UNIVERSITY OF BIRMINGHAM

ENCAPSULATION OF MODEL ACTIVES IN FLUID GELS

By

FABIO SMANIOTTO

A thesis submitted to
The University of Birmingham
for the degree of
DOCTOR OF PHILOSOPHY

School of Chemical Engineering
College of Engineering and Physical Sciences
The University of Birmingham

August 2020

Abstract

The present thesis seeks to extend the knowledge on fluid gel formulations and their potential applications by investigating how these systems can be utilised for the encapsulation of small molecular weight bioactives. This work builds upon previous studies on hydrocolloid-based fluid gels which have shown that these systems can be produced at an industrial scale and can alter food texture. In general, the two main objectives of this research are:

- To investigate the encapsulation of bioactives during the production process of alginate fluid gels and to assess the impact of process parameters on the encapsulation and release behaviours of bioactives of/from these materials.
- To study the effect of freeze-drying on alginate fluid gels properties and to evaluate this technique for the encapsulation of bioactives in fluid gels particles. In addition, the freeze-drying of these systems was studied as a way to extend the shelf-lives of the encapsulated actives as well as of the whole formulations.

This thesis considers first the microstructure and the formation of alginate fluid gels in order to understand the impact of specific formulation constituents (alginate and $CaCl_2$) and processing conditions used during their production, on the final properties of the materials.

Small molecular weight model actives were then encapsulated within alginate fluid gels, during their production, confirming that the presence of the actives does not interfere with the alginate fluid gels formation mechanism nor with their final particle dimensions and/or rheological properties. The encapsulation efficiency of all actives was initially very low, but significantly increased upon storage in the case of hydrophobic actives only. The encapsulation mechanism of hydrophobic actives into alginate fluid gel particles was investigated. It was concluded that hydrophobic actives were selectively encapsulated due to the formation of active-matrix hydrophobic interactions that significantly increased upon storage. Release analyses, conducted under sink conditions, revealed that the (hydrophobic) active fraction entrapped within alginate fluid gel particles does not migrate into the used aqueous acceptor phase. Release experiments conducted in simulated gastric fluids revealed the partial release of the fraction of actives encapsulated into alginate fluid gel particles, due to the disruption of the gel network when exposed to acidic conditions.

Freeze-drying studies of alginate fluid gels were performed and their rehydration revealed that, in general, the properties of these systems, i.e. particle size and rheological behaviour, were not significantly affected by this process. In addition, the encapsulation and release behaviour of actives, loaded in these systems before freeze-drying, were not altered by the drying process. Dried materials showed to be able to extend the shelf-life of both easy-degradable bioactives loaded as well as of the alginate fluid gel matrix, due to water removal. In conclusion, the research presented here promotes current understanding on fluid gel formulations by investigating the use of alginate fluid gels as nano/microcarriers for bioactives. Overall, this work extends the potential applications of hydrocolloid-based fluid gels to include their utilisation for the development of novel encapsulation and release approaches of bioactives relevant to the foods area.

Acknowledgements

I wish to express my infinite gratitude to my supervisor Dr. Fotis Spyropoulos for having given me this Ph.D. opportunity and for his constant support and friendship during these years. Additionally, I would like to thank Dr. Ioanna Zafeiri, the research fellow who assisted me throughout this project, for her assistance and help.

I would like to thank the University of Birmingham for the sponsorship of this work.

A special thanks to Dr. Valentina Prosapio for her big support during my research and life in Birmingham. I would like to thank all the people of the Microstructure Engineering Research Group for their support through this project, especially all my Ph.D. fellows. Thank you for all the assistance and help to all my colleagues at the University of Birmingham for all the great memories and lasting friendships. Thanks to all my friends in Italy for the invaluable time spent together during holiday breaks and for the at distance support.

Thanks to my mum Paola for all her unconditional love and support through the highs and lows of these last three years and throughout my whole life. Thanks to my dad Antonio for all his advice on life and work, for all the times that he put me back on track and for that crazy journey that we did together three years ago for my relocation in Birmingham.

Thanks Lucrezia: I have met you during this journey and you are the best gift I could have received from this experience. You make me feel happy.

Thank you!

“E voi materialisti, col vostro chiodo fisso,
che Dio è morto e l’uomo è solo in questo abisso,
le verità cercate per terra, da maiali,
tenetevi le ghiande, lasciatemi le ali.”

“And you materialists with your obsession
that there is no God and that we’re alone in this endless abyss,
you look for the truth down on the ground, like pigs,
just keep your acorns, and I’ll keep my wings.”

Francesco Guccini - “D'amore di morte e di altre sciocchezze” (1996)

List of Contents

List of Figures

List of Tables

Symbols

a_w – Water Activity

t_s – Storage time

w/w – Weight per weight

$D_{3,2}$ – Particle surface weighed mean diameter

$D_{4,3}$ – Particle volume weighed mean diameter

Span – Indication of the width of particle size distribution

η – Shear viscosity

$\dot{\gamma}$ – Shear rate

K – Consistency constant

n – Power-law index

R^2 – Coefficient of determination

M_t – Cumulative amount of active released at time t

M_∞ – Cumulative amount of active released at infinite time (complete release)

k_r – Release kinetic constant

n_r – Release exponent related to the mechanism of release

o/w – Oil in water emulsion

≈ – Approximately

°C – Celsius degree

$CaCl_2$ – Calcium Chloride

Abbreviations

AAFG – Ascorbic Acid Fluid Gel

AFG – Alginate Fluid Gel

AGP – Alginate Gel Particle

ALG – Alginate

ASC – Ascorbic acid

CMC – Critical Micelle Concentration

CRMF – Critical Ratio for Microparticles Formation

DLS – Dynamic Light Scattering

EE – Encapsulation Efficiency

EFSA – European Food Safety Authority

FD – Freeze drying

GIT – Gastro Intestinal Tract

NAS – Nicotinamide and Alginate Solution

NFG – Nicotinamide Fluid Gel

NIC– Nicotinamide

NMC – Normalised Moisture Content

PEPT – Positron Emission Particle Tracking

PSD – Particle Size Distribution

R.T. – Room Temperature

RPM – Revolutions Per Minute

SD – Standard Deviation

SDS – Sodium Dodecyl Sulphate

SGF – Simulated Gastric Fluid

SIF – Simulated Intestinal Fluid

TAS – Tryptophan and Alginate Solution

TFG – Tryptophan Fluid Gel

TRP – Tryptophan

VAN – Vanillin

VAS – Vanillin and Alginate Solution

VFG – Vanillin Fluid Gel

WHO – World Health Organisation

HPLC – High-Performance Liquid Chromatography

USA – United States of America

UK – United Kingdom

NL – The Netherlands

DE – Germany

DK – Denmark

Chapter 1: INTRODUCTION

1.1 Background

An essential part of the development of food products is the understanding of what consumers want and how they choose which products to buy [1]. The development of new food products is driven by the design of its formulation, in terms of ingredients composition and texture/structure. Understanding the properties of various ingredients composing foods is a fundamental concept for the development of products that meet the costumer's needs [2]. During the last decades, consumers have been seeking healthier food options, reduced in fat, salt and/or sugar**,** as well as enriched with micronutrients, i.e. vitamins, minerals and antioxidants. Concurrently people are still looking for tasty foods, requiring efforts from food industries to develop "nutritious and delicious" food alternatives**.** Fat content contributes to food texture, palatability, flavour and aroma, which is the reason why consumers are attracted to such high fat food products [3, 4]. On the other hand, fat is also the most concentrated source of energy in foods, providing 9 kcal per gram [5]. In addition, individuals following specific diets (e.g. vegan, gluten-free or dairy-free) are demanding for food options that fall within their dietary needs, while mimic the texture and flavour of "traditional" products, which do not fall within their dietary needs. Therefore, food products are often formulated using novel food ingredients to meet customer requirements, using the typically formed "microstructural approach".

The microstructure of food is the organisation and interaction of food components producing a unique microscopical phase, displaying specific properties and texture [6]. This structure is determined by the ingredients used to obtain the final product and by the conditions used to process these ingredients. By having a good understanding of the effect of ingredients and process conditions on the food textures, it is possible to design products using healthier and/or novel ingredients to obtain desired structures and/or properties. These characteristics are usually obtained by adding texture modifiers, stabilisers, thickening and gelling agents to food formulations. Hydrocolloids are high molecular weight polysaccharides and proteins that are widely used for these purposes, usually within semi-solid and liquid food formulations [7]. Hydrocolloids are able to absorb large amounts of water and swell forming a gel structure

that provides a specific texture to foods in which they are used. Studies revealed that these materials can display a similar rheological behaviour to that of fats present in food products and can mimic their palatability/consistency during the chewing process [8, 9]. For this reason, over the last decades hydrocolloids have been used in food formulations as fat replacers. In particular, polysaccharides can be added to foods to replace, or at least reduce their fat content, without a significant loss of sensory characteristics [10]. Lower calorie products can, therefore, be produced and the addition of non-digestible hydrocolloids would also increase consumer' satiety, as a consequence of their high fibre content, leading to further health benefits [11]. Examples of fat-reduced foods in which polysaccharides are commercially used are spread-cheese [12], mayonnaise [13], yoghurts [14] and ice creams [15].

In addition to the above, in the pharmaceutical and food supplement areas hydrocolloids are extensively applied as encapsulating agents for drugs and bioactives [16, 17]. Protection of the loaded active(s) from harsh environmental conditions to improve its/their stability, activity, avoid degradation and achieve a release targeted to the site of action/absorption in controlled and quantitative ways, are the main advantages/challenges of using encapsulation matrices. Specifically for food formulations, encapsulation matrices have been used to protect and deliver bioactives and living cells in the gastrointestinal tract [18]. For this reason, food and pharmaceutical industries constantly explore new encapsulation approaches and materials to overcome drug protection and/or delivery issues [16]. Research is currently conducted to find processing methods/conditions and matrix materials that allow the production of large (industrial scale) amounts of microparticles loaded with bioactives, to be used in food formulations [19]. In fact, these entities are quite easy to be made on a research/lab-scale, but there are still some big challenges to obtain large-scale productions of microparticle-based encapsulation systems [18]. In addition, research is oriented towards means to enhance the preservation and storage of these materials to extend shelf-life of microencapsulating systems on an industrial level [18, 20].

In the last decades, hydrocolloid-based fluid gels have been studied as a way to produce micrometre-scale particles in an industrially feasible way [21, 22]. These materials are dispersions of gelled particles in water, produced by shearing a hydrocolloid solution undergoing gelation [10]. Rheological and tribological studies of fluid gels revealed their

potential application for the replacement of fat droplets of emulsion-based foods; e.g. mayonnaise and yoghurts, since they were shown to have similar textures/sensory characteristics. However, it is important that gel particles are not detected during oral manipulation so that the food product mouthfeel remains unchanged. Detectability depends on particle characteristics as well as on the medium surrounding these. Hard/sharp particles in a low viscosity medium have been shown to be detected during oral processing at smaller sizes than those that are soft/smooth and are suspended in a higher viscosity medium. For example, alumina particles (hard particles) are firstly detected at a size of ~10 μm [7, 23]. Fluid gel systems seem to be ideal candidates for food applications, since soft-solid particles smaller than a few microns can be easily produced [24] and can be dispersed in high viscosity media, making their in-mouth detection even more difficult [7]. Consequently, fluid gel particles could be used to reformulate fat-based foods with a view to reduce their lipid and caloric content and providing similar textures to their low-fat counterparts.

Although the encapsulation and release of bioactives have been extensively investigated in hydrocolloid-based gel particles, fluid gel formulations have not been largely explored as matrices for the release of bioactives in foods. However, they were studied as biocompatible carriers for pharmaceutical application: for example, Chouhan *et.al.* (2019) developed an eye drop formulation, based on gellan gum fluid gel, which showed a high degree of ocular retention, enhancing the delivery of decorin, previously loaded within the formulation [25]. Another study of Mahdi *et al.* (2014), showed the potential application of gellan gum fluid gels as oral-liquid carriers for the controlled release of ibuprofen in the intestine [26]. Ibuprofen release was controlled by triggering the fluid gel stiffness, as a function of different gastric pH and as of its exposure time to the gastric environment. In addition to that, fluid gels can be used for big-scale production of hydrocolloid-based microparticles and this can be beneficial in order to use these particles for the encapsulation and release of actives in foods. In fact, these materials can be used for several purposes: to prevent actives degradation during food processing and/or storage; to control the delivery of bioactives into different parts of the gastrointestinal tract; to mask undesirable taste, odour and colour of some nutraceuticals, which will affect consumer's acceptance [27]. However, a deep scientific understanding of the relationship between fluid gel structures and their active encapsulation/release behaviours is needed and it is the overarching aim of this work. Studying the encapsulation of model actives in fluid gel systems is therefore essential to disclose their potential applications in the field of encapsulation in food products.

1.2 Aims and Objectives

The aim of this project is to gain insight into the encapsulation and release of small molecular weight active species within hydrocolloid-based fluid gel particles/formulations. In order to achieve this aim the following objectives were investigated:

- Investigate the formation of Alginate Fluid Gels (AFG) within a pin-stirrer device, used as an easily-scalable production route.
- Study the effect of freeze drying (FD) and rehydration on AFG properties, i.e. particle sizes and rheological behaviour.
- Assess the potential of FD as a technique to encapsulate actives within AFG and to extend the shelf-life of easily degradable bioactives.
- Investigate the encapsulation behaviour of hydrophilic and hydrophobic actives in AFG matrices and study their release overtime.

1.3 Thesis outline

The work presented in this thesis is organised into 9 Chapters. The experimental chapters (chapters 3-8) have all been written in the style of peer-reviewed publications, composed of an abstract, introduction, materials and methods, results and discussion, conclusion (and references) sections. A summary of each of these chapters is presented below:

In chapter 1, the background as well as the aim behind this project/thesis are reported. In addition, publications and conference presentations that arose from this project are listed.

In chapter 2 a critical literature review is presented, with a particular focus on hydrocolloid fluid gels and microencapsulation of bioactives.

Chapter 3 details the studies on AFG formation within a pin-stirrer device. The aim of this chapter was to study the formation mechanism of AFG and understand the impact of process parameters, such as residence time and shear rate used for their production, on their rheological properties and particle size distribution.

Chapter 4, published in “Food Hydrocolloids” under the title “Freeze drying and rehydration of alginate fluid gels”, describes the impact of FD and rehydration on AFG properties [28]. In addition, preliminary encapsulation experiments, using nicotinamide as a hydrophilic active,

are reported, aiming to investigate the impact of FD on the loading/release behaviour of this active from AFG.

Chapter 5, describes the ability of FD to extend the shelf-life of AFG when these are used as encapsulation matrices of easily degradable bioactives, specifically ascorbic acid, by reducing their water content.

Chapter 6, published in "Chemical Engineering Transactions" under the title "Use of alginate fluid gel microparticles to modulate the release of hydrophobic actives", describes the microencapsulation of tryptophan, used as a model hydrophobic active, into AFG [29]. Tryptophan was loaded into AFG during their production, to assess the concurrent encapsulation of hydrophobic actives during AFG formation. The effect on AFG properties due to active encapsulation were studied in terms of fluid gels' viscosity behaviour and particle size distribution.

Chapter 7 investigates the encapsulation of different small molecular weight actives in AFG as a function of active hydrophilic/hydrophobic character and of AFG particle size. Several experiments were conducted in order to correlate the active encapsulation efficiency with its release profile.

Chapter 8 offers an in-depth description of the encapsulation mechanism of hydrophobic actives, specifically in reference to vanillin, within AFG and macrogel alginate particles. Vanillin release was studied mimicking the conditions of different compartments of the gastrointestinal tract, for the potential development of stimuli-responsive formulations for controlled release applications.

Chapter 9 provides a summary of the main conclusions obtained from this work and proposes research ideas for future work.

This study is relevant from a scientific and industrial point of view, as it reveals new potential applications of fluid gels in the field of actives encapsulation. By disclosing new potential applications of fluid gels it would be possible to develop food formulations with less ingredients, since the texture modifiers will also be used as encapsulating matrices for bioactives.

1.4 Dissemination of research findings

The results obtained from this thesis have been disseminated as follows:

Publications:

- Smaniotto, F., Zafeiri, I., Prosapio, V., & Spyropoulos, F. (2019), Use of alginate fluid gel microparticles to modulate the release of hydrophobic actives. Chemical Engineering Transactions, 74, 1219-1224. (Chapter 6)
- Smaniotto, F., Prosapio, V., Zafeiri, I., & Spyropoulos, F. (2020), Freeze drying and rehydration of alginate fluid gels. Food Hydrocolloids, 99, 105352. (Chapter 4)
- Smaniotto, F., Zafeiri, I., Prosapio, V., & Spyropoulos, F., Freeze-drying of alginate fluid gels: a way to extend bioactives shelf life (i*n preparation*). (Chapter 5)
- Smaniotto, F., Zafeiri, I., Prosapio, V., & Spyropoulos, F., Understanding the encapsulation and release of small molecular weight model actives from alginate fluid gels (i*n preparation*). (Chapter 7)

Oral presentations (speaker underlined):

- Smaniotto, F., Zafeiri, I., Prosapio, V., & Spyropoulos, F., Use of alginate fluid gel microparticles to modulate the release of hydrophobic actives, 14th International Conference on Chemical and Process Engineering, Bologna (IT), 26-29th May 2019 (https://www.aidic.it/icheap14).
- Smaniotto, F., Zafeiri, I., Prosapio, V., & Spyropoulos, F., Encapsulation of model actives in fluid gels, The 20th Gums & Stabilisers for the Food Industry Conference, San Sebastian (ES), 11-14th June 2019 (https://foodhydrocolloidstrust.org.uk).

Poster presentation:

- Smaniotto, F., Norton, I. T., & Spyropoulos, F., Microencapsulation of model actives in polysaccharide fluid gels, EPSRC CIM in Food Conference, Nottingham (UK), 26-27th March 2018.

1.5 References

1. Frewer, L. and H. Van Trijp, *Understanding consumers of food products*. 2006: Woodhead Publishing.
2. Kacprzyk, J., Y. Avramenko, and A. Kraslawski, *Product Design: Food Product Formulation*. 2008.
3. Drewnowski, A., *Taste preferences and food intake.* Annual Review of Nutrition, 1997. **17**(1): p. 237-253.
4. Drewnowski, A. and E. Almiron-Roig, *Human Perceptions and Preferences for Fat-Rich Foods*. 2010.
5. Rolls, B.J., *The relationship between dietary energy density and energy intake.* Physiology & behavior, 2009. **97**(5): p. 609-615.

6. Verboven, P., T. Defraeye, and B. Nicolai, *Measurement and visualization of food microstructure: Fundamentals and recent advances*, in *Food Microstructure and Its Relationship with Quality and Stability*, S. Devahastin, Editor. 2018, Woodhead Publishing. p. 3-28.
7. Burey, P., et al., *Hydrocolloid Gel Particles: Formation, Characterization, and Application.* Critical Reviews in Food Science and Nutrition, 2008. **48**(5): p. 361-377.
8. Lucca, P.A. and B.J. Tepper, *Fat replacers and the functionality of fat in foods.* Trends in Food Science & Technology, 1994. **5**(1): p. 12-19.
9. Sandoval-Castilla, O., et al., *Microstructure and texture of yogurt as influenced by fat replacers.* International Dairy Journal, 2004. **14**(2): p. 151-159.
10. Norton, Jarvis, and Foster, *A molecular model for the formation and properties of fluid gels.* International Journal of Biological Macromolecules, 1999. **26**(4): p. 255-261.
11. Gabriele, A., F. Spyropoulos, and I.T. Norton, *A conceptual model for fluid gel lubrication.* Soft Matter, 2010. **6**(17): p. 4205-4213.
12. Brummel, S.E. and K.E.N. Lee, *Soluble Hydrocolloids Enable Fat Reduction in Process Cheese Spreads.* Journal of Food Science, 1990. **55**(5): p. 1290-1292.
13. Amin, M.H., et al., *Development of low fat mayonnaise containing different types and levels of hydrocolloid gum.* J Agroaliment Proc Technol, 2014. **20**(1): p. 54-63.
14. Keogh, M.K. and B.T. O'Kennedy, *Rheology of Stirred Yogurt as Affected by Added Milk Fat, Protein and Hydrocolloids.* Journal of Food Science, 1998. **63**(1): p. 108-112.
15. Varela, P., A. Pintor, and S. Fiszman, *How hydrocolloids affect the temporal oral perception of ice cream.* Food Hydrocolloids, 2014. **36**: p. 220-228.
16. Mustafa, A., *Encapsulation importance in pharmaceutical area, how it is done and issues about herbal extraction.* 2015.
17. Gibbs, F., et al., *Encapsulation in the food industry: a review.* International Journal of Food Sciences and Nutrition, 1999. **50**(3): p. 213-224.
18. Nedovic, V., et al., *An overview of encapsulation technologies for food applications.* Procedia Food Science, 2011. **1**: p. 1806-1815.
19. Silva, P.T.d., et al., *Microencapsulation: concepts, mechanisms, methods and some applications in food technology.* Ciência Rural, 2014. **44**(7): p. 1304-1311.
20. Đorđević, V., et al., *Trends in encapsulation technologies for delivery of food bioactive compounds.* Food Engineering Reviews, 2015. **7**(4): p. 452-490.
21. Garrec, D.A. and I.T. Norton, *Understanding fluid gel formation and properties.* Journal of Food Engineering, 2012. **112**(3): p. 175-182.
22. Gouin, S., *Microencapsulation: industrial appraisal of existing technologies and trends.* Trends in Food Science & Technology, 2004. **15**(7): p. 330-347.
23. Engelen, L., et al., *Oral size perception of particles: effect of size, type, viscosity and method.* Journal of Texture Studies, 2005. **36**(4): p. 373-386.
24. Fernández Farrés, I., *Fluid gel production and tribological behaviour of alginate and agar*. 2015, University of Birmingham.
25. Chouhan, G., et al., *A self-healing hydrogel eye drop for the sustained delivery of decorin to prevent corneal scarring*. Biomaterials, 2019. **210**: p. 41-50.
26. Mahdi, M.H., Conway, B.R., Smith, A.M., *Evaluation of gellan gum fluid gels as modified release oral liquids*. International Journal of Pharmaceutics, 2014. **475**(1–2): 335-343.

27. Sobel, R., R. Versic, and A.G. Gaonkar, *Chapter 1 - Introduction to Microencapsulation and Controlled Delivery in Foods*, in *Microencapsulation in the Food Industry*, A.G. Gaonkar, et al., Editors. 2014, Academic Press: San Diego. p. 3-12.
28. Smaniotto, F., et al., *Freeze drying and rehydration of alginate fluid gels.* Food Hydrocolloids, 2020. **99**: p. 105352.
29. Smaniotto, F., et al., *Use of Alginate Fluid Gel Microparticles to Modulate the Release of Hydrophobic Actives.* 2019.

Chapter 2: LITERATURE REVIEW

Abstract

This chapter aims to provide an overview of the relevant literature. It is divided in two main sections: the first one describes the physicochemical properties of hydrocolloids and specifically of alginate, since this is the hydrocolloid used for the fulfilment of this thesis. The production and properties of alginate fluid gels are also discussed. The second section provides an overview in the area of encapsulation materials and techniques, with a particular focus on the encapsulation of bioactives in foods.

2.1. Food hydrocolloids

Hydrocolloids are high molecular weight materials, usually polysaccharides and proteins, able to yield a gel material in the presence of water [1]. Polysaccharides and proteins are the two families of hydrocolloids that are commonly used in food products for different purposes, like structure stability, texture enhancement and flavour release [2]. A biopolymer solution is firstly obtained by dissolving/dispersing the polymer powder in water. Polymer chains are then crosslinked in a gelation step, which consists in the random association of polymer segments. These gels are classified into two categories depending on their cross-linking nature:

- Chemical, which have covalent/permanent junctions between polymer chains. This is obtained via different chemical reactions, depending on the polymer used and on the functional groups involved in the cross-linking. For example, the gelation can occur via radical polymerization, polycondensation, Schiff base reactions or Diels-Alder cycloaddition [3].
- Physical, also called reversible, when networks are held together by molecular interactions, including hydrogen bonds, ionic, hydrophobic interactions or combinations of these. These interactions are non-permanent and can be disrupted by environmental conditions, like pH changes or ions exchange. Natural hydrocolloids, like polysaccharides and proteins, are usually physically cross-linked.

The physical gelation can be obtained in several ways, depending on the gelation mechanism of polymer chains involved [4]. Three mechanisms are known [5]:

- Ionotropic gelation, which is due to the introduction of anions/cations in the polymer solution, allowing the formation of ionic bridges between polymer chains. Alginate and chitosan are examples of hydrocolloids able to gel in the presence of multivalent cations and anions, respectively.
- Cold-set gelation, which occurs when the polymer is dissolved at high temperature, forming a dispersion, and then cooled below a specific temperature, which is dependent on the polymer used, forming enthalpically-stabilized inter-chain helix structures. Agar, whey and soy proteins, gelatin, are probably the most known hydrocolloids displaying a cold-set gelation mechanism [6].
- Heat-set gelation, which occurs when the polymer is dissolved at low temperature and then heated above a specific temperature, which is dependent on the polymer used. The heating process unfolds the polymer chains that subsequently rearrange in a crosslinked network. Glucomannan, methyl-cellulose and starch are hydrocolloids that form gel structures via heat-set gelation [6].

Hydrocolloids are extensively used in food products as rheology modifiers, i.e. they are able to modify the flow behaviour of liquids in foods and their mechanical properties. They are used to meet consumer's desired sensory properties as thickening agents, gelling agents, emulsifiers and stabilisers [2]. Common thickening agents are starch, xanthan gum and cellulose derivatives, while gelling agents are alginate, pectin, gelatin and agar. Hydrocolloids are worldwide permitted as food additives according to the *Codex Alimentarius* of the World Health Organisation (WHO) [2].

2.1.1 Polysaccharides

Polysaccharides are complex carbohydrates derived from plants, seaweeds and microbial sources, consisting of sugar repeating units linked together via glycosidic bonds. They display a high hygroscopic character and they bind large amounts of water, exhibiting thickening properties [7]. Carrageenan, pectin, agar, xanthan gum and alginate are some examples of industrially used polysaccharides.

2.1.1.1 Alginate

Alginic acid, also called alginate (ALG), is an anionic natural polysaccharide, extracted from brown algae after treatment with alkali solutions, usually NaOH [8]. It is a linear-copolymer constituted by homopolymeric blocks of (1-4)-linked β-D-mannuronate (M) and its C-5 epimer α-L-guluronate (G) residues, covalently linked in different sequences [8]. Its structure is reported in Figure 2.1. Monomers can appear in consecutive blocks of G-residues, M-residues or alternating M/G-residues [9]. ALG is widely used in foods, textile printing and pharmaceutical industries as thickening and gelling agent. It gelates in the presence of divalent cations, like Ca^{2+} or Ba^{2+}. Ca^{2+} is the most used one, due to its high biocompatibility and low cost [10]. G-residues adopt a 2-fold symmetry giving rise to a buckled structure in which Ca^{2+} are accommodated. This 3D-network is called "egg-box model" and is reported in Figure 2.1.

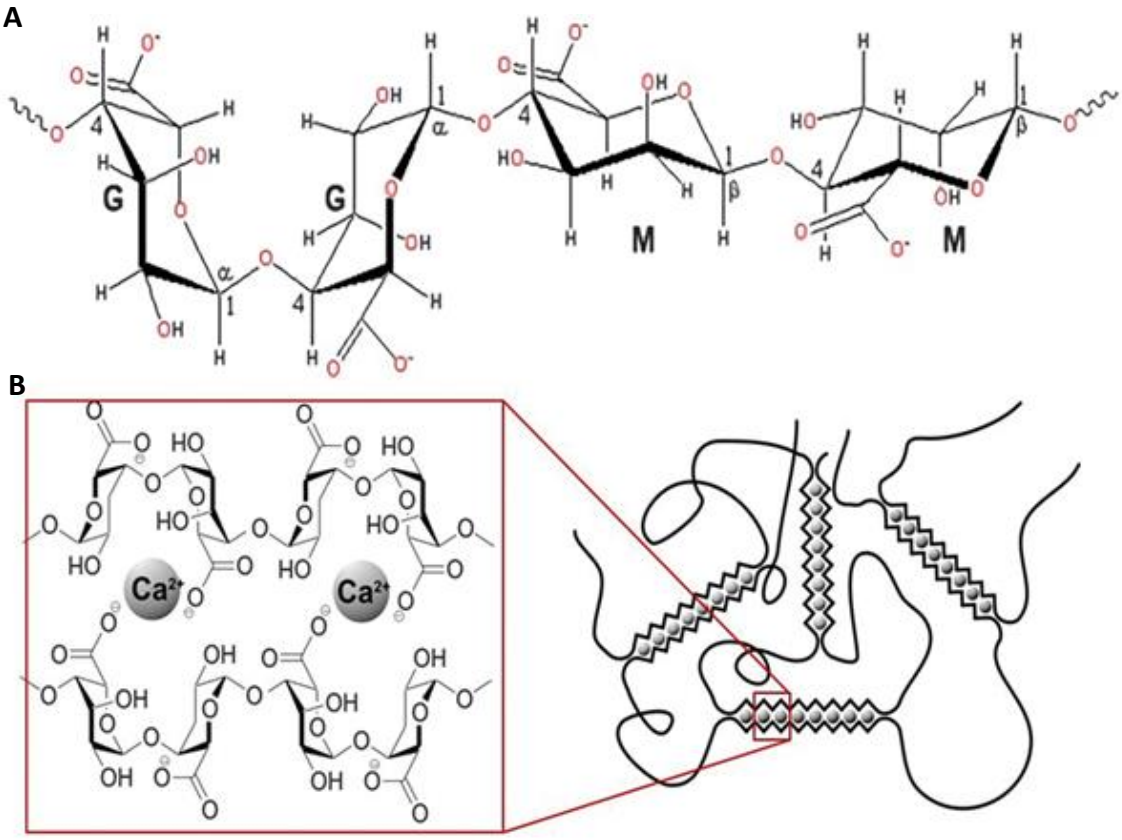

Figure 2. 1 - Alginate: (A) polymer chain composed by G: α-L-guluronic acid and M: (1–4)-linked β-D-mannuronic acid units; (B) alginate gelation in the presence of Ca^{2+} ions forming the "egg-box" structure [11]

The final gel strength depends on ALG source (algal species), on its concentration, its degree of polymerization and cation concentration. The ratio between M/G has been studied in

depth, revealing a significant impact on the final gel properties. ALG having a high G-residue content form strong and brittle gels, since G-residues are responsible for the interactions with cations. On the other hand, ALG gels rich in M-residues are softer and more elastic [8]. The calcium gelation of ALG can be obtained using two different approaches: diffusion method and *in-situ* calcium release. The first one involves the direct mixing of an ALG solution with a $CaCl_2$ water solution. This gelation is instantaneous, but the kinetic of gelation can be controlled by adjusting the diffusion rate of Ca^{2+} through the ALG solution. The *in-situ* calcium release into ALG is achieved by using an insoluble calcium salt in water, usually $CaCO_3$. The release of Ca^{2+} in water is achieved by lowering the pH, for example using HCl. $CaCO_3$ reacts with HCl as by the reaction reported in Equation 2.1:

$$CaCO_3 + 2HCl \rightarrow CaCl_2 + CO_2 + H_2O \qquad \text{(Equation 2.1)}$$

Due to the high-water solubility of $CaCl_2$, Ca^{2+} ions are progressively released into water, allowing ALG cross-linking. For this method the gelation kinetics is controlled by the acid addition and, therefore, it can be easily manipulated [12].

2.1.2 Hydrocolloid gel particles

Hydrocolloid gel particles can be obtained via several techniques, depending on the gelation mechanism of the hydrocolloid, i.e. thermal or ionic gelation. The essential step of particles production is the breakup of the gelled matrix that determines the final dimensions and strength of particles, together with the gelling mechanism [4]. These techniques can be divided in continuous phase formation and dispersed phase formation. The first is obtained when a large gel phase is formed and then broken up in smaller particles. On the contrary, dispersed phase formation mechanism involve first the formation of droplets and then their gelation [4]. Techniques for the production of hydrocolloid-based gel particles formed via continuous phase mechanism are coacervation and shear processes, while for dispersed phase are extrusion and emulsion. Coacervation involves the separation of a colloidal solution into two liquid phases, the coacervate, more concentrated in the colloid component and the equilibrium solution, less concentrated in the colloid [4]. Phase separation is obtained by the addition of electrolytes, desolvated by the addition of an immiscible solvent or temperature/pH changes [4]. This technique is widely used for the encapsulation of bioactives and cells in polymer materials [13]. Gelatin is probably the most used hydrocolloid that form gel particles via coacervation. The use of shear to breakup an hydrocolloid solution to form

discrete gel particles has been investigated in the last decades [14, 15]. Formed materials are known as shear/fluid gel and are later described more in depth.

2.1.2.1 Alginate Particles

Many techniques have been studied for the formation of Alginate Gel Particles (AGP), depending on the final properties desired, i.e. particles size and strength. In general, AGP are formed using a disperse phase formation, due to their ionic gelation mechanism, using emulsion or extrusion methods. Extrusion is commonly used for lab scale productions and its simplest version involves extruding an ALG solution through a needle into a $CaCl_2$/hardening bath [4]. The obtained droplet size is a function of the diameter of the needle used, of the flow rate and viscosity of the ALG solution. Typical AGP sizes are in the range between 0.5 mm to few mm. However, modified techniques, which use electrically charged needle or a nozzle spray, have been studied to atomize the extruded ALG droplets, obtaining smaller particles having dimensions of hundreds of microns [16]. Emulsion-based techniques can be used to obtain smaller AGP, which dimensions can be adjusted as a function of several parameters, like oil phase viscosity, oil/hydrocolloid/water ratios, type of emulsifier, emulsifier concentration and applied shear rate to create the emulsion [17]. Particle dimensions are usually in the range between 0.2 to few hundreds µm. Oil phase removal is the major difficulty of this technique, that add a separation process and increase process complexity and costs [4]. Both extrusion and emulsion techniques present issues, like the needs of sophisticated equipment and scale-up difficulties. In addition, final materials retain high amounts of water, increasing transportation and storage costs. The extrusion method is difficult to be used for the preparation of few micrometre particles, which are needed for food applications. Dry particles can be produced via spray-drying or dried after their production, to minimize transport and storage costs/volumes. Spray-drying is used on lab and industrial scales for preserving different materials for long period of time, including alginate, milk powder and fruit juices, and for the microencapsulation of nutraceuticals, probiotics and drugs in hydrocolloid-based systems [4, 18]. However, this technique present low yields of particle production due to the loss of product on the walls of the drying chamber and particles smaller than 2 µm usually pass into the exhaust air due to ineffective separation [19].

2.1.2.2 Applications of hydrocolloid gel particles

Gel particles have many applications in foods, pharmaceuticals, agrochemicals and cosmetics [4]. Texturisers, rheology modifiers and encapsulation moieties are common applications for gel particles. Examples of non-food applications are coatings, oil recovery systems, inks, and cream formulations in cosmetic [20]. Similar applications are of value in foods, however the range of polymer materials available is restricted by food-grade regulatory approval. Hydrocolloids are fundamental to achieve the physical stability of food products and desired product mouth-feel properties [21]. Hydrocolloid microparticles are widely used for encapsulation applications of drugs and food nutrients. Encapsulation in hydrocolloid particles is particularly attractive as it can overcome poor solubilities issues of the active or achieve specific time/site release as a function of environmental conditions. For example, gel particles have been extensively investigated for the encapsulation of probiotics to improve their survival rate in the gastric environment to maximize their colon delivery [4]. Other examples of food encapsulations include the use of AGP to encapsulate vitamin C and flavours and pectin-based particles for insulin encapsulation [4].

2.1.3 Fluid Gels

Fluid gels, also called shear gels, are defined as gelled hydrocolloid particles in a continuous medium, usually water. They are formed by applying a shear regime to a gelling biopolymer solution [14]. Their particle formation process is described as a two steps process: an aggregation of polymer chains step followed by a nucleation and particle growth step. Particles grow until they reach an equilibrium droplet size, controlled by the applied shear environment [12]. Particle sizes and shapes are also function of the polymer solution viscosity [15, 22]. Potentially all equipment able to provide shear can be used for the production of fluid gels. On a lab scale and for study purposes, the shear environment can be provided by a rotational rheometer, which allows the fine control of shear rate and temperature, allowing to study the formation kinetics of fluid gels [12]. To scale up the process a jacked pin-stirrer vessel can be used to produce fluid gels in a continuous way. This device is constituted by a rotating central shaft and by a fix jacked, that allows to adjust the vessel temperature by using a circulating hot/cold liquid, and on both internal parts pins are installed. A visual representation of the pin-stirrer set-up, used for the production of AFG, and pictures of the vessel, used for the fulfilment of this project, are reported in Figure 2.2.

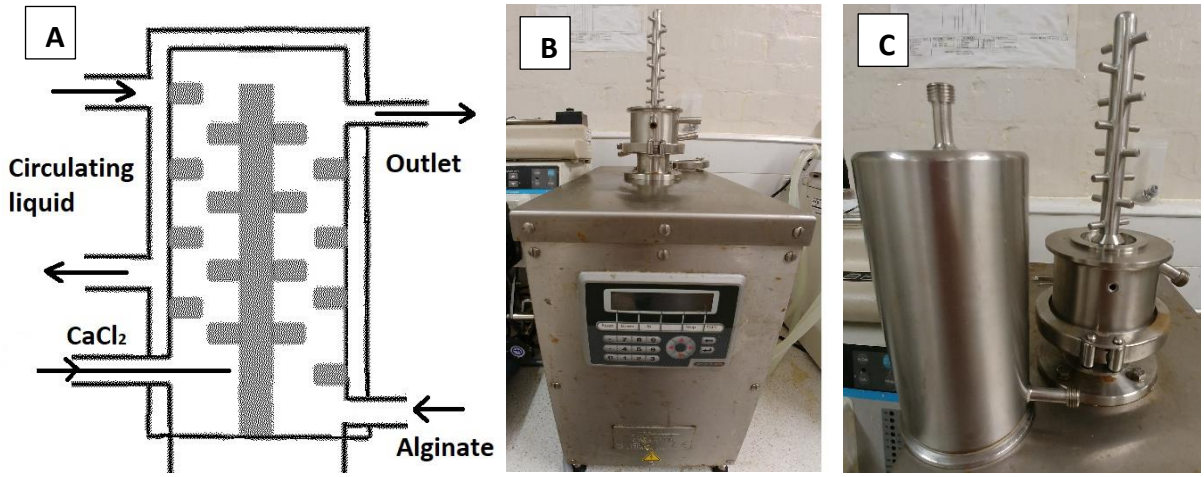

Figure 2. 2- Pin-stirrer vessel set-up diagram (A), used for Alginate fluid gel preparation, and pin-stirrer pictures (B&C)

2.1.3.1 Temperature set fluid gels

For temperature gelled hydrocolloids the fluid gel formation is obtained within a pin-stirrer vessel, in which the temperature of the jacked wall is adjusted to induce gelation. For example, Ellis *et al.* (2017) obtained agar based fluid gels by feeding 1% w/w agar solution at 70 °C into a pin-stirrer cooled to 5 °C [23]. Agar fluid gel formed at approx. 30 °C, depending on the concentration of agar used. A similar setting was used by Garrec *et al.* (2013) for the production of κ-carrageenan fluid gels: the inlet temperature was set at 50 °C, while the outlet temperature at 5 °C with a gelation temperature of approx. 35 °C [24]. Gabriele *et al.* (2009) showed that biopolymer concentration and process parameters, i.e. cooling rate and shear rate, were both responsible for the final fluid gels properties obtained via thermal gelation mechanism. In particular, when the cooling rate was reduced the final viscosity of the system increases as a result of a faster and more abundant formation of nuclei of gelation that leads to more interactions between particles [25]. Micrographs of κ-carrageenan fluid gels revealed that at low shear rate irregular-shaped large particles were formed, probably due to the break up process of a large gel structure. By increasing the applied shear rates smaller and almost spherical particles were obtained, as can be seen in Figure 2.3. It was concluded that the mechanism of fluid gel formation is a nucleation and growth process: small gel nuclei are firstly formed, growth, and final sizes are determined by the applied shear environment. Overall particle size decrease by increasing the shear rates [25]. These experimental findings were in agreement with what reported by Carvalho *et al.* (1997): the formation and growth of small nuclei during thermal-set fluid gel formation is a process mainly dictated by the

cooling rate, while coalescence and break-up processes of the formed gel are controlled by the shear rate applied [26].

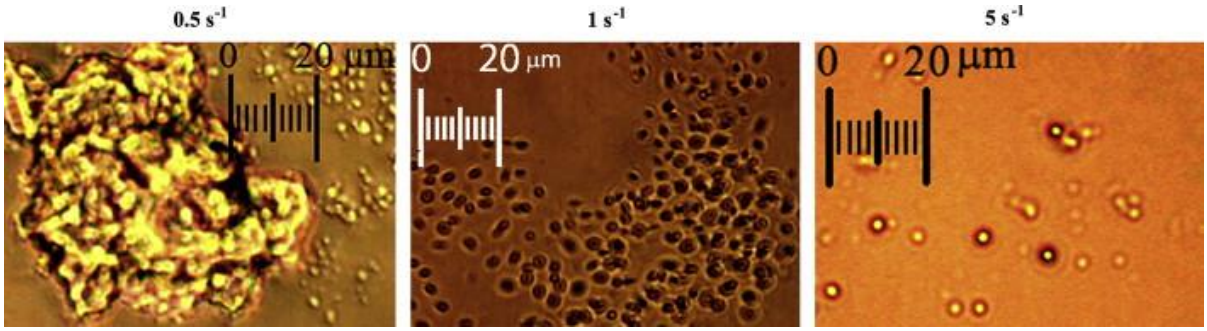

Figure 2. 3- Micrographs of κ-carrageenan fluid gel particles produced using a rotational rheometer at different shear rates [25]

2.1.3.2 Ionically set fluid gels

Opposite to the formation of thermal-set fluid gels, which is a process controlled by the rate of cooling/heating and by the timescale of the applied shear, ionic-set fluid gels present another formation mechanism. Alginate (ALG) is one of the most used ionically gelled biopolymer and it was previously used for fluid gels production [27]. The major difficulty in producing Alginate Fluid Gels (AFG) arises from the rapid gelation in the presence of Ca^{2+} ions. As such, Ca^{2+} introduction into ALG solution should be conducted inside the pin-stirrer at the same time of shear application. The process of AFG formation has been previously investigated by Farrés *et al.* [27]. ALG and $CaCl_2$ streams were injected separately into the pin-stirrer and $CaCl_2$ was injected as close as possible to the rotating shaft, to ensure a fast mixing of the two streams. The authors suggested that particles shapes and sizes were determined by a combination of nucleation and growth process of fluid gel particles, similar to the process observed for thermal-set fluid gels, competing with a break-up process induced by the applied shear [12]. In the same study, authors recognized that the gelation kinetic was poorly controlled, due to the instantaneous gelation of ALG in the presence of Ca^{2+} ions, and it was not possible to obtain a homogeneous particle size distribution. This was also affected by the non-uniform shear environment inside the pin-stirrer vessel. Gabriele *et al.* (2009) showed the residence behaviour of fluid gel particles in different parts of the pin-stirrer mixing chamber, during fluid gel formation, by using PEPT imaging technique [28]. Regions experiencing higher and lower residence times were identified, due to different mixing

magnitudes, as shown in Figure 2.4. It is important to notice that the pin-stirrer studied/used by Gabriele *et al.* is the same equipment used for the formation of AFG within this thesis.

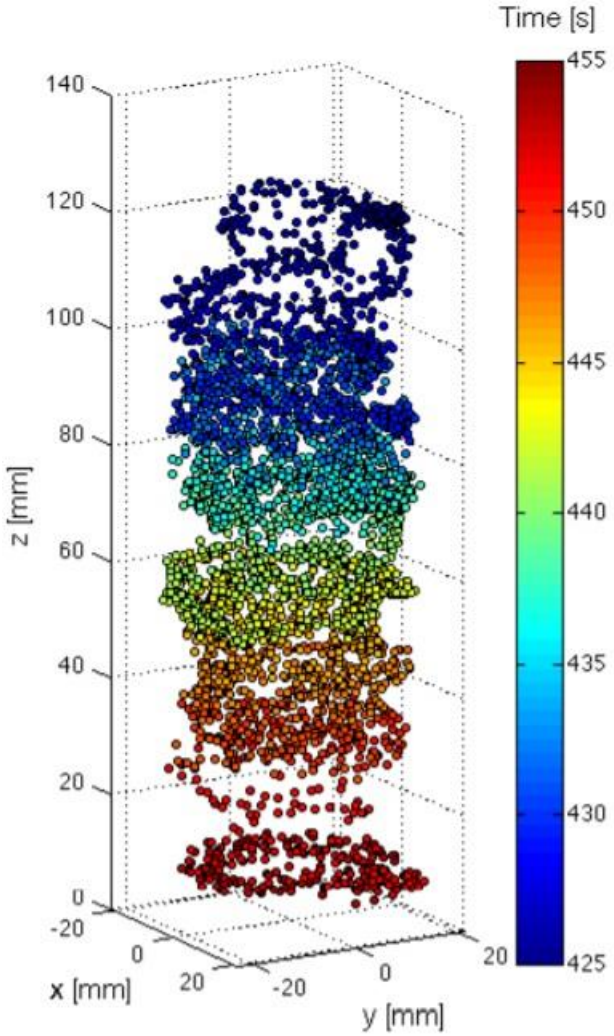

Figure 2. 4- Three-dimensional plot of particle residence in the pin-stirrer mixing chamber as a function of time. It can be appreciated the spiral flow of particles and the non-uniform shear environment [28]

To overcome this issue, a rotational rheometer to provide a more homogeneous shear environment was used by Farrés *et al.* (2014) for AFG production [12]. In this case the release of Ca^{2+} was obtained *in-situ*, by progressively liberating cations from the non-water soluble $CaCO_3$ by reaction with H^+ released from the slow hydrolysis of glucono-δ-lactone [12]. This more controlled introduction of cations into ALG prevented the formation of large blocks of gel and produced a more uniform particle size distribution.

2.1.3.3 Fluid gel rheology

Rheology is the science that study the deformation and flow of materials in response to an applied force. In the food area it enables the scientific characterisation of food structures and

consistencies. The flow behaviour of suspensions, i.e. heterogeneous systems in which solid particles are dispersed in a continuous medium, is dictated by the particle specific mechanical properties, i.e. deformability or modulus, and by the ratio between particles and liquid phase [32]. In general, for low solid fraction suspensions particle-particle interactions are not significantly formed and the viscosity of the system is mainly dictated by the flow behaviour of the solvent [33]. By increasing the solid fraction, particles start to collide and additional energy is required to make the material flowing. In fluid gel systems, the volume fraction of particles has been reported to be close to the maximum particle packing fraction, therefore, particles significantly interact with each other, increasing the viscosity of the system [12, 32]. This was observed, for example, in whey protein and agar fluid gels, where viscosity changed as a function of the particle solid fraction and by particle deformability [34, 35]. Deformability is an intrinsic characteristic of the material used to make particles, but it is also a function of particle size: big particles are easier to deform, when compared to more rigid smaller ones [29]. In general, the viscosity of systems with similar solid fractions is affected by the dimensions of particles; smaller particles produce a higher number of particles per volume unit, increasing their surface area exposed to the liquid phase. Therefore, particle-particle interactions are enhanced, usually leading to an increase in viscosity, if compared to a sample formed by bigger particles [33].

The rheological behaviour of fluid gels, which are suspensions of hydrocolloid gelled particles in water, was extensively investigated, both during their production process and after their set-up. The effect of applied shear during κ-carrageenan fluid gel production was investigated by Gabriele *et al.* [25]. These fluid gels were produced in a rotational rheometer and their viscosity was recorded as a function of the applied shear rate, during gelation. Viscosity started to increase upon the formation of nuclei of gelation, at the gelation temperature of κ-carrageenan. Upon lowering the temperature, particles grew until an equilibrium size, determined by the shear rate applied. Bulk viscosity continued to increase, as can be seen in Figure 2.5, due to an increase of both number and volume fraction of particles.

The process parameters used during fluid gel formation has an impact on their final rheological behaviour; for example, by increasing the concentration of hydrocolloids a higher bulk viscosity is obtained and this is true for both ionically and thermally gelled materials [24,

30, 31]. On the contrary, an increase of the applied shear rate, during fluid gel preparation, lead to a decrease in viscosity, as shown in Figure 2.5 [25, 32].

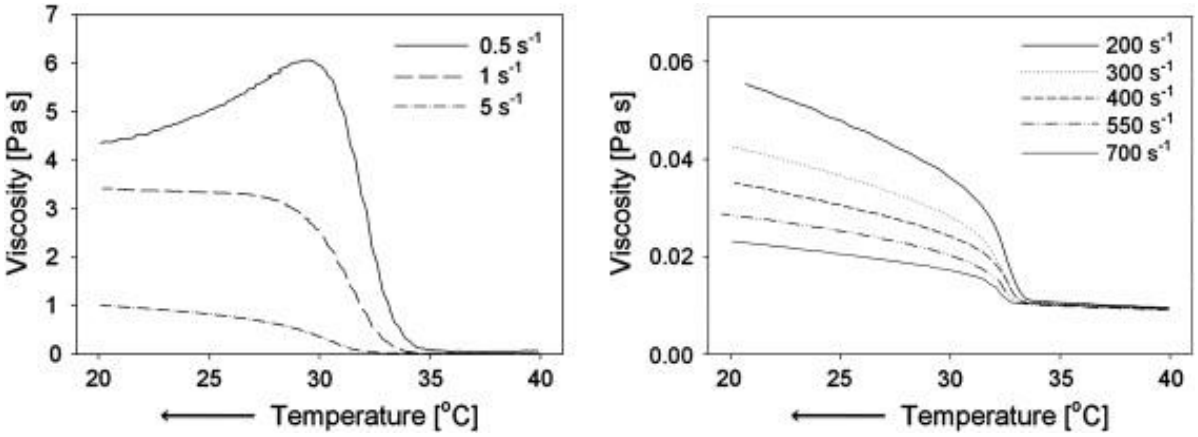

Figure 2. 5- Viscosity of κ-carrageenan fluid gels, during production, as a function of the applied shear rate [25]

Viscosity tests, conducted after fluid gel set-up, showed a typical non-Newtonian shear thinning behaviour, i.e. viscosity decreases by increasing the shear applied [24]. Particle packing has a big impact on their flow ability, as the flow behaviour of highly concentrated particle suspensions is characterized by the relative flow of particles one to another [32]. The lower the ratio between particles and the continuous phase, i.e. the larger the space between particles, the easier is for the system to flow. During rheological measurement inter-particle interactions are broken and the systems viscosity is therefore a direct function of the intrinsic elasticity and packing of particles [14]. For example, frequency sweeps tests were carried out on κ-carrageenan fluid gels showing that, at low frequencies, these systems displayed a viscous-liquid behaviour, while at higher frequencies particles entanglements provide an elastic response [33]. κ-carrageenan gel, produced without the application of a shear regime, behaved as a "strong" gel while κ-carrageenan fluid gels displayed characteristics between a "weak" and a "strong" gel. The authors concluded that this difference of gel strength was due to interactions between fluid gel particles. These were closely packed, forming an elastic network that was disrupted by applying a shear environment and the material started to flow. The bulk gel strength was function of the elasticity of particles and it increased with particle stiffness [24]. A rheological study of Farrés *et al.* (2014) on AFG revealed yield stress phenomena due to significant inter-particle interactions [31]. This is generally associated with a 3D rigid network that deforms before flowing. For suspensions of non-aggregated particles, yield stress indicates the formation of attractive forces between particles. The authors

concluded that AFG behave as a suspension of charged particles, forming Ca^{2+} interactions between them after their production and setting. Dynamic rheology experiments were also carried out displaying fluid gels ability to flow under low strain and to recover their initial structure/behaviour after the removal of shear. In addition, Farrés *et al.* (2014) reported that by increasing the calcium content, AFG particle stiffness was increased. However, this did not change the viscosity of the material in a significant way [31].

2.1.3.4 Fluid gel tribology

Tribology is the science that study the interaction of surfaces in relative motion and aims to understand the friction, lubrication and wear phenomena happening between them. Since the 1980's tribology was used to study oral processing of food in order to predict the in-mouth sensory perception of food consumption [21]. The eating process involves the interaction of several surfaces in relative motion, like palate, tongue and the food itself. The food sensory perception is strongly influenced by the resistance against moving due to the food presence in mouth, making the food to be perceived for example as thick, brittle, crispy, hard, soft, spongy, smooth or creamy [21, 34]. Rheology is a good technique to determine thickness, hardness or elasticity behaviours of food in mouth, while tribology can better predict smoothness, creaminess and slipperiness properties [35].

Tribological studies and sensory trials of fluid gel formulations showed lubrication properties of these materials. In mouth they were perceived as "smooth" and fluid gel particles were not prone to be detected during consumption, due to their soft-solid behaviour [36]. In particular, AFG particles behaved as deformable entities, in tribological analyses, mimicking the behaviour of fat droplets of o/w emulsions [27]. In addition, AFG are thermally stable materials, i.e. they do not melt upon heating at the high temperatures commonly used in the food industry processes, like pasteurisation at 100 °C. Because of this unique characteristics, they can be potentially applied in food formulations as fat replacers [12].

2.2 Bioactives

A bioactive is a substance that displays a biological activity, due to its ability to modulate at least one metabolic processes [37]. In humans, bioactives consumption is made with the goal of promoting a better health condition. In the food field, bioactives are also called nutraceuticals and used as formulation ingredients. They are also defined as "a food (or part

of it) that provides health benefits, including the prevention and/or treatment of diseases". They include vitamins, antimicrobials, antioxidants, flavours and minerals [38]. However, some bioactives should be encapsulated into carriers in order to display or increase their beneficial effects on human health, since some of them are degraded by environmental conditions, because of their chemical properties, sensitivity to high temperatures, low pH or high water activities environments. Encapsulating matrices can provide protection against degradation, potentially increasing their shelf-life. Additionally, some bioactives present a low bioavailability in humans and encapsulating matrices can slow down their release at their site of action/absorption, increasing overall their absorption in comparison with an uptake of high dosages of the same non-encapsulated active [39-41]. Different types of systems have been developed to deliver bioactives at their site of action/absorption in the gastrointestinal tract, like solutions, emulsions, suspensions and gels that are widely used in the pharmaceutical and food fields [20, 42].

2.3 Encapsulation

Encapsulation is the process of loading a substance, called active ingredient, within another material. This material is called in several ways, e.g. coating agent, membrane, capsule, carrier material, external phase, or matrix [43]. Actives encapsulation, using different methodologies and encapsulating materials, is widely used and studied in the food industry for several reasons: it is useful to improve the delivery of nutraceuticals, like antioxidants, minerals, vitamins, fatty acids and probiotics specifically to the gastrointestinal tract, where they are absorbed [44]. This is mainly due to actives protection and controlled/prolonged release effects. Usually bioactives are degraded due to harsh environment, food processing and gastrointestinal conditions. The encapsulation material cover them with a physical barrier that protects the active from surroundings, prolonging their shelf life. The matrix could also control the release of the active over prolonged periods of time and/or under specific conditions [43]. Encapsulation in foods is also applied for preserving bioactives during industrial processing and storage, reducing their inhibition due to oxidation and/or hydrolysis reactions [45]. Encapsulation is also used to build a physical barrier around actives known to have undesirable flavours/aroma, masking in this way their bad taste or smell in foods [43].

Bioactives can be encapsulated into different dimensions and shapes particles, spherical or irregular, simple or multi walled, having a single/multiple active core or having the active homogeneously dispersed in the whole matrix. Examples of encapsulating particles structures are reported in Figure 2.6.

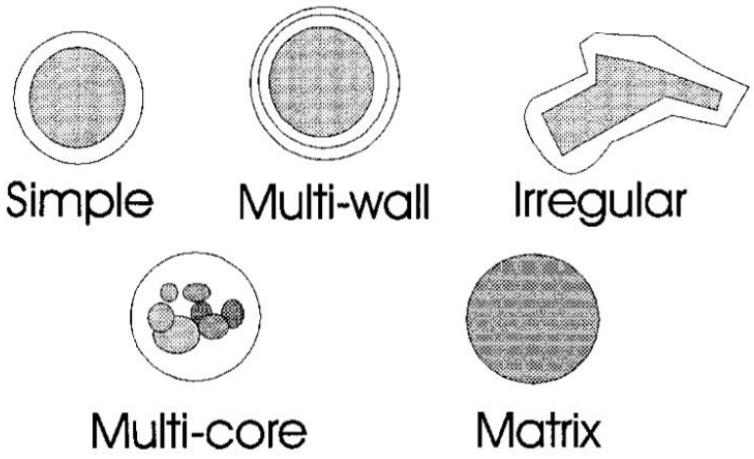

Figure 2. 6- Different types of encapsulating systems. Active is represented in grey and carrier in white [20]

2.3.1 Encapsulation materials

Different materials have been studied and used to encapsulate solid and liquid bioactives. However, several matrices, generally used in drug formulations, are not approved and not certified for food applications. Several organisations, like the European Food Safety Authority (EFSA) or the Food and Drug Administration (FDA) in the USA, are responsible to certify a substance as "safe" for food applications, by giving to it the status of "generally recognized as safe" (GRAS) [46]. Coating materials used for food encapsulation must be food-grade, biodegradable and able to protect the active from its surroundings. In addition, they do not have to react with the encapsulated compounds and they should have good rheological properties, depending on their applications. Polysaccharides are the most widely used materials for food encapsulation: starch, cellulose, dextrins and maltodextrins, Arabic gum, xanthan gum, gellan gum, carrageenan, alginate, pectins and chitosan are some examples of them. Polyunsaturated fatty acids, vitamins, minerals, antioxidants, probiotics, pigments and antimicrobial molecules are only some examples of nutraceuticals that have been successfully encapsulated in polysaccharide-based materials [47]. Proteins, like milk proteins, whey proteins, caseins, gelatine and gluten, and lipids, like fatty acids, waxes, glycerides and phospholipids, are also largely used for encapsulation purposes. Choosing the best encapsulation technology and material for a specific active is often a trial and error process.

However, knowing the active physicochemical properties is fundamental to determine their interactions, stability, release and digestion behaviours in a specific matrix [48]. Cost reduction is also a fundamental factor to consider when choosing an appropriate encapsulation coating/procedure [43].

2.3.1.1 Alginate as encapsulating material

Alginate has been widely used in pharmaceutical and food industries as encapsulating material for bioactives, drugs and probiotics. Alginate is very sensitive to pH changes: at pH below its pKa (<3.4), the majority of its carboxylic acid groups are in the non-ionized form (COOH) and so alginate is not soluble in water. By increasing the pH, more and more carboxylic acid groups became ionized (COO^-); at pH>4.4 the electrostatic repulsion of COO^- groups causes the expansion of alginate polymer chains, making them to be soluble and to swell water. The highest expansion and water swelling have been reported to be at pH=7.4 [49]. Due to this particular behaviour, alginate has been largely studied and used for the development of colon-selective drug release formulation, taking advantages of the pH variations along the gastrointestinal tract [50, 51]. Alginate has been widely used for the encapsulation/protection of probiotics in foods, since bacteria, and some actives, are known to be easily degraded by high temperatures. Thanks to its ionic gelation, which is performed under mild conditions, AGP are ideal matrices for the entrapment of easy degradable nutraceuticals. In addition, alginate gelation is easy to perform, does not involve the presence of toxic solvents or chemicals, is biocompatible and cost effective [52].

2.3.2 Encapsulation techniques

Several techniques are available for active encapsulation into food-grade matrices. Spray-drying, spray-chilling, extrusion coating, fluidized bed coating, liposome entrapment, and coacervation are the most used ones [20, 46]. Approx. 80-90% of encapsulated products are obtained via spray-drying. It is a flexible, continuous and economical process, able to produce small particles (<40 μm) with a high encapsulation efficiency [46]. However, it display some disadvantages such as equipment complexity, non-uniform drying into the drying chamber and non-homogeneous particle size distribution. In addition, it uses high temperatures to perform the drying step, which is not always suitable for temperature sensitive actives.

Extrusion methods consist of dripping droplets of an aqueous solution of an ionically set hydrocolloid, e.g. alginate, mixed with the active into a gelling bath, like $CaCl_2$ solution,

through a nozzle. Nozzles of various geometries, or an atomization disk apparatus, can be used to adjust the final particle sizes and shapes [46]. Simple extrusion method can only produce big particles and its modified versions, which can potentially produce smaller particles, are difficult to scale-up. Therefore, this method is mainly limited to lab-scale productions [53].

Emulsification method is often used in case of water soluble actives. Water/oil or oil/water emulsions and water/oil/water double emulsions are different types of formulations used for this purpose. Dry products are then obtained by drying these emulsions via different methods, like spray/freeze-drying. Emulsification methods usually involve the use of emulsifiers to stabilize the emulsion and prevent its gravitational separation, flocculation and coalescence, increasing process costs and requiring complicated and high-cost apparatus set-up, which are difficult to scale-up [54, 55].

Freeze-drying is a drying process that operates at the freezing point of the solvent [46]. It is a very gentle drying method, which prevents the degradation of low-stability actives during their encapsulation. In fact, freeze-drying has been extensively used for the encapsulation of thermo-sensitive actives, but its major disadvantages are the high energy and the long drying time required (24-48 h). This technique is therefore used for the encapsulation of high-added value compounds, mainly in the pharmaceutical field [56].

2.3.3 Microencapsulation

Microencapsulation is a method of packing solids, liquids or gases in micrometre scale particles or droplets [57]. Active containing core is entrapped into thin coating layers made of food-grade materials, providing a physical barrier to the surrounding environment. Microencapsulation is one of the most used approach to encapsulate bioactives in foods: it can prevent, or at least reduce, the active reactivity with the environment, decrease the active transfer from the core to the outside of the capsule by controlling its release rate and mask unwanted tastes/flavours [57, 58]. In addition, the use of few micrometre scale particles is ideal for the application in foods, since particles bigger than 20-40 μm are normally detected into food products changing the product mouthfeel, providing an undesired gritty texture [59]. The core may be in the crystalline, emulsion or suspension form. Spray-drying, spray-chilling/cooling, extrusion coating, freeze-drying, coacervation, and co-crystallization are the most used techniques for the production of microcapsules and for microencapsulation, even

though spray-drying is the most used one [57, 60]. Usually, the most appropriate method for microparticle formation is selected after choosing the best coating material for the encapsulation of a particular active. In fact, the coating material is the main determinant of microcapsule properties. In general, a good coating material should have good rheological properties, easy workability, homogeneously distribute the active into its structure and protect it from the environment. In addition, it should not react with the active, retain it during processing and storage, be inexpensive and food-grade [61]. Usually, more than one coating is employed, in combinations with other components, like antioxidants, chelating agents and surfactants, in order to obtain all the desired properties [57]. Generally, hydrocolloids are used to encapsulate organic and non-water soluble materials; on the contrary, water-insoluble polymers are used for water-soluble actives [57]. Natural or synthetic polymers, polysaccharide and protein hydrocolloids can be used as coating materials, depending on the active properties and on the desired final characteristics of the formulation. Studies have been conducted in literature to understand the encapsulation behaviour of actives into hydrocolloids-based microparticles after their production. The diffusion of bioactives, like glucose, tryptophan and α-lactoalbumin, into AGP was studied by Tanaka *et al.* (1987), showing a very fast diffusion of these actives into ALG microparticles when placing unloaded particles into actives aqueous solutions [62]. Hariyadi *et al.* (2016) studied the encapsulation efficiency of ibuprofen within alginate gel microparticles, by suspending AGP in a 0.1M NaOH of ibuprofen. After storage for 24 h they reported an ibuprofen loading of 23-29% w/w due to active diffusion into particles, but encapsulations at longer storage times were not evaluated [63]. Mahdi *et al.* (2014) loaded ibuprofen in gellan gum fluid gels during their production into a rheometer [64]. They proved the encapsulation of ibuprofen as solid crystals inside gellan gum particles, via microscopy imaging, due to the formation of a gellan gum acid gel at pH 1.2 that caused the crystallization of ibuprofen [64].

2.3.3.1 Examples of microencapsulation in foods

As previously said, one of the main purpose of actives encapsulation is to improve their final stability. Probiotics are known to be sensitive to pH variations, mechanical stress and degraded by digestive enzymes. Currently, they represent the main driving force in functional food design, in order to provide health benefits to the human microbiota. Probiotics need to survive to food processes, storage and food digestion to increase the population of the

intestinal flora. Their encapsulation into edible carriers has been demonstrated to increase their bioavailability [43]. However, gentle microencapsulation approaches are required, like extrusion techniques and freeze-drying. Typical coating agents are protein isolates, skim milk powder, Arabic gum, alginate, modified starch and maltodextrins [46, 65, 66]. Another main application of microencapsulation is to preserve volatile organic flavours, which are usually expensive. Aroma are covered with protective coatings to reduce their evaporation rate, prevent chemical reactions, like oxidation and flavour-flavour interactions, or migration into the food itself [67, 68]. Spray-drying and spray-chilling are the mainly used methods to load carrier particles usually made of mono- and disaccharides, maltodextrins, Arabic gum, proteins and gelatin with flavours [67]. The ultimate goal of flavours encapsulation is to control their release and to improve their stability during processing and consumption. As previously said, it can also be used to mask unpleasant aroma and tastes, such as bitter and astringent tastes of some polyphenols, like tannins, which have a high antioxidant activity in human body [43].

2.3.4 Encapsulation efficiency

Encapsulation efficiency (EE) is defined as the weight of active, W_t, incorporated in the matrix, over the initial weight of active, W_i, introduced during material preparation [69]. EE is calculated using Equation 2.2:

$$EE = (W_t/W_i) \times 100 \qquad \text{(Equation 2.2)}$$

EE of particles dispersed in a liquid phase is generally determined by analysing the active concentration in the liquid phase itself. An appropriate analytical technique, depending on the used active, e.g. UV-Vis, IR, HPLC or titration, is used after separating the liquid phase from particles via centrifugation, dialysis or filtration. By knowing the active concentration in the liquid phase is possible to back calculate the encapsulated fraction W_t by knowing W_i [69]. EE into microparticles is usually affected by several factors, e.g. polymer concentration and its solubility in the used solvent, the polymer/continuous phase ratio, active solubility in the continuous phase, active-polymer interactions and active/polymer ratios [70].

2.3.5 Release

Active release is the ultimate goal of encapsulation. In this step, the encapsulated active is unloaded from the matrix, in order to display its functional/biological effect. Controlled

release is defined as a method by which active ingredients become available at a desired site and/or at a specific time/rate [67]. Controlled release can be obtained using several triggers: active diffusion through the matrix, matrix degradation, matrix swelling and osmotic pressure are the most common approaches [71]. The release of actives from the formulation core can be divided into several steps, depending on the type of release system: active diffusion within the core, active dissolution/partitioning between the core and the matrix, diffusion through the matrix, transport into the bulk substrate away from the matrix [72]. If the release rate-limiting step is the diffusion through the wall of the capsule, the release rate from the core can be adjusted, changing the coating film thickness, its contact surface with the release medium and/or the permeability of the film [71]. Another case involves matrix degradation or erosion: the active is dispersed homogeneously within the matrix and its release is obtained during matrix erosion [67]. However, the surface area exposed to the release environment decreases with time, resulting in a decreased release rate overtime. This issue can be overcome by loading a higher active concentration in the interior layers than in the surface ones, or by changing the polymer matrix so that its erosion rate is slower initially and it increases overtime [71]. Release can also be controlled by matrix swelling when the active is unable to diffuse to a significant rate through the matrix. In this case, by selecting an appropriate matrix compatible with the release medium, its swelling is obtained, allowing the active diffusion into the release medium and its migration outside the particle. In swelling systems, the matrix changes from a solid moiety to a gel-like one upon fluid absorption. Polymer chains in this state have a higher mobility if compared to the solid state, allowing a faster active diffusion [20]. In reality, the active release can be due to a combination of diffusion, erosion and swelling behaviours. Another release method is applied in osmotic pressure-controlled systems. The active agent is loaded within a polymeric membrane selectively permeable to water, that present a small orifice on its surface. When water permeates through the membrane, if the active is highly water-soluble, a large osmotic pressure is generated and the active is released when the osmotic pressure become higher than the maximum force that the membrane can tolerate [71]. Ideally, the release of active should be site-specific or time-specific, and it can start by changes in temperature, pH, osmotic pressure or due to the presence of a specific solvent [71].

2.3.5.1 Release modelling

In vitro experiments are conducted on active loaded formulations to study their release behaviour under specific conditions and to design the best formulation for a specific application. Therefore, it is essential to analyse their overtime release data to elucidate the release mechanisms involved at molecular level and understand their structure-function relationship. Mathematical models can help to analyse release data and understand release mechanisms. In general, active diffusion, matrix swelling and matrix degradation are the main driving forces of active release from polymer matrices [72]. Mathematical models have been developed to describe actives release based on each of these mechanisms and by fitting experimental data into these models it is possible to clarify the specific release mechanism of a specific formulation. Release involves multiple steps, e.g. solvent moving towards the matrix interface, adsorption at the liquid-solid interface and back diffusion of active molecules toward the bulk solution, making difficult to produce a mathematical model able to describe the whole process [72]. During the years, several models have been developed to describe release phenomena from erodible-polymer systems (e.g. Hopfenberg's model), polymer-dissolution systems (e.g. Narasimhan-Peppas's model), and diffusion-controlled systems [72]. One of the most widely used models to describe release phenomena mainly due to a drug diffusion mechanism is the Korsemeyer-Peppas model [73]. This model is a simple relationship that described drug release from a polymeric system. To find the mechanism of drug release, the first 60% drug release data are usually fitted into Equation 2.3:

$$\frac{M_t}{M_\infty} = k\mathrm{t}^n \qquad \text{(Equation 2.3)}$$

where M_t and M_∞ are respectively the cumulative amount of active released at time *t* and at infinite time (complete release). The *n* value is related to the release mechanism. As reported by Korsmeyer *et al.* (1983), n=0.5 is related to a pure diffusion mechanism (Fickian diffusion), n=1 is related to polymer swelling-controlled mechanism and $0.5<n<1$ is attributed to a mix of both mechanisms [74]: the closer the *n* value to 0.5 the higher the degree of drug release due to diffusion mechanism, the closer to 1 the higher the degree due to polymer swelling. The *k* parameter is characteristic of each drug-matrix system and can be useful to understand potential interactions between the active and the formulation [74]. Several simultaneous processes are considered within this model, like diffusion of solvent in the matrix, diffusion

of active out of the formulation and dissolution of the matrix [73]. This model can provide a good description of active released due to diffusion and matrix-swelling mechanisms, but it is less accurate for matrix degradation mechanism or when a combination of diffusion and matrix erosion happens [73].

2.4 References

1. Omidian, H. and K. Park, *Introduction to Hydrogels*. Biomedical applications of hydrogels handbook. Springer, New York, 2010. p. 1-16.
2. Saha, D. and S. Bhattacharya, *Hydrocolloids as thickening and gelling agents in food: A critical review*. Vol. 47. 2010. 587-97.
3. Redaelli, F., M. Sorbona, and F. Rossi, *Synthesis and processing of hydrogels for medical applications*, in *Bioresorbable Polymers for Biomedical Applications*. 2017, Elsevier. p. 205-228.
4. Burey, P., et al., *Hydrocolloid Gel Particles: Formation, Characterization, and Application.* Critical Reviews in Food Science and Nutrition, 2008. **48**(5): p. 361-377.
5. Clark, A.H., *Biopolymer gels.* Current Opinion in Colloid & Interface Science, 1996. **1**(6): p. 712-717.
6. Saha, D. and S. Bhattacharya, *Hydrocolloids as thickening and gelling agents in food: A critical review.* Journal of food science and technology, 2010. **47**: p. 587-97.
7. Gopinath, V., et al., *A review of natural polysaccharides for drug delivery applications: Special focus on cellulose, starch and glycogen.* Biomedicine & Pharmacotherapy, 2018. **107**: p. 96-108.
8. Yong Lee, K. and D. J Mooney, *Alginate: Properties and biomedical applications*. Vol. 37. 2012. 106-126.
9. Pawar, S.N. and K.J. Edgar, *Alginate derivatization: A review of chemistry, properties and applications.* Biomaterials, 2012. **33**(11): p. 3279-3305.
10. George, M. and T.E. Abraham, *Polyionic hydrocolloids for the intestinal delivery of protein drugs: Alginate and chitosan — a review.* Journal of Controlled Release, 2006. **114**(1): p. 1-14.
11. Goff, H.D. and Q. Guo, *The Role of Hydrocolloids in the Development of Food Structure.* Handbook of Food Structure Development, 2019: p. 1-28.
12. Fernández Farrés, I., R.J.A. Moakes, and I.T. Norton, *Designing biopolymer fluid gels: A microstructural approach.* Food Hydrocolloids, 2014. **42**: p. 362-372.
13. Gouin, S., *Microencapsulation: industrial appraisal of existing technologies and trends.* Trends in Food Science & Technology, 2004. **15**(7): p. 330-347.
14. Norton, Jarvis, and Foster, *A molecular model for the formation and properties of fluid gels.* International Journal of Biological Macromolecules, 1999. **26**(4): p. 255-261.
15. Wolf, B., W.J. Frith, and I.T. Norton, *Influence of gelation on particle shape in sheared biopolymer blends.* Journal of Rheology, 2001. **45**(5): p. 1141-1157.
16. Murakata, T., et al., *Control of particle size of calcium alginate gel bead by application of electric field to interface between aqueous and organic phases.* Journal of chemical engineering of Japan, 2001. **34**(3): p. 299-305.

17. Reis, C.P., et al., *Review and current status of emulsion/dispersion technology using an internal gelation process for the design of alginate particles.* Journal of microencapsulation, 2006. **23**(3): p. 245-257.
18. Bhandari, B., *Spray drying and powder properties.* Food drying science and technology: Microbiology, chemistry, applications, 2008: p. 215-249.
19. Sosnik, A. and K.P. Seremeta, *Advantages and challenges of the spray-drying technology for the production of pure drug particles and drug-loaded polymeric carriers.* Advances in Colloid and Interface Science, 2015. **223**: p. 40-54.
20. Gibbs, F., et al., *Encapsulation in the food industry: a review.* International Journal of Food Sciences and Nutrition, 1999. **50**(3): p. 213-224.
21. Malone, M.E., I.A.M. Appelqvist, and I.T. Norton, *Oral behaviour of food hydrocolloids and emulsions. Part 1. Lubrication and deposition considerations.* Food Hydrocolloids, 2003. **17**(6): p. 763-773.
22. Wolf, B., et al., *Shear behaviour of biopolymer suspensions with spheroidal and cylindrical particles.* Rheologica Acta, 2001. **40**(3): p. 238-247.
23. Ellis, A.L., et al., *Stabilisation of foams by agar gel particles.* Food Hydrocolloids, 2017. **73**: p. 222-228.
24. Garrec, D.A., B. Guthrie, and I.T. Norton, *Kappa carrageenan fluid gel material properties. Part 1: Rheology.* Food Hydrocolloids, 2013. **33**(1): p. 151-159.
25. Gabriele, A., F. Spyropoulos, and I.T. Norton, *Kinetic study of fluid gel formation and viscoelastic response with kappa-carrageenan.* Food Hydrocolloids, 2009. **23**(8): p. 2054-2061.
26. de Carvalho, W. and M. Djabourov, *Physical gelation under shear for gelatin gels.* Rheologica Acta, 1997. **36**(6): p. 591-609.
27. Fernández Farrés, I., M. Douaire, and I.T. Norton, *Rheology and tribological properties of Ca-alginate fluid gels produced by diffusion-controlled method.* Food Hydrocolloids, 2013. **32**(1): p. 115-122.
28. Gabriele, A., *Fluid Gels: formation, production and lubrication*, U.o. Birmingham, Editor. 2011.
29. Moakes, R., A. Sullo, and I. Norton, *Preparation and rheological properties of whey protein emulsion fluid gels.* RSC advances, 2015. **5**(75): p. 60786-60795.
30. Gladkowska-Balewicz, I., I.T. Norton, and I.E. Hamilton, *Effect of process conditions, and component concentrations on the viscosity of κ-carrageenan and pregelatinised cross-linked waxy maize starch mixed fluid gels.* Food Hydrocolloids, 2014. **42**: p. 355-361.
31. Fernández Farrés, I. and I.T. Norton, *Formation kinetics and rheology of alginate fluid gels produced by in-situ calcium release.* Food Hydrocolloids, 2014. **40**: p. 76-84.
32. Gładkowska-Balewicz, I., *Mixed fluid gels formation, structure and rheological properties*. 2017, University of Birmingham.
33. Garrec, D.A. and I.T. Norton, *Understanding fluid gel formation and properties.* Journal of Food Engineering, 2012. **112**(3): p. 175-182.
34. Prakash, S., D.D.Y. Tan, and J. Chen, *Applications of tribology in studying food oral processing and texture perception.* Food Research International, 2013. **54**(2): p. 1627-1635.
35. Fernández Farrés, I. and I.T. Norton, *The influence of co-solutes on tribology of agar fluid gels.* Food Hydrocolloids, 2015. **45**: p. 186-195.

36. Garrec, D.A. and I.T. Norton, *Kappa carrageenan fluid gel material properties. Part 2: Tribology.* Food Hydrocolloids, 2013. **33**(1): p. 160-167.
37. Angiolillo, L., M.A. Del Nobile, and A. Conte, *The extraction of bioactive compounds from food residues using microwaves.* Current Opinion in Food Science, 2015. **5**: p. 93-98.
38. Kalra, E., *Nutraceutical -Definition and Introduction*. Vol. 5. 2003. E25.
39. Munin, A. and F. Edwards-Lévy, *Encapsulation of Natural Polyphenolic Compounds; a Review*. Vol. 3. 2011. 793-829.
40. Davidov-Pardo, G. and D.J. McClements, *Resveratrol encapsulation: Designing delivery systems to overcome solubility, stability and bioavailability issues.* Trends in Food Science & Technology, 2014. **38**(2): p. 88-103.
41. Joye, I.J., G. Davidov-Pardo, and D.J. McClements, *Nanotechnology for increased micronutrient bioavailability.* Trends in Food Science & Technology, 2014. **40**(2): p. 168-182.
42. Tiwari, D.G., et al., *Drug delivery systems: An updated review*. Vol. 2. 2012. 2-11.
43. Nedovic, V., et al., *An overview of encapsulation technologies for food applications.* Procedia Food Science, 2011. **1**: p. 1806-1815.
44. Whitton, C., et al., *National Diet and Nutrition Survey: UK food consumption and nutrient intakes from the first year of the rolling programme and comparisons with previous surveys.* The British journal of nutrition, 2011. **106**(12): p. 1899-1914.
45. Lesmes, U. and D.J. McClements, *Structure–function relationships to guide rational design and fabrication of particulate food delivery systems.* Trends in Food Science & Technology, 2009. **20**(10): p. 448-457.
46. Zuidam, N. and V. Nedovic, *Encapsulation Technologies for Active Food Ingredients and Food Processing*. 2010.
47. Raybaudi-Massilia, R.M. and J. Mosqueda-Melgar, *Polysaccharides as carriers and protectors of additives and bioactive compounds in foods.* The complex word of polysacharides. Editorial InTech, Rijeka, Croacia. Cap, 2012. **16**: p. 429-53.
48. Wandrey, C., A. Bartkowiak, and S.E. Harding, *Materials for encapsulation*, in *Encapsulation technologies for active food ingredients and food processing*. 2010, Springer. p. 31-100.
49. Alvarez-Lorenzo, C., et al., *Crosslinked ionic polysaccharides for stimuli-sensitive drug delivery.* Advanced Drug Delivery Reviews, 2013. **65**(9): p. 1148-1171.
50. Agüero, L., et al., *Preparation and characterization of pH-sensitive microparticles based on polyelectrolyte complexes for antibiotic delivery.* Polymer Engineering & Science, 2015. **55**(5): p. 981-987.
51. Agüero, L., et al., *Alginate microparticles as oral colon drug delivery device: A review.* Carbohydrate Polymers, 2017. **168**: p. 32-43.
52. Dong, Q.Y., et al., *Alginate-based and protein-based materials for probiotics encapsulation: A review.* International Journal of Food Science & Technology, 2013. **48**.
53. Ching, S.H., N. Bansal, and B. Bhandari, *Alginate gel particles–A review of production techniques and physical properties.* Critical Reviews in Food Science and Nutrition, 2017. **57**(6): p. 1133-1152.
54. McClements, D., E.A. Decker, and J. Weiss, *Emulsion-Based Delivery Systems for Lipophilic Bioactive Components.* Journal of Food Science, 2007. **72**: p. R109-R124.

55. Serdaroglu, M., A. Kara, and B. Öztürk Kerimoğlu, *Multiple emulsions and their applications in food*. 2013.
56. Rezvankhah, A., Z. Emam-Djomeh, and G. Askari, *Encapsulation and delivery of bioactive compounds using spray and freeze-drying techniques: A review.* Drying Technology, 2020. **38**(1-2): p. 235-258.
57. Achinna, P. and A. Kuna, *Microencapsulation technology: A review.* J Res Angrau, 2010. **38**.
58. Singh, M.N., et al., *Microencapsulation: A promising technique for controlled drug delivery.* Research in pharmaceutical sciences, 2010. **5**(2): p. 65-77.
59. Edwards, W.P., *Sweets and candies | Sugar Confectionery*, in *Encyclopedia of Food Sciences and Nutrition (Second Edition)*, B. Caballero, Editor. 2003, Academic Press: Oxford. p. 5703-5710.
60. Ozkan, G., et al., *A review of microencapsulation methods for food antioxidants: Principles, advantages, drawbacks and applications.* Food Chemistry, 2019. **272**: p. 494-506.
61. Desai, K.G.H. and H. Jin Park, *Recent Developments in Microencapsulation of Food Ingredients.* Drying Technology, 2005. **23**(7): p. 1361-1394.
62. Tanaka, H., M. Matsumura, and I. Veliky, *Diffusion characteristics of substrates in Ca-alginate gel beads.* Biotechnology and bioengineering, 1984. **26**(1): p. 53-58.
63. Hariyadi, D., et al., *Diffusion loading and drug delivery characteristics of alginate gel microparticles produced by a novel impinging aerosols method.* Journal of drug targeting, 2010. **18**: p. 831-41.
64. Mahdi, M.H., Conway, B.R., Smith, A.M., *Evaluation of gellan gum fluid gels as modified release oral liquids*. International Journal of Pharmaceutics, 2014. **475**(1–2): 335-343.
65. Fang, Z. and B. Bhandari, *Encapsulation of polyphenols – a review.* Trends in Food Science & Technology, 2010. **21**(10): p. 510-523.
66. de Vos, P., et al., *Encapsulation for preservation of functionality and targeted delivery of bioactive food components.* International Dairy Journal, 2010. **20**(4): p. 292-302.
67. Madene, A., et al., *Flavour Encapsulation and Controlled Release - a Review.* International Journal of Food Science & Technology, 2006. **41**: p. 1-21.
68. Roos, K., *Effect of texture and microstructure on flavor retention and release.* International Dairy Journal, 2003. **13**: p. 593-605.
69. Piacentini, E., *Encapsulation Efficiency*, in *Encyclopedia of Membranes*, E. Drioli and L. Giorno, Editors. 2016, Springer Berlin Heidelberg: Berlin, Heidelberg. p. 706-707.
70. Jyothi, N., et al., *Microencapsulation Techniques, Factors Influencing Encapsulation Efficiency: A Review.* The Internet Journal of Nanotechnology, 2008. **3**: p. 187-197.
71. Pothakamury, U.R. and G.V. Barbosa-Cánovas, *Fundamental aspects of controlled release in foods.* Trends in Food Science & Technology, 1995. **6**(12): p. 397-406.
72. Fu, Y. and W.J. Kao, *Drug release kinetics and transport mechanisms of non-degradable and degradable polymeric delivery systems.* Expert opinion on drug delivery, 2010. **7**(4): p. 429-444.
73. Singhvi, G. and M. Singh, *In-vitro drug release characterization models.* International Journal of Pharmaceutical Studies and Research, 2011. **2**(1): p. 77-84.
74. Korsmeyer, R.W., et al., *Mechanisms of solute release from porous hydrophilic polymers.* International Journal of Pharmaceutics, 1983. **15**(1): p. 25-35.

Chapter 3: BLANK ALGINATE FLUID GELS

Abstract

The aim of this chapter was to study the formation process of Alginate Fluid Gel (AFG) in a pin-stirrer vessel. The pin-stirrer was employed as an easy scalable method to provide shear to the gelling alginate (ALG) and, therefore, obtain a flowable gel structure. Firstly, it was investigated the influence of the AFG formulation, i.e. ALG and $CaCl_2$ concentrations. Then, it was assessed the effects of pin-stirrer process parameters, specifically the shear rate, the residence time and the diameter of the needle used to inject the $CaCl_2$ stream into the device. The obtained materials were analysed in terms of particle size distribution (PSD) and viscosity behaviour. The ALG/$CaCl_2$ ratio, used during AFG production, revealed to be responsible for the final particle dimensions, while the ALG concentration was responsible for the final viscosity. On the contrary, the pin-stirrer process parameters did not influence the PSD and/or the viscosity behaviour. This was done in order to better understand the formation mechanism of AFG and its final properties in order to properly design future encapsulation experiments of model actives in these materials.

3.1 Introduction

Fluid gels are formed by applying shear to a biopolymer solution undergoing gelation. The formation and properties of these materials have been largely investigated using both thermal and ionic gelled biopolymers. For thermally produced fluid gels, different microstructures can be obtained with minor changes to processing parameters while using the same biopolymer. For example, Gabriele *et al.* (2009) showed that κ-carrageenan fluid gels produced big and irregular shaped particles when low shear rates were used during gelation, while small and spherical ones were obtained when high shear rates were employed [1]. Also, for ionically-gelled biopolymers similar studies were conducted; for example, Farrés *et al.* investigated the effect of changing the ALG concentration of AFG, on their particle sizes and tribological properties [2, 3]. The formation of bigger particles was observed when decreasing the ALG concentration, which was explained as a result of the lower shear stress applied on the forming particles because of the reduced viscosity of the system [3]. In addition,

they stated that Ca^{2+} ions were able to diffuse throughout the sample at a higher rate, because of the less viscous matrix. They concluded that particles were formed as a result of two competing processes: the network formation due to the Ca^{2+} crosslinking of ALG chains and the shear induced break-up process of clusters formed. However, the authors said that the method presented the limitation of a poor control on the competing parameters of mixing and gelation because the shear regime inside the stirring vessel was not uniform. Particles sizes were evaluated via optical microscopy and they were not homogeneous in dimensions, ranging from 3-9.5 µm. In another study, Farrés *et al.* (2014) studied more in depth the properties of AFG produced using a rheometer to provide a more homogeneous shear environment, via *in-situ* Ca^{2+} release [4]. Different ALG and Ca^{2+} concentrations and different applied shear rates were studied. They concluded that by increasing the shear rate, during fluid gels preparation, a higher number of particles was obtained, but this did not change the final viscosity of the system. More significantly, it was highlighted that the kinetics of fluid gel formation were strongly influenced by the ALG molecular weight and by the used concentration of Ca^{2+} ions. However, production of AFG within a rheometer has obvious limitations in terms of industrial relevance and applicability.

Within this work, AFG were produced using a pin-stirrer vessel, in order to use a more industrially feasible approach for their production. Overall, the effect of several pin-stirrer process parameters and of some constituents' concentrations on the final properties of AFG were not previously investigated, e.g. the effect of changing the $CaCl_2$ concentration, the shaft speed and the residence time within the vessel. As reported by Lee *et al.* (2012), Ca^{2+} ions bind solely to G-blocks of ALG polymer chains to form the "egg-box" cross-linked structure [5]. Therefore, the use of a proper $CaCl_2$/ALG ratio is essential for the formation of a fully crosslinked network.

The aim of this chapter is to better understand the effects of process parameters, used during AFG production, on the final properties of these materials. It was investigated the effect of changing the used $CaCl_2$/ALG ratio, the applied shear regime, the residence time and the needle diameter used to inject the $CaCl_2$ stream on the final particle sizes and viscosity properties of AFG. It was concluded that the final particle dimensions changed as a function of the used $CaCl_2$/ALG ratio, while the ALG concentration affected the final viscosity of the material. All the other parameters tested did not influence the final properties of AFG.

3.2 Materials and methods

3.2.1 Materials

Sodium alginate was purchased from Sigma-Aldrich® (CAS: 9005-38-3, W201502, lot.# MKBT7870V, Sigma–Aldrich Company Ltd., Dorset, UK). Calcium chloride ($CaCl_2$, anhydrous, 93%) was purchased from Alfa Aesar™ [6]. All materials were used without further purification. Milli-Q distilled water was used for all water-based preparations and it was produced using an Elix® 5 distillation apparatus (Millipore®, USA). Concentrations of all materials are given as percentages of the weight of the specific substance over the total weight of the system in which it is contained (i.e. solution, fluid gel formulation, etc.) and are reported as '% w/w'.

3.2.2 Pin-stirrer production

AFG were produced into a jacked pin-stirrer device, which is schematically represented in Figure 2.2., using the following procedure [2]. Firstly, a 2% w/w ALG solution was prepared, unless otherwise specified, by dissolving the required amount of ALG in distilled water at 95 °C for 45 min under stirring to ensure complete powder dissolution. Thereafter, the solution was left to cool down to room temperature. A separate aqueous solution of $CaCl_2$ was also prepared by dissolving the required amount $CaCl_2$ at room temperature under magnetic stirring. AFG were formed using a pin-stirrer vessel (Het Stempel, NL) which has an available processing volume of 150 mL, 16 pins placed on the rotating shaft and 16 pins fixed on the internal wall. A pin-shaft speed of 1000 RPM was normally used for AFG preparations, unless otherwise stated, and it could not be increased over 2000 RPM due to equipment limitations. The ALG solution was pumped into the pin-stirrer using a peristaltic pump (Masterflex L/S Peristaltic, DE) at a rate of 33 mL/min, unless otherwise specified. The $CaCl_2$ solution was injected into the pin-stirrer, through a stainless steel needle of 1.25 mm internal diameter, unless otherwise specified, using a syringe pump (Cole-Parmer Single-syringe, USA) at a rate of 4.02 mL/min, unless otherwise specified. The residence time of AFG within the pin-stirrer could not be lower than 2.5 min, due to pumps limitations, as they were not able to generate flowrates higher enough to produce a shorter residence time.

3.2.3 Rheological measurements

The rheological properties of fluid gels were determined by shear viscosity tests using a rotational rheometer (Kinexus™, Malvern®, UK) equipped with a 40 mm diameter sand blasted plate geometry. The analyses were carried out at 25 °C using a shear rate ramp between 0.01 and 100 s^{-1} and a gap of 300 μm. All measurements were carried out in triplicate and all data are presented/plotted as the mean value± the standard deviation (SD). In order to assess bulk viscoelasticity, the shear viscosity profiles of all AFG formulations were fitted to a simple power-law model, reported in Equation (3.1) [7]:

$$\eta = K\,\dot{\gamma}^{\,n-1} \qquad \text{(Equation 3.1)}$$

where *K* is the consistency constant and *n* is the power-law index.

3.2.4 Particle size analysis

3.2.4.1 Mastersizer

The particle size distribution (PSD) of fluid gels was evaluated using laser diffraction (Mastersizer-2000, Malvern®, UK). Few drops of sample were placed into the mixing chamber of the instrument and were mixed for 10 min at 1300 RPM before performing the analysis. PSD was evaluated as numerical particle size percentage by the Mastersizer software, using a refractive index of 1,335. $D_{3,2}$ diameter, also known as Surface Weighed Mean, and Span values were calculated by Mastersizer software. All measurements were carried out in triplicate and all data are presented/plotted as the mean value± SD.

3.2.3.2 Dynamic Light Scattering

The PSD of fluid gels was also evaluated with Zetasizer (Malvern Instruments Ltd., UK) via Dynamic Light Scattering (DLS) analysis. Samples were diluted with water before analysis to yield a suitable scattering intensity and measured at 25 °C. PSD curves were evaluated as numerical particle sizes percentage. All measurements were performed at 25 °C in triplicate and all data are presented/plotted as the mean value± SD.

3.2.3.3 Optical microscopy

Optical microscope (DM 2500 LED, Leica®, CH) was used to observe and record alginate microparticles. Samples were, firstly, diluted with distilled water using a water to sample ratio of 10:1 and they were mixed using a vortex mixer (VM20, Rigal Bennet®, UK) for 20 seconds.

DIC settings were employed to increase the contrast, allowing the average dimensions of particles to be measured. Images were captured using a CCD camera (DFC450 C, Leica®, CH) coupled to the microscope. Image analysis software IPP (LAS 4.8.0, Leica®, CH) was used to evaluate the dimensions of the microparticles through the images.

3.3 Results

3.3.1 $CaCl_2$/ALG ratio

The effect of changing the $CaCl_2$ concentration on the formation of AFG was investigated. Initially, a 2% w/w ALG concentration was used, while the concentration of $CaCl_2$ was changed to 0.15%, 0.25% and 0.35% w/w, producing respectively samples AFG_2%_0.15%, AFG_2%_0.25% and AFG_2%_0.35%. PSD curves and microscope imaging of this materials are reported in Figure 3.1:

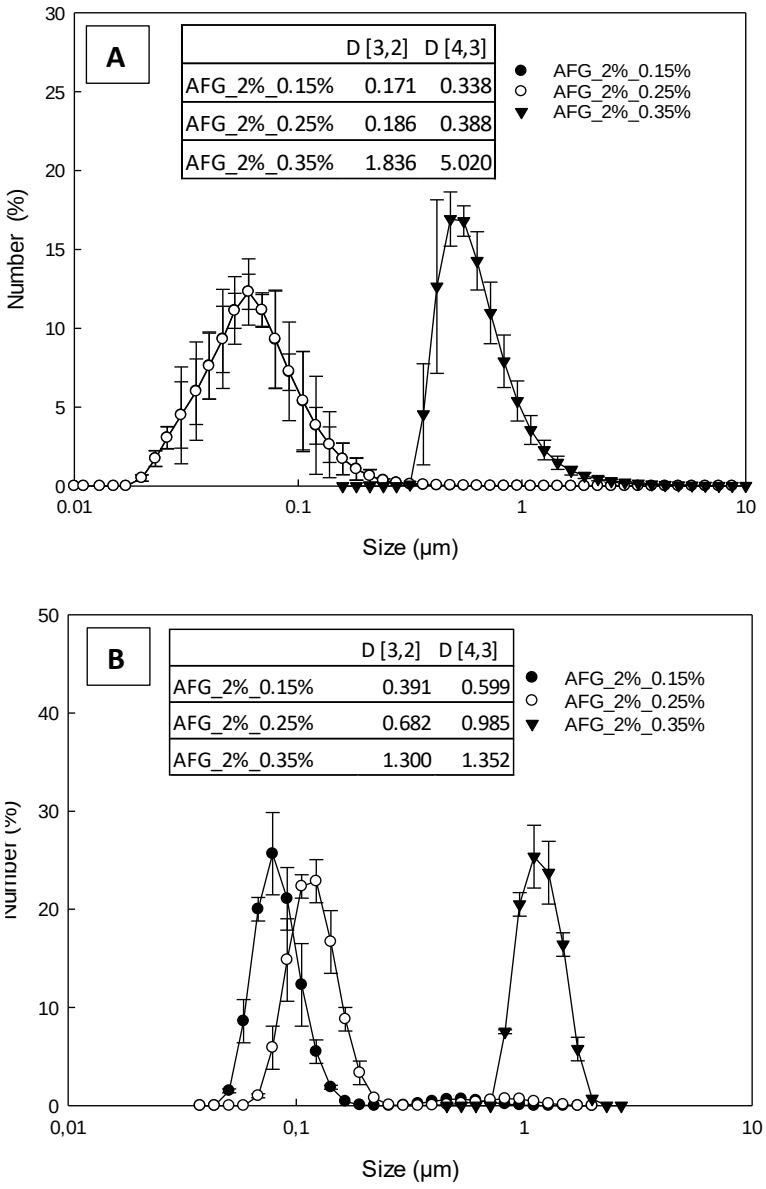

Figure 3. 1 - Particle sizes of AFG produced by using 2% ALG (w/w): (A) Light scattering (B) Laser diffraction (C) Optical microscopy of AFG_2%_0.35%. In Fig. A, AFG_2%_0.15% and AFG_2%_0.25% curves are perfectly overlapping.

PSD curves of AFG_2%_0.35% were in the range between 0.5 and 5 µm, while AFG_2%_0.15% and AFG_2%_0.25% were in the range between 0.02 µm and 0.2 µm. Particle dimensions were also studied using optical microscopy: due to their small dimensions particles in samples AFG_2%_0.15% and AFG_2%_0.25% could not be visualised using this imaging technique, while particles of AFG_2%_0.35% could be visualised, due to their micrometre dimensions, as can be seen in Figure 3.1.C. It is important to notice that the particle dimensions obtained using Mastersizer and DLS analyses were consistent one with the other. In addition, particles of AFG_2%_0.35%, observed using the optical microscope, presented similar dimensions to the size values obtained via Mastersizer and DLS analysis. These observations lead to the conclusion that particle dimensions can be determined using any of these techniques. For later analyses, particle sizes were evaluated only via Mastersizer, since this equipment was able to provide correct values of PSD of AFG, was easier to run and provide faster results in comparison to DLS and optical microscopy.

Four other AFG samples were produced using different percentages of ALG to identify the ratio between $CaCl_2$ and ALG necessary to obtain microparticles formation. ALG concentrations of 1% w/w were used together with a $CaCl_2$ concentration of 0.15% and 0.25% producing respectively samples AFG_1%_0.15% and AFG_1%_0.25%. ALG concentrations of 3% w/w were used together with a $CaCl_2$ concentration of 0.35% and 0.45% producing respectively samples AFG_3%_0.35% and AFG_3%_0.45%. PSD curves of these samples are reported in Figure 3.2:

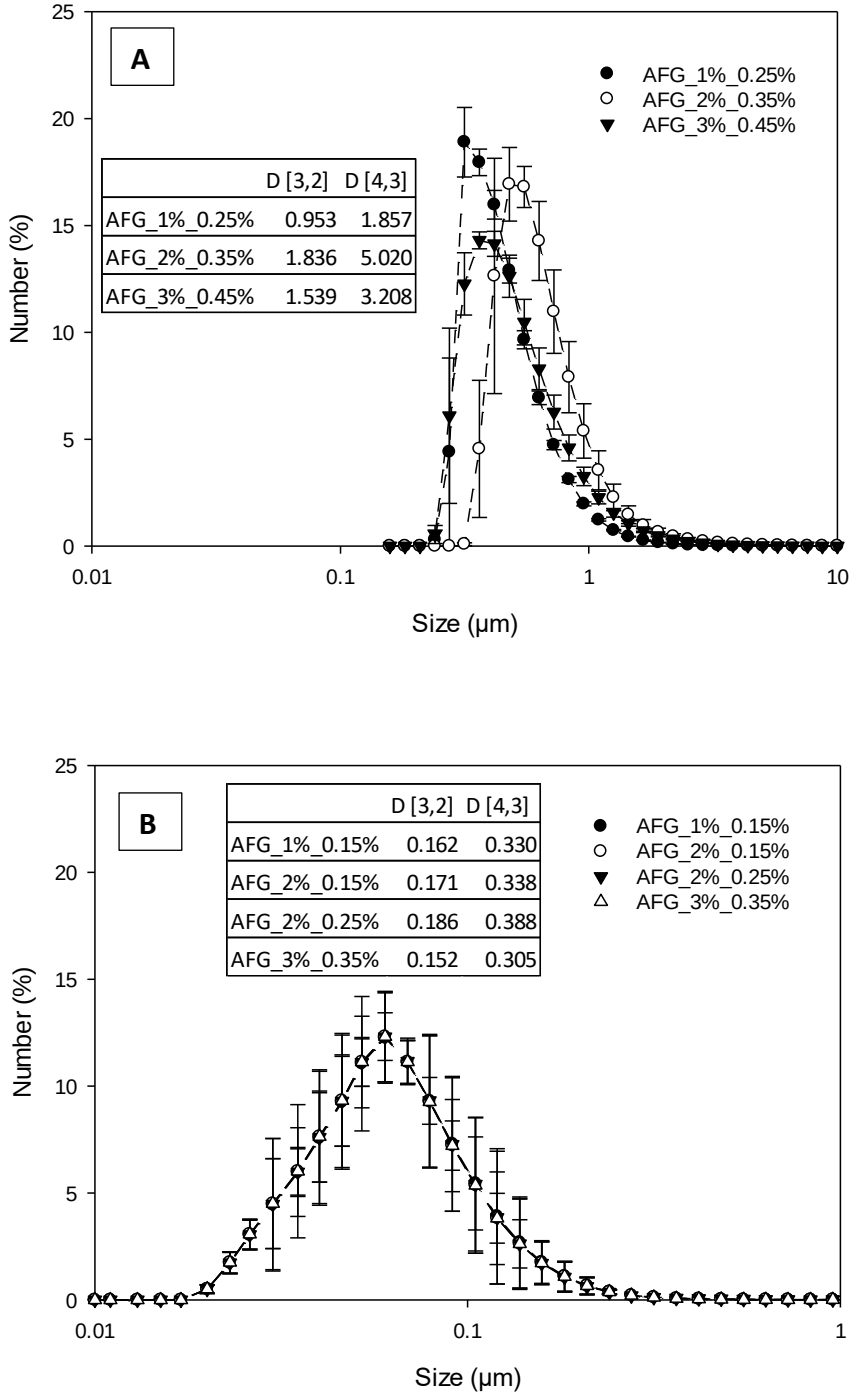

Figure 3. 2 - PSD curves of AFG produced by using 1% and 3% (w/w) ALG concentration: (A) Samples forming microparticles, (B) Samples forming nanoparticles

Mastersizer analyses revealed the formation of microparticles for samples AFG_1%_0.25% and AFG_3%_0.45%, while nanoparticles were detected for the samples AFG_1%_0.15% and AFG_3%_0.35%. These results showed that microparticles formation was achieved only when a critical ratio between ALG and $CaCl_2$ was used during sample preparation. The $CaCl_2$/ALG

ratios used for the preparation of samples that led to the formation of microparticles was considered for the estimation of this value, also with the ones used for samples preparation reported in later sections 3.3.2 Shear regime, 3.3.3 Residence time and 3.3.4 Effect of cross-sectional area of $CaCl_2$ injection. $D_{3,2}$ values of AFG as a function of their $CaCl_2$/ALG ratios are reported graphically in Figure 3.3. For the majority of AFG formulations a $CaCl_2$/ALG ratio higher than 0.150 led to the formation of microparticles. However, AFG samples made using a 1% w/w ALG concentration displayed the formation of nanoparticles when this ratio was used. In general, the ratio that led to the formation of microparticles was estimated to be around 0.155, and from now on this ratio will be called Critical Ratio for Microparticles Formation (CRMF).

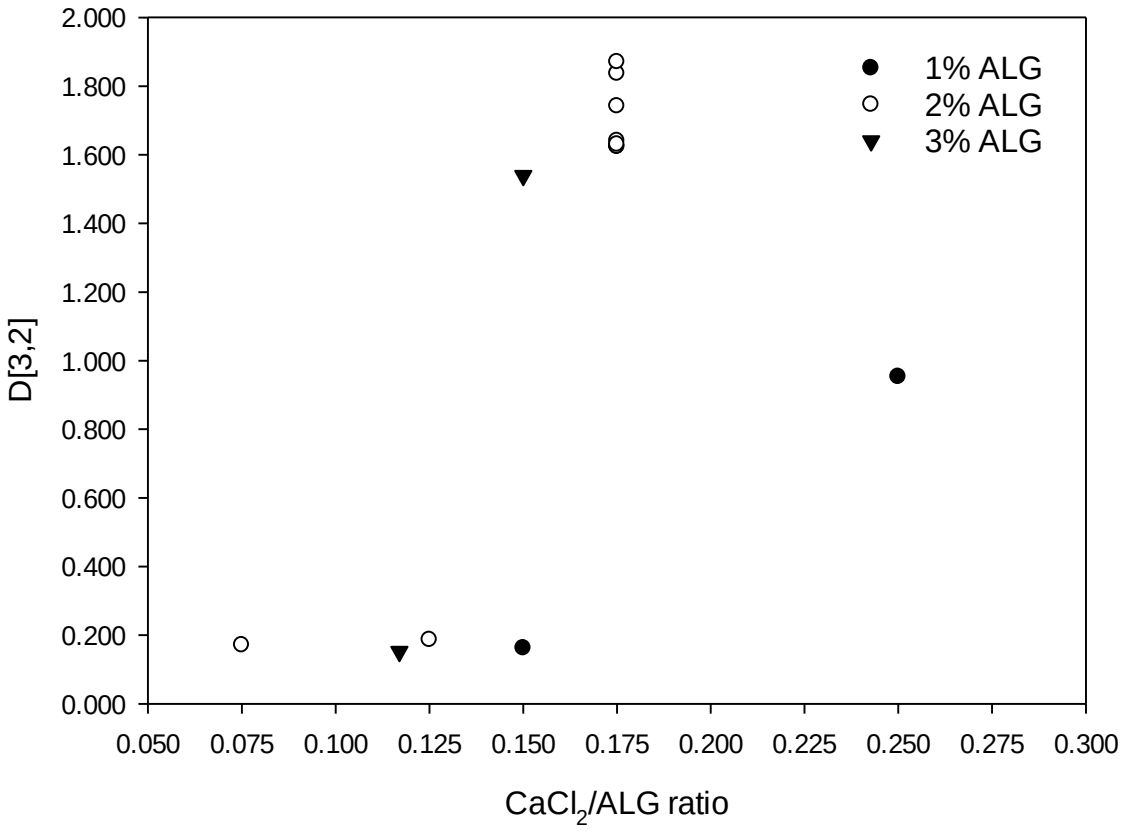

Figure 3. 3 – $D_{3,2}$ values of AFG particles as a function of $CaCl_2$/ALG ratios and ALG concentrations used for samples preparation

Viscosity analyses were conducted on AFG_2%_0.15%, AFG_2%_0.25% and AFG_2%_0.35% samples, to assess if the formation of microparticles affected in some way the final flow behaviour of AFG. Results are reported in Figure 3.4:

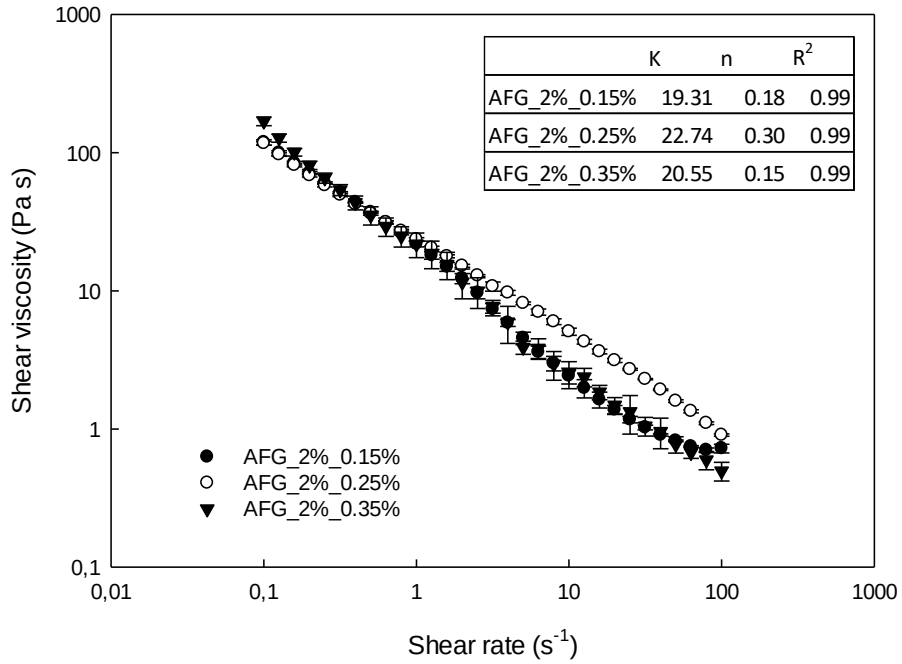

Figure 3. 4 - Effect of $CaCl_2$/ALG ratio on the viscosity of AFG

As can be seen from the above Figure, viscosity curves of samples AFG_2%_0.15%, AFG_2%_0.25% and AFG_2%_0.35% did not present different behaviours. It can be concluded that the flow behaviour of AFG was not dictated by the formation of micro/nanoparticles, but it was probably due to the concentration of ALG used during sample preparation. This was assessed by conducting similar viscosity analysis on samples AFG_1%_0.25% and AFG_3%_0.45%, which also consisted of microparticles. Results are reported in Figure 3.5:

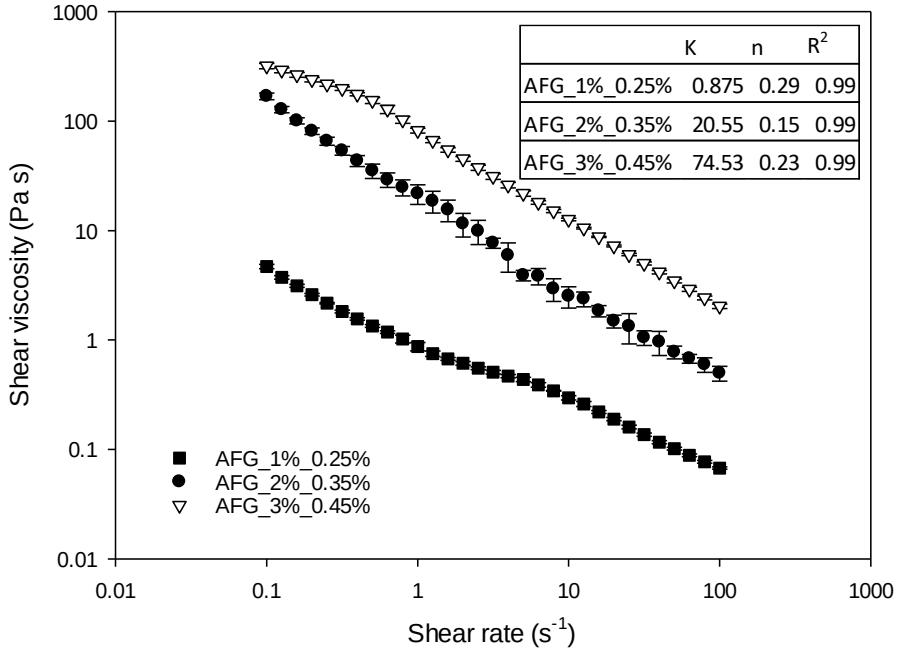

Figure 3. 5 - Effect of ALG concentration on the viscosity of AFG

Curves reported in Figure 3.5 clearly show that the increase of ALG concentration was responsible for an increase in viscosity, supporting the hypothesis that the flow behaviour of AFG was primarily dictated by ALG concentrations used during sample preparation.

3.3.2 Shear regime

The effect of changing the shear regime during AFG production in the pin-stirrer was investigated by producing samples with a 2% (w/w) ALG concentration and 0.35% (w/w) $CaCl_2$. These concentrations were selected in order to operate above the CRMF in order to obtain microparticles. The pin-stirrer shaft rotation was adjusted at 500, 1000, 1500 and 2000 RPM, producing respectively samples AFG_500, AFG_1000, AFG_1500 and AFG_2000. PSD and viscosity curves of these samples are reported, respectively, in Figure 3.6 and 3.7.

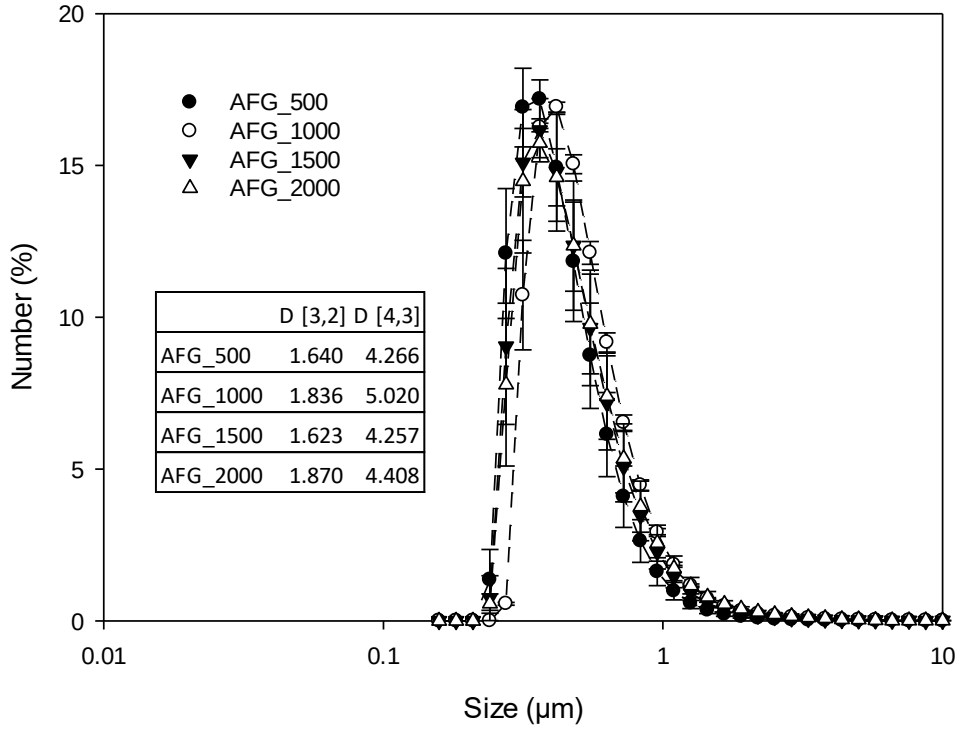

	D [3,2]	D [4,3]
AFG_500	1.640	4.266
AFG_1000	1.836	5.020
AFG_1500	1.623	4.257
AFG_2000	1.870	4.408

Figure 3. 6 - PSD curves of AFG at different shaft speeds

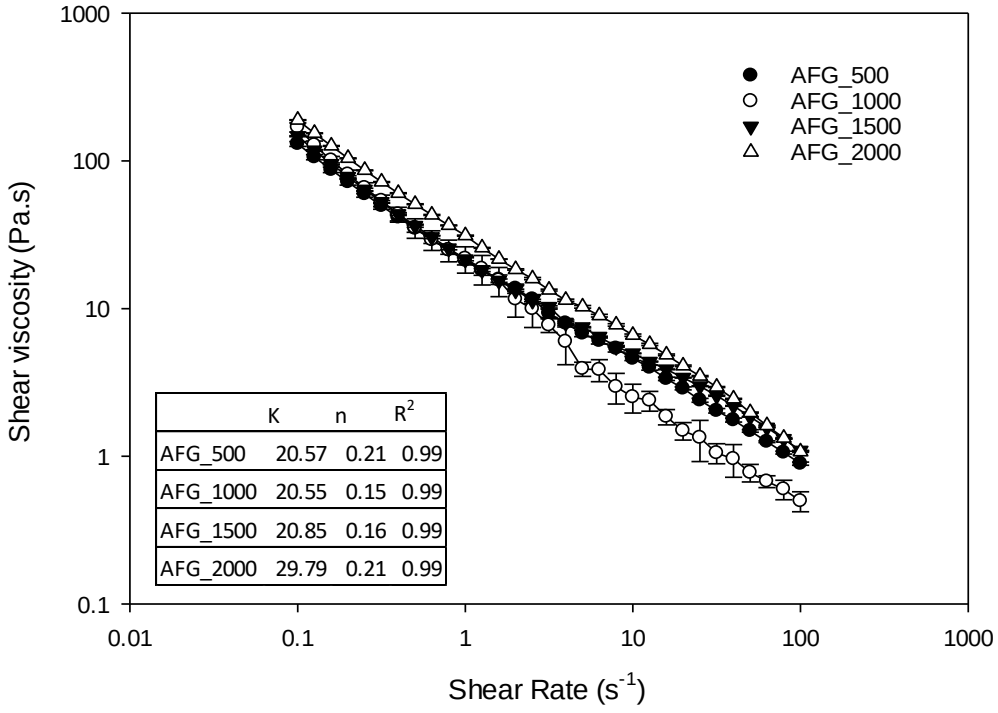

	K	n	R^2
AFG_500	20.57	0.21	0.99
AFG_1000	20.55	0.15	0.99
AFG_1500	20.85	0.16	0.99
AFG_2000	29.79	0.21	0.99

Figure 3. 7 - Effect of applied shear rate on the viscosity of AFG

As can be noticed the PSD curves were almost overlapping, revealing that the shaft speed did not affect AFG particle sizes. This is probably due to the fact that the formation of ALG particles is mainly dictated by the crosslinking of ALG chains. The shaft rotation provided the necessary shear for the formation of a fluid gel structure and not of a quiescent gel, i.e. a non-sheared gel. Experiments were also conducted using a shaft speed below 500 RPM, but this produced the formation of big clusters of ALG gel that blocked the out pipe of the pin-stirrer, leading inlet pumps to stop and to experiment failures. In conclusion, the shaft rotation did not contribute significantly to the AFG break up process, explaining why particles were not different in size. However, the magnitude of applied shear is fundamental to obtain the formation of a fluid gel structure, rather than a quiescent gel. In fact, a shaft speed rotation below 500 RPM produced the formation of big quiescent gel-like aggregates, which clogged up the pin-stirrer. In addition, viscosity analysis revealed that the final flow behaviour of AFG was not affected by the applied shear rate used during AFG production.

3.3.3 Residence time

The residence time of AFG in the pin-stirrer is dictated by the flowrates of the pumps used to inject the $CaCl_2$ and the ALG streams into the device. These were changed to assess the effect of changing the residence time on the final AFG properties. Pump flowrates were calculated knowing that the internal volume of the pin-stirrer was of 150 mL. Three different residence times were used to conduct this set of experiments, specifically 2.5min, 4 min and 8 min, which produced, respectively, samples AFG_2.5t, AFG_4t and AFG_8t. These samples were produced by fixing the ALG concentration at 2% (w/w) and the $CaCl_2$ concentration at 0.35% (w/w), in order to obtain the formation microparticles, and by using a shaft speed of 1000 RPM. Results of PSD and final viscosity are reported respectively in Figure 3.8 and 3.9.

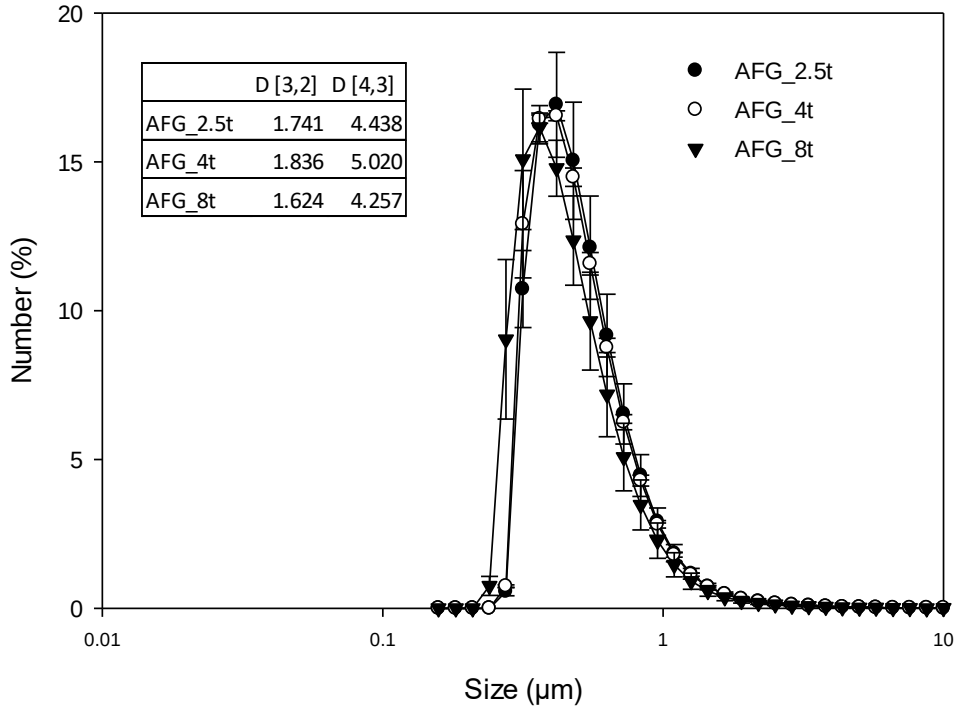

Figure 3. 8 - Effect of residence time in the pin-stirrer on the PSD of AFG

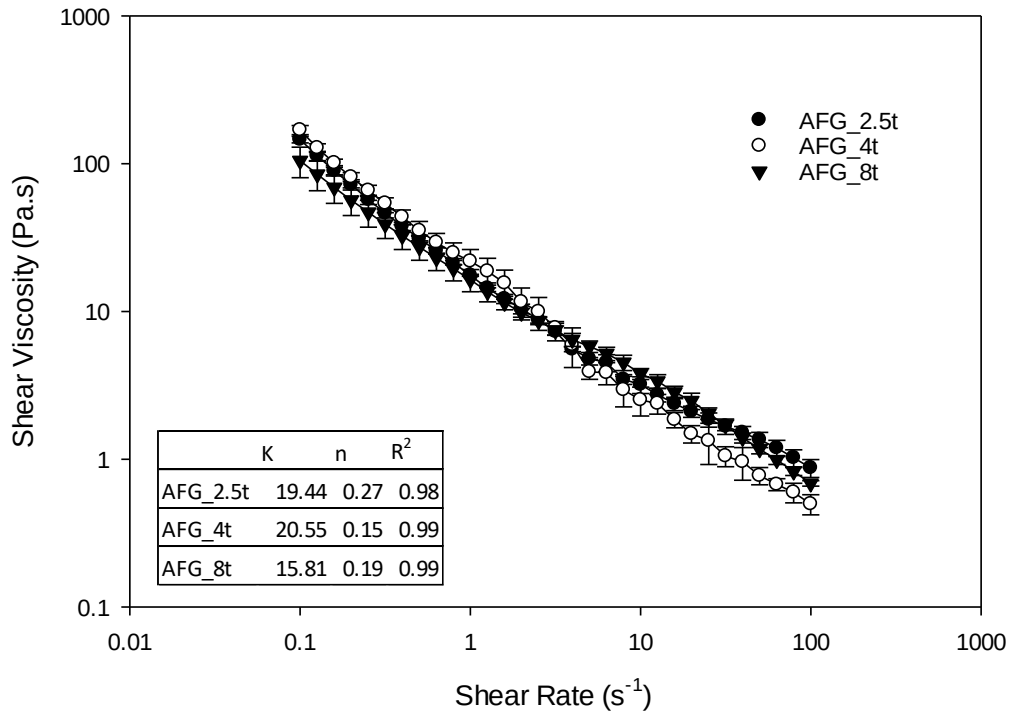

Figure 3. 9 - Effect of residence time in the pin-stirrer on the viscosity of AFG

As it is possible to notice both AFG viscosities and PSD were not influenced by the residence time used, at least within the interval between 2.5 and 8 min. It is possible to conclude that since the ALG gelation is a very fast process the residence time did not influence the particle dimensions. This confirmed that the breaking process of the gel structure, due to its exposure to the mixing environment, was not a significant process during AFG production. In fact, as previously reported in section 3.3.2 Shear regime, the magnitude of induced shear was fundamental to obtain the formation of a fluid gel structure and not the formation of a quiescent gel. On the contrary, the length of exposure to mixing did not change the final viscosity and/or particle sizes of AFG.

However, both the magnitude of applied shear and the length of exposure to mixing could affect other AFG properties, for example inter-particle interactions. Although the yield stress was not studied in this work, Gabriele *et al.* (2009) conducted a specific study on yield stress of κ-carrageenan fluid gels [1]. They reported that process parameters, specifically shear rate and cooling profile, used during fluid gel formation, changed the final particles size and the interactions between particles. In fact, yield stress phenomena were related to the formation of inter-particle interactions. These were formed during fluid gel formation and developed further overtime under rest conditions. Interactions between particles increased by increasing the cooling rate used during fluid gel formation. In addition, a higher shear rate used during fluid gel preparation reduced inter-particle interactions and, therefore, yield stress. Similar effects were reported by Farrés *et al.* (2014), when studying the yield stress of AFG; an increase of ALG concentration produced an increase of both particle phase volume and particle stiffness, enhancing inter-particle interactions [2]. Therefore, the applied shear regime and/or the residence time of AFG within the pin-stirrer could affect the material properties, such as inter-particle interactions, but this was investigated in the present study.

Overall, it can be stated that the AFG formation mechanism was mainly dictated by the Ca^{2+} ions presence, which were responsible for the formation of the first nuclei of gelation, while the shear regime was responsible for confining the gel growth in the region around these nuclei, as previously reported by de Carvalho and Djabourov [8]. In their study, the formation mechanism of gelatin fluid gels was described as a nucleation and growth process. These two processes were dictated by the gelation of gelatin, while shear regime blocked the growth of particles around the nuclei of gelation and did not allow the formation of an extended gel

network across the whole sample. The conclusion that the applied shear regime did not caused any particle disruption for AFG is in contrast to what reported by Garrec *et al.* [9]. They reported that κ-carrageenan particles grew after the formation of the gelation nuclei, due to the presence of the cooling environment, which promoted the gelation of the hydrocolloid. Particles grew only until the break-up process, caused by shaft rotation, started to occur. Therefore, the final particle dimensions of κ-carrageenan fluid gels could be controlled by changing the shear applied: the higher the shear, the lower the particle dimensions obtained. However, in the same paper, authors reported that it was not possible to control the shape of fluid gel particles when using agarose as hydrocolloid, due to its more rapid gelation mechanism of approx. 2–3 orders of magnitude faster than κ-carrageenan. They concluded that a fast gelation led to the growth of large anisotropic particles [9]. It is possible to conclude that since ALG gelation is almost instantaneous and faster than agarose, the effect of changing the residence time on the final particle dimensions is not relevant. As can be seen from Figure 3.9, the viscosity curves of AFG samples were almost overlapping, confirming that the final viscosity was not influenced by the residence time used during AFG production.

3.3.4 Effect of cross-sectional area of $CaCl_2$ injection

The effect of changing the internal diameter of the needle used to introduce $CaCl_2$ into the pin-stirrer was investigated. Two custom made stainless steel needles were used to perform this set of experiments. Both needles had the same length, in order not to change the injection distance of $CaCl_2$ from the rotating shaft. The internal diameters of the needles were 1.25 mm and 2.5 mm, producing, respectively, samples AFG_1.25 mm and AFG_2.5 mm. It is important to notice that the used $CaCl_2$ flowrate and the $CaCl_2$/ALG ratio used were identical in both samples; only the internal cross-sectional area of needles used to inject $CaCl_2$ changed. This was made in order to assess if an initial larger contact area between the $CaCl_2$ stream with the ALG stream could change the final properties of AFG, in particular the particles size. Samples were produced fixing the ALG concentration at 2% (w/w) and the $CaCl_2$ concentration at 0.35% (w/w), in order to obtain the formation of microparticles. The shaft speed and the residence time were fixed at 1000 RPM and 4 min. Results of final PSD and viscosities are reported, respectively, in Figure 3.10 and 3.11.

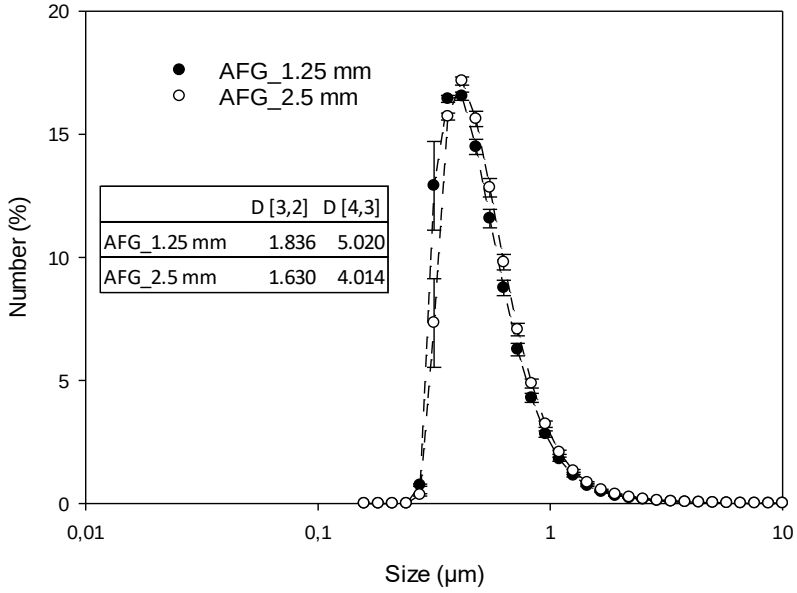

Figure 3. 10 - Effect of needle internal diameter, used for introducing the $CaCl_2$ stream in the pin-stirrer, on the PSD of AFG

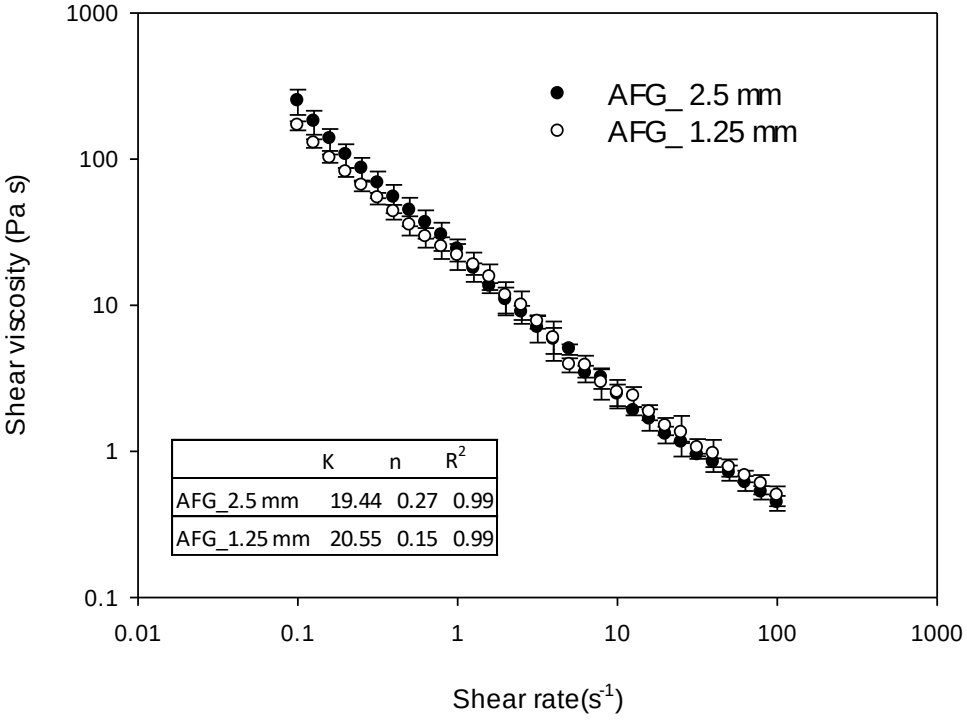

Figure 3. 11 - Effect of needle internal diameter, used for introducing the $CaCl_2$ stream in the pin-stirrer, on the viscosity of AFG

It is possible to notice that both viscosity and PSD were not affected by the internal diameter of the needle used to inject $CaCl_2$ into the pin-stirrer. This was probably related to the

unchanged $CaCl_2$/ALG ratio; on a molecular level, the amount of Ca^{2+} ions provided did not changed, neither did the rate by which this was provided, leading to the same final rate and extent of crosslinking and, therefore, to the same final particle dimensions. The mixing regime was efficient to minimize the effect of using a larger initial contact area between the $CaCl_2$ and the ALG streams, when a needle of 2.5 mm internal diameter was used. In conclusion, the diameter of the needle used did not influence the final properties of AFG.

3.3.5 Conclusions

The production of AFG using a pin-stirrer vessel was investigated in order to better understand its formation mechanism and the impact of different process and formulation parameters on the final AFG microstructure and rheological properties. The pin-stirrer was used to produce AFG in an easy industrially scalable approach. The $CaCl_2$/ALG ratio, the applied shear regime, the residence time and the needle internal diameter, for $CaCl_2$ injection, were changed. It is possible to conclude that since the ALG gelation is due to the formation of Ca^{2+} bridges between polymer chains and because this process happens really fast, the only parameter affecting the final particle dimensions was the used $CaCl_2$/ALG ratio. In addition, the final viscosity of materials could be adjusted as a function of the used ALG concentration. The other tested parameters did not influence the final PSD or the materials' flow behaviour. It was also observed that the pin-stirrer did not produce a shear regime strong enough to induce the breakage of AFG particles, but the magnitude of applied shear was fundamental to obtain the formation of a fluid gel material. In fact, a low shaft rotation during AFG production led to the formation of a quiescent gel structure. Overall, changes of the $CaCl_2$/ALG ratio affected the final PSD, while the ALG concentration changed the final viscosity behaviour. These two parameters can be tailored independently one from another based on the final properties desired from a specific AFG formulation.

3.4 References

1. Gabriele, A., F. Spyropoulos, and I.T. Norton, *Kinetic study of fluid gel formation and viscoelastic response with kappa-carrageenan.* Food Hydrocolloids, 2009. **23**(8): p. 2054-2061.
2. Fernández Farrés, I., R.J.A. Moakes, and I.T. Norton, *Designing biopolymer fluid gels: A microstructural approach.* Food Hydrocolloids, 2014. **42**: p. 362-372.

3. Fernández Farrés, I., M. Douaire, and I.T. Norton, *Rheology and tribological properties of Ca-alginate fluid gels produced by diffusion-controlled method.* Food Hydrocolloids, 2013. **32**(1): p. 115-122.
4. Fernández Farrés, I. and I.T. Norton, *Formation kinetics and rheology of alginate fluid gels produced by in-situ calcium release.* Food Hydrocolloids, 2014. **40**: p. 76-84.
5. Yong Lee, K. and D. J Mooney, *Alginate: Properties and biomedical applications*. Vol. 37. 2012. 106-126.
6. Varela, P., A. Pintor, and S. Fiszman, *How hydrocolloids affect the temporal oral perception of ice cream.* Food Hydrocolloids, 2014. **36**: p. 220-228.
7. Barnes, H.A., J.F. Hutton, and K. Walters, *An introduction to rheology*. Vol. 3. 1989: Elsevier.
8. de Carvalho, W. and M. Djabourov, *Physical gelation under shear for gelatin gels.* Rheologica Acta, 1997. **36**(6): p. 591-609.
9. Garrec, D.A. and I.T. Norton, *Understanding fluid gel formation and properties.* Journal of Food Engineering, 2012. **112**(3): p. 175-182.

Chapter 4: FREEZE DRYING AND REHYDRATION OF ALGINATE FLUID GELS

Smaniotto, F., Prosapio, V., Zafeiri, I., & Spyropoulos, F. (2020). Freeze drying and rehydration of alginate fluid gels. Food Hydrocolloids, 99, 105352.

Abstract

The aim of this work was to study the effect of freeze drying (FD) and rehydration on alginate fluid gels (AFG). FD was employed as a widely used drying method in order to evaluate whether its application causes any change in the material characteristics crucial for AFG behaviour. Rehydration studies were performed to assess if AFG properties could be restored after drying and rehydration processes. First, it was investigated the influence of the material formulation (alginate (ALG) and calcium chloride ($CaCl_2$) concentrations) on the particle size distribution (PSD) and the rheological properties. The used ALG/$CaCl_2$ ratio demonstrated to be responsible for forming nanoparticles or microparticles. The impact of fluid gel particle dimensions on drying and rehydration processes was also investigated. Overall, particle dimensions do not have a significant effect on drying kinetics. Analyses on rehydrated samples showed that the PSD is not affected by the processing, whereas the same viscosity was completely recovered only for samples formed by ALG and $CaCl_2$ in quantities leading to nanoparticles formation. Preliminary encapsulation experiments were also carried out to highlight the impact of this process on the release behaviour of the loaded active from AFG. Results obtained from *in vitro* release studies and their model fitting showed that the active release behaviour from AFG was not affected by FD when AFG was formed of nanoparticles. On the contrary, the active release behaviour was affected by FD when AFG was formed by microparticles.

Keywords: Fluid gel; freeze-drying; rehydration; rheological properties; encapsulation

4.1 Introduction

Fluid gels are suspensions of gel particles in a non-gelled continuous medium and are formed by applying shear forces to a polymeric solution undergoing a sol-gel transition [1]. They can be prepared using both biological (polysaccharides and proteins) and synthetic polymers [2], and can be produced using typical shear devices, such as a jacketed pin-stirrer, which allows a continuous process. Fluid gels can be temperature and/or ionically set, depending on the hydrocolloid used and to its gelation mechanism [3, 4]. The particle size can be controlled by varying the polymer concentration and the shear rate [2, 5].

Fluid gels show unique characteristics: at low deformations their flow behaviour tends to resemble that of quiescent gels, whereas at high deformations exhibits yield and flow characteristics like a viscoelastic fluid [6]. Due to this rheological performance, fluid gels find applications in the food industry as fat replacers [7, 8], texturing [9], satiety enhancers [10] and emulsion stabiliser [11]. A novel application involves their use for encapsulation of bioactive molecules to protect them from the surrounding environment, to control their release in a specific medium and/or to mask their flavour [12, 13]. The use of fluid gels as encapsulating material has the following advantages compared to other carriers (such as microcapsules, liposomes, etc.): organic solvents are not needed, the process can be run in continuous and can be easily scaled-up, mild operating conditions can be employed and good control over particle size is provided.

Being formed by a large amount of water, the shelf-life of fluid gels is relatively short and microbial spoilage can easily occur. This limitation can be overcome by drying the material, as water removal prevents bacteria proliferation. A dried product can be considered as safe if it is characterised by water activity (a_w) lower than 0.6 [14] and normalised moisture content (NMC) lower than 0.1 [15, 16]. In addition, the lower volume/weight of the product allows packaging, transport and storage costs to be reduced [17, 18]. On the other hand, drying of food products has been reported to cause some damage to the product microstructure according to the method and conditions employed, leading to low rehydration capacity and poor recovery of the initial properties [19]. Among the most common drying methods, freeze-drying (FD) showed the best performance in terms of water desorption, retention of the product characteristics and rehydration of the dried material [20, 21]. Specifically, for the dehydration of microstructures/formulations containing encapsulated matters, FD can be a

suitable method to prevent the degradation of thermosensitive compounds, as it involves the freezing of the product, followed by ice sublimation under vacuum conditions [22, 23].

The drying of quiescent gels has been extensively investigated using different materials (gellan gum [24, 25], starch [26, 27], cellulose [28, 29], agarose [30], silica [31], chitosan [32], etc.) and techniques (air-drying, FD, supercritical carbon dioxide drying, microwave drying [33, 34]). Tiwari *et al.* (2015) analysed the structure of freeze-dried gellan gum and agar gels; they observed for both materials that mechanically stable cellular solids were produced [35]. Cassanelli *et al.* (2019) studied the drying of gellan gum gels using oven drying, FD and supercritical carbon dioxide drying; they observed that the gel microstructure was better preserved when FD was employed, leading to a significantly higher rehydration capacity compared to the other methods [34]. Hu *et al.* (2013) employed air drying, microwave vacuum drying and FD to dry hairtail fish meat gels and stated that FD samples showed better quality attributes in terms of moisture content, water absorption index, protein degradation and sensory acceptance than air and microwave-dried ones [33].

Despite the potentiality in providing long/safe storage and protection of the actives, the drying of fluid gels has not been studied so far. In order to fill the gap in the current literature, this work investigates the FD of alginate fluid gels (AFG). Alginate is a hydrocolloid that undergoes gelation in the presence of multivalent cations, usually Ca^{2+} [36]. AFG were prepared in a pin-stirrer and thereafter freeze-dried. Rheological measurements were carried out on both unprocessed and processed fluid gels to verify if the material properties (particle size and viscosity) can be completely recovered after drying and rehydration. In addition to the preservation of rheological behaviour upon rehydration, the capacity of the fluid gels to modulate the release of a model active (present within the fluid gel microstructure) prior and following FD was investigated. Preliminary encapsulation experiments were also performed, using Nicotinamide as model active, to investigate the release behaviour before and after drying/rehydration, and identify possible changes due to the processing.

4.2 Materials and methods

4.2.1 Materials

Sodium alginate (CAS: 9005-38-3, W201502, lot.# MKBT7870V) and nicotinamide (NIC, ≥98%, HPLC) were purchased from Sigma-Aldrich® (Sigma–Aldrich Company Ltd., Dorset, UK).

Calcium chloride ($CaCl_2$, anhydrous, 93%) was purchased from Alfa Aesar™ (Varela, #159). All materials were used without further purification. Milli-Q water was made using an Elix® 5 distillation apparatus (Millipore®, USA) and was used for all water-based preparations.

4.2.2 Gel preparation

4.2.2.1 Blank fluid gels

Firstly, an alginate solution was prepared by dissolving different amounts of ALG (1%, 2%, 3% (w/w), calculated on the final weight of the material) in distilled water at 95 °C for 45 min under stirring to ensure complete powder dissolution, as reported by Farrés *et al.* [37]. Thereafter, the solution was cooled at room temperature (R.T.). Secondly, another solution was prepared by dissolving $CaCl_2$ at a different concentration for each experiment (0.15%, 0.25%, 0.35% (w/w), calculated on the final weight of the material) in water at R.T.. Alginate Fluid Gels (AFG) were prepared using a pin-stirrer vessel (Het Stempel, HL) having a volume of 150 mL, 16 pins placed on the rotating shaft and 16 pins fixed on the internal wall. 1000 RPM shaft speed was used for AFG production. The alginate solution was pumped using a flowrate of 33 mL/min with a peristaltic pump (Masterflex L/S Peristaltic, DE), while the $CaCl_2$ solution was injected using a flowrate of 4.02 mL/min with a syringe pump (Cole-Parmer Single-syringe, US) through a stainless steel needle of 1.25 mm internal diameter.

4.2.2.2 Nicotinamide fluid gels

Firstly, a solution of 2% (w/w) was prepared by dissolving ALG in distilled water at 95 °C for 45 min under stirring to ensure complete powder dissolution. Then, the solution was cooled at R.T.. Secondly, three solutions at 0.10% (w/w) were prepared by dissolving NIC in distilled water at R.T.. To these solutions different amounts of $CaCl_2$ (0.15%, 0.25%, 0.35% (w/w), calculated on the final weight) were dissolved at R.T.. Nicotinamide Fluid Gels (NFG) were then prepared using a pin-stirrer vessel as described above (2.2.1 Blank fluid gels).

4.2.3 Rheological properties

The rheological properties of fluid gels were determined by shear viscosity tests using a rotational rheometer (Kinexus™, Malvern®, UK) equipped with a 40 mm diameter sand blasted plate geometry. The analyses were carried out at 25 °C using a shear rate ramp of 31 points between 0.01 and 100 s^{-1}. Measurements were performed in triplicate.

4.2.4 Particle Size Distribution

4.2.4.1 Mastersizer

The particle size distribution (PSD) of fluid gels was evaluated using a Mastersizer-2000 (Malvern®, UK). Few drops of sample were placed into the mixing chamber and stirred for 10 min at 1300 RPM before performing the analysis to disrupt any possible macro-aggregation. PSD was evaluated as numerical particle sizes percentage by the Mastersizer software, using a refractive index of 1,335. Measurements were performed in triplicate.

4.2.4.2 Dynamic light scattering

The PSD of fluid gels was also evaluated with Zetasizer (Malvern Instruments Ltd., UK) via Dynamic Light Scattering (DLS) analysis. Samples were diluted with water before analysis to yield a suitable scattering intensity and measured at 25 °C. PSD curves were evaluated as numerical particle sizes percentage. All measurements were performed at 25 °C in triplicate and all data are presented/plotted as the mean value± SD.

4.2.5 Optical microscopy

Optical microscope (DM 2500 LED, Leica®, CH) was used to observe and record alginate microparticles. Samples were, firstly, diluted with distilled water using a water to sample ratio of 10:1 and they were mixed using a vortex mixer (VM20, Rigal Bennet®, UK) for 20 seconds. DIC settings were employed to increase the contrast, allowing the average dimensions of particles to be measured. Images were captured using a CCD camera (DFC450 C, Leica®, CH) coupled to the microscope. Image analysis software IPP (LAS 4.8.0, Leica®, CH) was used to evaluate the dimensions of the microparticles through the images.

4.2.6 Freeze drying

Fluid gels were frozen at -20 °C overnight and then lyophilised using a bench top Freeze Dryer (SCANVAC Coolsafe™, model 110-4, DK), condenser temperature -110 °C, pressure 10 Pa, condition that is defined by the equipment. Drying time was varied from 2 to 48 h to investigate the drying kinetics. Experiments were performed in triplicate for each condition investigated.

4.2.7 Moisture content analysis

Moisture content analyses were carried out measuring the sample weight before and after drying. Moisture content was expressed as NMC (Normalised Moisture Content) and calculated through the following Equation (4.1):

$$NMC = \frac{(Md - Ms)}{(Mo - Ms)} \qquad \text{(Equation 4.1)}$$

where M_s is the solid sample mass, M_d the sample mass after drying and M_o the pre-dried sample. The drying kinetics was determined plotting NMC as a function of the drying time. Analyses were carried out in triplicate.

4.2.8 Water activity analysis

Water activity (a_w) of dried samples was measured using an AquaLab® dew point water activity meter (model 4TE, Decagon Devices Inc., Pullman, WA, USA). The temperature-controlled sample chamber was set to 25 °C. Analyses were carried out in triplicate.

4.2.9 Rehydration of samples

After dehydration, amounts of distilled water were placed in each sample in order to obtain the same sample weight before FD. Samples were then transferred in a shacking incubator (Incu-Shake MIDI, SciQuip, UK), in order to obtain a homogeneous rehydration of the material, for different times at 400 RPM and 20 °C.

4.2.10 *In vitro* release

In vitro release studies from NFG were performed using a UV-Vis spectrophotometer (Orion Aquamate, Thermo Scientific, UK) to determine the concentration of NIC in the medium over time. A weighed amount of NFG (approximatively 2.5 g) was enclosed in a dialysis sack (Sigma–Aldrich Company Ltd., Dorset, UK, dialysis tubing cellulose membrane, width 43 mm, M.W. cut-off of 14000 Da) and placed in 500 mL of distilled water at room temperature (thermostated at 21.5 °C), under stirring at 150 RPM. At regular intervals, aliquots of 2 mL were withdrawn, measured using the spectrophotometer at 214 nm wavelength and then poured again into the medium. A calibration curve was made at 214 nm wavelength (NIC maximum of absorbance) and was set for concentrations between 0.08 and 45 µg/mL and

was used to correlate the absorbance value to the actual concentration of NIC into the release medium. Each analysis was carried out in triplicate.

4.2.11 Data fitting

Data obtained from NIC *in vitro* release studies from NFG were model fitted using Equation (4.2):

$$\frac{M_t}{M_\infty} = kt^n \qquad \text{(Equation 4.2)}$$

where M_t and M_∞ are respectively the cumulative amounts of drug released at time t and at time when the release plateaux was reached, k is the kinetic constant and n is an exponent characterizing the diffusional mechanism. The use of Equation (4.2) is validated by several authors and it is generally used to understand the release mechanism of drugs and bioactives from formulations from release data obtained in *in vitro* release experiments [38-40].

4.2.12 Statistical analysis

Statistical analysis of data groups was determined via single factor analysis of variance (ANOVA). P values < 0.05 were considered as statistically significant.

4.3 Results and discussion

In the first part of the experimentation, the amounts of alginate (ALG) and $CaCl_2$ were varied to identify the minimum ratio between $CaCl_2$ and ALG required to obtain microparticles formation. Both formulations (forming and non-forming particles) were used as matrices for the encapsulation of nicotinamide. *In vitro* release behaviour of NIC from these materials was then studied. FD experiments on AFG were carried out to investigate the effect of this method on fluid gel properties (particle size and viscosity) and to identify the conditions needed to assure the complete removal of free water (NMC < 0.1 and a_w < 0.6) [15, 41, 42]. The effect of $CaCl_2$ concentration in AFG on the FD kinetics was also investigated. Afterwards, a second set of release experiments was performed on NFG to study the effect of the FD process and rehydration on the release behaviour of NIC from AFG.

4.3.1 Effect of ALG/$CaCl_2$ ratio

The amount of $CaCl_2$ needed to obtain the complete gelation of AFG was investigated by producing several samples at fixed ALG concentration and changing the $CaCl_2$ one; the final properties of the obtained materials in terms of PSD were then assessed. Samples compositions used in this part of the work alongside their acronyms are reported in Table 4.1.

Table 4. 1 - ALG and $CaCl_2$ concentrations used for sample preparations

Sample	ALG concentration (w/w)	$CaCl_2$ concentration (w/w)
AFG_2%_0.15%	2%	0.15%
AFG_2%_0.25%	2%	0.25%
AFG_2%_0.35%	2%	0.35%

4.3.1.1 Particle size distribution

Particle dimensions were evaluated using the Mastersizer and DLS as reported in section 4.2.4 Particle Size Distribution. PSD curves obtained using both techniques are reported in Figure 4.1.

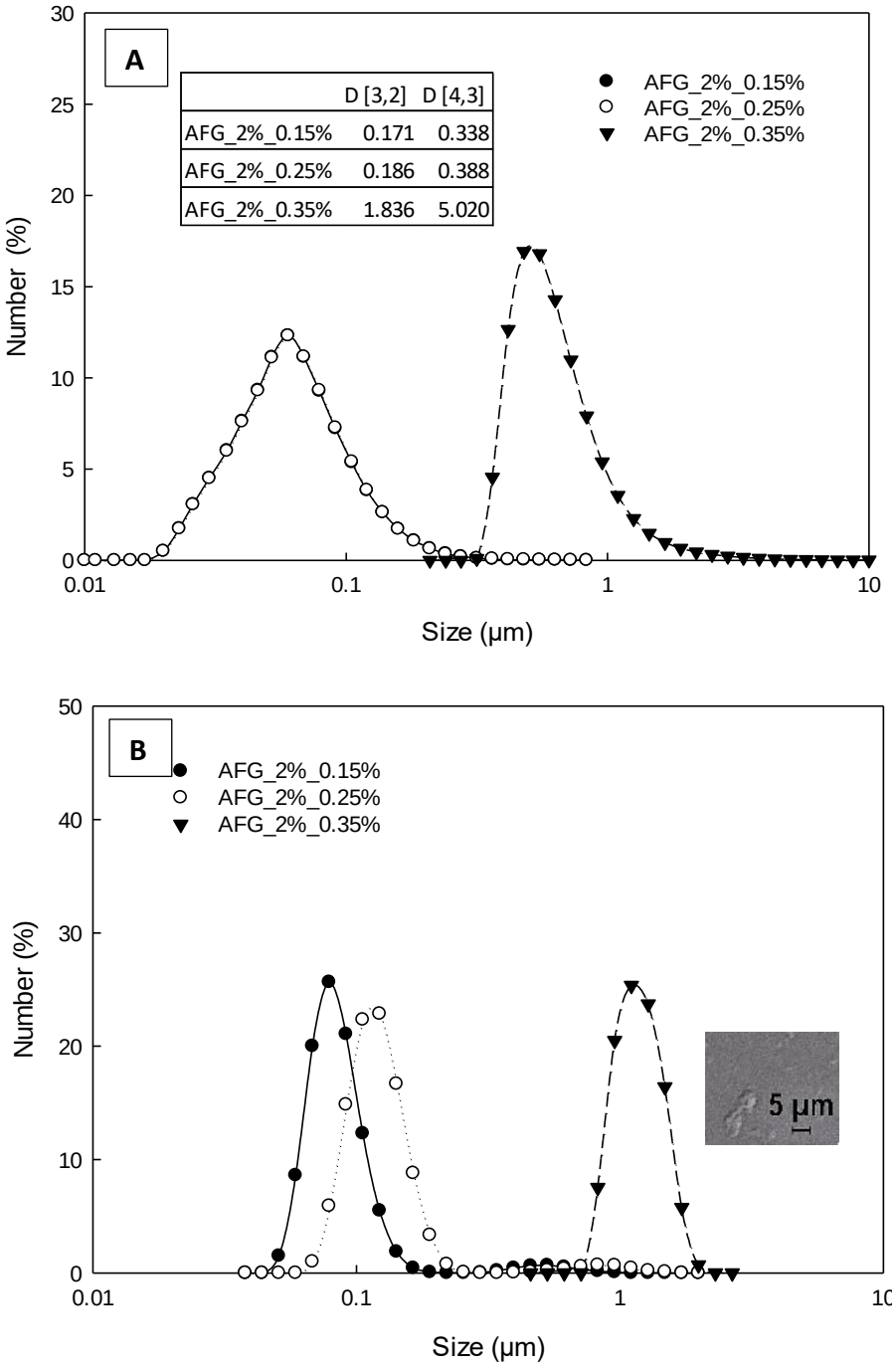

Figure 4. 1- PSD curves of AFG produced by using 2% ALG (w/w): (A) Mastersizer, (B) DLS. In Fig. A, AFG_2%_0.15% and AFG_2%_0.25% curves are perfectly overlapping

Mastersizer and DLS curves of AFG_2%_0.35% displayed a PSD in the range of 0.5 to 5 µm, while AFG_2%_0.15% and AFG_2%_0.25% were in the range between 0.02 µm and 0.2 µm. The particle formation behaviour of samples was also studied using light microscopy (as shown in Figure 4.1B).

Due to the small dimensions, particles in samples AFG_2%_0.25% and AFG_2%_0.15% could not be recorded/visualised by optical microscopy analysis, while it can be noticed the presence of microparticles for AFG_2%_0.35% (Figure 4.1B). Samples were also produced using different percentages of ALG to identify the ratio between $CaCl_2$ and ALG necessary to ensure particle formation. Samples compositions used are reported in Table 4.2.

Table 4. 2 - ALG and $CaCl_2$ concentrations used for sample preparations

Sample	ALG concentration (w/w)	$CaCl_2$ concentration (w/w)
AFG_1%_0.15%	1%	0.15%
AFG_1%_0.25%	1%	0.25%
AFG_3%_0.35%	3%	0.35%
AFG_3%_0.45%	3%	0.45%

Microparticles formation was observed for samples AFG_1%_0.25% and AFG_3%_0.45%, while nanoparticles were detected for the samples AFG_1%_0.15% and AFG_3%_0.35%. These results showed that microparticles formation was achieved only when a critical ratio of approx. 0.155 between ALG and $CaCl_2$ was used during sample preparation, as previously discussed in section 3.3.1 $CaCl_2$/ALG ratio. This ratio (CRMF) was estimated considering the used percentages of $CaCl_2$ and ALG in samples that consisted of microparticles. However, even in samples produced with a $CaCl_2$/ALG ratio lower than the CRMF, PSD curves showed the presence of nanoparticles in the range of 100 nm and due to these very small dimensions they could not be visualised using optical microscopy. In accordance with results reported by Badita *et al.* (2016), these nano-domains can be attributed to the alginate polymer chains morphology [43]. Additionally, the authors observed the formation of an alginate secondary structure in the presence of Ca^{2+} ions, but only when a Ca^{2+} concentration higher than a critical concentration was used. Nano-domains dimensions of AFG produced using a $CaCl_2$/ALG ratio lower than the CRMF were in accordance with the values obtained by Badita *et al.* [43]. In addition, He *et al.* (2016) reported the formation of "nuclei" of gelation when $CaCl_2$/ALG ratio lower than a critical value was used [44]. When a $CaCl_2$/ALG ratio lower than the CRMF was used for the production of AFG, some cross-linking points were generated; however, it

appears that the Ca^{2+} concentration was not enough to crosslink all the α-L-guluronate (G) monomers of ALG that are responsible for the formation of the egg-box model [45]. The non-crosslinked residues of polymer chains were able to interact with other non-crosslinked chains, explaining the formation of an extended network all over the whole material. Samples produced with a $CaCl_2$/ALG ratio higher than the CRMF were able to fully form microparticles. The folding of ALG polymer chains on themselves is a process induced by the applied shear regime. Ca^{2+} ions can "lock" ALG chains in position only when a concentration high enough to achieve a full crosslinking is used. After the removal of the shear regime, due to the full crosslinking of ALG, polymer chains were unable to unfold and interact with other ALG chains, but stable microparticles could still be formed. Even when a $CaCl_2$/ALG ratio lower than the CRMF was used, ALG folded on themselves, but due to the lack of a complete crosslinking, they were able to unfold and interact with each other, obtain an extended matrix, after the removal of the shear regime. In that case, only "pre-particles" within an ALG matrix could be identified by PSD analyses. However, due to their small dimensions they could not be visualised using the optical microscope.

4.3.1.2 Release behaviour

Nicotinamide loaded alginate fluid gels NFG-025 and NFG-035 were produced respectively using a $CaCl_2$/ALG ratio lower (0.25% $CaCl_2$ concentration) and higher (0.35% $CaCl_2$ concentration) than the CRMF; they were produced in the presence of NIC (0.10% w/w), as described in the section 4.2.2.2 Nicotinamide fluid gels. These two formulations were chosen with a view to understand how the release behaviour of the incorporated active compound is affected by the formed particle sizes. NIC was chosen as a model active because of its small dimension and its low molecular weight (122.13 g/mol) to avoid its physical entrapment into the gel-network, which would limit the diffusion into the release medium. Additionally, NIC is a highly hydrophilic molecule and displays a very high water solubility (>500 mg/mL at 25 °C), which is a suitable characteristic for the production of water-based fluid gels [46]. Additionally, the release profiles of these materials were compared to that of a NIC water solution and a NIC and ALG (2% w/w) water solution, both containing 0.10% w/w of the active, in order to fully understand if and how the $CaCl_2$ presence affects release behaviour (Figure 4.2).

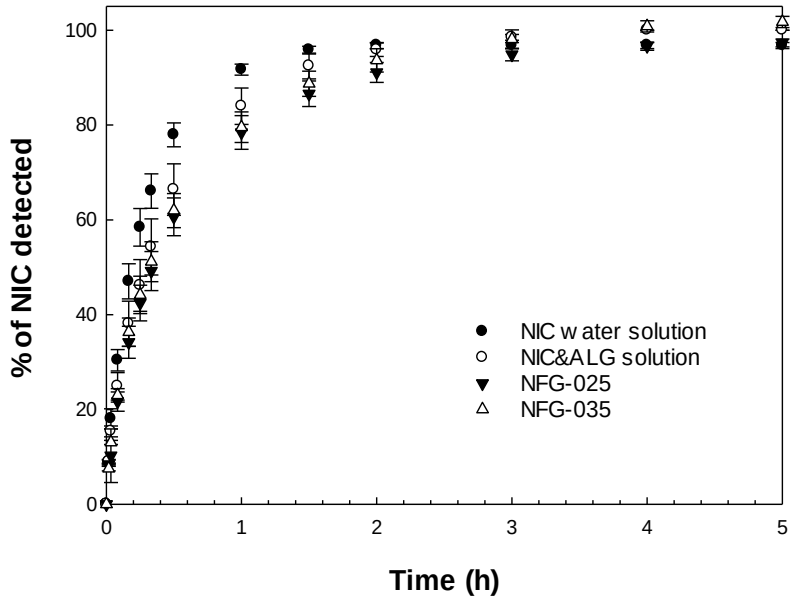

Figure 4. 2- In vitro release profile of nicotinamide from NIC in aqueous medium, NIC&ALG solution, and NIC-loaded alginate fluid gels produced using different concentrations of $CaCl_2$ (NFG-025 and NFG-035. No significant differences [p > 0.05] were found between in vitro release experiments of all formulations

As depicted from Figure 4.2, the formation of microparticles did not prevent the diffusion of NIC out of AFG. In fact, NFG-025 and NFG-035 presented the same release profile. Comparing these two curves with the one of NIC water solution, it can be observed that both AFG formulations were able to slightly slow down the release of NIC. This delay is obvious even when comparing the NIC&ALG solution curve with the NIC water solution one; however, the delay effect is enhanced in the presence of $CaCl_2$. It is possible to conclude that AFG are able to slow down the diffusion of the loaded NIC and this effect is due to a combination of the ALG and $CaCl_2$ presence. The delay ability can be attributed to the increase of viscosity of the solutions as suggested by Secouard *et al.* (2003), in a release experiments of limonene from three different polysaccharide based water solutions and gel systems [47]. They suggested that materials viscosities contribute significantly to limonene retention with the formulation and on its release behaviour.

4.3.2 Freeze drying

FD experiments were carried out to investigate the effect of processing time and $CaCl_2$ concentration, used during material production step, on samples moisture content and water activity. Rheological properties and particle size distributions were studied on both non

freeze-dried (AFG) and freeze-dried and rehydrated (FD-AFG) fluid gels formulations. ALG concentration was fixed at 2% w/w and three different fluid gels were prepared using $CaCl_2$ concentration of 0.15%, 0.25% and 0.35.

4.3.2.1 Moisture content and water activity

Normalised moisture content (NMC) and water activity (a_w) were measured for 48 h at different time intervals during the FD experiments. The values obtained alongside the corresponding standard deviations are shown in Figure 4.3.

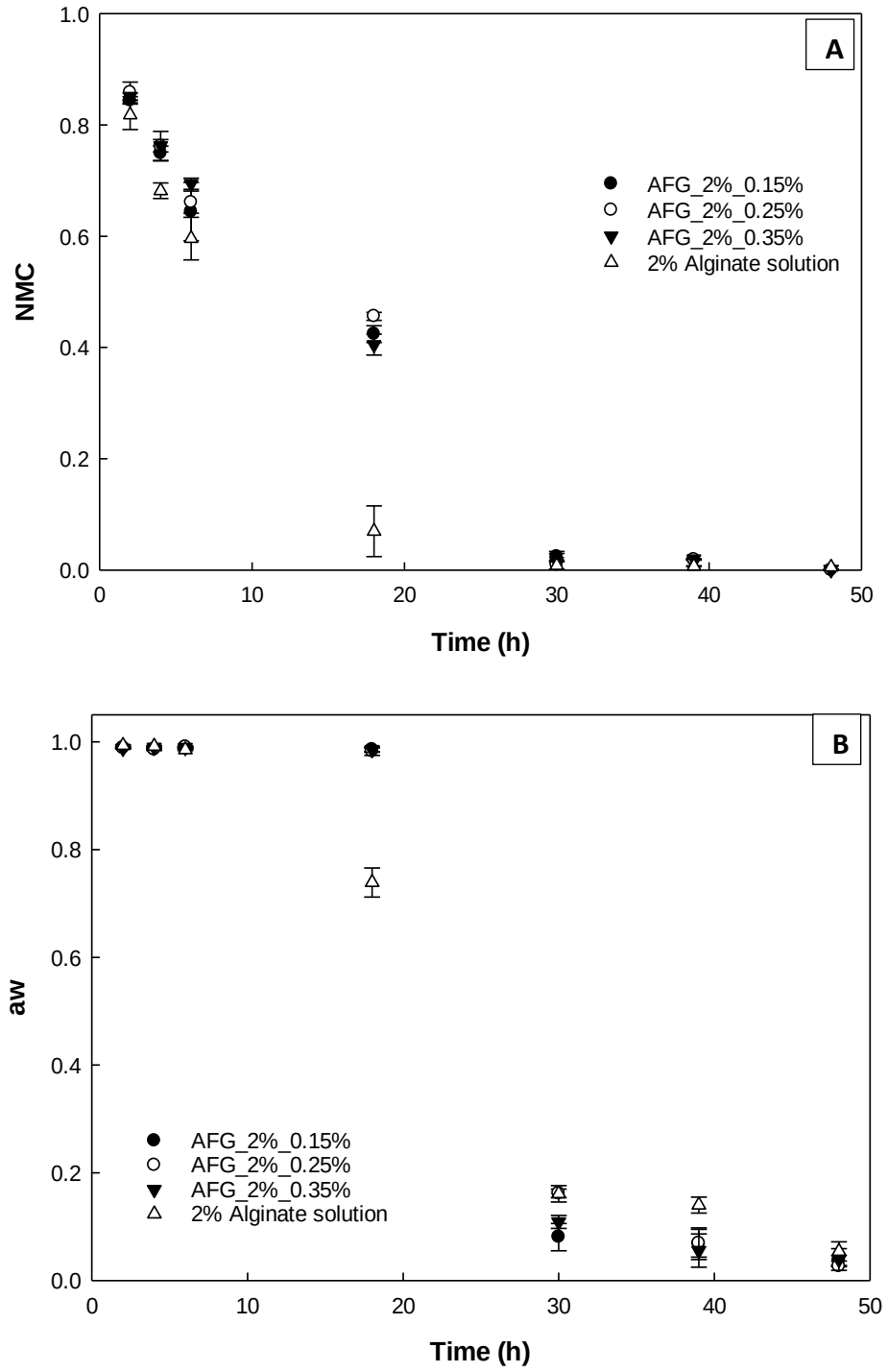

Figure 4. 3- Drying kinetics of fluid gels at 2% ALG (w/w) and different $CaCl_2$ concentrations: (A) Normalised Moisture Content; (B) water activity

From Figure 4.3A, it is possible to observe that the first stage of drying (about 18 h) was quite fast and characterised by a constant rate. Specifically, for AFG at this stage sublimation of the ice formed from inter-particle water took place, with a drying rate of about 0.02 h^{-1}, whereas for the alginate solution the process was faster (approx. 0.05 h^{-1}), likely due to the absence of aggregates that act as a resistance to heat and mass transfer. As a result, AFG at 18h drying

still showed an NMC around 0.4, while the solution was already dried. Thereafter, for fluid gels a falling rate was observed up to 30 h, related to the intra-particle ice sublimation. After 30 h, a zero drying rate with no substantial changes to moisture content was recorded, i.e. all free water was removed from the samples. The experimental values measured for a_w of the materials during drying, reported in Figure 4.3B, showed a slightly different behaviour in the first stage. In fact, water activity remained nearly unchanged for 6h in the case of the alginate solution and 18 h in the case of AFG and then gradually decreased until achieving a constant value at 48 h. From these diagrams, it can be concluded that at least 48 h drying is needed for AFG to lower both a_w and NMC under the threshold limits (0.6 and 0.1, respectively [14, 15]) and, therefore, prevent microbial growth.

The effect of fluid gel formation on alginate drying behaviour can be appreciated in the first hours of drying (until 18 hours). In fact, for the sample not formed by a fluid gel (no $CaCl_2$ added), the NMC decreased more rapidly if compared to materials in which some amount of $CaCl_2$ was used. A similar trend can be identified from the water activity (a_w) curves; especially at 18 hours of drying time big differences between samples can be seen. The slower drying kinetics of AFG, when compared to an ALG solution in which no $CaCl_2$ was added, can be due to the formation of a gel network in which water is entrapped between alginate polymer chains leading to more time being required to remove water from that network. Additionally, comparing the a_w and NMC curves obtained at different $CaCl_2$ concentrations for AFG samples (Figure 4.3A and 4.3B), it can be seen that there is negligible difference among them, suggesting that once the network is formed, this parameter does not have substantial effect on the gel drying.

4.3.2.2 Rehydration performance

FD samples were rehydrated, following the procedure reported in section 4.2.9 Rehydration of samples, to assess the impact of the freezing/drying on the material properties of fluid gels. Rehydration is one of the key parameters that quantify the quality of a dried product as it describes its ability to reacquire the initial amount of water within its structure. Rehydration is a complex phenomenon, in which different mechanisms take place: water absorption into the dried product, diffusion through the porous network and swelling of the structure [48-50]. Rehydrated samples were characterised in terms of viscosity, PSD and release behaviour and compared with unprocessed (non-freeze dried) fluid gels.

4.3.2.3 Recovery of rheological properties

The rheological behaviour of rehydrated fluid gel samples having different $CaCl_2$ content was compared to that of systems prior to FD. Samples were rehydrated for 1 hour before recording viscosity measurements. Viscosity curves for the different formulations are presented in Figure 4.4.

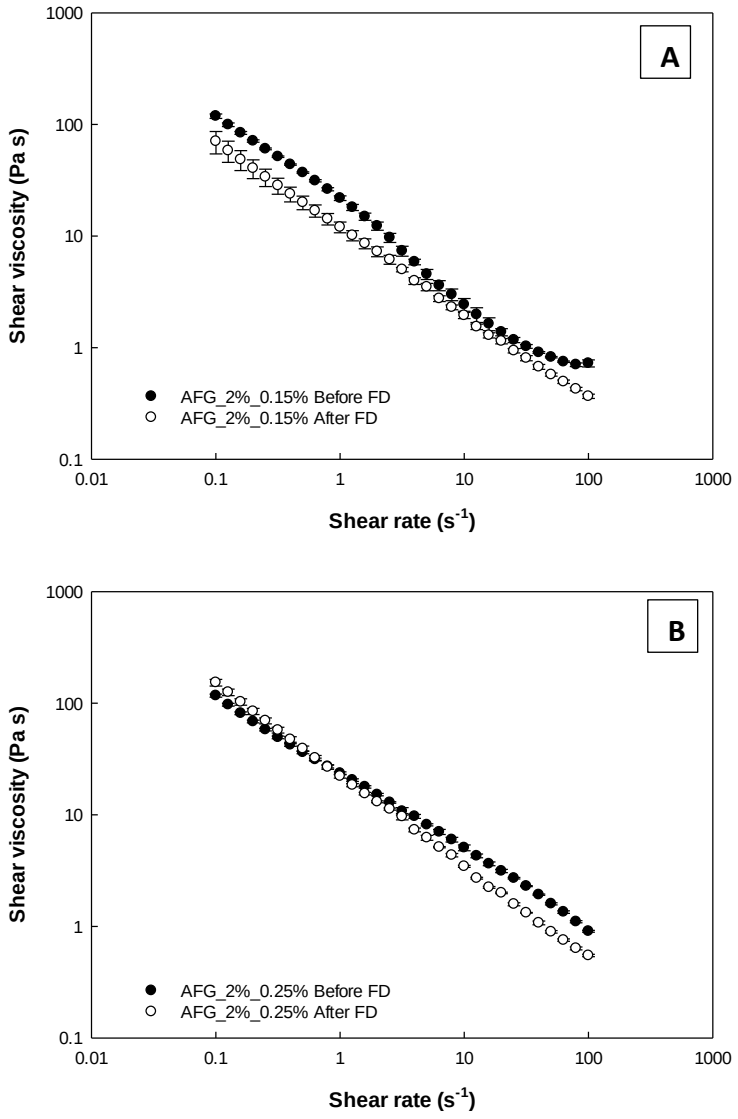

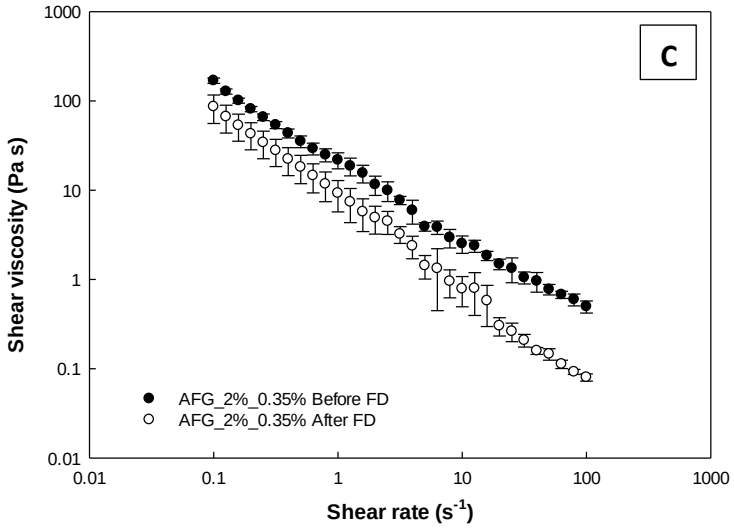

Figure 4. 4-Shear viscosity curves of blank AFG before FD and after drying/rehydration: (A) 0.15% $CaCl_2$; (B) 0.25% $CaCl_2$; (C) 0.35% $CaCl_2$

It is possible to notice that for AFG_2%_0.15% and AFG_2%_0.25%, viscosity curves before FD and after FD/rehydration are almost overlapping. It can be stated that freeze-dried materials with a $CaCl_2$ concentration of 0.15% or 0.25% were able to fully recover the rheological behaviour they had before FD. AFG_2%_0.15% and AFG_2%_0.25% were produced using a 2% ALG concentration and, as shown in Figure 4.1, they were not able to produce microparticles. The comparison between the viscosity curves of AFG_2%_0.35% in the fresh and dried/rehydrated form showed more significant changes (Figure 4.4C). More specifically, an overall decrease in the shear viscosity can be observed and, in particular, the difference with the untreated material becomes more evident as shear rate increases. This behaviour can be due to the inability of AFG_2%_0.35% to fully reabsorb the added water or by its delay in doing that. Additional rehydration experiments were carried out on freeze-dried AFG_2%_0.35%, increasing the rehydration time up to 48h, to assess if they were able to recover the rheological properties they had before FD by prolonging the time of the rehydration step; however, the viscosity profile was not restored even after 2 days of rehydration in the shaker incubator. This behaviour suggests that AFG produced using a $CaCl_2$/ALG ratio higher than the CRMF, i.e. when microparticles formation is achieved, cannot recover the rheological properties they had before FD. This set of experiments showed that the rehydration of AFG, and the complete recovery of the rheological properties they had before the FD, is achievable only when materials were prepared using a $CaCl_2$/ALG ratio lower than CRMF. Below that ratio, polymer chains are not fully cross-linked leaving some empty

zones between them in the alginate gel formed. Because of the presence of less cross-linking junctions, polymer chains present a higher mobility than polymer chains of fully cross-linked materials (when a $CaCl_2$/ALG ratio higher than the CRMF was used). The rehydrated AFG_2%_0.35% samples were not visually homogeneous and regions having higher particle concentration and regions at higher water concentration could be identified. This higher mobility may explain why viscosity profiles before and after FD completely match solely for samples not completely cross-linked. In fact, the more mobile polymer chains are less rigid and they can move more and faster to fit the water molecules between them. In contrast, polymer chains having a lower mobility due to the presence of more cross-linking points, take more time to fit all water molecules or just a fraction of the removed water molecules can be reabsorbed.

In order to identify the time needed for AFG produced using a $CaCl_2$/ALG ratio lower than the CRMF to recover the viscosity they had before FD, an additional rehydration experiment was carried out on AFG_2%_0.25% using a rehydration time of 5 min and 10 min in the shacking incubator before performing the rheological test. A comparison among the resulting viscosity curves is reported in Figure 4.5.

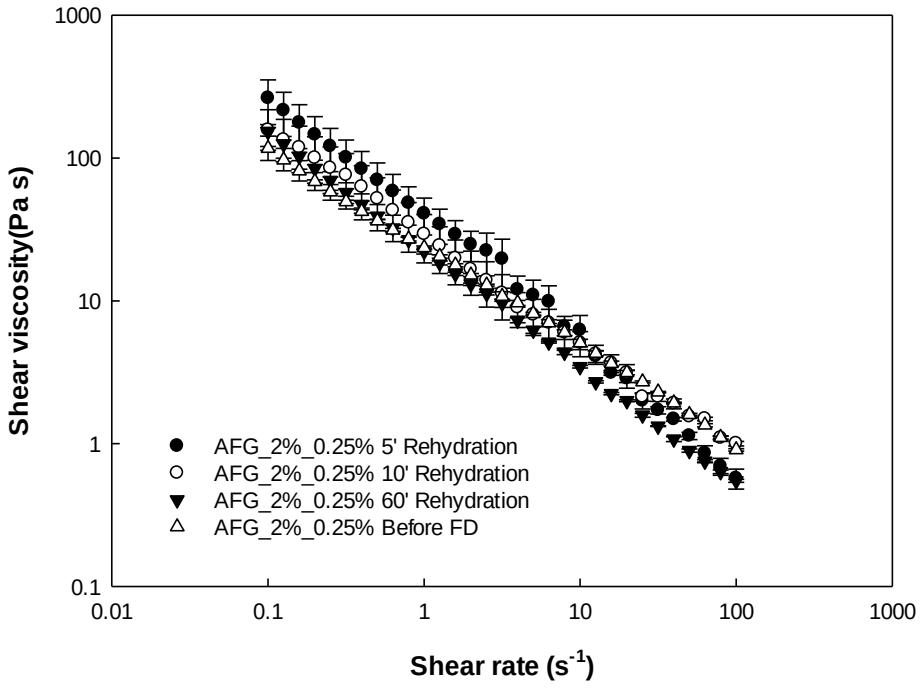

Figure 4. 5- Shear viscosity curves of AFG-025 as a function of the rehydration time

From Figure 4.5 becomes evident that the complete recovery of viscosity was achieved after approximately 10 min of rehydration time. It can be concluded that AFG produced using a $CaCl_2$/ALG ratio lower than the CRMF are able to fully recover the rheological properties they had before FD in a short time.

4.3.2.4 Particle Size distribution

The PSD of rehydrated samples of AFG_2%_0.15%, AFG_2%_0.25% and AFG_2%_0.35% were compared to those of the samples before FD to identify if some particle aggregation was induced by the drying process. Samples were rehydrated for 1 hour before performing particle size measurements using the Mastersizer, as described in section 4.2.4.1 Mastersizer. PSD curves are displayed in Figure 4.6.

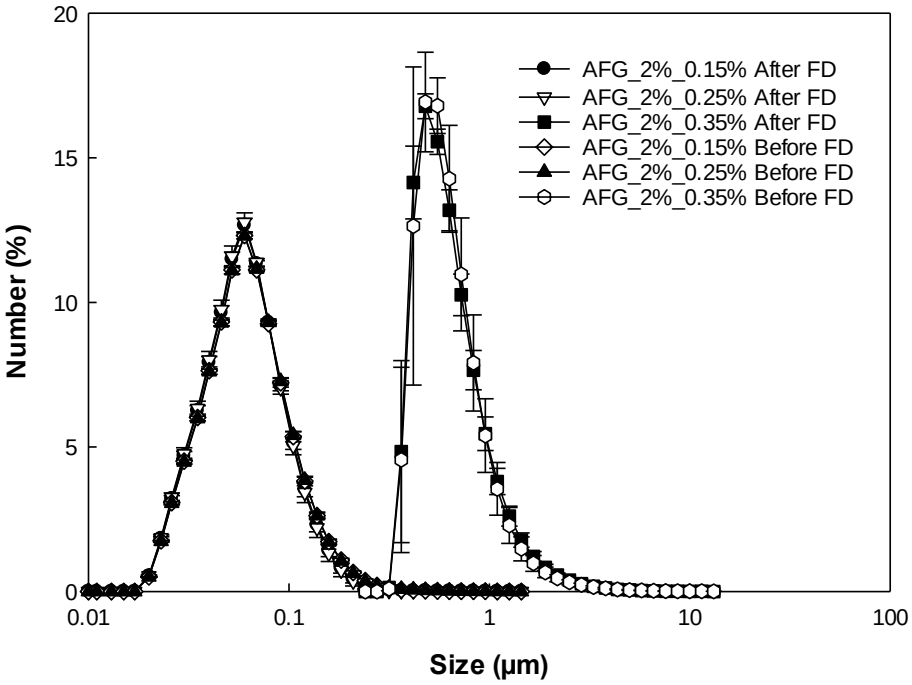

Figure 4. 6- PSD curves of blank (no active) AFG before FD and after drying and rehydration

The PSD curves after rehydration were perfectly overlapping with the curves obtained from materials before FD. It is possible to conclude that AFG do not form aggregates during the freeze-drying process and that they can retain their initial sizes.

4.3.2.5 Release behaviour of nicotinamide-loaded fluid gels

After NFG production, a fraction of both NFG_025 and NFG-035 was freeze-dried, as described in section 4.2.6 Freeze drying, until constant weight (48 h). Freeze-dried samples were then rehydrated for 1 hour and release of the active over time was studied, as described

in section 4.2.10 *In vitro* release, to highlight the influence of FD on the release behaviour of NIC. The NIC release profiles from FG before drying and following drying and rehydration are depicted in Figure 4.7 for two different concentrations of the active:

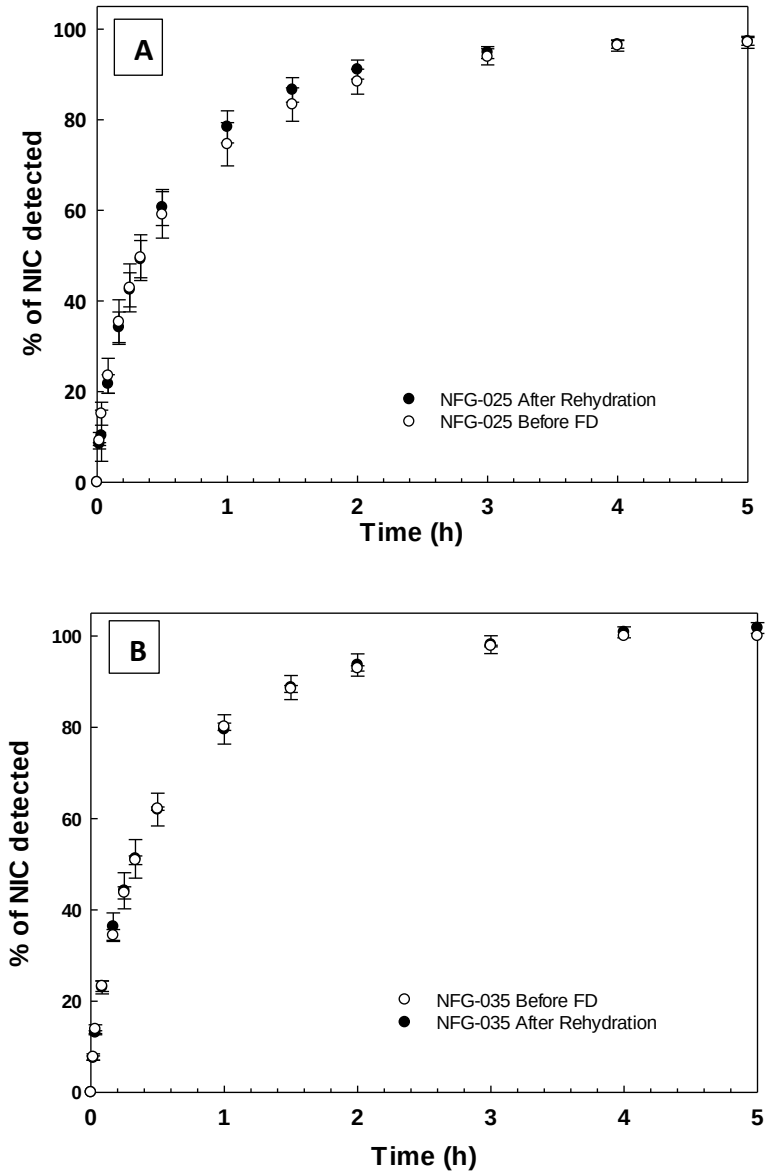

Figure 4. 7- In vitro release profiles of NIC from forming nanoparticles AFG (A) and forming microparticles AFG (B) before FD and after drying and rehydration (no significant differences [p > 0.05] were found between in vitro release experiments of FD and rehydrated NFG and the corresponding formulations not submitted to FD)

As can be seen in Figure 4.7A-B, both FD and rehydration processes do not seem to affect the release behaviour of NIC from AFG; in fact, release curves are almost overlapping. In order to better understand the release behaviour of NIC a model fitting analysis was conducted: data obtained from *in vitro* release studies of NFG formulations were used to fit a mathematical

model, as described in section 4.2.11 Data fitting, and the obtained parameters are reported in Table 4.3:

Table 4. 3 - k, n, R^2, parameters obtained from Equation 4.2 data fitting

	NFG-0.25	NFG-025 after rehydration	NFG-0.35	NFG-0.35 after rehydration	NIC Solution	NIC&ALG
k	0.9526 (± 0.0835)	0.8835 (± 0.0518)	0.9187 (± 0.0785)	0.3911 (± 0.0504)	1.3440 (± 0.1925)	0.9814 (± 0.0488)
n	0.5826 (± 0.0654)	0.5118 (± 0.0413)	0.5578 (± 0.0625)	0.5600 (± 0.0396)	0.5851 (± 0.0887)	0.5464 (± 0.0361)
R^2	0.995	0.997	0.995	0.998	0.994	0.998

As described by Rinaki *et al.* (2003), the *n* parameter obtained from data fitting of Equation 4.2 describes the mechanism of drug release [40]. As can be noticed from Table 4.3, this value is almost constant for all *in vitro* experiments and it is in the range between 0.51-0.59. As reported by the same authors and by Korsmeyer *et al.* (1983), n values in the range 0.4-0.65 are related to pure diffusion mechanism (anomalous non-Fickian diffusion) of drug [38, 40]. In NFG the release of NIC can be related to its diffusion through the ALG matrix; this is very similar to the diffusion of NIC from a water solution or from a water and alginate solution. This supports the theory that no drug-matrices interactions were formed between NIC and AFG. In a previous reported study, the interaction between tryptophan and AFG were recorded [51]. However, in that case the amount of drug detected during *in vitro* release studies was not equal to the overall amount of drug introduced in AFG and the amount released was also affected by storage time, suggesting a possible interaction between tryptophan and alginate polymer chains, as reported in literature by Yang *et al.* [52]. As described by Korsmeyer *et al.* (1983), the kinetic constant *k* is characteristic of each drug-matrix system [38]. As can be seen in Table 4.3, *k* values of NFG-0.35 are substantially different between the "untreated" material and the one after the drying and rehydration processes. As reported above (see section 4.3.2.2 Recovery of rheological properties), AFG made using a $CaCl_2$/ALG ratio higher than the CRMF, as in the case of NFG-0.35, were not able to be completely rehydrated and their rheological properties were affected by the drying and rehydration steps. Changes in *k* values of NFG-0.35 confirm that AFG made using a $CaCl_2$/ALG ratio higher than the CRMF cannot be completely rehydrated. This is not true for AFG made using a $CaCl_2$/ALG ratio lower than the CRMF, as the *k* values of NFG-0.25 is very similar to the

one of the same sample submitted to FD and rehydration processes, confirming that a complete rehydration of the matrix can be achieved, as showed in section 4.3.2.2 Recovery of rheological properties.

It is possible to conclude that AFG are able to slow down the diffusion of the loaded NIC even after FD, if compared to a water solution of NIC. Additionally, FD is a suitable technique for preserving AFG by decreasing their moisture content and, consequently, their water activity, preventing the bacterial growth. Rehydration can restore the release behaviour they had before FD.

4.4 Conclusions

In this work, the suitability of FD as preservation method for alginate fluid gels was investigated. The effect of particle dimensions on drying kinetics and rehydration behaviour of these materials was studied. It was demonstrated that the drying and rehydration processes do not affect the particle size distribution. However, the rheological properties of AFG can be completely recovered only when materials where made using a $CaCl_2$/ALG ratio that allowed the formation of nanoparticles. Preliminary encapsulation experiments of NIC in AFG were also carried out, showing that the release behaviour of this active from AFG was not modified by the drying/rehydration processes when AFG were composed of nanoparticles. This showed to be the most suitable system to deliver the active compound. On the other hand, data fitting models of *in vitro* release experiments showed some changes in the release behaviour of NIC after FD and rehydration of AFG made of microparticles. This is probably due to the fact that microparticles-based AFG cannot be fully rehydrated. More experiments should be conducted in the future, loading other types of actives in AFG to investigate their usage as materials for the controlled release overtime of actives. These results can be relevant from both a scientific and industrial point of view, since they lead to a better understanding of the AFG behaviour and suggest that FD can be applied to extend their shelf life, without any compromise in the material properties.

Acknowledgement

This research was funded by the Engineering and Physical Sciences Research Council [grant number EP/K030957/1], the EPSRC Centre for Innovative Manufacturing in Food.

4.5 References

1. Garrec, D.A. and I.T. Norton, *Understanding fluid gel formation and properties.* Journal of Food Engineering, 2012. **112**(3): p. 175-182.
2. Norton, D.A. Jarvis, and T.J. Foster, *A molecular model for the formation and properties of fluid gels.* International Journal of Biological Macromolecules, 1999. **26**(4): p. 255-261.
3. García, et al., *Gellan gum fluid gels: influence of the nature and concentration of gel-promoting ions on rheological properties.* Colloid and Polymer Science, 2018. **296**(11): p. 1741-1748.
4. Wang, Y., et al., *Rheology and microstructure of heat-induced fluid gels from Antarctic krill (Euphausia superba) protein: Effect of pH.* Food Hydrocolloids, 2016. **52**: p. 510-519.
5. García, et al., *Gellan gum fluid gels: influence of the nature and concentration of gel-promoting ions on rheological properties.* Colloid and Polymer Science, 2018.
6. Norton, et al., *Functional food microstructures for macronutrient release and delivery.* Food & Function, 2015. **6**(3): p. 663-678.
7. Chung, C., B. Degner, and D.J. McClements, *Development of Reduced-calorie foods: Microparticulated whey proteins as fat mimetics in semi-solid food emulsions.* Food Research International, 2014. **56**: p. 136-145.
8. Le Révérend, B.J.D., et al., *Colloidal aspects of eating.* Current Opinion in Colloid & Interface Science, 2010. **15**(1): p. 84-89.
9. Fernández Farrés, I., R.J.A. Moakes, and I.T. Norton, *Designing biopolymer fluid gels: A microstructural approach.* Food Hydrocolloids, 2014. **42**: p. 362-372.
10. Norton, W.J. Frith, and S. Ablett, *Fluid gels, mixed fluid gels and satiety.* Food Hydrocolloids, 2006. **20**(2): p. 229-239.
11. García, et al., *Influence of polysaccharides on the rheology and stabilization of α-pinene emulsions.* Carbohydrate polymers, 2014. **105**: p. 177-183.
12. Mahdi, M.H., et al., *Gellan gum fluid gels for topical administration of diclofenac.* International Journal of Pharmaceutics, 2016. **515**(1): p. 535-542.
13. Torres, O., B. Murray, and A. Sarkar, *Emulsion microgel particles: Novel encapsulation strategy for lipophilic molecules.* Trends in Food Science & Technology, 2016. **55**: p. 98-108.
14. de Bruijn, J., et al., *Effect of vacuum microwave drying on the quality and storage stability of strawberries.* Journal of Food Processing and Preservation, 2016. **40**: p. 1104-1115.
15. Brown, Z.K., et al., *Drying of agar gels using supercritical carbon dioxide.* The Journal of Supercritical Fluids, 2010. **54**(1): p. 89-95.
16. Prosapio, V. and I. Norton, *Simultaneous application of ultrasounds and firming agents to improve the quality properties of osmotic + freeze-dried foods.* LWT, 2018. **96**: p. 402-410.
17. Brown, Z.K., et al., *Drying of foods using supercritical carbon dioxide — Investigations with carrot.* Innovative Food Science & Emerging Technologies, 2008. **9**(3): p. 280-289.
18. Prosapio, V., I. Norton, and I. De Marco, *Optimization of freeze-drying using a Life Cycle Assessment approach: Strawberries' case study.* Journal of Cleaner Production, 2017. **168**: p. 1171-1179.

19. Vega-Gálvez, A., et al., *Influence of drying temperature on dietary fibre, rehydration properties, texture and microstructure of cape gooseberry (physalis peruviana l.).* Journal of Food Science and Technology, 2015. **52**: p. 2304-2311.
20. Prosapio, V. and I. Norton, *Influence of osmotic dehydration pre-treatment on oven drying and freeze drying performance.* LWT - Food Science and Technology, 2017. **80**: p. 401-408.
21. Karam, M.C., et al., *Effects of drying and grinding in production of fruit and vegetable powders: a review.* Journal of Food Engineering, 2016. **188**: p. 32-49.
22. Barbosa, J., et al., *Comparison of spray drying, freeze drying and convective hot air drying for the production of a probiotic orange powder.* Journal of Functional Foods, 2015. **17**: p. 340-351.
23. Sanchez, V., et al., *Freeze-Drying Encapsulation of Red Wine Polyphenols in an Amorphous Matrix of Maltodextrin.* Food and Bioprocess Technology, 2013. **6**(5): p. 1350-1354.
24. Cassanelli, M., et al., *Acidified/basified gellan gum gels: The role of the structure in drying/rehydration mechanisms.* Food Hydrocolloids, 2018. **82**: p. 346-354.
25. Bonifacio, M.A., et al., *Insight into halloysite nanotubes-loaded gellan gum hydrogels for soft tissue engineering applications.* Carbohydrate Polymers, 2017. **163**: p. 280-291.
26. De Marco, I. and E. Reverchon, *Starch aerogel loaded with poorly water-soluble vitamins through supercritical CO2 adsorption.* Chemical Engineering Research and Design, 2017. **119**: p. 221-230.
27. Franco, P., et al., *Supercritical Adsorption of Quercetin on Aerogels for Active Packaging Applications.* Industrial & Engineering Chemistry Research, 2018. **57**(44): p. 15105-15113.
28. Jin, H., et al., *Nanofibrillar cellulose aerogels.* Colloids and Surfaces A: Physicochemical and Engineering Aspects, 2004. **240**(1-3): p. 63-67.
29. Long, L.Y., Y.X. Weng, and Y.Z. Wang, *Cellulose aerogels: Synthesis, applications, and prospects.* Polymers, 2018. **8**(6).
30. Mao, B., T. Divoux, and P. Snabre, *Impact of saccharides on the drying kinetics of agarose gels measured by in-situ interferometry.* Scientific Reports, 2017. **7**: p. 41185.
31. Smirnova, I., J. Mamic, and W. Arlt, *Adsorption of Drugs on Silica Aerogels.* Langmuir, 2003. **19**(20): p. 8521-8525.
32. Cardea, S., P. Pisanti, and E. Reverchon, *Generation of chitosan nanoporous structures for tissue engineering applications using a supercritical fluid assisted process.* Journal of Supercritical Fluids, 2010. **54**(3): p. 290-295.
33. Hu, Y., et al., *Effect of Different Drying Methods on the Protein and Product Quality of Hairtail Fish Meat Gel.* Drying Technology, 2013. **31**(13-14): p. 1707-1714.
34. Cassanelli, M., et al., *Role of the Drying Technique on the Low-Acyl Gellan Gum Gel Structure: Molecular and Macroscopic Investigations.* Food and Bioprocess Technology, 2019. **12**(2): p. 313-324.
35. Tiwari, S., A. Chakkaravarthi, and S. Bhattacharya, *Imaging and image analysis of freeze-dried cellular solids of gellan and agar gels.* Journal of Food Engineering, 2015. **165**: p. 60-65.
36. McHugh, D., *Production, properties and uses of alginates.* 1987. **288**: p. 58-115.

37. Fernández Farrés, I., M. Douaire, and I.T. Norton, *Rheology and tribological properties of Ca-alginate fluid gels produced by diffusion-controlled method.* Food Hydrocolloids, 2013. **32**(1): p. 115-122.
38. Korsmeyer, R.W., et al., *Mechanisms of solute release from porous hydrophilic polymers.* International Journal of Pharmaceutics, 1983. **15**(1): p. 25-35.
39. Siepmann, J., A. Streubel, and N.A. Peppas, *Understanding and Predicting Drug Delivery from Hydrophilic Matrix Tablets Using the "Sequential Layer" Model.* Pharmaceutical Research, 2002. **19**(3): p. 306-314.
40. Rinaki, E., G. Valsami, and P. Macheras, *The power law can describe the 'entire' drug release curve from HPMC-based matrix tablets: a hypothesis.* International Journal of Pharmaceutics, 2003. **255**(1): p. 199-207.
41. Ratti, C., *Hot air and freeze-drying of high-value foods: a review.* Journal of Food Engineering, 2001. **49**: p. 311-319.
42. Stevenson, A., et al., *Is there a common water-activity limit for the three domains of life?* The ISME Journal, 2015. **9**: p. 1333-1351.
43. Badita, C.R., et al., *The study of the structural properties of very low viscosity sodium alginate by small-angle neutron scattering.* AIP Conference Proceedings, 2016. **1722**(1): p. 220007.
44. He, X., et al., *Single-stranded structure of alginate and its conformation evolvement after an interaction with calcium ions as revealed by electron microscopy.* RSC Advances, 2016. **6**(115): p. 114779-114782.
45. Braccini, I. and S. Pérez, *Molecular Basis of Ca2+-Induced Gelation in Alginates and Pectins: The Egg-Box Model Revisited.* Biomacromolecules, 2001. **2**(4): p. 1089-1096.
46. Budavari, S., *The Merck Index - An Encyclopedia of Chemicals, Drugs, and Biologicals.* 1996, Whitehouse Station, NJ.: Merck and Co. 1114.
47. Secouard, S., et al., *Release of limonene from polysaccharide matrices: viscosity and synergy effect.* Food Chemistry, 2003. **82**(2): p. 227-234.
48. Maldonado, S., E. Arnau, and M. Bertuzzi, *Effect of temperature and pretreatment on water diffusion during rehydration of dehydrated mangoes.* Journal of Food Engineering, 2010. **96**(3): p. 333-341.
49. Ratti, C., *Advances in food dehydration*. 2008: CRC Press.
50. Lopez-Quiroga, E., et al., *Model discrimination for drying and rehydration kinetics of freeze-dried tomatoes.* Journal of Food Process Engineering, 2019: p. e13192.
51. Smaniotto, F., et al., *Use of Alginate Fluid Gel Microparticles to Modulate the Release of Hydrophobic Actives*. 2019.
52. Yang, Y., J. Qian, and D. Ming, *Docking polysaccharide to proteins that have a Tryptophan box in the binding pocket.* Carbohydrate Research, 2015. **414**: p. 78-84.

Chapter 5: FREEZE-DRYING OF ALGINATE FLUID GELS: A WAY TO EXTEND BIOACTIVES SHELF LIFE

F. Smaniotto*, V. Prosapio, I. Zafeiri, F. Spyropoulos

School of Chemical Engineering, University of Birmingham, Edgbaston, Birmingham B15 2TT, United Kingdom

*fxs680@student.bham.ac.uk

Abstract

Bioactives encapsulation and controlled release from biopolymer-based gels has been studied widely in the last decades for pharmaceuticals and food applications. Fluid gels are a special class of soft-solid particles produced by applying a shear environment to a hydrocolloid solution undergoing gelation. Their use as entrapment entity for bioactives of therapeutic or nutritional interest has not been deeply investigated. The aim of this work was to assess if alginate fluid gels (AFG) are able to extend the shelf-life of bioactives that easily degrade, specifically ascorbic acid (ASC), by creating a protective environment. Degradation tests, conducted at R.T., confirmed that ASC was fast degraded in AFG formulations. For this reason, the effect of freeze-drying (FD) to prevent ASC degradation within AFG was studied. This technique was able to avoid the ASC degradation. Afterwards, dried materials were rehydrated and they were able to fully recover the ASC encapsulation behaviour they had before FD. Overall, this study expands the possible applications of AFG in the field of food formulations as materials to prevent bioactives degradation for long shelf-life periods.

Keywords: Fluid gel; freeze-drying; rehydration; shelf-life extension.

5.1 Introduction

In the food area, encapsulation of bioactives is employed for different purposes, such as to improve their delivery at the site of action, prolong activity in human body, controlling release and protect sensitive actives from degradation, induced by environmental conditions, like high moisture content, acidity and presence of enzymes [1, 2]. Nutraceuticals, drugs and probiotics are some examples of compounds that have been introduced in edible matrices [3]. Specifically, microencapsulation has been largely studied for the protection of actives against harsh environmental conditions, known to cause active degradation during food processing, storage and consumption [4]. The few micrometre dimensions of these systems are ideal for food applications, since particles bigger than 20-40 μm are usually detected in mouth during chewing, affecting the food mouthfeel [5].

Hydrocolloid-based microparticles are biocompatible, renewable and natural materials that find applications as texturisers, thickening agents and stabilisers due to their soft-solid particles nature. Recent studies revealed their potential application as encapsulation and slow-release matrices for bioactives [6, 7]. Over the last two decades fluid gel production has been investigated as a continuous and easy scalable way to produce hydrocolloid-based microparticles [8, 9]. Fluid gels are suspensions of gelled microparticles in water, produced by shearing a biopolymer solution undergoing gelation [8, 10]. Tribological and rheological studies of fluid gels have shown their ability to provide lubrication during chewing and impart a sensory response similar to that typically associated by fats [11]. Due to their small particle dimensions (<10 μm) fluid gel particles are not prone to be detected during chewing, finding potential applications in the food industry as fat replacers [12, 13], texturizers [14], satiety enhancers [15] and emulsion stabiliser [16]. A rheological and tribological investigation, conducted by Farrés *et al.* (2014), on Alginate Fluid Gels (AFG) revealed that their microparticles behaved in similarly to oil droplets in an o/w emulsion and can be potentially used for the development of fat-reduced foods [14]. A novel application of fluid gels is for the encapsulation of bioactives [17, 18]. A previous study revealed AFG potential applications for the encapsulation and delivery of tryptophan [19]. However, AFG shelf-life is relatively short, due to the presence of a large amounts of water, rendering them vulnerable to microbial spoilage. Studies shown that a dried product can be considered safe from bacterial/moulds growth if it has a water activity (a_w) value lower than 0.6 [20, 21]. However, the drying of food

products has been reported to cause some damage to their microstructure, leading to poor recovery of their initial texture and structure upon rehydration [22]. FD is a low temperature dehydration process that involves freezing the materials and apply vacuum to remove the solvent by sublimation [23]. FD operates at the freezing point of the solvent and, among drying methods, removes the highest rate of water and best retain the food texture and structure after rehydration [24, 25]. In a previous study, the stability of AFG formulations to FD was studied, revealing that drying and rehydration processes do not affect their PSD [26]. FD is also used as an encapsulation method for easily degradable bioactives in food and pharmaceutical formulations, due to its gentle process conditions [27].

ASC, commonly known as vitamin C, is a natural antioxidant that is fast degraded in high a_w environments [28]. It oxidizes first to dehydroascorbic acid, then to diketogulonic acid, oxalic acid and threonic acid, which leads to its irreversible degradation, as shown in Figure 5.1:

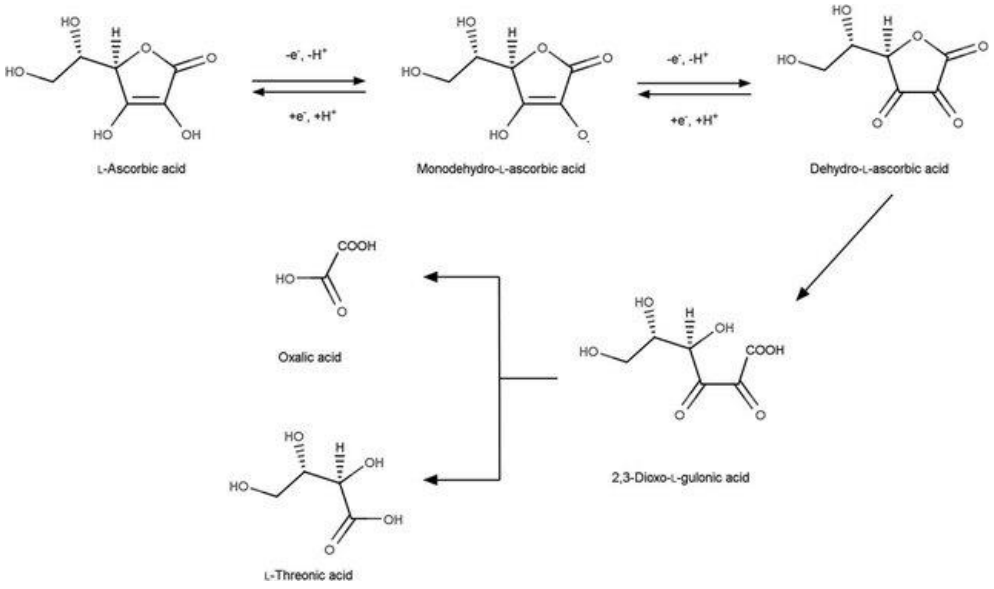

Figure 5. 1 - Degradation mechanism of ASC [28]

ASC content in food decreases during food preparation, storage and its rate of degradation is strongly influenced by temperature [29]. To compensate for ASC losses, foods are often fortified with ASC to increase their stability, shelf-life and to meet the population daily requirement of this vitamin [30].

In a previous study, AFG encapsulation of nicotinamide, used as hydrophilic model active, revealed that these materials were able to slow down its release and this effect was attributed to the increased bulk viscosity, if compared to a water solution of the same active [26]. In

addition to this, the long diffusion path of the active, due to the presence of a very high fraction of dispersed particles, significantly delayed its diffusion from AFG materials, even though the continuous medium surrounding these particles can be assumed to possess a "local" viscosity similar to water.

The current study investigated the impact of FD on AFG formulations loaded with ASC, chosen as a model hydrophilic active (water solubility at 25 °C ≈330 mg/mL). The final scope was to prevent ASC degradation as well as to increase the shelf-life of AFG formulations by recovering their release behaviour of ASC upon rehydration, taking advantage of the behaviour of hydrophilic actives of not being entrapped within AFG particles. The degradation of ASC in AFG was firstly investigated and the impact of ASC presence/concentration on AFG particle sizes and rheological properties was assessed too.

5.2 Materials and methods

5.2.1 Materials

Sodium alginate (CAS: 9005-38-3, W201502, lot.# MKBT7870V) and ascorbic acid (ASC, ≥99.0%, HPLC) were purchased from Sigma-Aldrich® (Sigma–Aldrich Company Ltd., Dorset, UK). Calcium chloride ($CaCl_2$, anhydrous, 93%) was purchased from Alfa Aesar™ (Varela, #159). All materials were used without further purification. Milli-Q water was made using an Elix® 5 distillation apparatus (Millipore®, USA) and was used for all water-based preparations.

5.2.2 Gel preparation

5.2.2.1 Blank fluid gels

Firstly, an alginate solution was prepared by dissolving 2% w/w of ALG, calculated on the final weight of the material, in distilled water at 95 °C until complete powder dissolution. The solution was cooled at R.T.. Another solution was prepared by dissolving $CaCl_2$ in water at R.T. using concentrations of 0.25%, 0.35% w/w, calculated on the final weight of the material, depending on the final $CaCl_2$/ALG ratio needed. Alginate Fluid Gels (AFG) were then prepared as described in section 4.2.2.1 Blank fluid gels.

5.2.2.2 Ascorbic acid fluid gels

Solutions having different concentrations of ASC, specifically 0.05%, 0.10% and 0.20% (w/w), were prepared by dissolving ASC in distilled water at R.T.. Then, different amounts of $CaCl_2$,

specifically 0.25%, 0.35% w/w, calculated on the final weight, were dissolved at R.T., depending on the final $CaCl_2$/ALG ratio needed. Ascorbic Acid Fluid Gels (AAFG) were then prepared in a pin-stirrer vessel using a 2% w/w ALG solution by following the procedure reported in section 2.2.1 Blank fluid gels.

5.2.3 Rheological measurements

The rheological properties of fluid gels were determined by shear viscosity tests using a rotational rheometer (Kinexus™, Malvern®, UK) equipped with a 40 mm diameter sand blasted plate geometry. The analyses were carried out at 25 °C using a shear rate ramp between 0.01 and 100 s^{-1} and a 0.3 mm gap. All measurements were carried out in triplicate and all data are presented/plotted as the mean value± the standard deviation (SD).

5.2.4 Particle Size Distribution

The particle size distribution (PSD) of fluid gels was evaluated using a Mastersizer (Mastersizer-2000, Malvern®, UK). Few drops of sample were placed into the mixing chamber and stirred for 10 min at 1300 RPM before performing the analysis to disrupt any possible macro-aggregation. PSD was evaluated as numerical particle sizes percentage by the Mastersizer software, using a refractive index of 1,335. All measurements were carried out in triplicate and all data are presented/plotted as the mean value± SD. PSD values obtained with this technique were validated in a previous study using DLS measurements and optical microscope imaging, confirming that Mastersizer is a suitable technique for the particle size determination of AFG [26].

5.2.5 Freeze-drying

Fluid gels were frozen at -24 °C overnight and then lyophilised using a bench top freeze dryer (110-4, SCANVAC Coolsafe™, DK), with a condenser temperature set at -110 °C and a vacuum pressure of 10 Pa. These conditions were defined by the equipment.

5.2.6 Water activity analysis

Samples water activity (a_w) was measured using a dew point water activity meter (4TE AquaLab®, Decagon Devices Inc., Pullman, WA, USA). The analysis chamber temperature was set to 25 °C. Analyses were carried out in triplicate.

5.2.7 UV-Vis measurements

The UV absorbance of the aqueous solutions of actives was measured using an UV-Vis spectrophotometer (Orion AquaMate 8000, Thermo-Scientific®, UK). Maximum absorbance wavelength of ASC was experimentally detected to be 248 nm and used for all UV-Vis analyses. Absorbance values were correlated to the corresponding active concentration using the Beer-Lambert equation via a calibration curve: this was made at 248 nm wavelength and was set for concentrations between 0.53 and 53 μg/mL. Analyses were carried out at R.T.. All measurements were carried out in triplicate and all data were presented/plotted as the mean value± SD.

5.2.8 Encapsulation efficiency

The encapsulation efficiency (EE) of ASC in AAFG particles was determined by ultracentrifugation: a weighed amount of sample (approx. 15g) was centrifuged using a refrigerated centrifuge (3K-30, Sigma®, DK), equipped with a 12150 rotor. Centrifugation was performed at 21 °C, 21,000 RPM for 45 minutes. These conditions were determined experimentally by performing preliminary tests (not reported here) and they revealed a sufficient separation between the AFG aqueous phase and particles, allowing easy sampling of the supernatant. A weighed amount of the supernatant (approx. 1.5 g) was placed in a 100 mL volumetric flask and filled with distilled water. The concentration of ASC within the flask was determined via UV-Vis analysis, as reported in section 5.2.7 UV-Vis measurements. The EE was calculated using Equation (5.1):

$EE = (W_t/W_i)\times 100$ (Equation 5.1)

where, W_i is the amount of ASC added initially to the AAFG sample preparation and W_t is the amount of encapsulated ASC. W_t was calculated as the difference between the theoretical concentration of ASC added into the sample and the concentration detected in the supernatant phase by UV-Vis analysis [31].

5.2.9 Release studies

In vitro release studies of ASC from AAFG were performed using sink conditions: a weighed amount of AAFG (approx. 2.5 g) was enclosed within a dialysis bag (Sigma–Aldrich Company Ltd., Dorset, UK, dialysis tubing cellulose membrane, width 43 mm, M.W. cut-off of 14000 Da) and placed in 500 mL of distilled water at R.T. (thermostated at 21.5 °C), under magnetic-

stirring at 150 RPM. At regular intervals, aliquots of 2 mL were withdrawn and ASC concentration was measured using the UV-Vis as described in section 5.2.7 UV-Vis measurements. Aliquots were poured back again into the release medium. All measurements were carried out in triplicate and all data were presented/plotted as the mean value± SD.

5.2.10 ASC determination in dry formulations

A weighed amount of freeze-dried AAFG sample (approx. 100 mg) was placed into 100 g of water inside a plastic pot and agitated into an incubating orbital shaker (Incu-Shake MIDI, SciQuip®, UK) for one hour at 400 RPM and 20 °C. Then the liquid was centrifuged (Sigma 2-5, SciQuip®, UK) at 4000 RPM for one hour. The concentration of ASC in the supernatant was measured using an UV-Vis spectrophotometer as described in section 5.2.7 UV-Vis measurements. Each analysis was carried out in triplicate.

5.2.11 Rehydration of freeze-dried materials

AAFG were weighed before being freeze-dried. The samples rehydration was performed by adding to dry materials amounts of distilled water to obtain the same sample weight they had before FD. Samples were then transferred into an incubating orbital shaker (Incu-Shake MIDI, SciQuip®, UK), in order to obtain a homogeneous rehydration of the material, for one hour at 400 RPM and 20 °C.

5.2.12 Statistical analysis

Statistical analysis of data groups was determined via single factor analysis of variance (ANOVA). P values < 0.05 were considered as statistically significant.

5.3 Results and discussion

In the first part of the study, ASC was loaded into AFG, in order to identify if they were able to encapsulate the active. A previous study showed that the $CaCl_2$/ALG ratio used during AFG production was responsible for the formation of nanometre or micrometre particles [26]. In particular, when a $CaCl_2$/ALG ratio of 0.125 was used nanoparticle materials were obtained, while 0.175 produced microparticles. Both these formulations were used to assess their ability to encapsulate ASC. “Blank” formulations were also prepared without the presence of ASC to see the effect of the active presence on AFG properties. In a previous study, conducted

on AFG loaded with tryptophan, the EE of this active was monitored over a time period of two weeks and release experiments were performed over the same time [19]. These tests revealed that the EE of tryptophan increased by increasing the storage time (t_s), i.e. the time elapsed from samples preparation until the analysis, and the amount of active detected in the release medium, after the plateau of release was reached, decreased by increasing t_s. It was concluded that tryptophan was prone to build hydrophobic interactions with the AFG network overtime, explaining the effects on EE and release experiments as a function of t_s. In the present study EE and release studies were performed on AAFG as a function of t_s to compare this results with what obtained from AFG loaded with tryptophan. This comparison was made also to assess the effect of active hydrophilicity on EE and release behaviours of AFG. Following that, FD experiments on AAFG were carried out. Dried materials were than rehydrated to investigate the possibility to prolong the shelf-life of both AFG and the ASC introduced in them.

5.3.1 Effect of ALG/$CaCl_2$ ratio

As a preliminary test, the amount of ASC introduced into AAFG was changed to identify if its concentration can affect the properties of AFG in terms of viscosity and PSD. ALG particles are known to undergo morphological shrinkage in a low pH environment, in particular below pH 4 [32]. ASC has a mild acidic behaviour (pKa values: 4.2 and 11.6) and a water solution of ASC at 5% w/w has a pH of 2,2–2,5 [33]. The viscosity and PSD behaviours were therefore studied in both micro/nanoparticles forming AFG formulations. The $CaCl_2$/ALG ratio, and the concentration of ASC used for samples preparations are reported in Table 5.1:

Table 5. 1 - $CaCl_2$/ALG ratio and ASC concentration used for sample preparations

	$CaCl_2$/ALG ratio	**ASC concentration (w/w)**
nano (micro)_AAFG_0.00%	0.125 (0.175)	0.00%
nano (micro)_AAFG_0.05%	0.125 (0.175)	0.05%
nano (micro)_AAFG_0.10%	0.125 (0.175)	0.10%
nano (micro)_AAFG_0.20%	0.125 (0.175)	0.20%

5.3.1.1 Particle size distribution

Particle dimensions were evaluated as reported in section 5.2.4 Particle Size Distribution. Results are reported in Figure 5.2.

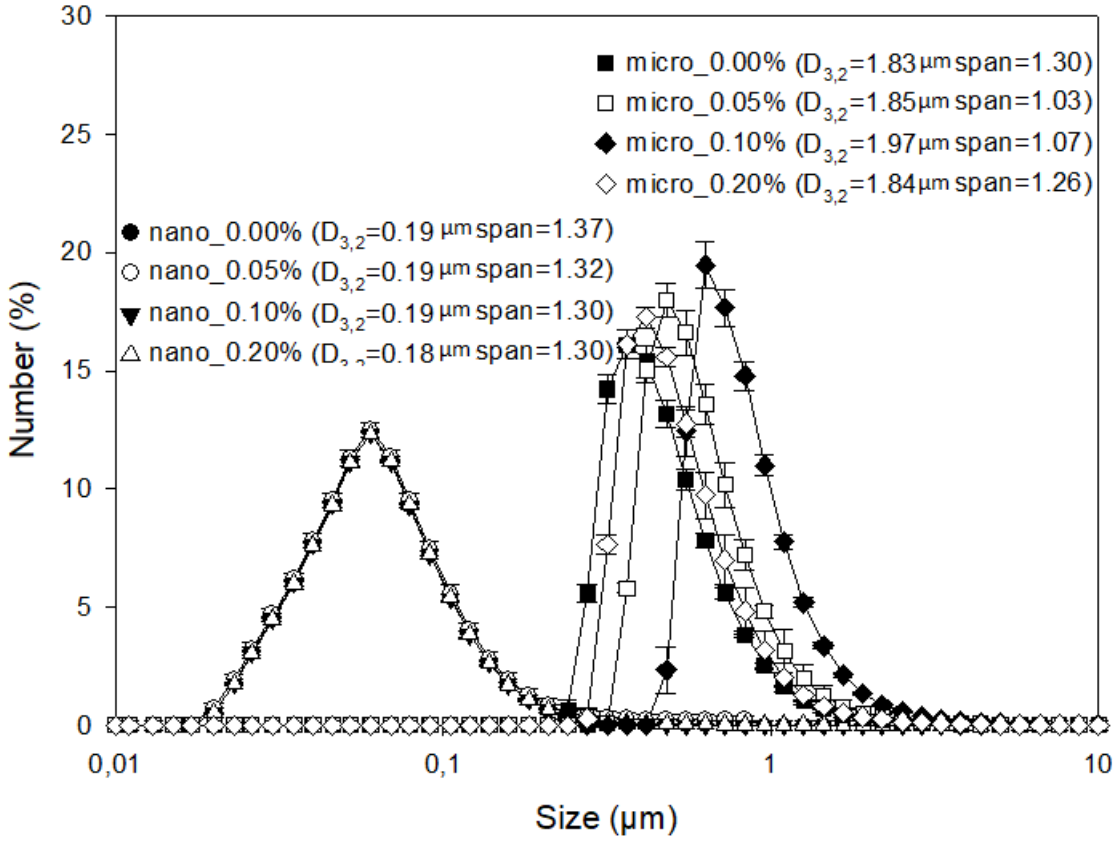

Figure 5. 2 - PSD curves of AAFG as a function of $CaCl_2$/ALG ratios

As can be noticed from Figure 5.2, particle dimensions of nano_AAFG had $D_{3,2}$ of 0.18-0.19 µm and span values of 1.30-1.37, and micro_AAFG samples had $D_{3,2}$ of 1.83-1.97 µm and span values of 1.03-1.30. These results were consistent with what reported in a previous study showing that $CaCl_2$/ALG ratio, used during AFG production, was responsible for the formation of nanometre or micrometre particles [26]. PSD curves of nano_AAFG samples were perfectly overlapping. The PSD of micro_AAFG samples presented some differences between them, but it was not possible to identify a trend for PSD variations as a function of ASC concentration.

5.3.1.2 Rheological properties

The rheological behaviour of rehydrated AAFG samples was tested as described in section 5.2.3 Rheological measurements. Viscosity curves are reported in Figure 5.3.

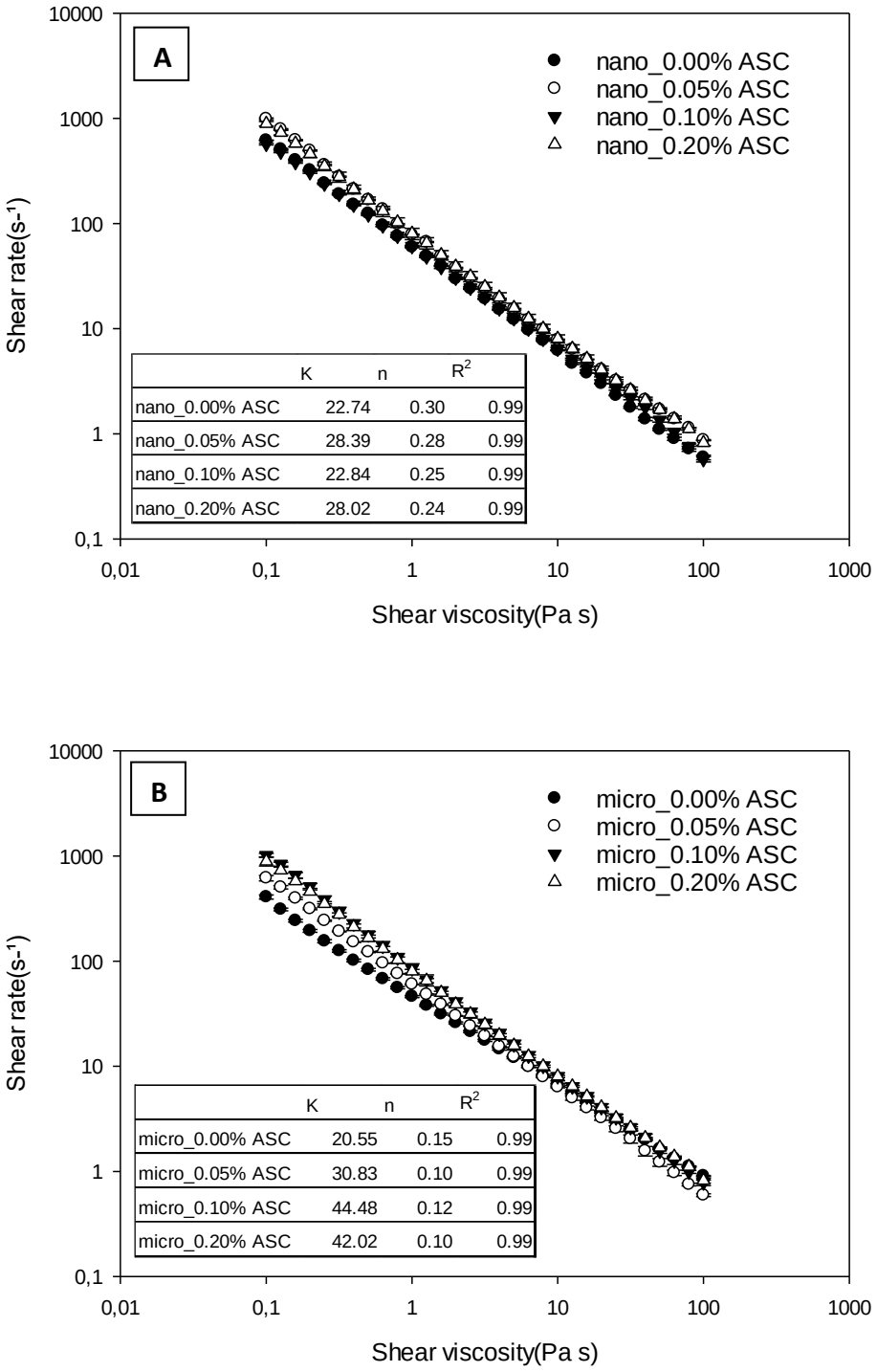

Figure 5. 3 - Shear viscosity curves of AAFG as a function of ASC concentration: (A) nanometre samples (B) micrometre samples

It is possible to notice that all viscosity curves of AAFG samples were almost overlapping, regardless of the used ASC concentration and/or the $CaCl_2$/ALG ratio used during samples preparation. The shear viscosity curves for all systems were comparable and displayed a similar shear thinning behaviour, as revealed by *n* parameters [34]. The flow behaviour of

AAFG formulations did not changed as a function of ASC presence and/or by its used concentration, probably because the used concentration of ASC was very low. The flow behaviour was not affected by gel particle dimensions and this is probably related to the microstructure of AFG. In fact, it has been reported that the flow behaviour of fluid gel systems is mainly dictated by the specific mechanical properties of the hydrocolloid used (ALG in this case) and by the particle fraction formed [10, 14]. For fluid gel systems, and specifically for AFG, this was reported to be close to the maximum packing fraction of particles and, therefore, particle-particle interactions are highly probable to happen within these materials [10, 14]. As both nano- and micro-AAFG were prepared using the same ALG concentration, a similar solid fraction was obtained, leading to similar particle-particle interactions and, therefore, to similar viscosities.

5.3.1.3 Encapsulation and release of ASC

The effect of AFG particle dimensions on the encapsulation and release behaviours of ASC was investigated by conducting EE and release tests as reported in sections 5.2.8 Encapsulation efficiency and 5.2.9 Release studies. A previous study showed that particles dimensions did not affect the release behaviour of nicotinamide from AFG, but AFG presence reduced its release rate when compared to a water/ALG solution of nicotinamide [26]. Similar tests were conducted also on AAFG to identify if the behaviour of ASC in AFG was similar to what observed for nicotinamide. Results are reported in Table 5.2 and Figure 5.4.

Table 5. 2 - EE results of AAFG samples

	Encapsulation Efficiency, EE (±SD)		
	1 Day	**1 Week**	**2 Weeks**
micro_AAFG_0.05%	3.9% (±0.5)	28.1% (±3.4)	93.6% (±4.2)
micro_AAFG_0.10%	4.7% (±0.4)	10.6% (±2.1)	29.6% (±3.1)
micro_AAFG_0.20%	1.5% (±0.3)	8.4% (±2.0)	16.9% (±2.7)
nano_AAFG_0.05%	1.2% (±0.7)	26.4% (±2.1)	86.9% (±4.8)
nano_AAFG_0.10%	4.7% (±1.5)	28.0% (±1.9)	35.0% (±4.1)
nano_AAFG_0.20%	1.1% (±0.9)	10.3% (±2.0)	19.5% (±2.9)

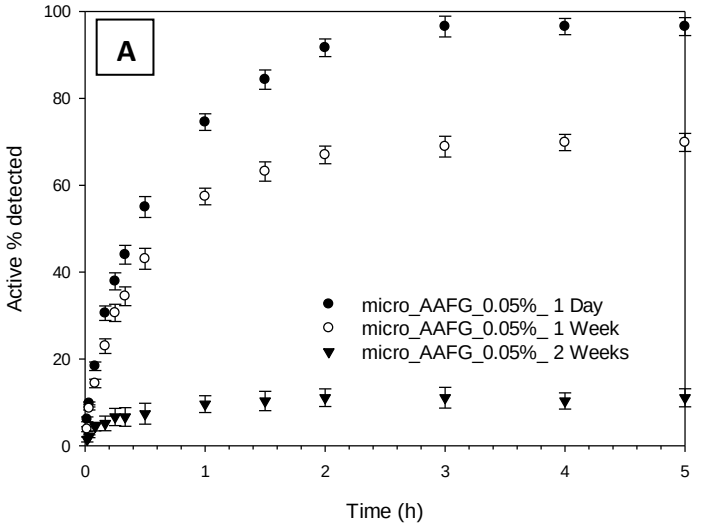
A
Active % detected
Time (h)
micro_AAFG_0.05%_ 1 Day
micro_AAFG_0.05%_ 1 Week
micro_AAFG_0.05%_ 2 Weeks

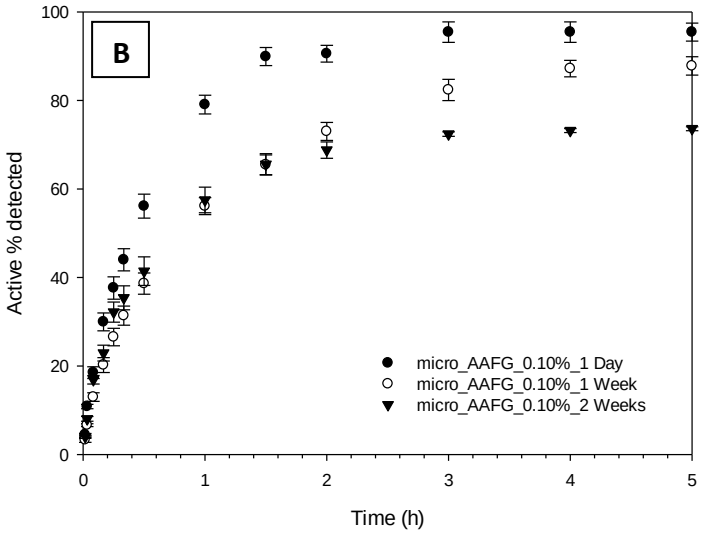
B
Active % detected
Time (h)
micro_AAFG_0.10%_1 Day
micro_AAFG_0.10%_1 Week
micro_AAFG_0.10%_2 Weeks

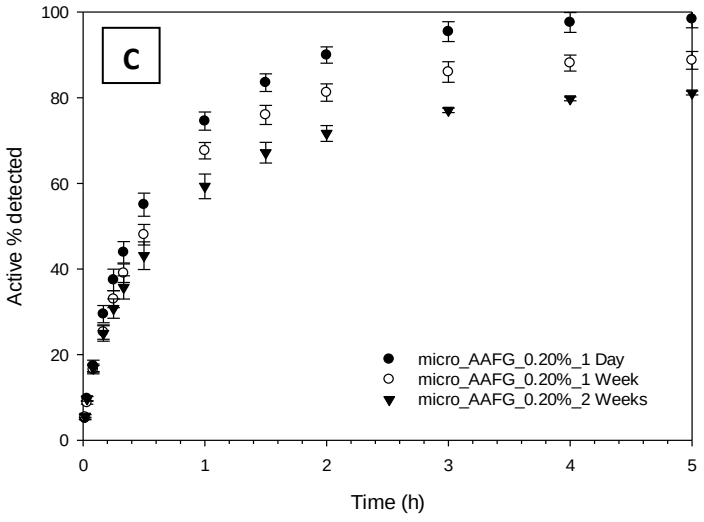
C
Active % detected
Time (h)
micro_AAFG_0.20%_1 Day
micro_AAFG_0.20%_1 Week
micro_AAFG_0.20%_2 Weeks

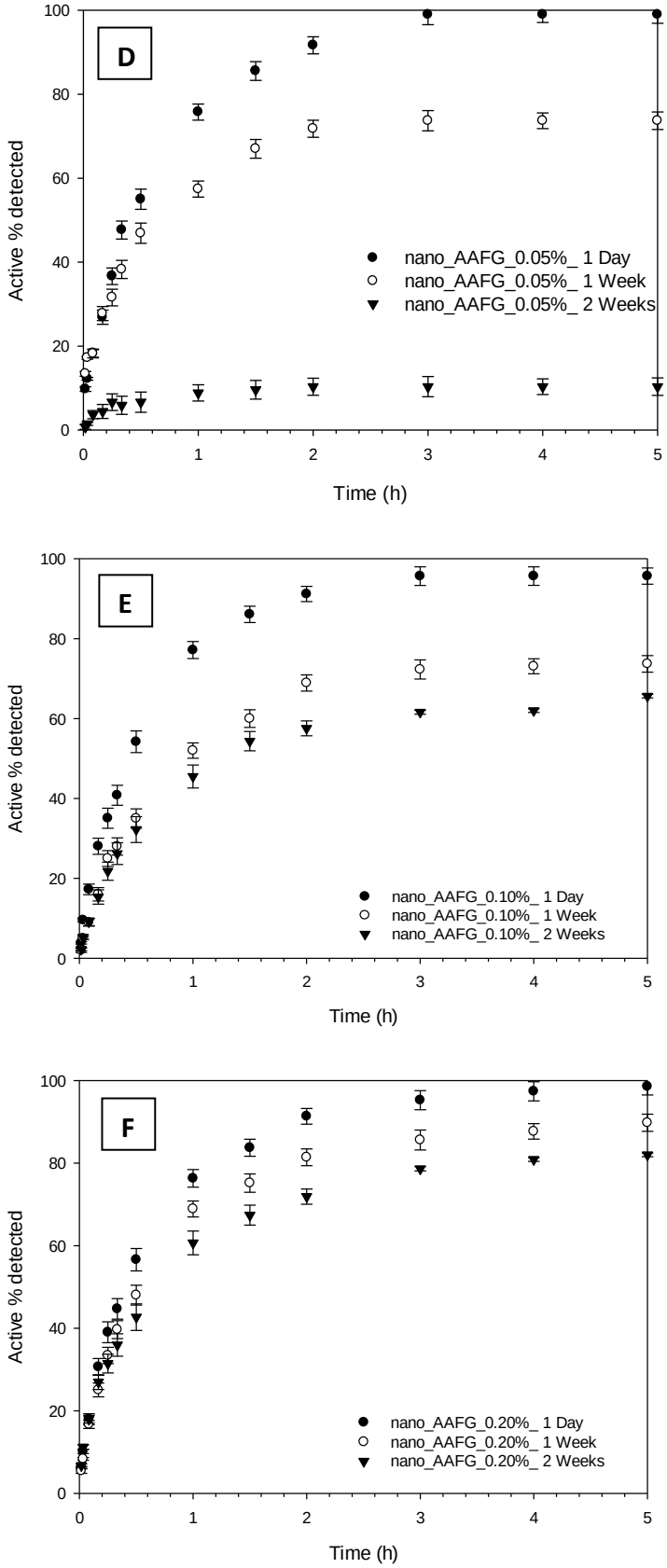

Figure 5. 4 - Release analyses of ASC from AAFG formulations as a function of storage time: (A) micro_AAFG_0.05% (B) micro_AAFG_0.10% (C) micro_AAFG_0.20% (D) nano_AAFG_0.05% (E) nano_AAFG_0.10% (F) nano_AAFG_0.20%

EE tests revealed that ASC was not highly encapsulated during production for all AAFG formulations. However, EE values increased as a function of t_s. What is more, for all AAFG formulations, the non-encapsulated ASC fraction, as determined from EE analyses (Table 5.2), and the maximum ASC cumulative release, as detected in the aqueous acceptor phase, in release studies (Figure 5.4), were practically identical, as can be seen in Figure 5.5. Here EE and release experiments data were converted from percentage basis to milligrams of ASC encapsulated/released per gram of AAFG formulation.

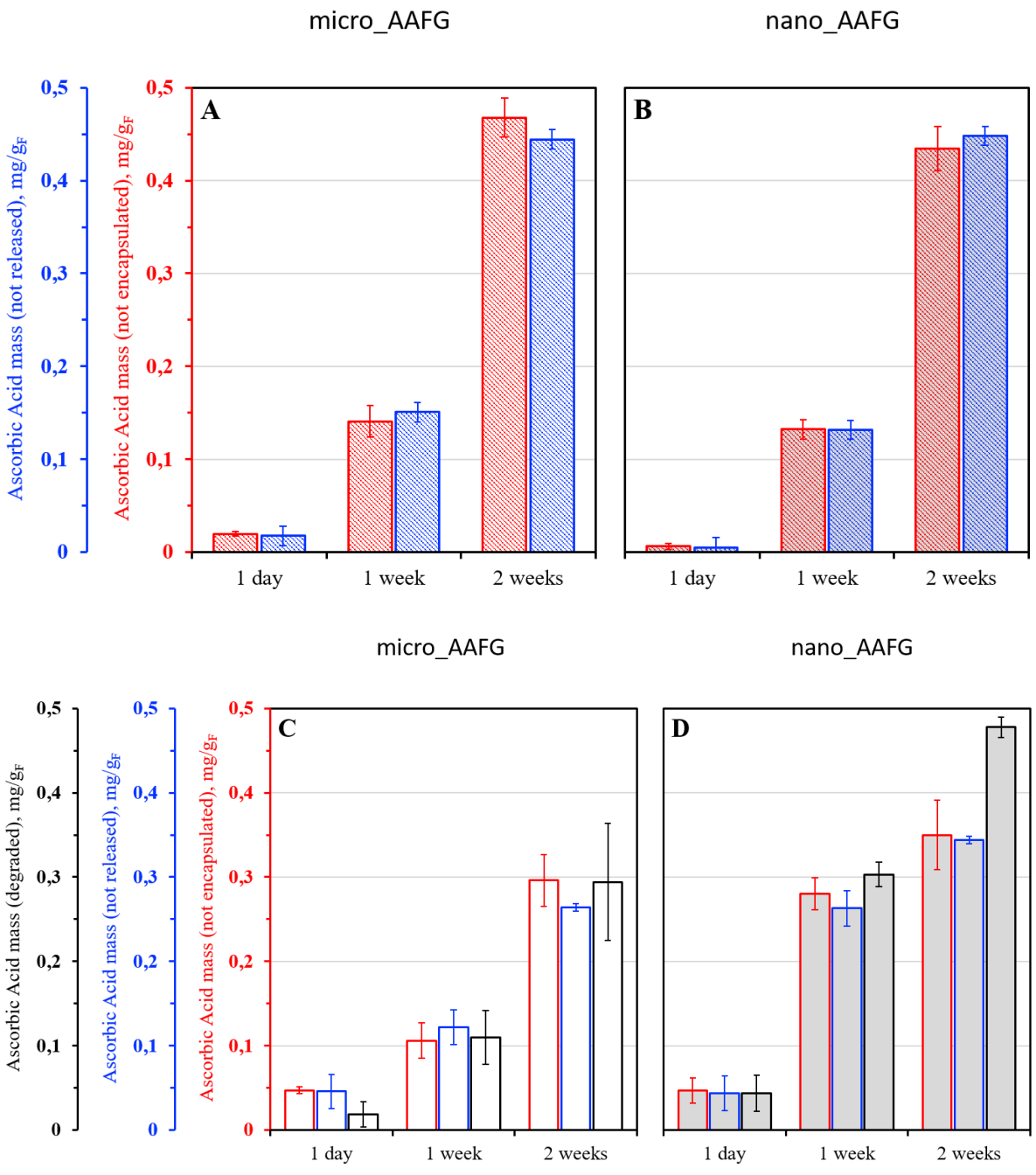

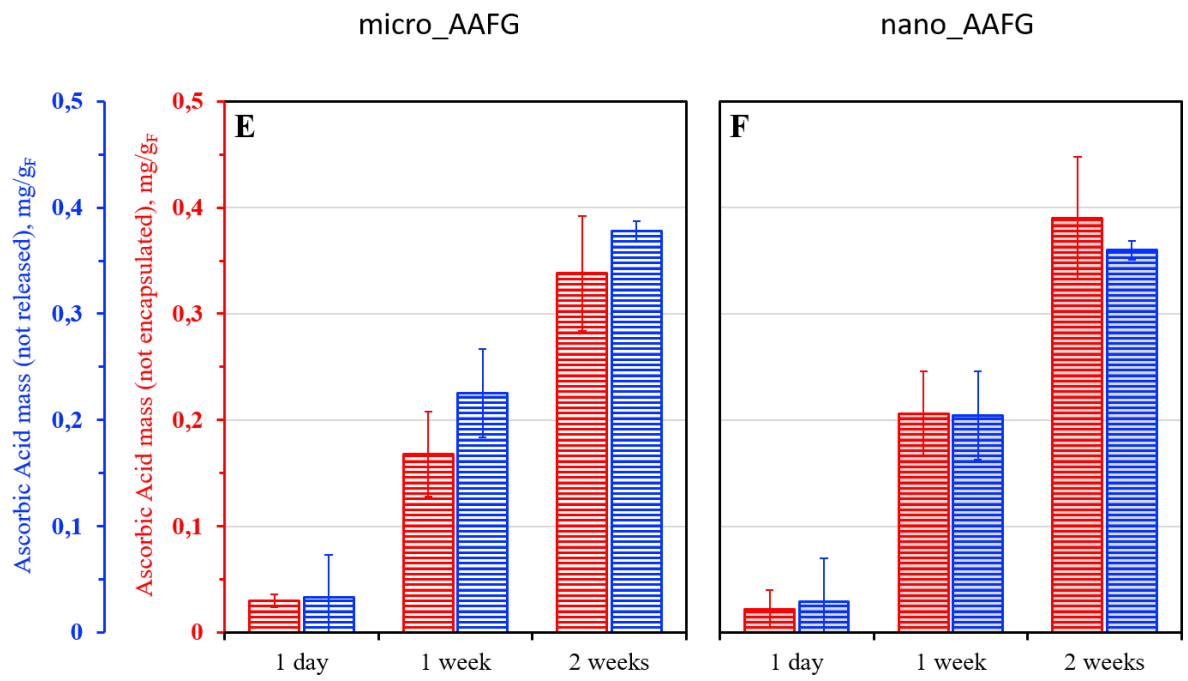

Figure 5. 5 - Comparison of encapsulation and release data of ASC from AAFG formulations as a function of storage time: (A, B) 0.05% ASC concentration (C, D) 0.10% ASC concentration (E, F) 0.20% ASC concentration

First, it is possible to notice that fractions of ASC encapsulated and released in AAFG were not affected by AFG particle dimensions, as for all ASC concentrations the mass of this active encapsulated/released did not change, when comparing similar t_s. However, an effect of ASC degradation overtime should be considered. In fact, EE was evaluated by detecting the ASC concentration in the continuous water phase outside particles and by knowing the concentration of ASC loaded during sample preparations. These tests only revealed that ASC concentration decrease in the water phase as a function of t_s. In a previous paper it was reported that hydrophilic actives were not prone to be entrapped in AFG [19, 26]. ASC is very hydrophilic, hence it is not expected to be irreversibly encapsulated into AFG. ASC degradation overtime could explain the observed increase of EE and the decreased amounts of ASC cumulative release as a function of t_s. To prove this hypothesis, ASC degradation studies of ASC-water solutions and of AAFG were performed.

5.3.2 Degradation of ASC

ASC degradation in high water activity environments overtime was extensively investigated in literature [30, 35-37]. As reported by Yuan *et al*. (1998), the degradation of ASC into its main degradation products 2-furoic acid, 3-hydroxy-2-pyrone and furfural, leads to a change in its of UV-Vis absorption [35]. In section 5.3.1.3 Encapsulation and release of ASC, EE

analyses were conducted using UV-Vis analysis, and therefore they could had been affected by ASC degradation. Peleg *et al.* (2016) reported that ASC degradation is time dependent, following a first-order kinetic of degradation, therefore explaining the observed increase of EE by increasing t_s [37]. ASC degradation experiments were conducted to prove that EE results were affected by ASC degradation and to determine the magnitude/rate of ASC degradation in AAFG vs. ASC-water solution.

5.3.2.1 ASC degradation in wet formulations

A 0.10% w/w ASC-water solution was prepared and divided in two aliquots into plastic sample pots wrapped with aluminium foil, to avoid potential light induced degradation. One was stored at R.T. and the other at 4 °C. Their ASC concentration was monitored via UV-Vis analysis every week over an eight weeks period. In addition, similar analyses were conducted on micro_AAFG_0.10% and nano_AAFG_0.10% using the same storage conditions. Results are reported in Figure 5.6 and they are presented as % of ASC not degraded as a function of time.

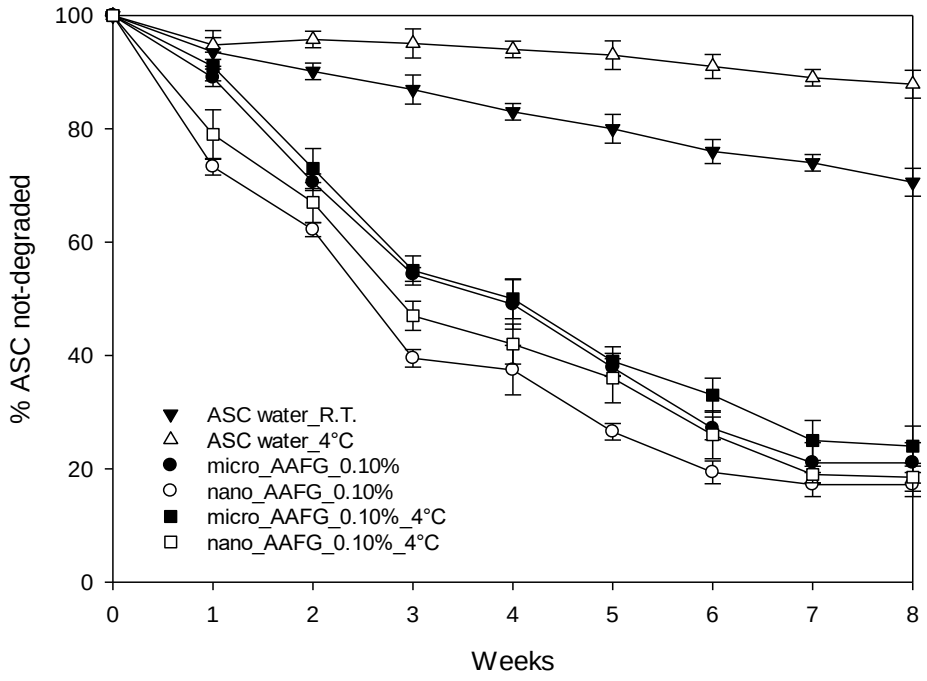

Figure 5. 6 - ASC degradation overtime in water solutions and in AAFG stored at R.T. and 4 °C (no significant differences [p > 0.05] were found between degradation experiments of AAFG sample, while significant differences [p < 0.05] were found between degradation experiments of ASC solutions stored at R.T. and at 4°C)

It can be noticed that ASC degradation in water happened almost constantly overtime: for the sample stored at R.T. approx. 3% w/w of ASC was degraded per week, while at 4 °C storage

approx. 1.5% w/w was degraded per week. Overall, fridge storage can decrease ASC degradation in water by approx. 50%. This is in accordance with what has been suggested by Klu *et al*. (2016) regarding storing formulations containing ASC under refrigeration/low temperature to minimize its degradation overtime [38]. However, decreasing ASC degradation by using low temperature was not observed for AAFG. In these samples ASC degradation happened significantly faster: after 8 weeks of storage only 20-30% of ASC was present in AAFG, while 70-90% was present in water solutions. ASC degradation rate in microparticle AAFG was slightly lower than the one in nanoparticles AAFG. However, this effect was almost negligible and it is possible to conclude that in both formulations ASC degraded at similar rates. The reason behind the faster ASC degradation in AAFG than in water solutions can be due to its anaerobic degradation, catalysed by metal ions presence, like Ca^{2+} used for ALG crosslinking, as reported by Pinholt *et al.* [39]. As can be appreciated in Figure 5.7 AAFG samples browned as a result of ASC degradation overtime, as previously seen in several studies [40, 41].

Figure 5. 7 - AFG sample aging: respectively from left to right, 1 day, 6 weeks and 8 weeks after production

In addition, as can be noticed from Figure 5.5 C&D, plotting the unencapsulated/unreleased ASC masses for 0.10% nano/micro_AAFG samples together with the amount of ASC degraded as a function of time, revealed that these two quantities were almost identical. Therefore, it can be concluded that the fractions of ASC encapsulated into nano/micro_AAFG samples, observes during EE and release tests, reported in section 5.3.1.3 Encapsulation and release of ASC, were in reality the fractions of ASC degraded as a function of time.

5.3.3 Freeze-drying

FD was studied as a method to prevent or delay ASC degradation within AAFG. Several studies showed that a decrease of moisture content delay ASC degradation in food products [36, 42]. FD studies were, therefore, conducted to assess if this process can avoid/reduce ASC degradation. Micro_AAFG_0.10% and nano_AAFG_0.10% were freeze-dried until constant weight and their a_w after FD was measured as reported in section 5.2.6 Water activity analysis, to verify that a complete drying was obtained a_w values are reported in Table 5.3.

Table 5. 3 - a_w values of freshly produced and freeze-dried micro/nano_AAFG_0.10%

	Water activity
micro_AAFG_0.10%	0.989 (±0.004)
micro_AAFG_0.10%_FD	0.080 (±0.016)
nano_AAFG_0.10%	0.992 (±0.008)
nano_AAFG_0.10%_FD	0.076 (±0.027)

An aliquot of each freeze-dried materials was taken and its ASC concentration was evaluated using the procedure reported in section 5.2.10 ASC determination in dry formulations. This procedure was repeated every week for an 8 week period, to compare ASC degradation rates in freeze-dried formulations with the ones obtained from untreated AAFG. Results are presented in Figure 5.8, comparing ASC degradation of freeze-dried and untreated AAFG and ASC-water solution stored at R.T..

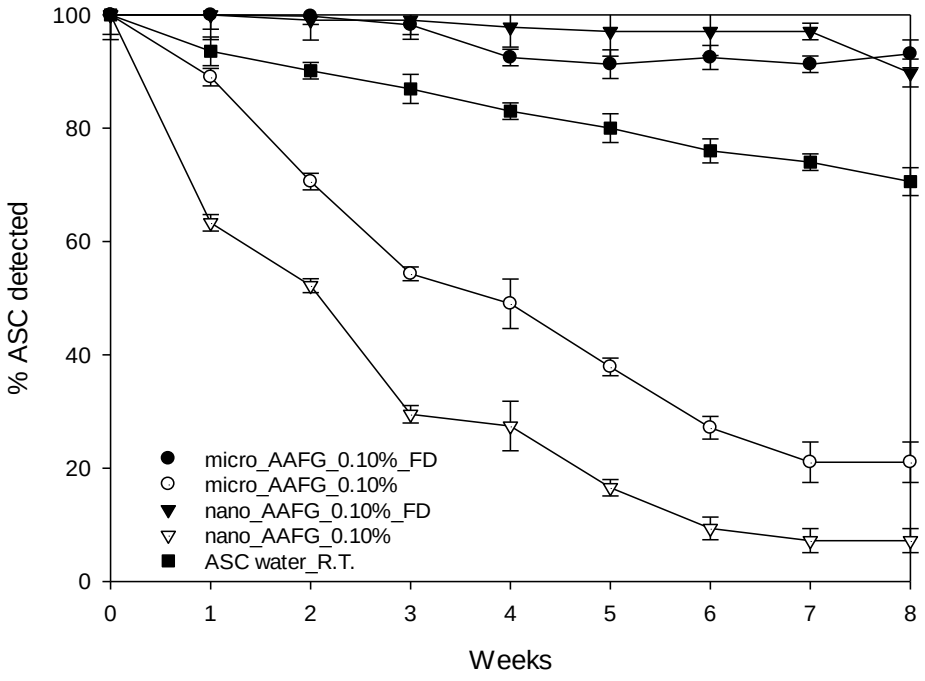

Figure 5. 8 - ASC degradation overtime in water solution, freeze-dried and untreated AAFG stored at R.T. (no significant differences [p > 0.05] were found between degradation experiments of AAFG_FD samples, while significant differences [p < 0.05] were found between degradation experiments of AAFG_FD samples, non-FD samples and ASC-water solution)

It is possible to notice that ASC degradation was significantly reduced by FD; less than 10% of ASC was degraded in freeze-dried AAFG after 8 weeks of storage at R.T.. The degradation of ASC in the solid state had been investigated extensively in literature [36, 38, 43]. Sanchez *et al.* (2018) reported a significant degradation rate of ASC in solid formulations when it was used at concentrations below 50% w/w [43]. In AAFG the ASC concentration was 0.10% w/w, explaining why approx. 10% of ASC degradation was observed even in the freeze-dried materials. However, the drying process was able to significantly reduce ASC degradation, even when compared with an ASC water solution. In addition, these rehydration experiments revealed that all ASC was able to be unloaded from AAFG after FD. This result confirmed that hydrophilic actives were not prone to form interactions with AFG strong enough to irreversibly encapsulate them. In conclusion, FD of AAFG was able to prevent ASC degradation and microbial growth in AFG, increasing the shelf-life of these materials as well. In fact, as reported by Beuchat *et al.* (1983), low water activity environments can prevent, or at least significantly reduce, the growth and proliferation of moulds, fungi and bacteria [44].

5.3.4 Rehydration effects

To evaluate the impact of FD on the encapsulation and release behaviours of ASC, EE and release experiments were conducted on AAFG that were freeze-dried and rehydrated. These were compared with results obtained from the same tests conducted on unprocessed AAFG. These tests were conducted after 1 day, 1 week and 2 weeks of storage, at R.T., following FD, to mimic the same aging of unprocessed AAFG samples. The rehydration was made following the procedure reported in section 5.2.11 Rehydration of freeze-dried materials, allowing the samples to fully reabsorb water. In a previous study, a rehydration time of 10 minutes was reported to be sufficient to restore the initial properties of AFG composed by nanoparticles [26]. On the contrary, the same study showed that the rehydration of AFG composed by microparticles cannot restore the material properties even at longer rehydration times, up to two days. Based on these results, a rehydration time of one hour was used to allow water to distribute homogeneously within freeze-dried AAFG and to provide consistency through all the experiments. Then, EE and release analyses were conducted, as described in sections 5.2.8 Encapsulation efficiency and 5.2.9 Release studies. Results are reported in Table 5.4 and Figure 5.9:

Table 5. 4 - EE results of freshly produced and rehydrated micro_AAFG_0.10% and nano_AAFG_0.10% samples

	Encapsulation Efficiency, EE (±SD)		
	1 Day	**1 Week**	**2 Weeks**
micro_AAFG_0.10%	4.7% (±0.4)	10.6% (±2.1)	29.6% (±3.1)
micro_AAFG_0.10%_REH	3.8% (±1.2)	4.0% (±1.5)	3.7% (±1.7)
nano_AAFG_0.10%	4.7% (±1.5)	11.8% (±1.9)	28.0% (±4.1)
nano_AAFG_0.10%_REH	3.9% (±1.1)	3.9% (±1.3)	3.6% (±1.8)

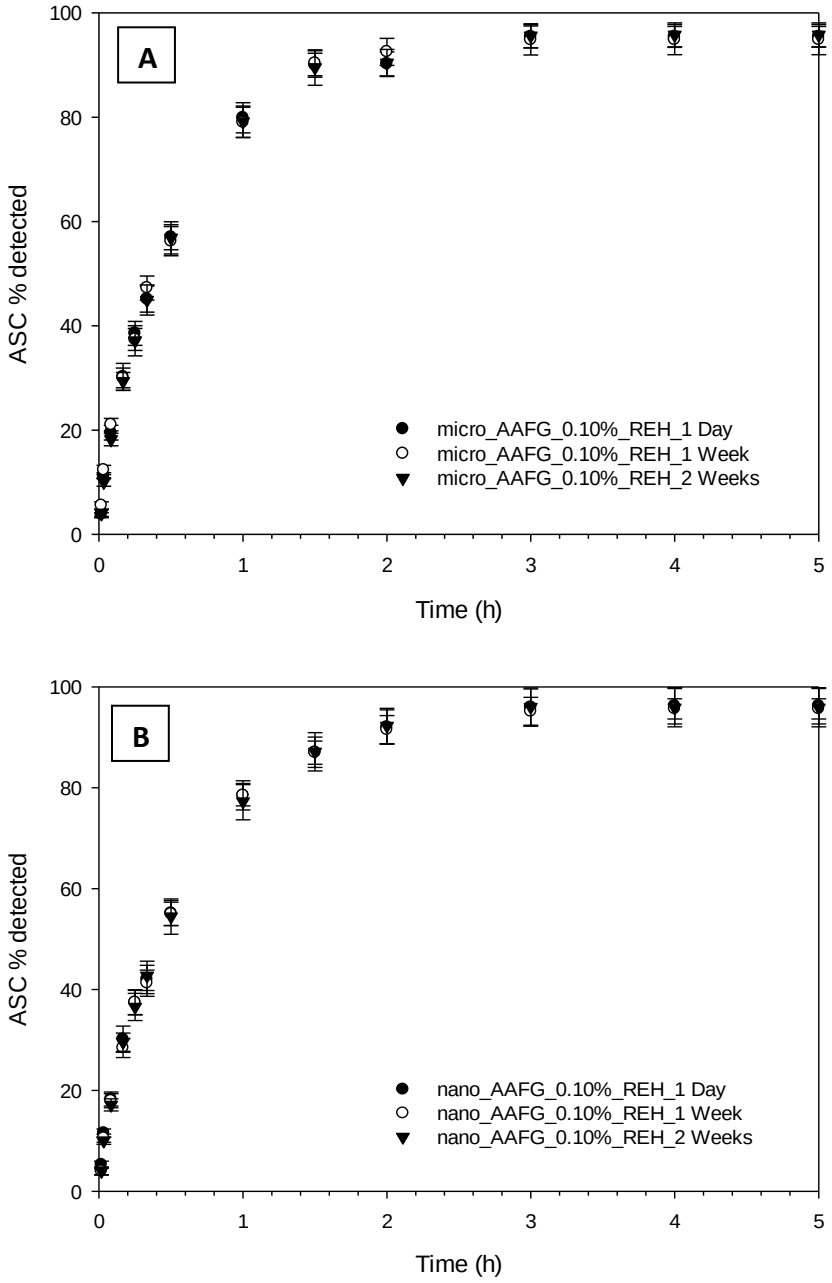

Figure 5. 9 - Release analyses of ASC from rehydrated AAFG formulations as a function of t_s after FD: (A) micro_AAFG_0.10%_REH (B) nano_AAFG_0.10%_REH (no significant differences [p > 0.05] were found between release experiments of FD and rehydrated AAFG samples rehydrated after 1 day, 1 week and 2 weeks)

EE tests clearly showed that FD was able to stop ASC degradation during two weeks of storage. Release experiments showed that the ASC fraction detected into the release medium, at the plateau of release, was almost identical to the percentage of ASC not degraded in AAFG formulations. In fact, release experiments showed that the percentage of ASC released did not change as a function t_s after FD, confirming that FD was able to stop ASC degradation. In addition, these tests confirmed that ASC was not irreversibly encapsulated within AFG particles, in contrast with what observed for hydrophobic ones [45]. FD and rehydration

processes did not influence the encapsulation and release behaviour of ASC within AFG and they were able to extend the shelf-life of the whole formulations.

5.4 Conclusions

In this work, the impact of ASC presence on AFG formulations and vice versa was investigated. It was concluded that ASC was not encapsulated in AFG particles. Although, the presence of AFG significantly accelerated the degradation of ASC, compared to that in an aqueous solution, the used $CaCl_2$/ALG ratio for AFG production, as well as the particle sizes of AFG, did not appear to further affect the rate of this phenomenon. FD of AFG loaded with ASC significantly decreased the rate of ASC degradation, due to water removal. What is more, freeze-dried formulations maintained their capacity to regulate the release of ASC upon rehydration. This study revealed a new potential method to preserve easy degradable actives within hydrocolloids systems that does not involve the use of preservatives. Overall, the current study offers new potential applications of AFG as encapsulation matrix and shelf-life enhancer for applications in the food fields.

Acknowledgement

This research was funded by the Engineering and Physical Sciences Research Council [grant number EP/K030957/1], the EPSRC Centre for Innovative Manufacturing in Food.

5.5 References

1. Wischke, C. and S.P. Schwendeman, *Principles of encapsulating hydrophobic drugs in PLA/PLGA microparticles.* International Journal of Pharmaceutics, 2008. **364**(2): p. 298-327.
2. Nedovic, V., et al., *An overview of encapsulation technologies for food applications.* Procedia Food Science, 2011. **1**: p. 1806-1815.
3. Gibbs, F., et al., *Encapsulation in the food industry: a review.* International Journal of Food Sciences and Nutrition, 1999. **50**(3): p. 213-224.
4. Ray, S., U. Raychaudhuri, and R. Chakraborty, *An overview of encapsulation of active compounds used in food products by drying technology.* Food Bioscience, 2016. **13**: p. 76-83.
5. Edwards, W.P., *Sweets and candies | Sugar Confectionery*, in *Encyclopedia of Food Sciences and Nutrition (Second Edition)*, B. Caballero, Editor. 2003, Academic Press: Oxford. p. 5703-5710.

6. Burey, P., et al., *Hydrocolloid Gel Particles: Formation, Characterization, and Application.* Critical Reviews in Food Science and Nutrition, 2008. **48**(5): p. 361-377.
7. Inês, M., I. Ferreira, and M. Barreiro, *Microencapsulation of bioactives for food applications.* Food & function, 2015. **6**.
8. Norton, Jarvis, and Foster, *A molecular model for the formation and properties of fluid gels.* International Journal of Biological Macromolecules, 1999. **26**(4): p. 255-261.
9. Shewan, H.M. and J.R. Stokes, *Review of techniques to manufacture micro-hydrogel particles for the food industry and their applications.* Journal of Food Engineering, 2013. **119**(4): p. 781-792.
10. Garrec, D.A. and I.T. Norton, *Understanding fluid gel formation and properties.* Journal of Food Engineering, 2012. **112**(3): p. 175-182.
11. Fernández Farrés, Moakes, and Norton, *Designing biopolymer fluid gels: A microstructural approach.* Food Hydrocolloids, 2014. **42**: p. 362-372.
12. Chung, C., B. Degner, and D.J. McClements, *Development of Reduced-calorie foods: Microparticulated whey proteins as fat mimetics in semi-solid food emulsions.* Food Research International, 2014. **56**: p. 136-145.
13. Le Révérend, B.J.D., et al., *Colloidal aspects of eating.* Current Opinion in Colloid & Interface Science, 2010. **15**(1): p. 84-89.
14. Fernández Farrés, I., R.J.A. Moakes, and I.T. Norton, *Designing biopolymer fluid gels: A microstructural approach.* Food Hydrocolloids, 2014. **42**: p. 362-372.
15. Norton, I.T., W.J. Frith, and S. Ablett, *Fluid gels, mixed fluid gels and satiety.* Food Hydrocolloids, 2006. **20**(2): p. 229-239.
16. García, M.C., et al., *Influence of polysaccharides on the rheology and stabilization of α-pinene emulsions.* Carbohydrate polymers, 2014. **105**: p. 177-183.
17. Mahdi, M.H., et al., *Gellan gum fluid gels for topical administration of diclofenac.* International Journal of Pharmaceutics, 2016. **515**(1): p. 535-542.
18. Torres, O., B. Murray, and A. Sarkar, *Emulsion microgel particles: Novel encapsulation strategy for lipophilic molecules.* Trends in Food Science & Technology, 2016. **55**: p. 98-108.
19. Smaniotto, F., et al., *Use of Alginate Fluid Gel Microparticles to Modulate the Release of Hydrophobic Actives*. 2019.
20. de Bruijn, J., et al., *Effect of vacuum microwave drying on the quality and storage stability of strawberries.* Journal of Food Processing and Preservation, 2016. **40**: p. 1104-1115.
21. Brown, Z.K., et al., *Drying of agar gels using supercritical carbon dioxide.* The Journal of Supercritical Fluids, 2010. **54**(1): p. 89-95.
22. Vega-Gálvez, A., et al., *Influence of drying temperature on dietary fibre, rehydration properties, texture and microstructure of cape gooseberry (physalis peruviana l.).* Journal of Food Science and Technology, 2015. **52**: p. 2304-2311.
23. Zuidam, N. and V. Nedovic, *Encapsulation Technologies for Active Food Ingredients and Food Processing*. 2010.
24. Prosapio, V. and I. Norton, *Influence of osmotic dehydration pre-treatment on oven drying and freeze drying performance.* LWT - Food Science and Technology, 2017. **80**: p. 401-408.
25. Karam, M.C., et al., *Effects of drying and grinding in production of fruit and vegetable powders: a review.* Journal of Food Engineering, 2016. **188**: p. 32-49.

26. Smaniotto, F., et al., *Freeze drying and rehydration of alginate fluid gels.* Food Hydrocolloids, 2020. **99**: p. 105352.
27. Rezvankhah, A., Z. Emam-Djomeh, and G. Askari, *Encapsulation and delivery of bioactive compounds using spray and freeze-drying techniques: A review.* Drying Technology, 2020. **38**(1-2): p. 235-258.
28. Toth, S., T. Lőrincz, and A. Szarka, *Concentration Does Matter: The Beneficial and Potentially Harmful Effects of Ascorbate in Humans and Plants.* Antioxidants & Redox Signaling, 2017. **29**.
29. Steskova, A., M. Morochovicova, and E. Leskova, *Vitamin C degradation during storage of fortified foods.* Journal of food and nutrition research, 2006. **45**: p. 55-61.
30. Abbas, S., et al., *Ascorbic Acid: Microencapsulation Techniques and Trends—A Review.* Food Reviews International, 2012. **28**(4): p. 343-374.
31. Piacentini, E., *Encapsulation Efficiency*, in *Encyclopedia of Membranes*, E. Drioli and L. Giorno, Editors. 2016, Springer Berlin Heidelberg: Berlin, Heidelberg. p. 706-707.
32. Ching, S.H., N. Bansal, and B. Bhandari, *Alginate gel particles–A review of production techniques and physical properties.* Critical Reviews in Food Science and Nutrition, 2017. **57**(6): p. 1133-1152.
33. Yussif, N., *Vitamin C - an Update on Current Uses and Functions.* 2018, Jean Guy LeBlanc, IntechOpen.
34. Fox, R.W., P.J. Pritchard, and A.T. McDonald, *Fox and McDonald's introduction to fluid mechanics*. 2011, Hoboken, NJ; Chichester: John Wiley & Sons, Inc. ; John Wiley [distributor].
35. Yuan, J.-P. and F. Chen, *Degradation of Ascorbic Acid in Aqueous Solution.* Journal of Agricultural and Food Chemistry, 1998. **46**(12): p. 5078-5082.
36. Shofian, N.M., et al., *Effect of freeze-drying on the antioxidant compounds and antioxidant activity of selected tropical fruits.* International journal of molecular sciences, 2011. **12**(7): p. 4678-4692.
37. Peleg, M., et al., *Modeling the degradation kinetics of ascorbic acid*. Vol. 58. 2016.
38. Klu, M., et al., *Effect of storage conditions on the stability of ascorbic acid in some formulations.* International Journal of Applied Pharmaceutics, 2016. **8**: p. 26-31.
39. Pinholt, P., et al., *Rate Studies on the Anaerobic Degradation of Ascorbic Acid IV: Catalytic Effect of Metal Ions.* Journal of Pharmaceutical Sciences, 1966. **55**(12): p. 1435-1438.
40. De'Nobili, M.D., et al., *Stability of L-(+)-ascorbic acid in alginate edible films loaded with citric acid for antioxidant food preservation.* Journal of Food Engineering, 2016. **175**: p. 1-7.
41. Bharate, S.S. and S.B. Bharate, *Non-enzymatic browning in citrus juice: chemical markers, their detection and ways to improve product quality.* Journal of Food Science and Technology, 2014. **51**(10): p. 2271-2288.
42. Rahman, M., et al., *Stability of Vitamin C in Fresh and Freeze-Dried Capsicum Stored at Different Temperature*. Vol. 52. 2013.
43. Sanchez, J.O., et al., *Degradation of L-Ascorbic Acid in the Amorphous Solid State.* Journal of Food Science, 2018. **83**(3): p. 670-681.
44. Beuchat, L.R., *Influence of Water Activity on Growth, Metabolic Activities and Survival of Yeasts and Molds.* Journal of Food Protection, 1983. **46**(2): p. 135-141.
45. Smaniotto, F., et al., *Use of Alginate Fluid Gel Microparticles to Modulate the Release of Hydrophobic Actives.* 2019.

Chapter 6: USE OF ALGINATE FLUID GEL MICROPARTICLES TO MODULATE THE RELEASE OF HYDROPHOBIC ACTIVES

Smaniotto, F., Zafeiri, I., Prosapio, V., & Spyropoulos, F. (2019), Use of alginate fluid gel microparticles to modulate the release of hydrophobic actives. Chemical Engineering Transactions, 74, 1219-1224

Abstract

The use of hydrocolloids-based microparticles in the field of bioactives microencapsulation is an area of great interest and research. However, their industrial scale production and their application in food products holds many technological challenges. The objective of this study was to investigate the microencapsulation of tryptophan, used as model active, into alginate microparticles obtained using the fluid gel route, as an easy industrial method for their production. Several alginate fluid gels, loaded with different amounts of tryptophan, were produced and characterized by particle size, rheological properties and encapsulation efficiency, then *in vitro* release kinetics using a dialysis approach were studied. Although the produced materials were unable to highlight a correlation between operating parameters and release kinetics, alginate fluid gels showed the ability to slow down the release of the drug compared to a water solution of tryptophan. Obtained microspheres showed very small sizes, which makes them suitable for the enrichment and delivery of actives in food products.

Keywords: Fluid gel, rheological properties, encapsulation, industrial process, release kinetic.

6.1 Introduction

Across different sectors, like foods, agrochemicals and pharmaceuticals, there is a big interest in developing a new generation of microparticles able to show “smart” behaviours, including the controlled release of bioactive molecules overtime [1-3]. A large variety of natural

polymers, especially polysaccharides and proteins, have been used during the last few years for the encapsulation of bioactives. In particular, alginate is a natural polysaccharide having attractive characteristics for encapsulation and delivery of actives and drugs, due to its biodegradability, low toxicity, low cost and biocompatibility. It forms stable water-based gels, called hydrogels, under mild conditions in presence of multivalent-cations [4-6]. Several techniques have been used for the production and encapsulation of actives in alginate microparticles, including spray-drying, coacervation, extrusion and emulsion methods [7]. However, all these approaches present some limitations, in terms of encapsulation of particular actives, for example due to the usage of high temperatures (spray-drying), presence of other materials, like emulsifiers and surfactants (emulsion), production of large particles and non-continuous production methods (extrusion) [8]. In the last few years, many studies have focused on the development of industrially feasible methods for the production of microparticles, particularly using the fluid gel route [9, 10]. Fluid gels are suspensions of gel particles in a continuous medium (usually water) that are produced by applying a shear environment to a polymer solution undergoing gelation [10, 11]. Alginate fluid gel particles can be easily obtained using continuous processes on a lab-scale; equipment able to provide a shear environment, like pin-stirrer, can produce alginate fluid gels in a reproducible and controlled way [12]. Studies have shown that fluid gels can find applications in the foods as stabilizers, thickeners, texturing materials and fat replacers [13-16]. Because of the rise in population health problems and obesity the development of low-fat foods that should meet the “traditional food” sensory characteristics and costumers’ tasty expectations is a potential area for the application of fluid gels. In general, the addition of ingredients in foods should not affect their flavour, colour or sensory properties and the addition of microparticles should not modify the food smoothness. As a consequence the addition of large particles is generally undesirable [17]. Alginate fluid gels particles are not prone to be detected in mouth, due to their small particle dimensions (<10 μm) and “soft solid” behaviour upon compression within the oral cavity [18]. However, alginate fluid gels particles have not been used so far as matrices for the encapsulation of bioactives. In order to fill the gap in the current literature, this work investigates the ability of alginate fluid gel to be used as material for the encapsulation and controlled release of tryptophan (TRP), used as model active. TRP was chosen because of its small dimension and low molecular weight (204.23 g/mol) in order to avoid its physical entrapment into the formed gel-network. Additionally, TRP presents a quite

low water solubility (13.4 mg/mL at 25 °C), which is an ideal characteristic to study the encapsulation of quite hydrophobic compounds; in fact, a small water solubility is a required characteristic to obtain homogeneous solutions for production of fluid gels. The viscosity and the particle size of fluid gels loaded with TRP were compared to the ones of unloaded fluid gels to clarify if the material properties are affected by the presence of the active. The encapsulation efficiency was determined and release experiments were conducted to assess the ability of the materials to control the release of the loaded active in controlled way overtime.

6.2 Materials and methods

6.2.1 Materials

Sodium alginate (CAS: 9005-38-3, W201502, lot.# MKBT7870V) and L-tryptophan (TRP) (reagent grade, ≥98% (HPLC)) were purchased from Sigma-Aldrich® (Sigma–Aldrich Company Ltd., Dorset, UK). Calcium chloride ($CaCl_2$, anhydrous, 93%) was purchased from Alfa Aesar™ (Varela, #159). All materials were used without further purification. Milli-Q water was made using an Elix® 5 distillation apparatus (Millipore®, USA) and was used for all water-based preparations.

6.2.2 Gel preparation

6.2.2.1 Blank fluid gels

Firstly, a solution of 2% (w/w) was prepared by dissolving ALG in distilled water at 95 °C for 30 min under stirring to ensure a complete powder dissolution [18]. Thereafter, the solution was cooled at R.T.. Secondly, a $CaCl_2$ solution having a concentration of 0.35% (w/w) was prepared by dissolving $CaCl_2$ at R.T.. All used concentrations were calculated on the final weight of the material. Alginate Fluid Gels (AFG) were prepared using a pin-stirrer vessel (Het Stempel, HL): the alginate solution was pumped into the pin-stirrer using a peristaltic pump (Masterflex L/S Peristaltic, DE), while the $CaCl_2$ solution was injected using a syringe pump (Cole-Parmer Single-syringe, US) through a stainless steel needle having an internal diameter of 1.25 mm.

6.2.2.2 Tryptophan loaded fluid gels

Firstly, a solution of 2% (w/w) was prepared by dissolving ALG in distilled water at 95 °C for 30 min under stirring to ensure complete powder dissolution. After the solution was cooled at R.T.. A second solution was prepared by firstly dissolving a calculated amount of TRP (0.025%, 0.05% or 0.10%) in water at R.T.. After the complete dissolution of TRP, 0.35% of $CaCl_2$ was added and dissolved at R.T.. All used concentrations were calculated on the final weight of the material. Tryptophan Fluid Gels (TFG) were then prepared using a pin-stirrer vessel, as described in section 6.2.2.1 Blank fluid gels.

6.2.3 UV-Vis measurements

The UV absorbance of water solutions of TRP was measured using an Orion AquaMate 8000 UV-Vis spectrophotometer (Thermo-Scientific®, UK) at 278 nm wavelength and correlated to the corresponding concentration by using the Beer-Lambert equation.

6.2.4 Encapsulation efficiency

The encapsulation efficiency (EE) of TRP in AFG particles was determined by ultracentrifugation: a weighed amount of sample (approximatively 15g) was centrifuged using a Sigma 3K-30 refrigerated centrifuge (Sigma®, D), equipped with a 12150 rotor, at 21,000 RPM at 21 °C for 45 minutes. A weighed amount of supernatant (approximatively 1.5 g) was placed in a 100 mL volumetric flask and filled with distilled water. The concentration of the active in the supernatant solution was quantified spectrophotometrically, as described in section 6.2.3 UV-Vis measurements. The EE was calculated using Equation 6.1:

$$EE = (W_t/W_i)\times 100 \qquad \text{(Equation 6.1)}$$

where, W_t is the amount of encapsulated TRP detected by UV and W_i is the quantity of TRP added during sample preparation [19].

6.2.5 Rheological properties

Rheological properties of fluid gels were determined by shear viscosity tests using a rotational rheometer (Kinexus™, Malvern®, UK) equipped with a 40 mm diameter sand blasted plate geometry. The analyses were carried out at 25 °C using a shear rate ramp between 0.01 and 100 s^{-1} and a gap of 300 µm. Measurements were performed in triplicate and all data are presented/plotted as the mean value± the standard deviation (SD).

6.2.6 Particle Size Distribution

The particle size distribution (PSD) of fluid gels was evaluated using a Mastersizer-2000 (Malvern®, UK). Few drops of sample were placed into the mixing chamber and stirred for 10 min at 1250 RPM before performing the analysis to disrupt any possible macro-aggregation. PSD was evaluated as numerical particle sizes percentage by the Mastersizer software, using a refractive index of 1,335. Measurements were performed in triplicate.

6.2.7 Drug release analysis

In vitro release studies of TRP from AFGs were performed by enclosing a known amount of material (approximately 2.5 g) into a cellulose dialysis tube (Sigma-Aldrich Company Ltd., Dorset, UK, width 43 mm, M.W. cut-off of 14000 Da). Dialysis membranes were soaked in distilled water for 10 min before filling with TFG. Tests were conducted at R.T. (thermostated at 21.5 °C) under stirring (150 RPM) using 500 mL of water as release medium. At regular intervals, aliquots of 2 mL were withdrawn, measured using the spectrophotometer and then poured back into the release medium. Each analysis was carried out in triplicate. Tests were conducted for a total of 5 hours each, since after that time no changes in concentration were observed in the release medium. The same analysis was performed also on a TRP water solution, prepared by dissolving 0.10% (w/w) of TRP in water.

6.3 Results and discussion

In the first part of the experimentation, three different samples of alginate fluid gels loaded with tryptophan (TFG) were prepared by changing the TRP concentration to 0.025%, 0.05% and 0.10% (w/w) (TFG-0.025, TFG-0.05, and TFG-0.10), to study the EE of TRP as function of its concentration. Additionally, an AFG formulation without TRP was prepared, in order to study the effect of TRP presence and its concentration on the rheological behaviour and PSD of AFG microparticles. Afterwards, a second set of experiments was performed on TFG to evaluate their TRP release kinetics overtime.

6.3.1 Encapsulation Efficiency

The EE of TRP in AFG was determined, as described in section 6.2.4 Encapsulation efficiency, and results are reported in Figure 6.1:

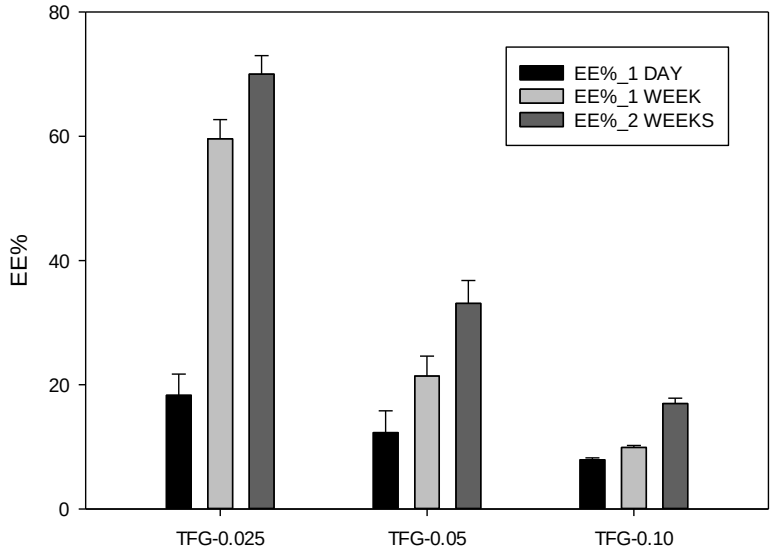

Figure 6. 1- EE of TRP in AFG as a function of storage time. Results are shown as mean ± st.dev. (n=3)

The EE of TRP in AFG was monitored over a 2 weeks period to assess if any changes occurred as a function of the storage time (t_s), where t_s was the time elapsed from the sample production. It is possible to notice that the EE increased as a function of t_s. It can be suggested that TRP diffuses into alginate microparticles, in order to fit their internal core that can be described as a more hydrophobic environment if compared to the continuous water phase surrounding particles. In fact, TRP is not very hydrophilic (water solubility of 13.4 mg/mL at 25 °C) and would preferentially be surrounded by alginate polymer chains. Several studies were conducted in the past revealing hydrophobic interactions between hydrocolloids polymer chains, including alginate and milk proteins, and hydrophobic molecules, like vanillin and sodium dodecyl sulphate [20-22]. The diffusion of TRP into particles as a function of time can be explained considering a similar effect, which justifies the increase of EE overtime.

6.3.2 PSD and Viscosities

Production parameters, apart from TRP concentration, were not changed and they are here reported: 2% ALG concentration, 0.35% $CaCl_2$ concentration, pin-stirrer shaft speed of 1000 RPM and 4 min of residence time in the pin-stirrer. Mastersizer curves, reported in Figure 6.2A, reveals that all materials have the same PSD, independently from the used concentration of TRP. Particle sizes were in the range between 0.2 µm to 7 µm, with particles mean size around 0.3/0.4 µm, and they had comparable dimensions with particles of AFGs produced without TRP. Viscosity profiles did not present substantial changes due to the

presence of TRP, as can be noticed from Figure 6.2B. Low percentages of TRP were used for materials preparation if compared to the percentage of other formulation constituents (i.e. ALG and $CaCl_2$). It is possible to conclude that the TRP addition, in the range of used TRP concentrations, does not affect the particle size and the rheological behaviour of AFG.

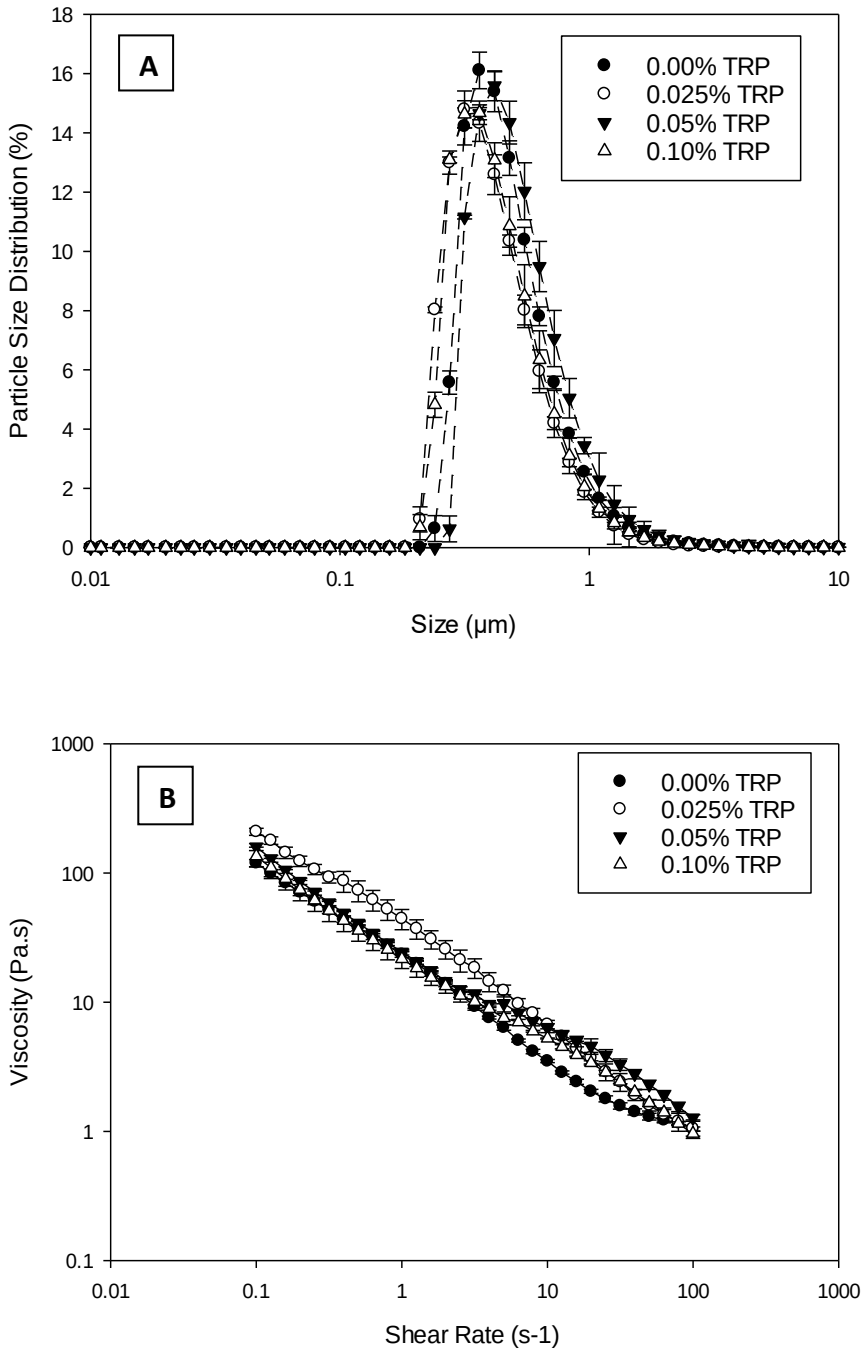

Figure 6. 2- TRP loaded alginate fluid gels: (A) Particle size distribution; (B) Viscosities. Results are shown as mean ± st.dev. (n=3)

6.3.3 *In vitro* release studies

TFG-0.025, TFG-0.05, TFG-0.10 were tested for *in vitro* release studies, as described in section 6.2.7 Drug release analysis. Curves are reported in Figure 6.3:

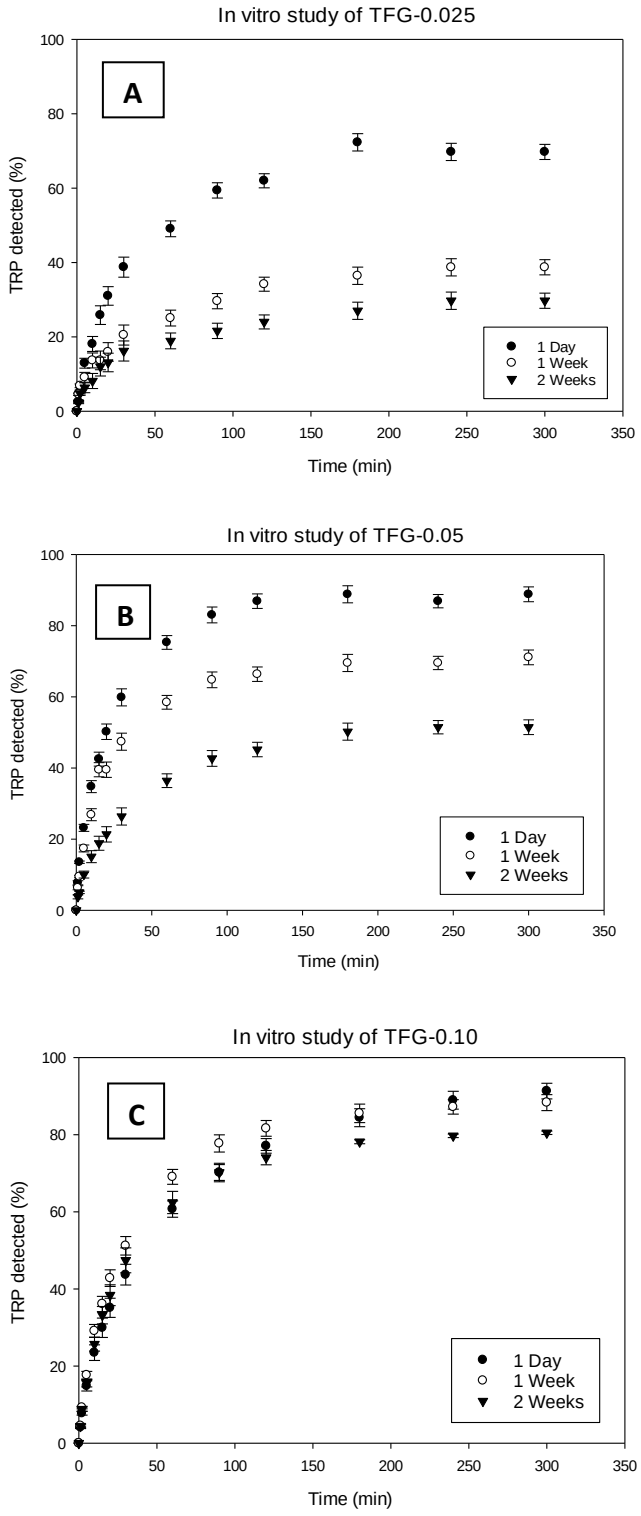

Figure 6. 3 – In vitro release studies as function of the storage time: (A) TFG-0.025; (B) TRP-0.05; (C) TRP-0.10. Results are shown as mean ± st.dev. (n=3)

As can be noticed even the *in vitro* tests were strongly influenced by t_s; the quantity of TRP detected in the release medium decreased as a function of t_s for the same material. In addition, none of TFG formulations was able to completely release 100% of the TRP added during sample preparation as can be noticed in Figure 6.3. To better understand the release behaviour of TRP within AFG, the non-encapsulated percentages of TRP and the percentages of TRP detected into the release medium after 5 hours of *in vitro* studies have been reported in Table 6.1 and Table 6.2, respectively.

Table 6. 1 - Percentages of non-encapsulated TRP in TFG

Sample	% TRP non-encapsulated (1 Day)	% TRP non-encapsulated (1 Week)	% TRP non-encapsulated (2 Weeks)
TFG-0.025	81.7	40.4	30.0
TFG-0.05	87.7	78.6	66.9
TFG-0.10	92.1	90.1	83.0

Table 6. 2 - Percentages of TRP detected after 5 hours in in vitro release studies of TFG

Sample	% TRP detected (1 Day)	% TRP detected (1 Week)	% TRP detected (2 Weeks)
TFG-0.025	69.8	38.7	29.7
TFG-0.05	88.8	71.1	51.5
TFG-0.10	91.3	88.4	80.5

Comparing data from Tables 6.1 and 6.2 can be noticed that the percentages of TRP able to diffuse out of AFG formulations were always lower than the percentages of non-encapsulate TRP. In addition, the amount of TRP detected in the release medium decreased as a function of t_s. Considering that the EE increased as a function of t_s, as reported in section 6.3.1 Encapsulation Efficiency, it is possible to conclude that only the TRP not encapsulated in the microparticles was able to diffuse from the formulation. This can explain why not all the 100% of TRP within AFG was never detected in the release medium of *in vitro* studies. It can be concluded that TRP cannot be released from microparticles. This behaviour may be due to hydrophobic interactions between the TRP molecule and ALG polymer chains. However, molecular modelling experiments should be conducted in order to assess these interactions.

The diffusion time of TRP from AFG was compared to the diffusion time of TRP from a water solution and the results are compared in Figure 6.4:

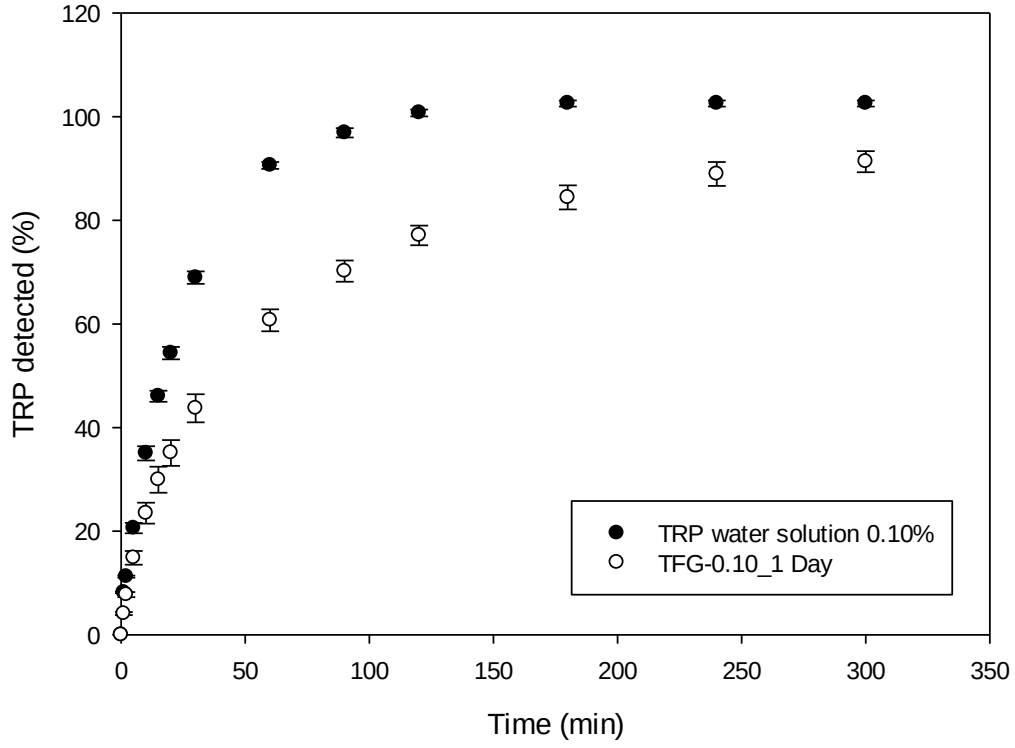

Figure 6. 4 - In vitro release studies of 0.10% (w/w) TRP water solution and TFG-0.10 (1 day of storage time). Results are shown as mean ± st.dev. (n=3)

As can be noticed the AFG formulation was able to slow down the diffusion of the active when compared to its diffusion from a water solution. This effect can be probably related to the higher viscosity of AFG.

6.4 Conclusions

The ability of AFG to be used as matrices for the encapsulation of TRP was investigated. The results showed that its EE is a function of t_s and that TRP cannot diffuse out of alginate microparticles, under the conditions used for the *in vitro* release tests. Further experiments should be conducted to verify the ability of AFG to release TRP under different conditions, like gastric or physiological environment. In fact, as the isoelectric point of TRP is 5.89 at 25°C (pKa1= 2.83, pKa2= 9.39), under water release conditions, used in this study, TRP existed dominantly in its zwitterion form. By changing the release environment pH, electrostatic interactions between TRP and the ALG matrix can be obtained, which can potentially affect the release rate of this active. Nevertheless, this study showed the ability of AFG to slow down the diffusion of TRP in *in vitro* studies when compared to a TRP water solution, suggesting

that more studies should be conducted in order to investigate the usage of these materials for the development of formulations to control the diffusion of actives overtime.

Acknowledgment

This research was funded by the Engineering and Physical Sciences Research Council [grant number EP/K030957/1], the EPSRC Centre for Innovative Manufacturing in Food.

6.5 References

1. Dubey, R., *Microencapsulation technology and applications.* Defence Science Journal, 2009. **59**(1): p. 82.
2. Roy, A., et al., *Controlled pesticide release from biodegradable polymers.* Central European Journal of Chemistry, 2014. **12**(4): p. 453-469.
3. Caccavo, D., et al., *Hydrogel-based granular phytostrengtheners for prolonged release: production and characterization.* Chemical Engineering Transactions, 2015. **44**: p. 235-240.
4. Silva, P.T.d., et al., *Microencapsulation: concepts, mechanisms, methods and some applications in food technology.* Ciência Rural, 2014. **44**(7): p. 1304-1311.
5. Cardoso, M.J., R.R. Costa, and J.F. Mano, *Marine origin polysaccharides in drug delivery systems.* Marine drugs, 2016. **14**(2): p. 34.
6. Agüero, L., et al., *Alginate microparticles as oral colon drug delivery device: A review.* Carbohydrate Polymers, 2017. **168**: p. 32-43.
7. Goh, C.H., P.W.S. Heng, and L.W. Chan, *Alginates as a useful natural polymer for microencapsulation and therapeutic applications.* Carbohydrate Polymers, 2012. **88**(1): p. 1-12.
8. Madene, A., et al., *Flavour Encapsulation and Controlled Release - a Review.* International Journal of Food Science & Technology, 2006. **41**: p. 1-21.
9. Gouin, S., *Microencapsulation: industrial appraisal of existing technologies and trends.* Trends in Food Science & Technology, 2004. **15**(7): p. 330-347.
10. Garrec, D.A. and I.T. Norton, *Understanding fluid gel formation and properties.* Journal of Food Engineering, 2012. **112**(3): p. 175-182.
11. Norton, Jarvis, and Foster, *A molecular model for the formation and properties of fluid gels.* International Journal of Biological Macromolecules, 1999. **26**(4): p. 255-261.
12. Fernández Farrés, I., M. Douaire, and I.T. Norton, *Rheology and tribological properties of Ca-alginate fluid gels produced by diffusion-controlled method.* Food Hydrocolloids, 2013. **32**(1): p. 115-122.
13. Le Révérend, B.J., et al., *Colloidal aspects of eating.* Current Opinion in Colloid & Interface Science, 2010. **15**(1-2): p. 84-89.
14. Saha, D. and S. Bhattacharya, *Hydrocolloids as thickening and gelling agents in food: A critical review.* Journal of food science and technology, 2010. **47**: p. 587-97.
15. Chung, C., B. Degner, and D.J. McClements, *Development of reduced-calorie foods: microparticulated whey proteins as fat mimetics in semi-solid food emulsions.* Food research international, 2014. **56**: p. 136-145.

16. Fernández Farrés, I., R.J.A. Moakes, and I.T. Norton, *Designing biopolymer fluid gels: A microstructural approach.* Food Hydrocolloids, 2014. **42**: p. 362-372.
17. Champagne, C.P. and P. Fustier, *Microencapsulation for the improved delivery of bioactive compounds into foods.* Current opinion in biotechnology, 2007. **18**(2): p. 184-190.
18. Fernández Farrés, I. and I.T. Norton, *Formation kinetics and rheology of alginate fluid gels produced by in-situ calcium release.* Food Hydrocolloids, 2014. **40**: p. 76-84.
19. Piacentini, E., *Encapsulation Efficiency*, in *Encyclopedia of Membranes*, E. Drioli and L. Giorno, Editors. 2016, Springer Berlin Heidelberg: Berlin, Heidelberg. p. 706-707.
20. Chobpattana, W., et al., *Mechanisms of Interaction Between Vanillin and Milk Proteins in Model Systems*. Vol. 67. 2002. 973-977.
21. Yang, J., J. Zhao, and Y. Fang, *Calorimetric studies of the interaction between sodium alginate and sodium dodecyl sulfate in dilute solutions at different pH values.* Carbohydrate research, 2008. **343**(4): p. 719-725.
22. Yang, J., S. Chen, and Y. Fang, *Viscosity study of interactions between sodium alginate and CTAB in dilute solutions at different pH values.* Carbohydrate Polymers, 2009. **75**(2): p. 333-337.

Chapter 7: ENCAPSULATION OF MODEL ACTIVES IN ALGINATE FLUID GELS

Smaniotto, F., Zafeiri, I., Prosapio, V., & Spyropoulos, F., Understanding the encapsulation and release of small molecular weight model actives from alginate fluid gels (i*n preparation*).

Abstract

The encapsulation and release of actives from biopolymer-based gels has received significant research attention for applications in the pharmaceutical and food industries. The inclusion of actives within a range of formulated gelled systems has been extensively studied. Amongst these, gelled microparticles have generated substantial interest, but still face challenges for scalable production. Fluid gels are a special class of soft-solid particles produced by high shear approaches that are suitable for industrial scale manufacture. However, their use for the entrapment of species of therapeutic or nutritional activity in foods has been very little investigated. The aim of this work was to study the encapsulation of different small actives within AFG. It was confirmed that the presence of an active during Alginate Fluid Gel (AFG) formation does not interfere with the particle dimensions or bulk rheological behaviour (shear viscosity) of these materials. The Encapsulation Efficiency (EE) of all actives following AFG production was very low, but significantly increased upon storage. This primarily depends on the hydrophilicity of the used actives, with only hydrophobic ones exhibiting such behaviour. The rate and extent of active incorporation within AFG were governed by addenda concentration and AFG particle dimensions. Release analyses revealed that encapsulated matter remains within the AFG particles regardless of particle size and storage period. A hypothesis that elucidates the preferential transfer of actives within the AFG is presented and validated. Overall, the current study offers insight into the use of AFG as encapsulation media and presents original findings that expand the industrial applicability of these colloidal systems.

Keywords: Alginate; Fluid gels; Encapsulation Efficiency; Release.

7.1 Introduction

Material and microstructures that can enable the controlled release of active ingredients, like nutraceuticals and drugs, are increasingly used in the pharmaceutical and food industries. Microencapsulation matrices, such as liposomes, microgels, emulsions and/or microemulsions, have been studied for such purposes in foods [1]. These formulations can be designed for different purposes, such as to prolong the function of actives by delaying their release, protect sensitive components from adverse environmental conditions (e.g. high moisture content, acidity, presence of enzymes, etc.) and/or mask unwanted tastes [2].

Amongst all structures investigated as microencapsulation matrices, hydrocolloid gel particles have received significant research attention due to their biocompatibility, renewable and natural sourcing, as well as soft-solid texture. Food applications include their use as texturisers, thickening agents and stabilisers and, additionally, they have shown a promising behaviour as slow-release matrices for the encapsulation of actives like flavours, nutrients and pharmaceuticals [3]. However, the majority of microencapsulation technologies based on hydrocolloid microparticles face, challenges in terms of scalability [4]. Over the last two decades a new approach for the production of biopolymer-based microparticles, commonly termed as sheared or fluid gels, has been investigated [5, 6]. Fluid gels are suspensions of hydrocolloid gel particles in water, produced by applying shear to a biopolymer solution undergoing gelation [7]. Fluid gels can be produced continuously using typical shear devices (e.g. pin-stirrer) and as such their scalable manufacture is less problematic [8]. Fluid gels can find applications in food products as texturing materials because of their unique properties/characteristics [9-11]. In particular, tribological studies have shown the ability of fluid gel particles to provide lubrication, suggesting that they can impart a sensory response similar to that typically associated with fat in the mouth [11].

Despite their current uses in an array of different applications, literature on the utilisation of fluid gels for entrapment and delivery purposes is extremely scarce. The current authors used AFG to control the encapsulation of tryptophan and showed that overtime such matrices can slow down the release of the active [12]. In another study, ter Horst *et al*. (2019) studied the entrapment of skin cells in gellan gum fluid gels in order to enable their spray delivery onto burn wounds. The authors reported that cell viability was not compromised by encapsulation in the gellan particles nor by the subsequent spray application [13].

The present work aims to study the encapsulation of different small active molecules within AFG. The model actives used here were selected based on their hydrophilicity/hydrophobicity and water-solubility; vanillin and tryptophan were chosen to represent low water-solubility actives and nicotinamide to correspond to a model active of high water-solubility. Vanillin is a natural flavour, tryptophan is an essential amino acid and nicotinamide is a form of vitamin B_3 [14, 15]. AFG particle size and bulk rheological behaviour (shear viscosity) were measured both in the presence and absence of the actives. The EE of all actives was initially obtained upon AFG production, but was also monitored over a 2-week storage period. The release of all actives from the AFG formulations was carried out under sink conditions for both immediately produced and stored systems. Finally, the effects of the alginate to $CaCl_2$ ratio on AFG EE and release profiles for all actives were also studied. Overall, the current study offers new insight into the use of AFG as encapsulation matrices in an attempt to strengthen the industrial applicability of these colloidal systems.

7.2 Materials and methods

7.2.1 Materials

Sodium alginate (CAS: 9005-38-3, W201502, lot.# MKBT7870V), vanillin (VAN, ≥97%), nicotinamide (NIC, ≥98%, HPLC) and L-tryptophan (TRP, ≥98% HPLC) were purchased from Sigma-Aldrich® (Sigma–Aldrich Company Ltd., Dorset, UK). Calcium chloride ($CaCl_2$, anhydrous, 93%) was purchased from Alfa Aesar™ (Varela, #159). All materials were used without further purification. Milli-Q distilled water, produced using an Elix® 5 distillation apparatus (Millipore®, USA), was used for all water-based preparations Concentrations of all materials are given as percentages of the weight of the specific substance over the total weight of the system in which it is contained (i.e. solution, fluid gel formulation, etc.) and are reported as '% w/w'.

7.2.2 Production of alginate fluid gels

7.2.2.1 Blank fluid gels

Blank Alginate Fluid Gels (AFG) were produced as described in section 4.2.2.1 Blank fluid gels, by using a 2% w/w Alginate (ALG) solution and two different $CaCl_2$ solutions of 0.25% and 0.35% w/w concentrations.

7.2.2.2 Active-loaded fluid gels

Active-loaded AFG were prepared following a procedure similar to the production of blank AFGs. However, the procedure of making the aqueous $CaCl_2$ solution in this case was slightly modified. The active was firstly dissolved, at different concentrations (0.05% and 0.10% w/w), in distilled water at R.T. under magnetic stirring. $CaCl_2$ (0.25% and 0.35% w/w) was then dissolved in the active-containing aqueous solution under magnetic stirring. ALG solutions were prepared as previously described: Vanillin (VFG), Tryptophan (TFG) and Nicotinamide (NFG) loaded Fluid Gels were prepared by introducing both the ALG and the active-containing $CaCl_2$ aqueous solutions into the pin-stirrer as described above.

7.2.3 Rheological measurements

The rheological properties of fluid gels were determined by shear viscosity tests using a rotational rheometer (Kinexus™, Malvern®, UK) equipped with a 40 mm diameter sand blasted plate geometry. The analyses were carried out at 25 °C using a shear rate ramp between 0.01 and 100 s^{-1} and a gap of 300 µm. All measurements were carried out in triplicate and all data are presented/plotted as the mean value± the standard deviation (SD). In order to assess bulk viscoelasticity, the shear viscosity profiles of all AFG formulations were fitted to a simple power-law model [16]:

$$\eta = K\,\dot{\gamma}^{\,n-1} \qquad (7.1)$$

where η and $\dot{\gamma}$ are respectively the shear viscosity and the shear rate, *K* is the consistency constant and *n* is the power-law index.

7.2.4 Particle size analysis

The particle size distribution (PSD) of fluid gels was evaluated using laser diffraction (Mastersizer-2000, Malvern®, UK). Few drops of sample were placed into the mixing chamber of the instrument and were mixed for 10 min at 1300 RPM before performing the analysis. PSD was evaluated as numerical particle size percentage by the Mastersizer software, using a refractive index of 1,335. Particle dimensions of AFG were also validated in a previous study via DLS measurements [17]. $D_{3,2}$ diameter, also known as Surface Weighed Mean, and Span values were calculated by Mastersizer-2000 software. All measurements were carried out in triplicate and all data are presented/plotted as the mean value± SD.

7.2.5 UV-Vis measurements

The UV absorbance of the aqueous solutions of actives was measured using an Orion AquaMate 8000 UV-Vis spectrophotometer (Thermo-Scientific®, UK). Maximum absorbance wavelength of each active was experimentally detected and used for later UV-Vis analyses; specifically, 300 nm for VAN, 278 nm for TRP and 214 nm for NIC. Absorbance values were correlated to the corresponding active concentration using the Beer-Lambert equation and an active specific correlation parameter obtained via a calibration curve. Analyses were carried out at R.T.. All measurements were carried out in triplicate and all data are presented/plotted as the mean value± SD.

7.2.6 Encapsulation efficiency

The encapsulation efficiency (EE) of actives in AFG particles was determined by ultracentrifugation: a weighed amount of sample (approximatively 15g) was centrifuged using a Sigma 3K-30 refrigerated centrifuge (Sigma®, DK), equipped with a 12150 rotor. Centrifugation was carried out (at 21 °C) at 21,000 RPM for 45 minutes; preliminary tests (not reported here) revealed that these conditions provide sufficient separation between the AFG aqueous continuous phase and the formed AFG particles, thus allowing easy access (sampling) to the formed supernatant. A weighed amount of the supernatant (approximatively 1.5 g) was placed in a 100 mL volumetric flask and filled with distilled water. The concentration of the active in the supernatant solution was quantified spectrophotometrically (see section 7.2.5 UV-Vis measurements). The EE was calculated using Equation (7.2):

$EE = (W_t/W_i)\times 100$ (Equation 7.2)

where W_i is the amount of active initially added to the system during sample preparation and W_t is the amount of encapsulated active. The latter was calculated as the difference between the theoretical concentration of active added into the system and the concentration detected by UV, in the supernatant phase [18].

7.2.7 Release studies

The release of different actives from the formed AFG was monitored over time by UV-Vis. A weighed amount (approx. 2.5 g) of active-loaded AFG was enclosed in a dialysis sack (cellulose dialysis tubing membrane, width 43 mm, M.W. cut-off of 14000 Da; Sigma–Aldrich, UK) and placed in 500 mL of distilled water (acceptor phase) at R.T. (thermostated at 21.5 °C), under

mild mixing provided by the use of a magnetic stirrer at 150 RPM. At regular intervals during each release study, aliquots of 2 mL were withdrawn from the acceptor phase and measured using UV-Vis (see Section 7.2.5 UV-Vis measurements) to determine the concentration/amount of released active(s). Following UV-Vis analysis, withdrawn aliquots were reintroduced back into the acceptor phase. All measurements were carried out in triplicate and all data are presented/plotted as the mean value± SD.

7.2.8 Data fitting

Data obtained from release studies were fitted to Equation (7.3):

$$\frac{M_t}{M_\infty} = k_r \mathrm{t}^{n_r} \qquad \text{(Equation 7.3)}$$

where M_t and M_∞ are respectively the cumulative amount of active released at time t and at infinite time (complete release), respectively, k_r is a kinetic constant and n_r is an exponent related to the mechanism of release. The empirical model described by Equation (7.3) has been used by several studies as a tool to establish whether the release of drugs/actives from polymeric formulations is driven by diffusion ($n_r \approx 0.5$) or relaxation ($n_r \approx 1$) [19-21].

7.3 Results and discussion

First the effect of introducing different actives in AFG was tested. Actives were selected based on their water solubility and, consequently, on their hydrophilic behaviour. VAN (water solubility = 11 mg/mL) and TRP (water solubility = 13 mg/mL) were chosen as actives with relatively low water solubility, while NIC (water solubility = 500 mg/mL) as active with high water solubility. The effect of active concentration in the AFG formulation was also studied. The properties of active-containing AFG were evaluated in terms of Particle Size Distribution (PSD), rheological behaviour, EE and release of active under sink conditions. In order to investigate whether the presence of actives affects AFG properties, ALG and $CaCl_2$ concentrations were fixed to allow the formation of microparticles, as it was shown in a previous study [17]. EE measurements and release analyses were carried out 1 day, 1 week and 2 weeks following the AFG production in order to assess the capacity of these formulations to retain the actives and whether release characteristics are influenced by the storage period.

7.3.1 Effect of active type and concentration

AFG were produced in the presence of actives and the effects of active type and concentration were studied. Samples were produced by fixing the ALG concentration at 2% w/w and the $CaCl_2$ concentration at 0.35% w/w, respectively. ALG and $CaCl_2$ concentrations were chosen in accordance to a previous study, showing that when the $CaCl_2$/ALG ratio is higher than 0.150, AFG in the size range of 0.5-5 µm are obtained [17]. It was decided to study first the effect of actives hydrophobicity/hydrophilicity on AFG properties as well as their used concentrations. Given that AFG systems are primarily composed of water, it is essential that the active to be loaded within this matrix is used at a concentration below its aqueous saturation limit. As such, active concentration was tested at 0.05% to 0.10% w/w for VAN (VFG_0.05% and VFG_0.10% samples, respectively), TRP (TFG_0.05% and TFG_0.10% samples, respectively), and NIC (NFG_0.05% and NFG_0.10% samples, respectively).

7.3.1.1. PSD and Viscosity profiles

All AFG produced in the presence of actives were characterised in terms of PSD and rheological behaviour (shear viscosity). Results were compared to PSD and shear viscosity curves of "blank" AFG, i.e. AFG systems formed in the absence of an active. Size measurements, reported in Figure 7.1, revealed that all AFG systems had practically the same PSD, independently of the type of active and/or its used concentration. Additionally, "blank" and active-containing AFG particles presented similar $D_{3,2}$ (1.5-2 µm) and span values (1-2). These results were in accordance with what reported previously when looking at PSD of AFG loaded with TRP [12]. It can be concluded that active presence and its concentration in AFG did not affect this material PSD. Shear viscosity profiles are presented in Figure 7.2 together with a simple power-law fit of the data accordingly to Equation (7.1). The model described by Equation (7.1), also known as the Ostwald–de Waele power law, is a mathematical relationship used to describe the behaviour of non-Newtonian fluids [22]. The *K* and *n* parameters of the obtained shear viscosity curves were all comparable and consistently revealed a shear thinning behaviour; *n* parameter below 1 [22]. Overall, AFG formation, PSD and rheological performance were not affected by the presence of any of the actives, at their used concentrations. PSD and shear viscosities profiles, for all systems, were monitored over a 2-week period, following sample preparations, and no significant deviation to either of these features was observed (data not reported here).

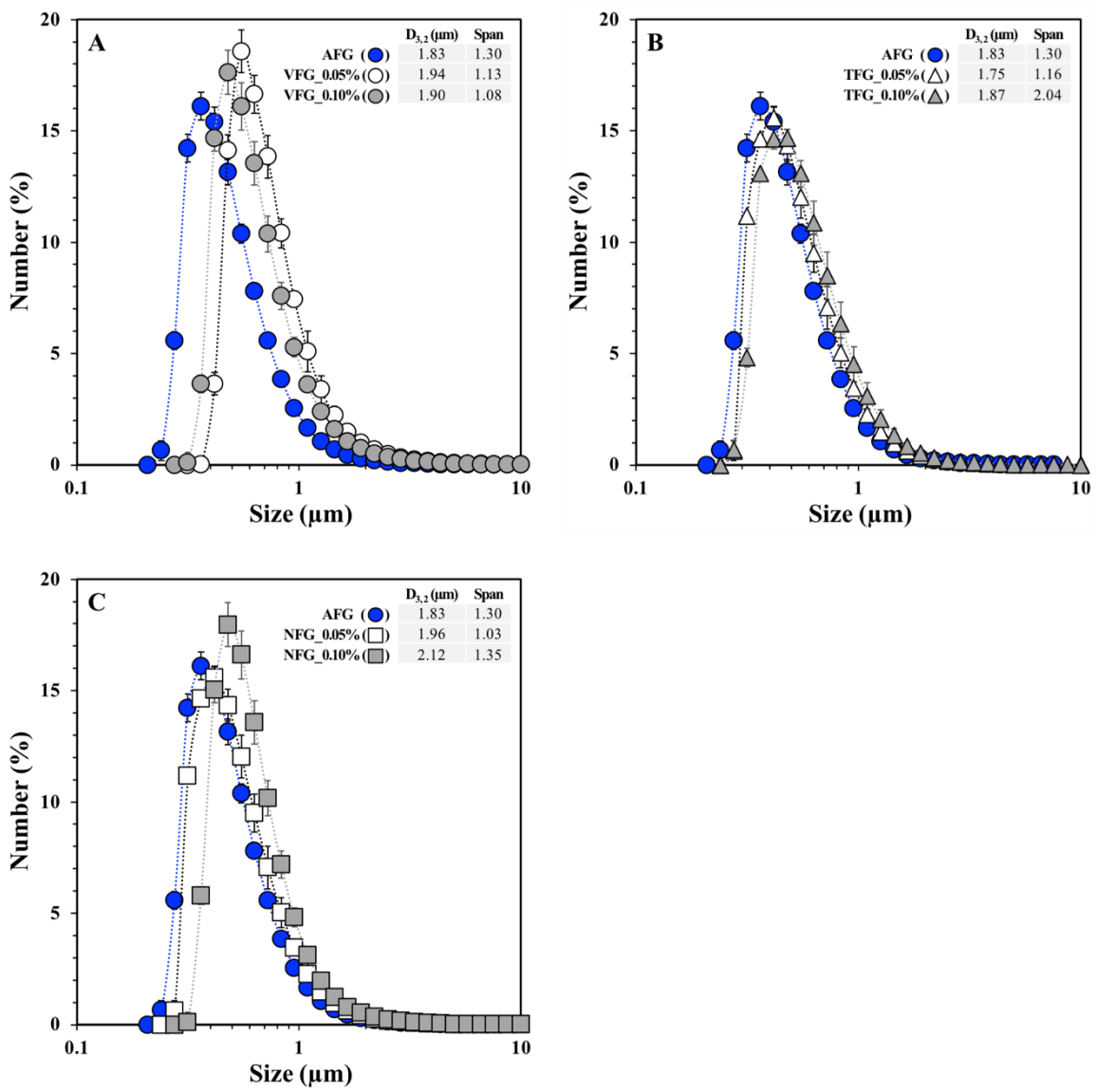

Figure 7. 1 - Particle size distributions (number %) for blank and as a function of active type and concentration AFG: VAN (A), TRP (B), NIC (C)

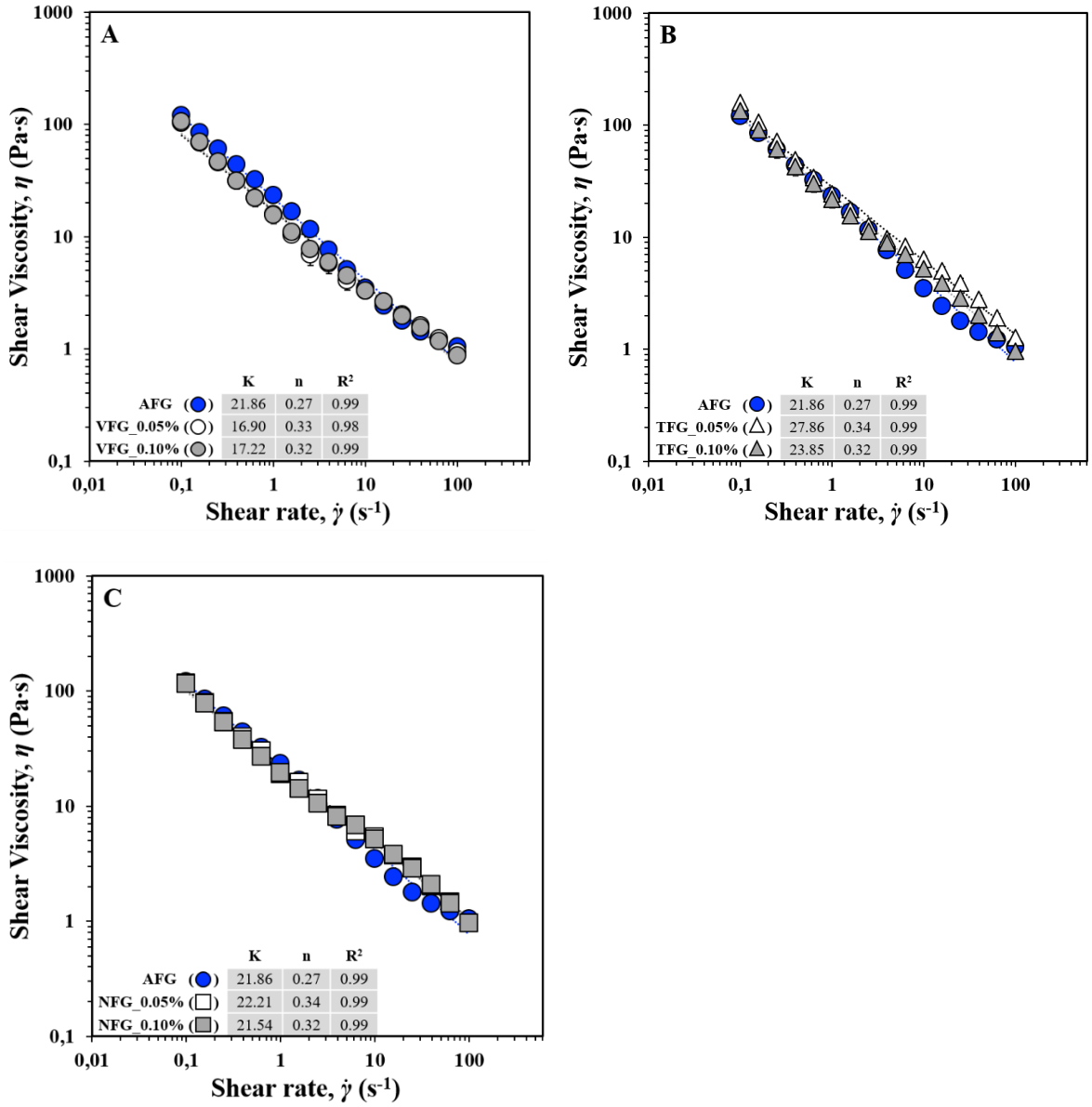

Figure 7. 2 - Shear viscosity curves for blank and as a function of active type and concentration AFG: VAN (A), TRP (B), NIC (C)

7.3.1.2. Encapsulation efficiency

The EE of different types and concentrations of actives within AFG was determined, as described in section 7.2.6 Encapsulation efficiency, and results are presented in Table 7.1. The EE was monitored over a 2 weeks period to assess changes that might occur as a function of storage time (t_s), i.e. the time elapsed between AFG production and EE analysis. Active loaded AFG were stored at R.T. (≈ 21 °C) in closed plastic pots. As can be seen from Table 7.1, EE data after 1 day of storage were quite low, for all the AFG systems. This can be explained considering the way these materials were prepared. Actives were introduced in the systems before performing gelation. Active encapsulation is therefore related to the probability of the

active molecule to be entrapped into a forming AFG particle, due to the injection of $CaCl_2$ in the system. Considering that these materials were produced using 2% w/w ALG, a low probability of active encapsulation was expected for these systems. However, EE analyses repeated over a 2-week period of storage clearly showed an increase of EE of VAN and TRP, within VFG and TFG respectively. On the other hand, the EE of NIC, within NFG, was practically unchanged over the same period.

Table 7. 1 - EE of actives in AFG as a function of storage time

	Encapsulation Efficiency, EE (±SD)		
	1 Day	**1 Week**	**2 Weeks**
VFG_0.05%	22.5% (±3.2)	48.3% (±3.1)	69.2% (±3.4)
VFG_0.10%	28.9% (±3.2)	25.2% (±2.9)	43.9% (±3.2)
TFG_0.05%	12.3% (±3.5)	21.4% (±3.2)	33.1% (±3.7)
TFG_0.10%	19.8% (±3.9)	22.1% (±3.2)	16.2% (±5.7)
NFG_0.05%	0.0% (±0.0)	0.0% (±0.0)	0.0% (±0.0)
NFG_0.10%	4.1% (±1.3)	5.6% (±1.1)	3.6% (±1.7)

EE data were used to calculate the mass of each active encapsulated in AFG as a function of t_s. Results are reported in Figure 7.3. Although the EE of VAN and TRP after 2 weeks was higher when a low active concentration (0.05% w/w) was used, the total mass of encapsulated species was higher in samples prepared at a higher active content (0.10% w/w). Considering that particle dimensions of these materials were not affected by the presence of actives or by their employed concentrations, as reported in Figure 7.1, it can be assumed that samples had the same number of particles per volume unit, independently of the active type/concentration used during production. Therefore, data suggested that by increasing the concentration of the active, during AFG formation, particles loaded a higher mass of active, over the same storage period. However, by operating in this way the overall efficiency of active encapsulation was reduced. This observation was only valid for actives having a low aqueous solubility, since NIC did not follow the same pattern.

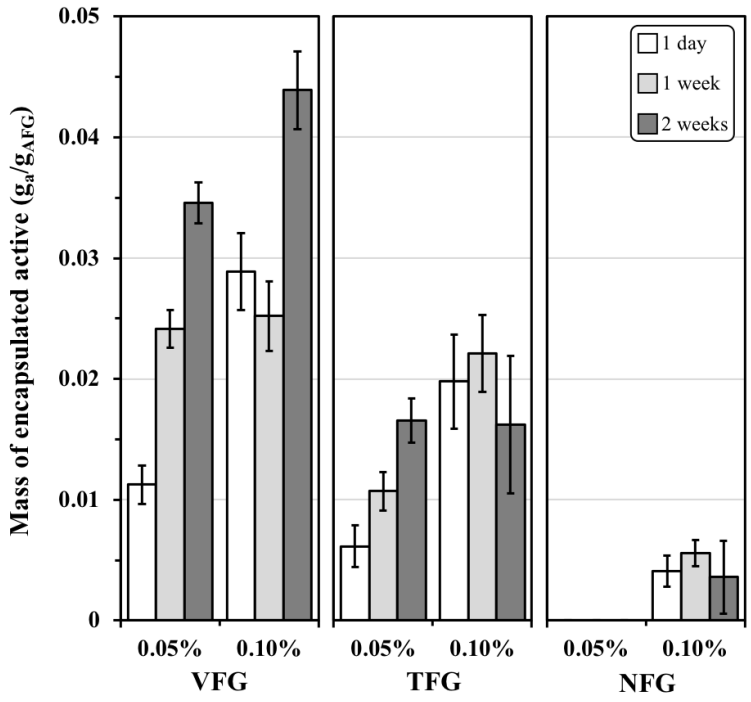

Figure 7. 3 - Mass of actives encapsulated in VFG, TFG and NFG as a function of the type and concentration of the actives and of t_s. Data are reported as mass of encapsulated active (g_a) over mass of active-containing AFG formulation (g_{AFG})

7.3.1.3. Release experiments

Release tests for all active-containing AFG as a function of the type and concentration of the active as well as t_s, were carried out under sink conditions, as described in section 7.2.7 Release studies. Results are presented in Figure 7.4. Release testing was carried out on "as-produced" AFG formulations, without separation of the formed particles from their continuous water phase nor dilution. Results were not adjusted to take into account the fraction of encapsulated active, determined by EE analysis. As such, release data reported here correspond to the cumulative release of each active (total amount of active detected in the acceptor phase) and are expressed as a percentage of the active content initially used during the production of all AFG formulations. Additionally, release experiments were conducted using aqueous solutions of the actives: Vanillin, Tryptophan and Nicotinamide Aqueous Solution (VAS, TAS and NAS respectively) were produced by dissolving the specific active to a final concentration of 0.10% w/w. This was done in order to assess whether AFG formulations affect the release of the active. All data were fitted to Equation (7.3) in order to assess the mechanism responsible for actives release. Obtained parameters are reported in Table 7.2.

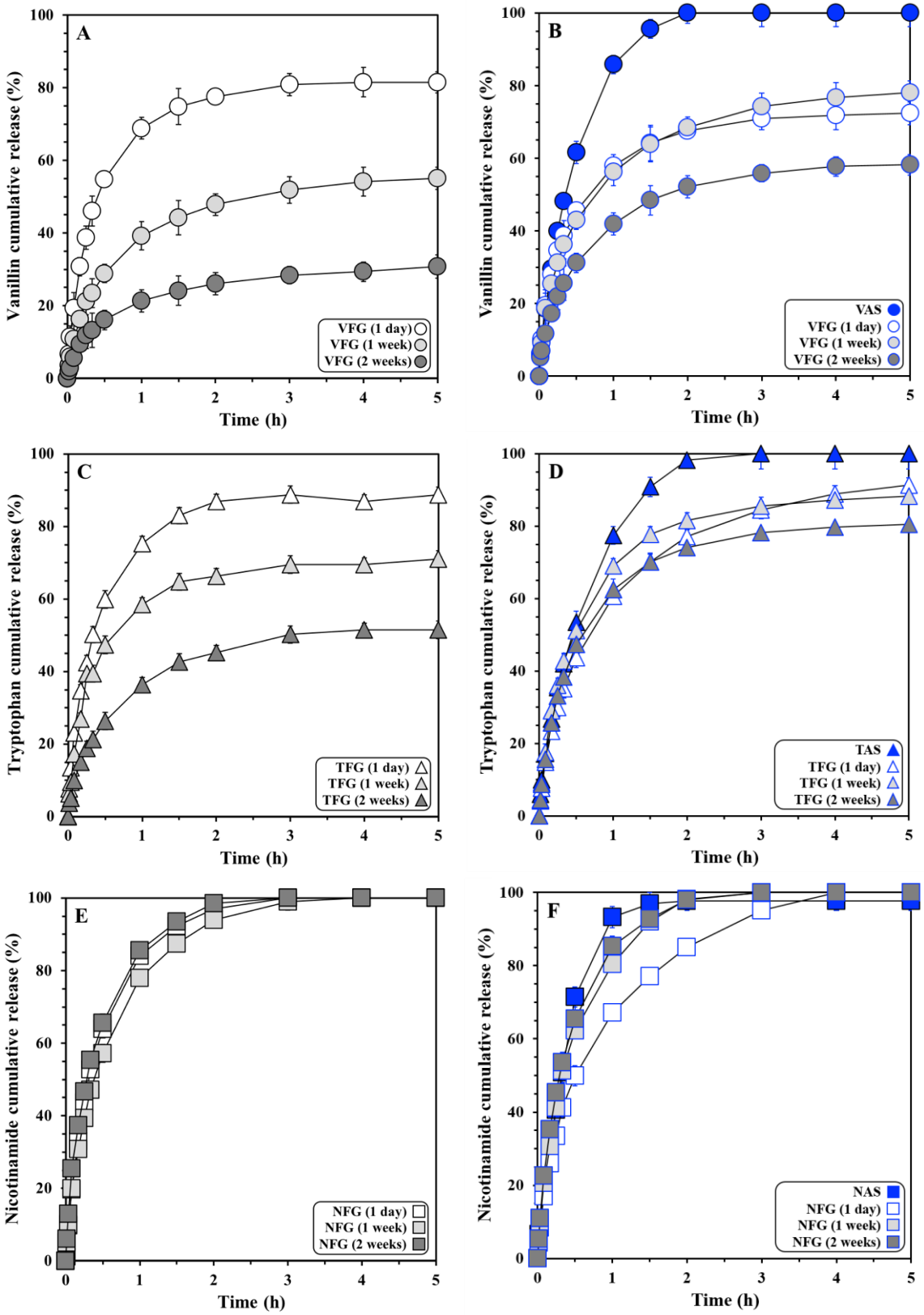

Figure 7. 4 - Release profiles under sink conditions for VFG (A & B), TFG (C & D) and NFG (E & F) as function of t_s and active concentrations: 0.05% w/w of active (A, C & E) and 0.10% w/w of active (B, D & F). Also shown is the release profiles of aqueous solutions of VAN, TRP and NIC of 0.10% w/w active concentration (VAS, TAS and NAS respectively)

It can be noticed that release curves followed similar trends for all formulations. All curves presented an "exponential-like" shape and plateaus of release were reached after 90 to 240 minutes from the beginning of release tests. However, the cumulative release values for these plateaus changed with the type and concentration of the active as well as with t_s. Percentages of VAN and TRP released, respectively from VFG and TFG, were effected by t_s, while the percentages of NIC released from NFG were not affected by t_s and all the NIC present in NFG was detected into the release medium. Regarding active aqueous solutions (VAS, TAS and NAS) it can be noticed that all the amounts of active loaded into the dialysis bags, used to performed the release tests, were detected into the release medium.

In order to better understand the release behaviour of actives from active-containing AFG samples, data obtained from release studies were used to fit Equation (7.3), as described in section 7.2.8 Data fitting. Obtained parameters are reported in Table 7.2.

Table 7. 2 - k_r, n_r, R^2, parameters obtained from data fitting of Equation 7.3 for release tests of VFG, TFG, NFG formulations as function of t_s

				k_r (±SD)	n_r (±SD)	R^2
VAN	**VFG**	**0.05%**	**1 day**	7.94 (± 1.43)	0.58 (± 0.06)	0.99
			1 week	4.37 (± 0.84)	0.56 (± 0.06)	0.99
			2 weeks	2.33 (± 0.66)	0.58 (± 0.09)	0.99
		0.10%	**1 day**	9.48 (± 2.44)	0.45 (± 0.08)	0.98
			1 week	7.76 (± 1.55)	0.47 (± 0.06)	0.99
			2 weeks	3.49 (± 0.01)	0.50 (± 0.04)	0.99
TRP	**TFG**	**0.05%**	**1 day**	9.60 (± 1.47)	0.55 (± 0.06)	0.99
			1 week	7.58 (± 3.28)	0.55 (± 0.14)	0.97
			2 weeks	4.03 (± 0.76)	0.56 (± 0.06)	0.99
		0.10%	**1 day**	5.50 (± 0.99)	0.62 (± 0.06)	0.99
			1 week	6.83 (± 1.89)	0.60 (± 0.09)	0.99
			2 weeks	6.02 (± 1.26)	0.61 (± 0.07)	0.99
NIC	**NFG**	**0.05%**	**1 day**	6.61 (± 2.85)	0.68 (± 0.14)	0.99
			1 week	6.56 (± 1.24)	0.66 (± 0.07)	0.99
			2 weeks	8.69 (± 2.32)	0.62 (± 0.10)	0.99
		0.10%	**1 day**	6.00 (± 1.28)	0.63 (± 0.07)	0.99
			1 week	6.83 (± 1.65)	0.66 (± 0.08)	0.99
			2 weeks	7.32 (± 1.73)	0.67 (± 0.09)	0.99

As reported by Rinaki *et al.* (2003), the n_r parameter, obtained from data fitting of Equation (7.3), describes the mechanism of drug release [21]. As can be seen from Table 7.2, n_r was in the range between 0.45-0.7. As reported by the same authors and by Korsmeyer *et al.* (1983), an n_r value of 0.5 is related to a pure drug diffusion mechanism (Fickian diffusion), while an n_r value of 1 is related to polymer swelling-controlled drug release mechanism; n_r values in between 0.5 and 1 can be attributed to a mix of both mechanism of drug release [19, 21]. In this range of n_r values the closer to 0.5 the higher the degree of drug release due to diffusion mechanism, the closer to 1 the higher the degree of drug release due to polymer swelling. Based on these considerations, the release of actives from AFG can be attributed mainly to diffusion. |On the other hand, the k_r parameter is characteristic of each drug-matrix system [19]. k_r changed significantly for active-containing AFG as a function of the loaded active, of its concentration and of t_s. It is, therefore, difficult to correlate changes of k_r to AFG formulation changes and/or storage periods.

In order to better understand the effect of the type of active and concentration on the obtained release profiles, EE measurements were also considered. Non-encapsulated active fractions, determined via EE analysis, were compared to plateau values (cumulative release percentages after 5 h) from the corresponding release profile, and results are presented in Figure 7.5. The comparison revealed that these two quantities, regardless of the type/concentration of the active and/or of t_s, were practically equivalent. It is, therefore, evident that the amount of active detected during release experiments was, in all cases, the fraction of the species that was not encapsulated. This further implies that once an active was entrapped then its release from AFG particles simply did not take place, even under sink conditions. As the EE and the mass of active within the AFG particles increased, the capacity of these systems to retain the entrapped species was maintained. This is obviously the case only for the systems exhibiting some level of entrapment and as such this behaviour was not observed for NFG formulations. For the latter systems release was indeed slightly delayed, in comparison to that observed simply for an aqueous solution of the active, most likely as a result of the increased viscosity of AFG formulations. Nonetheless, release did result in complete expulsion of the active (100%), realised approx. after 90 minutes for NAS and 120 minutes for NFG.

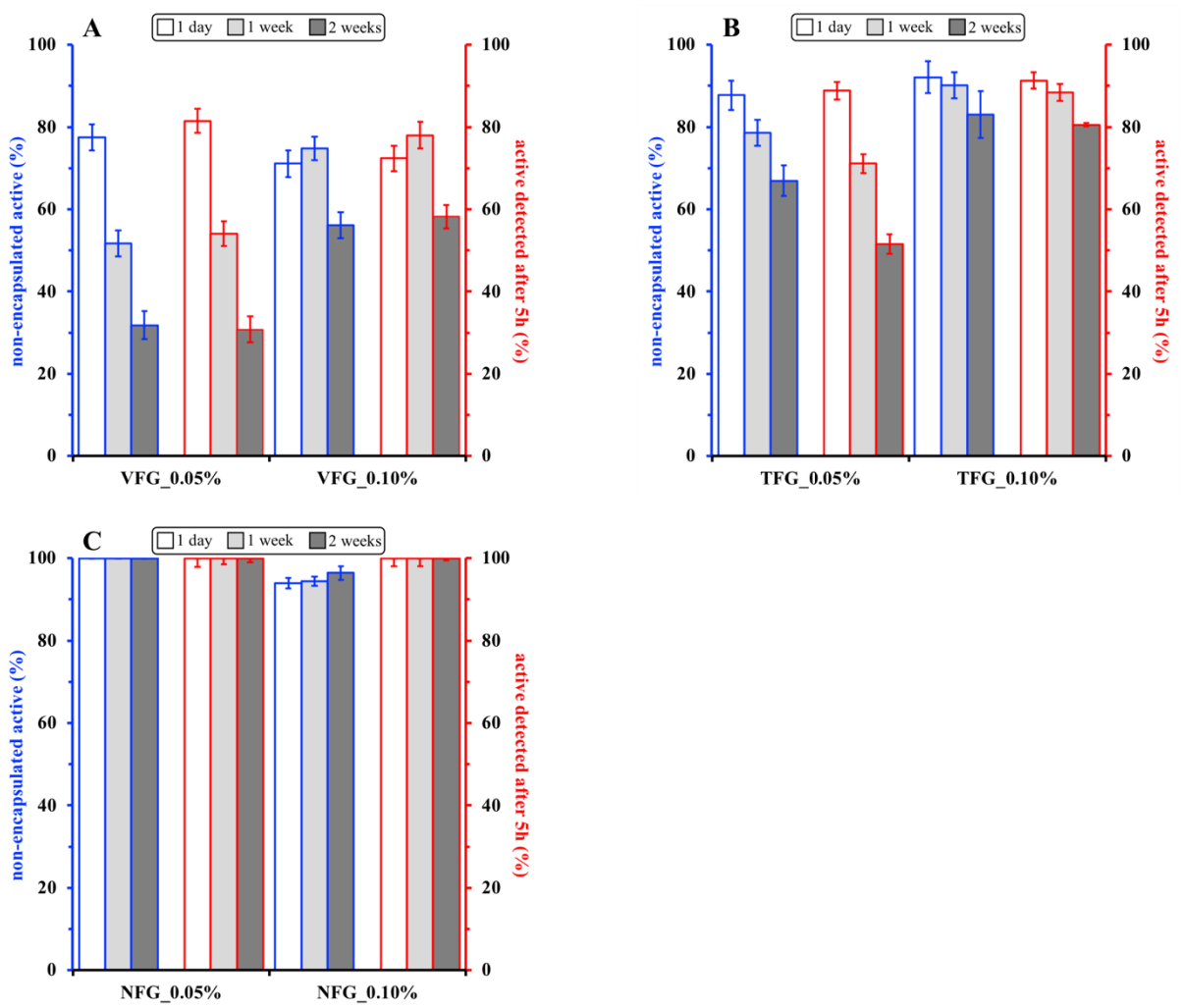

Figure 7. 5 - Active percentages non-encapsulated (Blue) and active percentages detected after 5 h of release testing in the acceptor phase (Red) for VFG (A), TFG (B) and NFG (C) as function of t_s

7.3.2 Effect of particle dimensions

It was previously shown that the water solubility of the active as well as t_s had a significant impact on EE of AFG and of their subsequent release under sink conditions. These behaviours are further explored in this section with reference to the role of AFG particle dimensions; the encapsulation of a low water soluble active tested previously, specifically VAN, was studied in microparticles and nanoparticles AFGs. VAN was selected as model active to be encapsulated, since it displayed higher changes of EE values and release behaviours as a function of t_s, in comparison to TRP, as shown in section 7.3.1.2. Encapsulation efficiency and 7.3.1.3. Release experiments. The ratio between $CaCl_2$/ALG used during AFG preparation played a significant role on the final dimensions of AFG particles, as shown in a previous study [17]. In particular, when a ratio $CaCl_2$/ALG higher than 0.150 was used for AFG production, particles in the micrometre range were obtained, while when a lower ratio was used particles

in the nanometre range were obtained. The dependency of ALG particle dimensions on the used concentration of calcium was also reported by Badita *et al*. (2016): at relatively low calcium concentrations, gelation was limited and ALG aggregates of spherical shape and rough surfaces were formed with a radius of gyration of approx. 300 nm [23].

7.3.2.1 Particle size distribution

In the present study, AFG were produced using a fixed ALG concentration of 2% w/w, a VAN concentration of 0.10% w/w and $CaCl_2$/ALG ratios of 0.125 and 0.175; thus, $CaCl_2$ concentration was at 0.25% w/w (sample VFG_A) and 0.35% w/w (sample VFG_B), leading to formation of nanometre and micrometre particles, respectively, as reported in Figure 7.6. Additionally, two "blank" AFG samples, i.e. systems formed in the absence of the active, were produced using the same ALG concentration and $CaCl_2$/ALG ratios for comparison. The PSD for both VFG_A and VFG_B practically overlap with those of their blank counterparts (AFG_A and AFG_B, respectively). The dimensions of the VFG_A and AFG_A systems were close to the sizes of the $CaCl_2$/ALG nano-assemblies (at equivalent concentrations) reported by Badita *et al.* (2016). Thus, as was the case for the AFG microparticles previously discussed, the presence of the active did not impact on the dimensions of the formed fluid gel system, even when the colloidal assemblies were formed by nanometre particles.

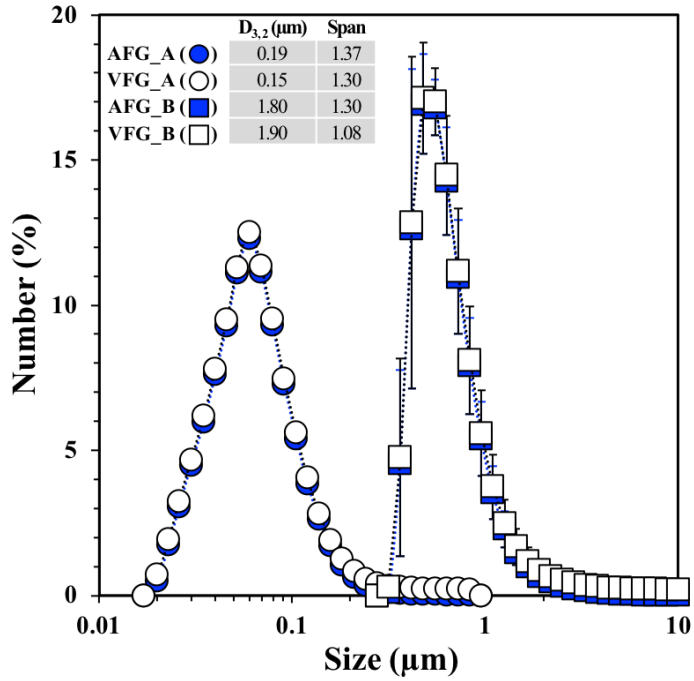

Figure 7. 6 - PSD (number %) for VAN-loaded and blank AFG as a function of $CaCl_2$/ALG ratios: 0.125 (VFG_A & AFG_A) and 0.175 (VFG_B & AFG_B)

7.3.2.2 Shear viscosity profile

The rheological behaviour (shear viscosity profiles) of VFG_A and VFG_B systems was also investigated and compared to that of their "blank" counterparts (AFG_A and AFG_B, respectively); data obtained are presented in Figure 7.7. The shear viscosity curves for all systems practically overlapped throughout the shear rate range studied. In addition, power law fitting parameters obtained from Equation (7.4) (also provided in Figure 7.7) revealed a similar magnitude of shear thinning behaviour across all fluid gel formulations. Besides the obvious conclusion that the presence of VAN did not affect the flow behaviour of these systems, it was also evident that shear viscosity was not significantly influenced by the difference in particle size between the AFG_A and AFG_B formulations.

The flow behaviour in the case of fluid gels was mostly dominated by the large fraction of dispersed particles typically obtained in these formulations (reported to be close to the maximum packing fraction) and gel particle-specific mechanical properties (e.g. stiffness) [7, 24]. The latter became increasingly influential at high particle fractions (higher tendency for particle-particle contacts to take place) and were proportional to polymer (in this case ALG) concentration [7, 24]. As both AFG_A and AFG_B formulations were formed using the same ALG concentration, it would be expected that particle gel strength was not dissimilar, although particle dimensions were different.

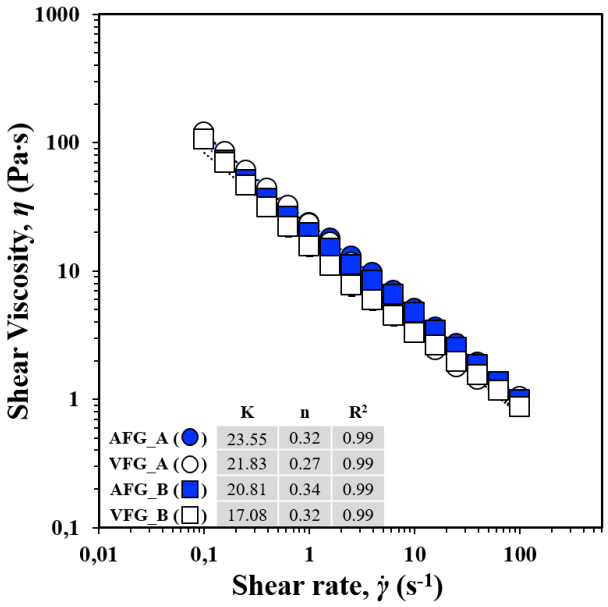

Figure 7. 7 - Shear viscosity curves for blank and VAN-loaded AFG as a function of $CaCl_2$/ALG ratios: 0.125 (VFG_A & AFG_A) and 0.175 (VFG_B & AFG_B)

7.3.2.3 Encapsulation efficiency

The EE of VAN in VFG formulations with particles of different dimensions (VFG_A and VFG_B) was also determined, as described in section 7.2.6 Encapsulation efficiency, as a function of t_s. Results are reported in Table 7.3. In both cases, EE increased over t_s, in a way similar to that observed previously for different concentrations of actives having a low water solubility (VAN and TRP; see Table 7.1). Nevertheless, the EE increase for VFG_A appeared to progress more rapidly and reached a higher value than that for VFG_B. As such there was some evidence that this behaviour was affected by particle size. As VAN is much smaller (radius of gyration of ≈ 0.47 nm [25]) than the reported average pore size of ALG gel network (≈ 5 nm [26]), it can be assumed that the observed migration of this active, from the bulk aqueous phase of VFG towards the interior of AFG particles, took place by a simple diffusion-controlled mechanism. In this case, Fick's second law should be sufficient to describe this process. As such, diffusion of VAN would depend on three parameters: its concentration difference between the exterior and the interior of the particle, the diffusion coefficient or diffusivity of the particle structure and the diffusion length or path [27]. The initial EEs for both VFG_A and VFG_B were more or less the same (Table 7.3), therefore a similar concentration differential (between bulk aqueous phase and AFG particles) driving diffusive migration was expected. Additionally, particles in both systems should consist of a similar “building block” structure; i.e. an assembly of ALG polymer chains. However, the presence of a higher Ca^{2+} concentration

in VFG_B could suggest that in this case the ALG network exhibited a higher degree of cross-linking, and thus lower diffusivity, as suggested by literature [26]. What is more, the diffusion path for VAN to be transported into the AFG_A particles was significantly shorter than that in the case of AFG_B, because of their different sizes. In conclusion, the observed difference in the amount of VAN that was accumulated in VFG_A over VFG_B particles, during the studied storage period, could be explained primarily due to the much smaller size of the former (VFG_A) and also because of the reduced diffusivity of the polymer network in the latter (VFG_B).

Table 7. 3 - EE of VAN in VFG as a function of their particle size and t_s

	Encapsulation Efficiency, EE (±SD)		
	1 Day	**1 Week**	**2 Weeks**
VFG_A	24.2% (±2.5)	49.5% (±3.3)	73.3% (±2.9)
VFG_B	28.9% (±3.2)	25.2% (±2.9)	43.9% (±3.2)

7.3.2.4 Release behaviour

Release tests were conducted on VFG_A and VFG_B samples as described in section 7.2.7 Release studies. Release curves obtained are reported in Figure 7.8. The concentrations of VAN detected into the release medium were obtained via UV-Vis analysis and they were not adjusted to take into account the fraction of VAN encapsulated into AFG particles. Additionally, in order to clarify the release behaviour of this active, data obtained from release experiments were fitted into Equation (7.3), as described in section 7.2.8 Data fitting, and the obtained parameters are reported in Table 7.4.

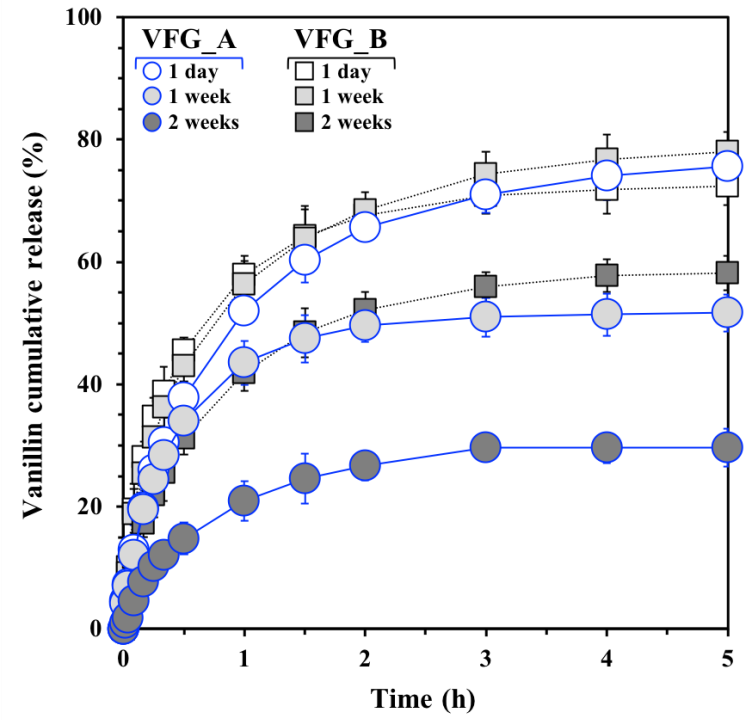

Figure 7. 8 - Release curves of VFG as function of t_s: VFG_A (Blue), VFG_B (Grey)

It can be noticed that the shape of release curves was similar to that exhibited by all other active-containing AFG formulations discussed previously (see Figure 7.4) and that the plateau of release of each curve was reached before the end of the release test (in between 120 and 240 minutes). However, this plateau was reached at different VAN amounts for each test, depending on the sample tested, i.e. VFG_A or VFG_B, and on t_s. In general, the amount of VAN released from these materials decreased by increasing t_s, but this effect was more pronounced for tests conducted on VFG_A, i.e. in the sample formed by nanoparticles, then for VFG_B. These results suggested that particle size of AFG had a significant impact on the release behaviour of VAN. As previously reported, in section 7.3.2.3 Encapsulation efficiency, because VAN is much smaller than the reported average pore size of the ALG gel network, it can be assumed that this active was able to freely diffuse inside AFG particles. In theory, VAN diffusion through ALG pores should happen also during release tests, allowing its release from particles. However, the release plateaus for both VFG_A and VFG_B did not reach 100% of VAN release, but only lower amounts. For some reasons VAN was released only to some extent and this was influenced by both the sample tested, i.e. VFG_A or VFG_B, and by t_s.

In order to better understand whether existed some correlation between the EE of VAN and its release behaviour from VFG_A and VFG_B, the results obtained from EE measurements

were also considered. Non-encapsulated VAN fractions, determined via EE analysis, and the cumulative amounts of VAN detected during release studies, i.e. the fraction of VAN detected in the aqueous acceptor phase after 5 h, were practically identical, as presented in Figure 7.9. In other words, the amount of VAN detected during release experiments was the fraction that was not encapsulated into AFG particles, confirming that once VAN was entrapped in AFG particles then its release did not take place, as reported previously in section 7.3.1.3. Release experiments. This behaviour was observed in both microparticle and nanoparticle AFG samples. However, a faster rate of VAN encapsulation into nanoparticles was observed. It can be assumed, as mentioned previously in section 7.3.2.3 Encapsulation efficiency, that both materials had a similar ALG structure and their only difference was the extension of the gel network. When VAN diffused through AFG particles, its diffusion path to be transported into nanoparticles was significantly shorter than that for microparticles. The smaller size of nanoparticles could also explain the faster decrease of VAN detected at the plateau of release as a function of t_s. This can be explained assuming that the fraction of VAN entrapped within particles was not able to back-diffuse into the bulk phase of AFG and so it could not be detected into the release medium. Only the fraction not encapsulated was able to freely move in the bulk water phase between particles, diffuse out of AFG and being detected into the release medium.

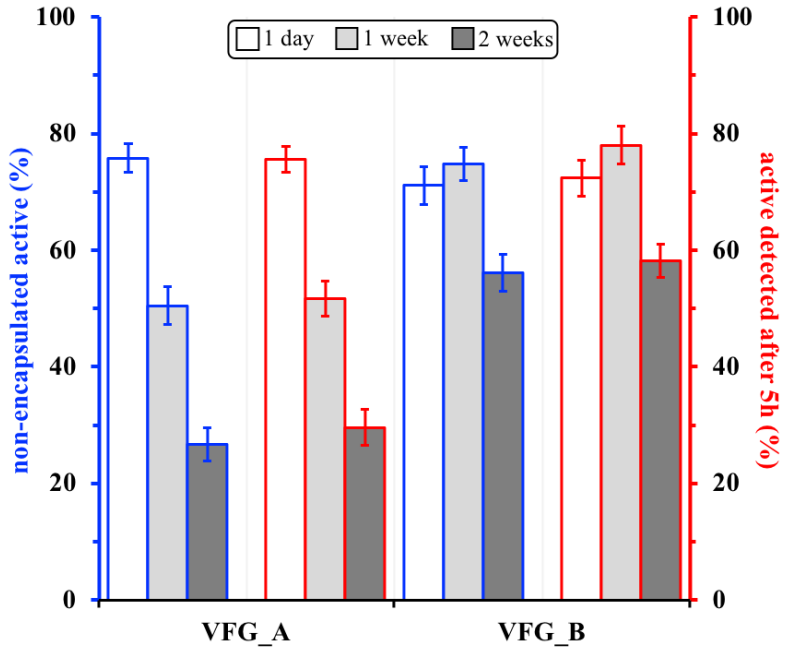

Figure 7. 9 - VAN percentages non-encapsulated (Blue) and VAN detected in the acceptor phase after 5 h of release testing (Red) for VFG_A and VFG_B as a function of t_s

In order to better understand the release behaviour of VAN, data obtained from release studies of VFG formulations were fitted to Equation (7.3), as described in section 7.2.8 Data fitting. Obtained parameters are reported in Table 7.4.

Table 7. 4 - k, n, R^2 parameters obtained from data fitting of Equation 7.3 for release tests of VFG_A and VFG_B

		k_r (±SD)	n_r (±SD)	R^2
VFG_A	**1 day**	6.48 (± 1.10)	0.54 (± 0.05)	0.99
	1 week	9.80 (± 2.61)	0.49 (± 0.08)	0.98
	2 weeks	3.91 (± 0.58)	0.51 (± 0.04)	0.99
VFG_B	**1 day**	9.48 (± 2.44)	0.45 (± 0.08)	0.98
	1 week	7.76 (± 1.55)	0.47 (± 0.06)	0.99
	2 weeks	3.49 (± 0.01)	0.50 (± 0.04)	0.99

As can be noticed n_r parameter was almost constant for all experiments and it was in the range between 0.45-0.54, revealing a pure diffusion mechanism of VAN release from VFG_A and VFG_B [19, 21].

7.3.3 Proposed mechanism for actives encapsulation in AFG

In this section a hypothesis to explain the mechanism of actives encapsulation/release in AFG is proposed. This hypothesis summarises all the data reported in previous sections and it is schematically presented in Figure 7.10.

During AFG formation actives are homogeneously distributed in the system. They can freely move through the gel network and diffuse into the formed particles due to their smaller sizes in comparison to gel pore dimensions, following Fick's second law. The diffusional loading of the actives in AFG particles depends on the difference of active concentrations between the exterior and the interior of the particle, the diffusion coefficient of the particle structure and diffusion length [27]. These influences were discussed earlier to explain the variation in the rate and magnitude of loading exhibited by AFG of nano- (VFG_A) and micro-particles (VFG_B) (Table 7.3). Nonetheless, the rate of VAN loading observed here was much lower than that reported for other actives within ALG gel particles by Tanaka *et al.* (1984). They studied the diffusion of several species into and from ALG gel beads, reporting that an equilibrium concentration of TRP in the particles was obtained after only 30 min of placing blank beads into an aqueous solution of the active. Hariyadi *et al.* (2010) studied the diffusional loading and release of ibuprofen within ALG microparticles [29]. Microparticles were added to a water

solution of ibuprofen and stored at R.T. for 24 h, producing an active loading in the range of 23-29% w/w.

Low water-soluble actives, after their diffusion in the core of AFG particles, are prone to build some interactions with the ALG network. In this way actives are entrapped within the particles and they cannot be released from them. In fact, the fraction of active entrapped within AFG particles is retained into the system and is not detected into the release medium when release experiments are made. The extent of interactions between these actives and the AFG matrix is time dependent and overtime the fraction entrapped in the particles increase, due to the diffusion of the active from the bulk water phase into AFG particles, leading to an increase of EE and to a decrease the amount of active detected during release experiments. On the other hand, high water-soluble actives are not prone to encapsulation due to the fact that they do not form interactions with the gel network. They can diffuse in AFG particles, but are not retained in them. When performing EE tests and/or release experiments these actives can back-diffuse from the particles core to the bulk phase and so to the release medium.

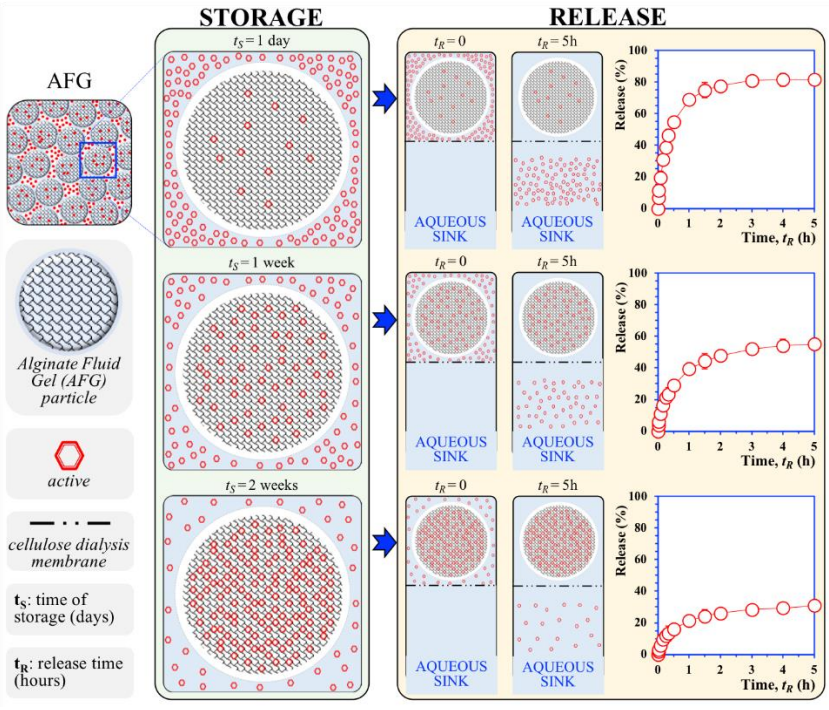

Figure 7. 10 - Graphical representation of hydrophobic active behaviour within AFG particles

7.3.3.1 Preliminary studies

In addition to previously reported EE tests and release experiments on active-containing AFG, release studies were conducted using a VAN (0.10% w/w) Aqueous solution (VAS) and an

aqueous solutions of VAN (0.10% w/w) in the presence of ALG (2% w/w), but without the addition of calcium (VAN-ALG). Both solutions were stored at R.T. in closed plastic pots and release tests were conducted on them, as described in section 7.2.7 Release studies, after 1 day, 1 week and 2 weeks from preparation, to mimic the same storage conditions and aging of VFG formulations (Figures 7.4B & 7.8). Results are reported in Figure 7.11 (only one curve is presented for VAS solution, since data obtained from release tests conducted at different t_s perfectly overlapped).

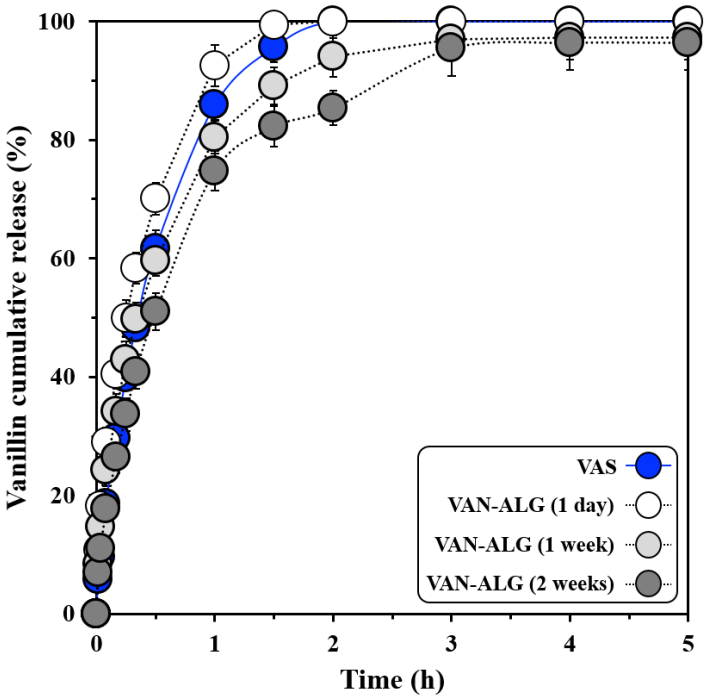

Figure 7. 11 - Release curves of 0.10% w/w VAN solutions as function of t_s: VAN-water solution (Blue), VAN-2% ALG solution (Grey)

VAN present in VAS was completely detected into the release medium at the plateau of release (≈120 minutes), and this behaviour did not change as a function of t_s. Since the concentration of VAN detected did not decrease by increasing t_s, it can also be concluded that VAN did not degrade during storage. This confirmed that the reduced concentration of actives in VFG and TFG overtime was due to the encapsulation of VAN and TRP in AFG particles and it was not related to actives degradation.

Also for the VAN-ALG solution, the amount of VAN introduced was completely detected into the release medium after the plateau of release was reached (≈120/180 minutes) and this did not decrease by increasing t_s. It can be concluded that interactions were only formed between

VAN and the ALG gel network and not with the non-crosslinked ALG polymer chains. To achieve active encapsulation, particles should be present and the crosslinking is therefore essential for the development of active-AFG interactions.

7.3.3.2 Encapsulation of actives

As previously reported, in section 7.3.2.3 Encapsulation efficiency, all the actives used in this study had dimensions much smaller than the reported average pore size of the ALG gel network. It can be assumed that ALG pores would not limit movements of actives in the gel network and that the transfer of actives into gel particles was predominantly driven by a diffusion mechanism. To clarify the mechanism of actives transfer in AFG particles, EE data for VFG and TFG were used to calculate the mass of actives encapsulated per gram of material. These data were plotted over the square root of storage time ($\sqrt{t_s}$). In addition, a diffusion-dominated transfer of actives into particles is displayed as a linear trend-line. Results are reported in Figure 7.12. The initial rate of transfer appeared to follow a similar pattern for all the formulations, which depended on the concentration of active initially placed in the system, regardless of the type of hydrophobic active and/or AFG particle dimensions. In fact, the slope of active transfer rate into particles was higher for samples in which was introduced a 0.10% w/w active concentration than for 0.05% w/w. This support the argument that at early stages of storage, inclusion of actives was primarily controlled by the concentration difference imposed into the system, i.e. by the difference in concentration of active between the bulk phase and the internal particle cores. Solid-straight lines, plotted in Figure 7.12, represent the theoretical encapsulation rate over the 2 weeks' time span if the rate of active transfer into particles continued to be only driven by the difference in active concentrations between the bulk phase and the internal particle cores; specifically, red line for actives concentration of 0.05% w/w and blue line for actives concentration of 0.10% w/w. After the initial stages, the transportation of actives into particles deviates from the calculated diffusion mechanisms, as can be seen from Figure 7.12, as other phenomena dominate: specifically, the diffusivity of the particles, imposed by the gel network, and the diffusion length, governed by the dimension of the particles. In fact, even after the initial stages, the active transfer rate in nanoparticle-AFG seemed to be predominantly governed by the difference in active concentration between the bulk phase and the internal particle cores. On the contrary, the active transfer rate in microparticle-AFG deviated more from this behaviour and it was more

affected by particle diffusivity and longer diffusion pathways. Additionally, in microparticle-AFG, over long t_s, the amount of active entrapped was also function of the type of added active and VAN was clearly more encapsulated than TRP.

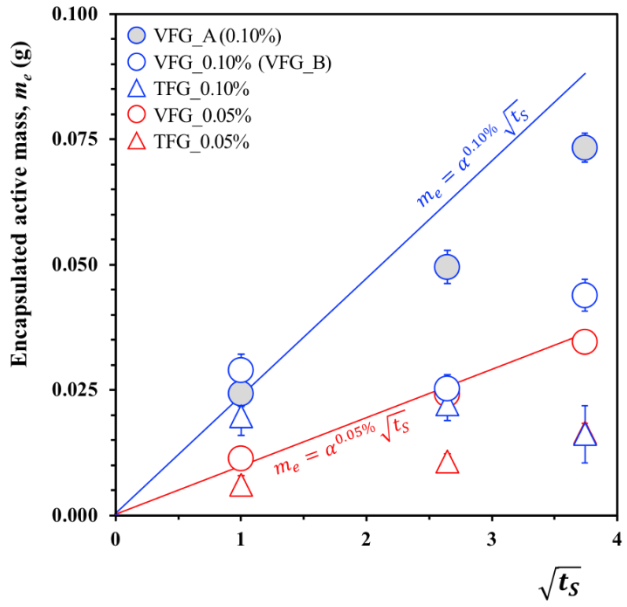

Figure 7. 12 - Grams of active encapsulated per gram of AFG formulation as a function of the used active (VAN and TRP), of particle dimensions (VFG_A and VFG_B) and of the active concentration in the sample (0.05% w/w-Red and 0.10% w/w-Blue) plotted over the square root of t_s

Once actives diffused into AFG particles two different behaviours were identified, based on the active hydrophilicity/hydrophobicity. In fact, as reported in section 7.3.1.2. Encapsulation efficiency, the EE of VAN and TRP increased as a function of t_s, while EE of NIC was not affected by t_s. AFG particles were formed by a network of crosslinked ALG chains and water was present both outside and inside particles. However, the core of particles was composed also by ALG chains, constituted of mannuronic acid (M) and guluronic acid (G) building blocks, and by Ca^{2+} ions. Thanks to the presence of hydrocarbon backbones and ions the core of particles had a more hydrophobic behaviour, if compared to the bulk water phase surrounding particles. VAN and TRP were specifically chosen as model actives because of their quite low water solubility and, for the purpose of this study, can be described as hydrophobic actives. Due to their low water solubility these actives would preferentially fitted hydrophobic environments, like the internal core of AFG particles. Once VAN and TRP diffused into AFG particles they built interactions with the matrix and they were retained in the particles. In fact, it was observed that the EE in VFG and TFG samples increased by increasing t_s and the amount of VAN and TRP released during release studies decreased by increasing t_s. The

formation of similar matrix-active interactions have been studied in the past: Yang *et al.* (2015) highlighted the formation of hydrophobic interaction between ALG polymer chains and the aromatic rings of TRP molecules [30]. Even though no study was conducted specifically on VAN interactions with ALG, a good number of works reported the interaction between VAN and different hydrocolloids. For example, VAN has been reported to interact with amino acids via hydrogen bonding, hydrophobic and electrostatic interactions and with a range of proteins, including β-lactoglobulin, sodium caseinate, bovine serum albumin, ovalbumin, whey, milk and soy protein [31-34]. In addition, a study of De Fenoyl *et al.* (2018) showed interactions between VAN and polysaccharides, specifically amylose and ι-carrageenan [35]. The hypothesis is that even in ALG systems some active-matrix interactions were formed. This can explain the increase of EE of VAN and TRP overtime and the decreased amount of these actives detected into the release medium during release experiments. In addition, the increase in EE was more pronounced in AFG formulation made of nanoparticles in comparison to microparticles ones and this can be explained considering the diffusion time of the active into particles. The diffusion path of the active to be transported into nanoparticles was significantly shorter than that for microparticles and, therefore, the active diffused faster in them. In fact, the diffusion time of actives through gel particles has been reported to be function of particle dimensions by Siepmann *et al*. (2004), in a study about the diffusion of 5-fluorouracil from microparticles of different sizes [36].

On the other hand, NIC was chosen as high water soluble/hydrophilic active. The hypothesis is that NIC was also able to freely diffuse through AFG particles, but it did not form any interactions with the AFG matrix. Because of that, NIC was able to back-diffuse out of particles. Additionally, NIC preferentially stayed in the continuous water phase surrounding AFG particles, due to the higher hydrophilic behaviour of this environment, if compared to the internal core of particles. In fact, no changes in EE were observed and all NIC was released from NFG during release experiments.

To summarise, an increase in EE by increasing t_s was observed only when VAN and TRP were used as actives, but not in the case of NIC. Therefore, it can be concluded that active-matrix interactions are formed only when low water-soluble actives are introduced in AFG systems. The hypothesis is that these interactions have a hydrophobic nature and only actives having a quite low water solubility, like VAN and TRP, can be encapsulated into AFG particles core.

Overall, an enthalpic advantage could be identified for hydrophobic actives to be solubilised in the water confined in the core of AFG particles, in order to be less in contact with the water present in the bulk phase. In fact, the hydrocarbon backbone of ALG polymer chains can reduce unfavourable interactions between hydrophobic actives and water molecules. The development of hydrophobic interactions with the matrix is time dependant, since it is subsequent to actives diffusion in the particles. On the contrary, actives having a high hydrophilic nature, like NIC, are not prone to be encapsulated and would preferentially stay in the continuous water phase outside particles. However, more experiments should be conducted to better understand the formation mechanism and the nature of these interactions.

7.4 Conclusions

In this work, the encapsulation of VAN and TRP, as hydrophobic model actives, and NIC, as hydrophilic one, in cross-linked AFG particles has been investigated. It was demonstrated that the presence of the active did not affect the dimensions and rheological properties of AFG particles. The EE and release behaviour of actives, loaded in AFG, were strongly influenced by the hydrophilicity of the active: highly water-soluble actives were not prone to encapsulation, while active showing quite low water solubility were successfully encapsulated. Several experiments revealed the formation of matrix-active interactions. The hypothesis is that these were due to hydrophobic interactions between low water soluble actives and the crosslinked ALG network. These interactions may be responsible for blocking the release of hydrophobic actives when encapsulated into AFG particles, during release experiments. However, future studies should be conducted in order to better clarify the nature of these interactions in AFG systems and to understand if these interactions can be formed in general between ALG particles and low water soluble actives. These results are scientifically relevant to clarify the encapsulation behaviour of actives in AFG. These materials can be potentially used for new applications in the field of encapsulation and controlled release of active compounds and drugs. In future, more experiments should be conducted on AFG loaded with hydrophobic actives in order to identify release environments/conditions that will lead to the release of the actives fraction encapsulated into the particles. In this way it would be possible to obtain a new class of stimuli responsive materials able to release the non-encapsulated

active fraction in water, or hydrophilic conditions, and to release the encapsulated fraction under a different release environment/conditions.

Acknowledgment

This research was funded by the Engineering and Physical Sciences Research Council [grant number EP/K030957/1], the EPSRC Centre for Innovative Manufacturing in Food.

7.5 References

1. Ray, S., U. Raychaudhuri, and R. Chakraborty, *An overview of encapsulation of active compounds used in food products by drying technology.* Food Bioscience, 2016. **13**: p. 76-83.
2. Wischke, C. and S.P. Schwendeman, *Principles of encapsulating hydrophobic drugs in PLA/PLGA microparticles.* International Journal of Pharmaceutics, 2008. **364**(2): p. 298-327.
3. Burey, P., et al., *Hydrocolloid Gel Particles: Formation, Characterization, and Application.* Critical Reviews in Food Science and Nutrition, 2008. **48**(5): p. 361-377.
4. Ozkan, G., et al., *A review of microencapsulation methods for food antioxidants: Principles, advantages, drawbacks and applications.* Food Chemistry, 2019. **272**: p. 494-506.
5. Norton, Jarvis, and Foster, *A molecular model for the formation and properties of fluid gels.* International Journal of Biological Macromolecules, 1999. **26**(4): p. 255-261.
6. Shewan, H.M. and J.R. Stokes, *Review of techniques to manufacture micro-hydrogel particles for the food industry and their applications.* Journal of Food Engineering, 2013. **119**(4): p. 781-792.
7. Garrec, D.A. and I.T. Norton, *Understanding fluid gel formation and properties.* Journal of Food Engineering, 2012. **112**(3): p. 175-182.
8. Fernández Farrés, I., M. Douaire, and I.T. Norton, *Rheology and tribological properties of Ca-alginate fluid gels produced by diffusion-controlled method.* Food Hydrocolloids, 2013. **32**(1): p. 115-122.
9. Chung, C., B. Degner, and D.J. McClements, *Development of Reduced-calorie foods: Microparticulated whey proteins as fat mimetics in semi-solid food emulsions.* Food Research International, 2014. **56**: p. 136-145.
10. Le Révérend, B.J.D., et al., *Colloidal aspects of eating.* Current Opinion in Colloid & Interface Science, 2010. **15**(1): p. 84-89.
11. Fernández Farrés, Moakes, and Norton, *Designing biopolymer fluid gels: A microstructural approach.* Food Hydrocolloids, 2014. **42**: p. 362-372.
12. Smaniotto, F., et al., *Use of Alginate Fluid Gel Microparticles to Modulate the Release of Hydrophobic Actives*. 2019.
13. ter Horst, B., et al., *A gellan-based fluid gel carrier to enhance topical spray delivery.* Acta Biomaterialia, 2019. **89**: p. 166-179.
14. Gibbs, F., et al., *Encapsulation in the food industry: a review.* International Journal of Food Sciences and Nutrition, 1999. **50**(3): p. 213-224.

15. Jelena, M., et al., *Microencapsulation of Flavors in Carnauba Wax.* Sensors, 2010. **10**.
16. Barnes, H.A., J.F. Hutton, and K. Walters, *An introduction to rheology*. Vol. 3. 1989: Elsevier.
17. Smaniotto, F., et al., *Freeze drying and rehydration of alginate fluid gels.* Food Hydrocolloids, 2020. **99**: p. 105352.
18. Piacentini, E., *Encapsulation Efficiency*, in *Encyclopedia of Membranes*, E. Drioli and L. Giorno, Editors. 2016, Springer Berlin Heidelberg: Berlin, Heidelberg. p. 706-707.
19. Korsmeyer, R.W., et al., *Mechanisms of solute release from porous hydrophilic polymers.* International Journal of Pharmaceutics, 1983. **15**(1): p. 25-35.
20. Siepmann, J., A. Streubel, and N.A. Peppas, *Understanding and Predicting Drug Delivery from Hydrophilic Matrix Tablets Using the "Sequential Layer" Model.* Pharmaceutical Research, 2002. **19**(3): p. 306-314.
21. Rinaki, E., G. Valsami, and P. Macheras, *The power law can describe the 'entire' drug release curve from HPMC-based matrix tablets: a hypothesis.* International Journal of Pharmaceutics, 2003. **255**(1): p. 199-207.
22. Fox, R.W., P.J. Pritchard, and A.T. McDonald, *Fox and McDonald's introduction to fluid mechanics*. 2011, Hoboken, NJ; Chichester: John Wiley & Sons, Inc. ; John Wiley [distributor].
23. Badita, C.R., et al., *The study of the structural properties of very low viscosity sodium alginate by small-angle neutron scattering.* AIP Conference Proceedings, 2016. **1722**(1): p. 220007.
24. Fernández Farrés, I., R.J.A. Moakes, and I.T. Norton, *Designing biopolymer fluid gels: A microstructural approach.* Food Hydrocolloids, 2014. **42**: p. 362-372.
25. Yaws, C.L. and A.S.Y. Leh, *Radius of gyration—Organic compounds*, in *Thermophysical Properties of Chemicals and Hydrocarbons*, C.L. Yaws, Editor. 2009, William Andrew Publishing: Norwich, NY. p. 661-668.
26. Yong Lee, K. and D. J Mooney, *Alginate: Properties and biomedical applications*. Vol. 37. 2012. 106-126.
27. Li, J. and D. Mooney, *Designing hydrogels for controlled drug delivery.* Nature Reviews Materials, 2016. **1**: p. 16071.
28. Tanaka, H., M. Matsumura, and I. Veliky, *Diffusion characteristics of substrates in Ca-alginate gel beads.* Biotechnology and bioengineering, 1984. **26**(1): p. 53-58.
29. Hariyadi, D., et al., *Diffusion loading and drug delivery characteristics of alginate gel microparticles produced by a novel impinging aerosols method.* Journal of drug targeting, 2010. **18**: p. 831-41.
30. Yang, Y., J. Qian, and D. Ming, *Docking polysaccharide to proteins that have a Tryptophan box in the binding pocket.* Carbohydrate Research, 2015. **414**: p. 78-84.
31. Houde, M., N. Khodaei, and S. Karboune, *Assessment of interaction of vanillin with barley, pea and whey proteins: Binding properties and sensory characteristics.* LWT, 2018. **91**: p. 133-142.
32. Wang, X., et al., *Application of molecular modelling and spectroscopic approaches for investigating binding of vanillin to human serum albumin.* Food Chemistry, 2011. **127**(2): p. 705-710.
33. Chobpattana, W., et al., *Mechanisms of Interaction Between Vanillin and Milk Proteins in Model Systems*. Vol. 67. 2002. 973-977.
34. Weerawatanakorn, M., et al., *Reactivity and stability of selected flavor compounds.* journal of food and drug analysis, 2015. **23**(2): p. 176-190.

35. De Fenoyl, L., et al., *Interfacial activity and emulsifying behaviour of inclusion complexes between helical polysaccharides and flavouring molecules resulting from non-covalent interactions.* Food Research International, 2018. **105**: p. 801-811.
36. Siepmann, J., et al., *Effect of the size of biodegradable microparticles on drug release: experiment and theory.* Journal of Controlled Release, 2004. **96**(1): p. 123-134.

Chapter 8: ACTIVES IN ALGINATE FLUID GEL: MECHANISMS OF ENCAPSULATION AND RELEASE

Abstract

The encapsulation and release of actives in fluid gel materials has been recently studied, especially for food applications. The encapsulation of hydrophilic and hydrophobic actives has been previously studied using Alginate Fluid Gels (AFG) composed by micro/nanoparticles as loading matrices. The aim of this work was to further investigate the mechanisms of encapsulation and release of hydrophobic actives into/from AFG particles as well as assessing further parameters that can be used for their control. This was obtained using both macrogel particles, produced via extrusion method, and micro/nanoparticles, produced via the fluid gel route. It was confirmed that VAN was encapsulated into alginate (ALG) particles due to the formation of active-matrix hydrophobic interactions that significantly increased upon storage. *In vitro* release experiments revealed that the exposure of these systems to acidic environments (simulated gastric fluid) led to release of the VAN fraction encapsulated into ALG particles, due to the disruption of the gel network. On the contrary, the exposure to neutral pH conditions (water and simulated intestinal fluid) did not trigger the release of VAN from particles. In addition, freeze drying (FD) was used to study the active encapsulation into AFG, revealing that this technique can be used to tune the amounts of VAN loaded into ALG particles. Overall, these experiments confirmed that the formation of active-matrix interaction in ALG particles happened only when hydrophobic molecules were placed in contact with these moieties. This study expands the knowledge about the mechanism of actives encapsulation in fluid gel systems and reveals the potential application of ALG systems for the development of pH-trigger release systems for the specific release of hydrophobic actives in low pH environments, e.g. stomach.

8.1 Introduction

Microstructures able to the control the release of drugs and nutraceuticals are widely used in pharmaceutical and food products [1]. Prolonging the activity of drugs, delaying their release and protecting sensitive actives from adverse environmental conditions, like high moisture content, acidity and high temperatures, are some of the reasons why microencapsulation systems have been widely studied and implemented over the last decades [2, 3].

Almost twenty years ago, fluid gel materials were studied and developed, revealing these to be an industrially scalable method to produce biopolymer-based microparticles [4]. More recently, microparticles produced via the fluid gel route have been studied as encapsulation matrices for bioactives. A study of ter Horst *et al.* (2019) studied the entrapment of cells in gellan gum fluid gels for wound healing applications [5]. The authors reported that encapsulation into a fluid gel formulation did not affect cell viability and was able to protect them during a subsequent spray application. The encapsulation of bioactives in AFG for food applications has been previously investigated, showing potential applications of these materials in this area [6, 7]. In fact, the ionic gelation of ALG is ideal for the entrapment of bioactives, as some of these are prone to be degraded by the high temperatures usually used for the gelation step of thermally gelled hydrocolloids, like agarose and gelatin [8-10]. AFG were studied for the encapsulation and release of tryptophan, revealing that these materials were able to encapsulate this active and slow down its release overtime [7]. The same materials were studied for the encapsulation of hydrophilic actives, specifically nicotinamide and ascorbic acid [6]. However, hydrophilic actives were not encapsulated in AFG particles, remaining in the continuous water phase surrounding these moieties. Overall, the encapsulation of hydrophobic and hydrophilic actives in AFG particles was investigated, showing that highly water-soluble actives are not prone to encapsulation in AFG, while actives having a low water solubility can be successfully encapsulated.

In past studies, ALG microparticles have been used as materials for bioactives encapsulation/release using different loading approaches. For example, Tanaka *et al*. (1984) studied the encapsulation of several compounds, like glucose, tryptophan and a-lactoalbumin via diffusion, by placing ALG gel particles into an aqueous solution containing the active [11]; Tu *et al*. (2005) loaded spray-dried ALG microparticles with 4-phenylazoaniline and methylene blue, respectively using an ethanol and water solutions of these actives [12]; Hariyadi *et al.*

(2010) studied the diffusional loading of ibuprofen within ALG microparticles, produced via an impinging aerosols method, using an aqueous solution of ibuprofen to load a suspension of ALG microparticles [13]. The main difference with these "traditional" methods for active encapsulation in ALG particles is that in the present work (as reported in chapters 4 to 7) this was conducted on "intact" formulations. In other words, AFG particles were not separated from the surrounding aqueous medium to perform encapsulation. In addition, AFG were not diluted further with an active containing solution, but actives were introduced within formulations at the same time of their production. Using this encapsulation approach, what appeared to mainly govern encapsulation in AFG particles was the rate of diffusion of the active through the continuous water phase surrounding particles. However, why the encapsulation of actives was obtained solely when hydrophobic actives were used, was not completely understood. In this study, more experiments were conducted to better clarify the encapsulation mechanism of hydrophobic actives in AFG and to study the nature of the formed matrix-active interactions. This was made using VAN as hydrophobic model active, due to its quite low water solubility of approx. 11 mg/mL at 25 °C.

Firstly, encapsulation experiments were performed on ALG particles of few millimetre dimensions, obtained via "standard" extrusion, to assess the general ability of this biopolymer to encapsulate VAN and not only when produced in the fluid gel form. Then, FD was studied as a way to modify the VAN fraction encapsulated in AFG, at the moment when the FD procedure was performed. In fact, it was previously observed that the EE of VAN in AFG increased as a function of t_s, i.e. the time elapsed from sample production. With FD, by removing the water content in AFG, it may be possible to stop the diffusion of VAN into particles. On the opposite, FD was also studied as a way to load VAN in AFG particles: blank AFG were freeze dried and rehydrated using a VAN-aqueous solution. The idea behind these experiments was to test whether the encapsulation of VAN was promoted by forcing the solvent, which carries the active, to access the core of particles. The hypothesis was that after removing the water phase associated with AFG particles, their rehydration will produced a greater driving force for the solvent to re-enter into dried particles, if compared to "standard" diffusion of the solvent in wet AFG particles. By performing the rehydration with a VAN-water solution, this active can be forced to penetrate into particles faster and/or in a larger amount.

Later on, to clarify the loading mechanism of VAN into AFG, experiments were conducted using Sodium Dodecyl Sulphate (SDS) as a proxy matrix, to study the encapsulation of VAN into SDS micelles, known to behave as hydrophobic moieties. In fact, understanding the VAN behaviour in the presence of hydrophobic moieties can clarify its encapsulation mechanism in AFG. Finally, the release of VAN form AFG particles was evaluated as a function of the used release medium. Release experiments in simulated gastric and intestinal fluids were performed to assess if the fraction of VAN encapsulated into AFG particles can be released under specific environmental conditions.

It was demonstrated that VAN was encapsulated into ALG particles due to the formation of hydrophobic interactions between the active and the ALG matrix. These interactions were disrupted by exposing ALG gels to an acidic environment, releasing a high percentage of the VAN fraction entrapped within these materials. These results are relevant from both a scientific and industrial point of view to clarify the encapsulation behaviour of AFG for potential uses in the field of encapsulation and controlled release of actives in food and drug formulations.

8.2 Materials and methods

8.2.1 Materials

Sodium alginate (CAS: 9005-38-3, W201502, lot.# MKBT7870V), vanillin (VAN, ≥97%) and sodium dodecyl sulphate (SDS, ≥99%) were purchased from Sigma-Aldrich® (Sigma–Aldrich Company Ltd., Dorset, UK). Calcium chloride ($CaCl_2$, anhydrous, 93%) was purchased from Alfa Aesar™ (Thermo Fisher Scientific, USA USA). All materials were used without further purification. Milli-Q distilled water, produced using an Elix® 5 distillation apparatus (Millipore®, USA), was used for all water-based preparations Concentrations of all materials are given as percentages of the weight of the specific substance over the total weight of the system in which it is contained (i.e. solution, fluid gel formulation, etc.) and are reported as '% w/w'.

8.2.2 Blank fluid gels

Firstly, a 2% w/w ALG solution was prepared by dissolving the required amount of ALG in distilled water at 95 °C for 45 min under stirring to ensure complete powder dissolution, as

reported by Fernández Farrés *et al.* [14]. Thereafter, the solution was cooled down to R.T.. A separate aqueous solution of $CaCl_2$ (at two different concentrations, 0.25% and 0.35% w/w) was also prepared by dissolving $CaCl_2$ at R.T. under magnetic stirring. AFG were formed using a pin-stirrer vessel (Het Stempel, NL) which has an available processing volume of 150 mL, 16 pins placed on the rotating shaft and 16 pins fixed on the internal wall [15]. A pin-shaft speed of 1000 RPM was used for all AFG preparations. The ALG solution was pumped into the pin-stirrer using a peristaltic pump (Masterflex L/S Peristaltic, DE) at a rate of 33 mL/min. The $CaCl_2$ solution was injected into the pin-stirrer, through a stainless steel needle of 1.25 mm internal diameter, using a syringe pump (Cole-Parmer Single-syringe, USA) at a rate of 4.02 mL/min. Flow rates of ALG and $CaCl_2$ streams were calculated to obtain a residence time of 4 min of samples in the pin-stirrer. This was shown to be an optimal residence time for the scope of this work based on preliminary experiments.

8.2.3 VAN-loaded fluid gels

VAN-loaded AFGs were prepared following a procedure similar to the production of blank AFGs. However, the procedure of making the aqueous $CaCl_2$ solution in this case was slightly modified. Firstly, 0.10% w/w of VAN was dissolved in distilled water at R.T. under magnetic stirring. Different amounts of $CaCl_2$, specifically 0.25% or 0.35% w/w, were then dissolved in the VAN-containing aqueous solution under magnetic stirring. The ALG solution was then prepared as described in section 8.2.2 Blank fluid gels and the final AFG containing VAN (VFG) sample was prepared as described in the same section.

8.2.4 Macrogel particles

Firstly, an ALG solution was prepared by dissolving the required amount of ALG in 50 mL of distilled water at 95 °C for 45 min under stirring to ensure complete powder dissolution. Thereafter, the solution was cooled down to R.T.. The gelling bath was prepared by dissolving the required amount of $CaCl_2$ in 500 mL of water under magnetic stirring. ALG particles were produced using a "standard" extrusion approach: ALG solution was loaded into a 50 mL plastic syringe, which was fitted into a syringe pump (AL-4000, World Precision Instruments, USA). The $CaCl_2$ solution was transferred into a 500 mL beaker and magnetically stirred at 50 RPM. The ALG solution was extruded dropwise through a stainless steel needle (26G-3/8") using a flowrate of 1 mL/min. The point of the needle was placed 5 cm above the gelling bath. 30 mL

of ALG solution was dropped into the $CaCl_2$ hardening solution. After that, formed particles were left within the $CaCl_2$ solution for other 30 minutes under magnetic stirring. Particles were then filtered using a kitchen sieve and washed with distilled water to remove the excess of $CaCl_2$ solution. Particles were collected into a disposable plastic pot and stored at 4 °C until needed for later experiments. However, they were not stored longer than 4 weeks to avoid the potential formation of moulds.

8.2.5 Macrogel particle size

The size of macrogel ALG particles was measured using a calliper. 20 beads per sample were collected and placed over an aluminium foil. Their diameters were recorded and the average values with standard deviations were calculated.

8.2.6 VAN loading in macrogel particles

Macrogel ALG particles were produced as described in section 8.2.4 Macrogel particles and then used for the encapsulation of VAN. Firstly, a VAN solution was prepared by dissolving approx. 15 mg of VAN in 500 mL of water in a volumetric flask. Then approx. 3 g of macrogel particles were weighed into a plastic pot and 100 mL of VAN solution was added to it. Pots were then transferred into an incubating orbital shaker (Incu-Shake MIDI, SciQuip, UK) and shaken at 400 RPM and 20 °C in order to obtain a homogeneous mixing of macrogel particles into the VAN solution, for the whole duration of the encapsulation experiments. This procedure were carried out in triplicate for each sample.

8.2.7 Freeze drying

Samples to Freeze Drying (FD) were frozen at -20 °C overnight and then lyophilised using a bench top freeze dryer (SCANVAC Coolsafe™, model 110-4, DK), condenser temperature -110 °C, pressure 10 Pa, conditions that were defined by the equipment. Samples were dried until constant weight.

8.2.8 Rehydration of samples

After dehydration, amounts of distilled water or VAN solution, depending on the purpose of the experiment, were placed in each dry sample in order to obtain the same sample weight before FD. When rehydration was performed using the VAN solution, this was prepared as described in section 8.2.6 VAN loading in macrogel particles. Samples were then transferred

into an incubating orbital shaker (Incu-Shake MIDI, SciQuip, UK), in order to obtain a homogeneous rehydration of the material, for different times at 400 RPM and 20 °C.

8.2.9 UV-Vis measurements

The UV absorbance of aqueous solutions of VAN was measured using an UV-Vis spectrophotometer (Orion AquaMate 8000, Thermo-Scientific®, UK). 300 nm was experimentally detected as the maximum absorbance wavelength of VAN and this value was used for later UV-Vis analyses. Absorbance values were correlated to the corresponding VAN concentrations using the Beer-Lambert equation and a VAN specific correlation parameter, determined via a calibration curve, which was made using VAN concentrations between 0.05 and 63 μg/mL. Analyses were carried out at R.T. in triplicate and all data are presented/plotted as the mean value± the standard deviation (SD).

8.2.10 Encapsulation efficiency

The encapsulation efficiency (EE) of VAN in VFG was determined by ultracentrifugation: a weighed amount of sample (approximatively 15g) was centrifuged using a Sigma 3K-30 refrigerated centrifuge (Sigma®, DK), equipped with a 12150 rotor. Centrifugation was carried out (at 21 °C) at 21,000 RPM for 45 minutes; preliminary tests (not reported here) revealed that these conditions provided sufficient separation between the VFG aqueous continuous phase and the formed VFG particles, thus allowing easy access (sampling) to the formed supernatant. A weighed amount of the supernatant (approximatively 1.5 g) was placed in a 100 mL volumetric flask and filled with distilled water. The concentration of the active in the supernatant solution was quantified spectrophotometrically (see section 8.2.9 UV-Vis measurements). The EE was calculated using Equation 8.1:

$EE = (W_t/W_i)\times 100$ (Equation 8.1)

where W_i is the amount of active initially added to the system during sample preparation and W_t is the amount of encapsulated active. The latter was calculated as the difference between the theoretical concentration of active added into the system and the concentration detected by UV, in the supernatant phase [16].

8.2.11 *In vitro* release of VAN

In vitro release studies of VAN from VFG and macrogel ALG particles were performed using a UV-Vis spectrophotometer (Orion AquaMate, Thermo Scientific, UK) to determine the concentration of VAN in the medium over time. A weighed amount of VFG (approximatively 2.5 g) was enclosed in a dialysis sack (Sigma–Aldrich Company Ltd., Dorset, UK, dialysis tubing cellulose membrane, width 43 mm, M.W. cut-off of 14000 Da) and placed in 500 mL of distilled water at R.T. (thermostated at 21.5 °C), under stirring at 150 RPM. At regular intervals, aliquots of 2 mL were withdrawn, measured using the spectrophotometer at 300 nm wavelength, as described in section 8.2.9 UV-Vis measurements, and then poured again into the medium. Each analysis was carried out in triplicate. Similar release experiments were performed on macrogel ALG particles loaded with VAN, but without using the dialysis sack. This was possible because macrogel particles were bigger than the tip of the pipette used to withdrawn the release medium. Therefore, only the release medium was collected for the UV-Vis analysis.

8.2.12 SDS proxy matrix experiments

100 mL of SDS-water solutions were prepared by dissolving amounts of SDS needed to obtain final concentrations of 0.5, 2, 3 and 10 times its CMC (8.2 mM at 25 °C), under magnetic stirring. VAN was dissolved into these solutions in order to obtain a final concentration of 0.10% (w/w), under magnetic stirring, producing respectively 0.5X, 2X, 3X and 10X SDS-VAN samples. The VAN concentration in solutions was monitored overtime using a UV-Vis, as described in section 8.2.9 UV-Vis measurements. This VAN concentration was compared to the theoretical one, weighed into the solutions initially. Similarly, SDS solutions having 0.5, 2, 3 and 10 times the CMC concentrations were prepared but without adding VAN in them and they were submitted to the same UV-Vis analysis. A VAN Aqueous Solution (VAS) was prepared by dissolving the required amount of VAN needed to obtain a 0.10% (w/w) concentration under magnetic stirring. VAS was used as a control solution and tested as for SDS-VAN solutions.

8.2.13 Simulated release in GIT

Similar release studies were conducted using different release medium to simulate the VAN release in the stomach and intestine environment. Simulated Gastric Fluid (SGF) and

Simulated Intestinal Fluid [18] were used as release media and they were prepared as follow. SGF: 2.00 g of NaCl were dissolved in approx. 900 mL of deionised water under magnetic stirring. 70 mL of 1 M HCl solution was added and the final volume was then adjusted to 1000 mL by adding distilled water. Small aliquots of 0.2 M HCl or NaOH solutions were added in order to adjust the final pH at 1.2, checking this value using a bench top pH meter (SevenCompact S220, METTLER TOLEDO, USA). This solution was stored at 4 °C and used within 7 days. SIF: 6.80 g of monobasic potassium phosphate (KH_2PO_4) were dissolved in approx. 900 mL of deionised water under magnetic stirring. 77.0 mL of 0.2 M NaOH solution was added under magnetic stirring and the final volume was then adjusted to 1000 mL by adding distilled water. Small aliquots of 0.2 M HCl or NaOH solutions were added in order to adjust the final pH at 6.8, checking this value using a bench top pH meter (SevenCompact S220, METTLER TOLEDO, USA). This solution was stored at 4 °C and used within 7 days.

In vitro release studies from VFG were performed using a dissolution apparatus (DIS 6000, Copley, UK) and a UV-Vis spectrophotometer (Orion AquaMate, Thermo Scientific, UK) was used to determine the concentration of VAN in the medium over time. A weighed amount of VFG (approximatively 2.5 g) was enclosed in a dialysis sack (Sigma–Aldrich Company Ltd., Dorset, UK, dialysis tubing cellulose membrane, width 43 mm, M.W. cut-off of 14000 Da) and attached to the mechanical shaft of the dissolution equipment. Tests were conducted using 500 mL of release medium, thermostated at 37 °C and 150 RPM stirring speed was used. At regular intervals, aliquots of 2 mL were withdrawn, measured using the spectrophotometer at 300 nm wavelength and then poured back into the release medium. A calibration curve was made at 300 nm wavelength (VAN maximum of absorbance) and was set for concentrations between 0.05 and 63 μg/mL. This was used to correlate the absorbance values of the release medium with its actual VAN concentration. Each analysis was carried out in triplicate.

8.2.14 Statistical analysis

Statistical analysis of data groups was determined via single factor analysis of variance (ANOVA). P values < 0.05 were considered as statistically significant.

8.3 Results

First the effect of introducing VAN in macrogel ALG particles was tested to better understand the behaviour of VAN in ALG matrix. In fact, it was observed previously that the EE of VAN into AFG particles increased as a function of storage time (t_s), i.e. the time elapsed from sample preparation. Therefore, encapsulation experiments of VAN were performed using millimetre size ALG particles to assess the general behaviour of VAN to migrate into ALG particles. After that, FD was studied as an alternative and gentle method to encapsulate VAN inside ALG gels: the effect of FD on VAN encapsulation and release behaviours into AFG was assessed. Additionally, blank AFG were freeze dried and rehydrated using a VAN solution, to evaluate if FD can be used as an encapsulation method for VAN in these materials. After that, experiments were conducted using SDS as proxy matrices to mimic the behaviour of AFG particles in water and study the encapsulation mechanism of VAN into hydrophobic moieties. Finally, release studies using different release media were conducted on VFG, in order to highlight if the VAN fraction encapsulated within AFG particles could be released in different release environments.

8.3.1 Macrogel particles production

Macrogel ALG particles were produced, as reported in section 8.2.4 Macrogel particles, using different concentrations of ALG and $CaCl_2$, reported in Table 8.1. Different concentrations were used in order to later study their effects on the encapsulation behaviour of VAN. The obtained particles, for all samples, were perfectly spherical and their dimensions were evaluated as described in section 8.2.5 Macrogel particle size. Results are reported in Table 8.1.

Table 8. 1 – ALG and $CaCl_2$ concentrations used for the production of macrogel ALG particles. Diameters of particles are also reported

	ALG (w/w)	$CaCl_2$ (w/w)	Diameter (mm)
AMP_2%_1%	2%	1%	2.72 (± 0.163)
AMP_2%_0.5%	2%	0.5%	2.74 (± 0.184)
AMP_2%_2%	2%	2%	2.71 (± 0.202)
AMP_1%_1%	1%	1%	2.71 (± 0.143)
AMP_3%_1%	3%	1%	2.75 (± 0.139)

As can be seen from Table 8.1 the final particle dimensions were not affected by the used concentrations of ALG and $CaCl_2$. This is in accordance with a study of Ching *et al*. (2015), were they reported that particle size and morphology of ALG macrogel are essentially a function of the needle diameter used to extrude ALG solution into the $CaCl_2$ bath, of the ALG solution flow rate and of the height between the ALG exit point and the $CaCl_2$ bath [19]. All these parameters were not changed during sample preparation, explaining why similar diameter of particles were obtained. In addition, Ching et *al.* (2015) reported that particle dimensions are function of the viscosity of ALG solution used for gel preparation [19]. The concentration of ALG used for making macrogel particles changed from 1% to 3% w/w. However, based on experimental observations, all these solutions displayed similar water-like viscosities that did not change as a function of the concentration of ALG used. This could explain why final particle dimensions did not change as a function of the ALG concentration used for the synthesis of macrogel particles.

8.3.2 VAN encapsulation in macrogel particles

All samples reported in Table 8.1 were used to conduct experiments of VAN loading as described in section 8.2.6 VAN loading in macrogel particles. The concentrations of VAN in solution used to load this active in macrogel particles were checked overtime via UV-Vis analysis, as described in section 8.2.9 UV-Vis measurements. By knowing the amounts of VAN introduced in the pots at the beginning of experiments and its concentration in the loading solution overtime it was possible to determine the amount of VAN encapsulated into macrogel particles. The concentration of VAN was checked also for a control test, in which no

macrogel particles were added. This was stored under the same conditions of other samples and its concentration of VAN did not change overtime, confirming that VAN was not degraded during these tests. Result of VAN encapsulation are reported in Table 8.2.

Table 8. 2 - Percentages of VAN encapsulated in millimetre size ALG particles, prepared using different percentages of ALG and $CaCl_2$, as a function of loading time (no significant differences [p > 0.05] were found between percentages of VAN encapsulated)

	0 day	**1 day**	**2 days**	**3 days**	**4 days**	**5 days**	**6 days**	**7 days**	**8 days**
AMP_2%_1%	0.0 (± 0.0)	2.4 (± 0.3)	17.3 (± 2.1)	41.3 (± 2.5)	77.4 (± 3.5)	76.2 (± 4.1)	75.5 (± 3.9)	73.4 (± 4.1)	72.0 (± 3.6)
AMP_2%_0.5%	0.0 (± 0.0)	8.1 (± 1.1)	21.6 (± 2.1)	32.3 (± 2.4)	42.1 (± 3.4)	50.0 (± 3.9)	57.9 (± 3.7)	62.2 (± 3.2)	66.5 (± 4.2)
AMP_2%_2%	0.0 (± 0.0)	6.9 (± 0.6)	38.6 (± 2.4)	60.3 (± 2.1)	71.5 (± 3.7)	80.0 (± 4.0)	77.8 (± 4.4)	75.8 (± 4.0)	74.1 (± 2.9)
AMP_1%_1%	0.0 (± 0.0)	7.8 (± 0.9)	33.3 (± 2.0)	52.8 (± 3.2)	72.2 (± 3.8)	70.5 (± 3.1)	73.3 (± 3.3)	72.7 (± 3.3)	70.6 (± 3.4)
AMP_3%_1%	0.0 (± 0.0)	9.3 (± 1.3)	29.9 (± 2.2)	49.6 (± 2.9)	69.2 (± 3.5)	67.5 (± 3.4)	72.3 (± 3.2)	73.7 (± 3.6)	71.7 (± 3.8)

From Table 8.2 it is possible to notice that all samples, with the exception of AMP_2%_0.5%, reached a plateaux of VAN loading after approx. 4 days. For sample AMP_2%_0.5% the VAN encapsulation took approx. 8 days and it was more gradual overtime, even though it was not statistically different from VAN encapsulation in other AMP materials. Probst *et al.* (1985) showed that Ca^{2+}, due to its ion-water interaction, can alter the structure of water [20]. This can potentially facilitate an enhancement of the water capacity to solubilise VAN within particles, as Ca^{2+} ions are only present within particles. This can explain the observed migration of this active within particle cores. In addition, a study of Soliman *et al.* (2013) showed that by increasing the concentration of $CaCl_2$, used for the formation of ALG gel particles, the EE of thyme, clove and cinnamon oil increased [21]. They reported that the maximum loading capacity of ALG particles changed as a function of the encapsulated active. However, increasing the $CaCl_2$ concentration over a specific percentage led to a decrease of

actives encapsulation. They concluded that by increasing the Ca^{2+} concentration a higher level of cross-linking was obtained, forming a more dense structure able to entrap higher amount of actives. However, increasing the Ca^{2+} concentration also reduced the pores size of ALG gels, limiting the ability of actives to permeate through them, which reduce the final loading capacity of the system. For the encapsulation of VAN in macrogel ALG particles a minimum concentration of 1% w/w of $CaCl_2$ was needed to obtain a complete VAN loading in 4 days. Reducing the concentration of $CaCl_2$ to 0.5% w/w a slower encapsulation of VAN was obtained. In addition, it is possible to conclude that the ALG concentration, used for samples synthesis, did not change the final amount of VAN encapsulated into macrogel ALG particles.

After 8 days of loading time, all particles of the sample (approx. 3 grams) were removed from VAN solution, using a stainless-steel colander, and washed with approx. 10 mL of distilled water, using a wash bottle over the colander, to remove the excess of VAN solution present on their surface. This procedure was repeated for all samples listed in Table 8.2.Then, release studies were performed on particles, as described in section 8.2.11 *In vitro* release of VAN. These experiments showed that no VAN was detected into the release medium. VAN was encapsulated into macrogel ALG particles and the non-encapsulated VAN fraction was removed/washed. As the washing step was performed very quickly, it was not expected for the encapsulated VAN to be released significantly from the core of particles. In order to prove this, water amounts used for washing samples were collected and their VAN concentration was determined via UV-Vis analyses. Results showed that the concentration of VAN was very low and in line with what expected from the solely removal of the excess of VAN on the surface of particles. Overall, particles were isolated and release experiments were conducted on them, revealing that they could not release VAN loaded in them. In fact, the use of macrogel ALG particles allowed to separate them completely from the continuous aqueous phase, thanks to their big dimensions, and perform release analysis only on the solid fraction. These experiments confirmed what observed previously about the encapsulation of hydrophobic actives into AFG: the encapsulated active fraction could not be released in water from AFG particles and only the active present in the bulk water phase surrounding particles was detected into the release medium during release experiments [7].

8.3.3 Freeze drying of VFG

Previous studies were conducted on the effects of FD on the encapsulation of hydrophilic actives, specifically nicotinamide and ascorbic acid, loaded into AFG [6]. Results showed that FD did not change the fraction of active that was encapsulated into AFG particles before performing the FD procedure. What is more, it was concluded that this technique could extend the shelf life of easy degradable actives, like ascorbic acid, and of AFG themselves, due to the removal of water from AFG formulations. Therefore, a similar study was conducted on VFG to assess the effects of FD on the encapsulation of VAN in AFG. VFG, composed of microparticles and nanoparticles, were produced using a 0.10% (w/w) VAN concentration, as described in section 8.2.3 VAN-loaded fluid gels, producing respectively samples VFG_2%_0.35% and VFG_2%_0.25%. Both samples were submitted to EE analyses, as described in section 8.2.10 Encapsulation efficiency, after one day from their production, and then freeze dried. Dry materials were rehydrated after one/two weeks of storage in their dry forms, as described in section 8.2.8 Rehydration of samples, with water and were shaken for one hour at 400 RPM and 20 °C in order to obtain a homogeneous rehydration. EE analyses were then repeated and results are reported in Table 8.3.

*Table 8. 3 – EE data of VAN in VFG samples 1 day after their production and after rehydration after a storage of 1 and 2 weeks in their dry forms (*no significant differences [p > 0.05] were found between EE values of non FD (EE_1 Day and FD samples(EE_dry-1 Week, EE_dry_2 Weeks)*

	EE_1 Day*	**EE_dry_1 Week***	**EE_dry_2 Weeks***
VFG_2%_0.35%	26.7 (± 3.0)	28.2 (± 3.2)	29.2 (± 3.5)
VFG_2%_0.25%	24.0 (± 2.9)	25.4 (± 3.3)	25.9 (± 2.9)

As can be seen from Table 8.3, FD was able to block the encapsulated percentage of VAN in AFG. In addition, FD did not alter the structure of AFG since the VAN fraction encapsulated into these materials before FD was retained within ALG particles. It can also be concluded that FD is a suitable technique to increase the shelf life of AFG, preventing the microbial/mould growth, without affecting the EE of actives, both hydrophilic and hydrophobic, loaded in it.

8.3.4 Rehydration of AFG with VAN solution

After assessing that FD did not change the EE of VAN and the structure of VFG, other experiments were conducted to study the rehydration of freeze dried "blank" AFG as a way to load VAN in these materials. AFG were produced, as described in section 8.2.2 Blank fluid gels, using different $CaCl_2$/ALG ratios, in order to obtain the formation of microparticles and nanoparticles, respectively for samples AFG_2%_0.35% and AFG_2%_0.25%. These materials were freeze dried, as described in section 8.2.7 Freeze drying, and then rehydrated for one hour using a VAN solution, as described in section 8.2.8 Rehydration of samples. After rehydration, EE and release experiments were conducted on these materials. Results are reported in Table 8.4 and Figure 8.1, in addition with data obtained from the same analyses performed on non-freeze dried VFG.

*Table 8. 4- EE of VAN in VFG as a function of their $CaCl_2$/ALG ratio in the "freshly produced" form and after FD and rehydration with VAN solution (*no significant differences [p > 0.05] were found between EE of FD and rehydrated samples and non-FD samples)*

	Encapsulation Efficiency, EE (±SD)		
	1 Day*	**1 Week***	**2 Weeks***
VFG_2%_0.25%_FD	21.3% (±3.4)	50.3% (±3.8)	72.2% (±3.9)
VFG_2%_0.25%_Fresh	24.2% (±2.5)	49.5% (±3.3)	73.3% (±2.9)
VFG_2%_0.35%_FD	21.6% (±4.2)	23.8% (±4.1)	42.5% (±3.5)
VFG_2%_0.35%_Fresh	28.9% (±3.2)	25.2% (±2.9)	43.9% (±3.2)

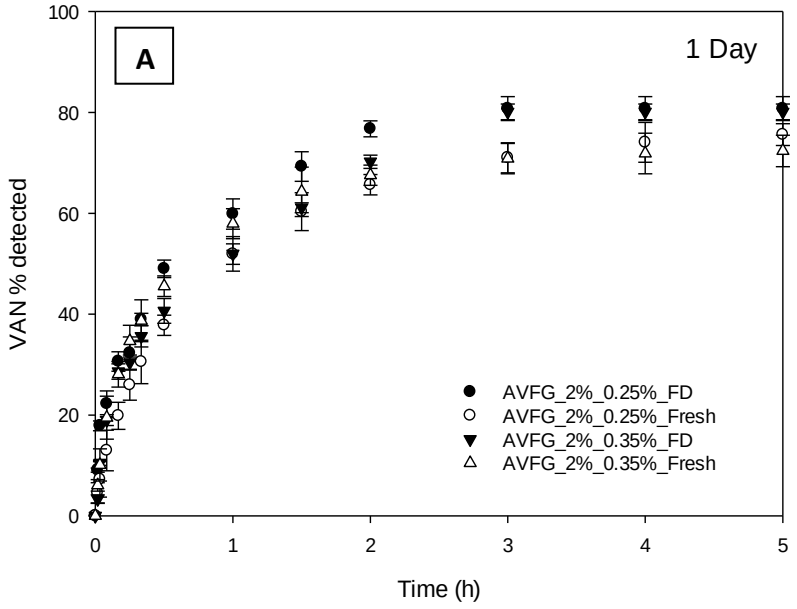
A
1 Day
VAN % detected
Time (h)
AVFG_2%_0.25%_FD
AVFG_2%_0.25%_Fresh
AVFG_2%_0.35%_FD
AVFG_2%_0.35%_Fresh

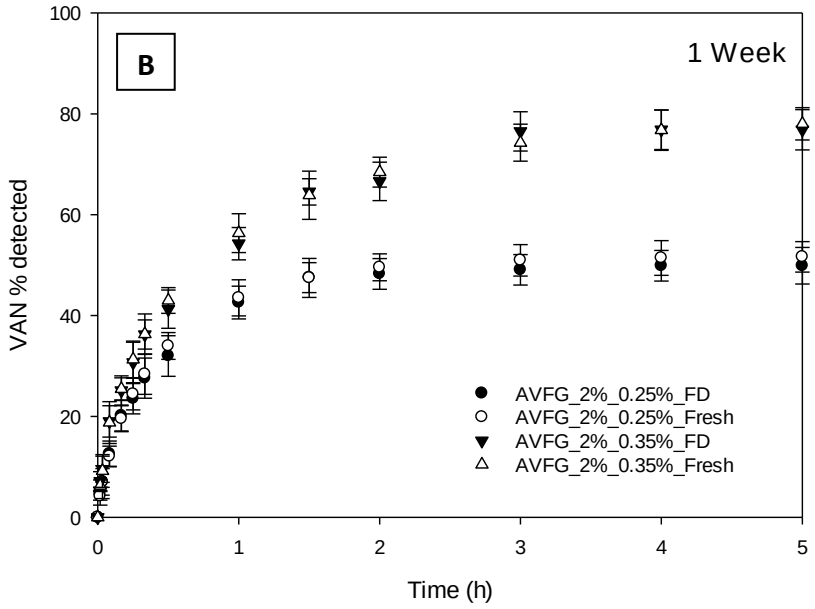
B
1 Week
VAN % detected
Time (h)
AVFG_2%_0.25%_FD
AVFG_2%_0.25%_Fresh
AVFG_2%_0.35%_FD
AVFG_2%_0.35%_Fresh

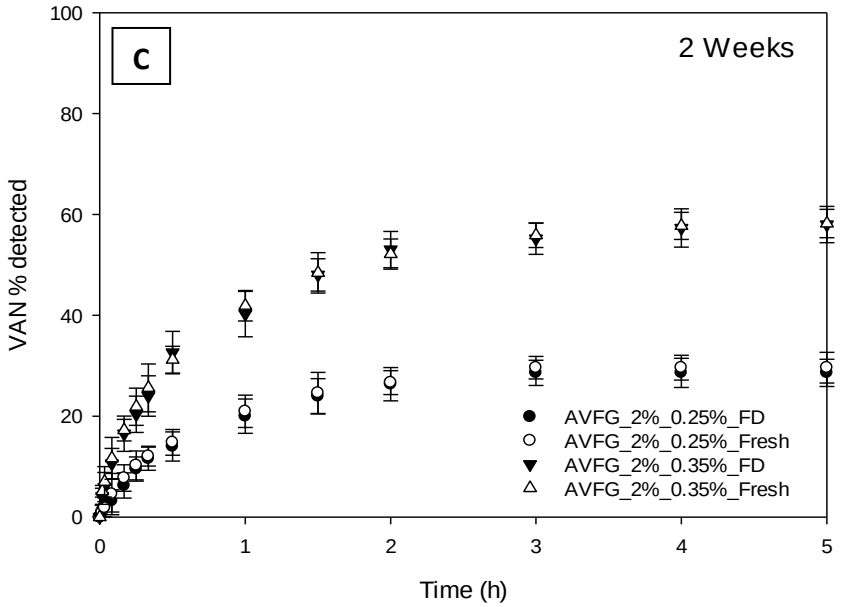

Figure 8. 1 - Release curves of VAN from VFG as a function of t_s in the "freshly produced" form and after FD and rehydration with VAN solution: (A) 1 day (B) 1 week (C) 2 weeks (no significant differences [p > 0.05] were found between data from release experiments conducted on FD and rehydrated samples and non-FD samples, at similar t_s times)

Comparing EE of non-freeze dried VFG samples with EE of the same materials after FD and rehydration with VAN solution it is possible to notice that these values were almost identical, after storing them for similar times. Also release experiments presented the same trends: release curves of non-freeze dried VFG samples and of the same materials after FD and rehydration with VAN solution were almost overlapping, after the same time of samples storage. These results suggested that the encapsulation of VAN in AFG did not take place during fluid gel formation. Firstly, VAN was distributed in the whole sample and, as a function of time, it migrated into particles. The rate of VAN loading into AFG particles, dry or "fresh", was mainly driven by diffusion, which was controlled by the high viscosities of AFG systems. In addition, it is possible to confirm, again, that FD did not affect the AFG structure, since dried materials were able to absorb VAN when rehydrated with a VAN solution and their loading rate was similar to the one of non-freeze dried VFG.

8.3.5 Encapsulation mechanism of VAN in alginate particles

In order to clarify the encapsulation reason/mechanism of VAN and, more in general, of hydrophobic actives in ALG particles, experiments were conducted using SDS as micelle forming materials. It is widely known that, when SDS is dissolved in water above a critical concentration called Critical Micelle Concentration (CMC), micelles with a hydrophobic core

and a hydrophilic surface are formed and their size is in between 12.0 Å and 20.3 Å [22, 23]. In a study of Chobpattana *et al.* (2002) SDS was used as bond disrupting agent to break interactions between VAN and bovine serum albumin, revealing some interactions between VAN and SDS itself [24]. In the present study, SDS micelles were used to replicate the presence of hydrophobic repositories in the water phase as that hypothesised to be offered by AFG particles. This was made to test the enthalpic advantage of introducing hydrophobic moieties in water and observe the behaviour of VAN in this amphiphilic mixture. VAS and SDS-VAN solutions were prepared as described in section 8.2.12 SDS proxy matrix experiments, and they were submitted to UV-Vis analysis to evaluate VAN concentration in them. Results are reported in Figure 8.2. In addition, the UV-Vis absorbance of SDS solutions without any VAN added was analysed and it was equal to zero, showing that SDS and SDS micelles cannot be detected at 300 nm wavelength. SDS presence did not affect the UV-Vis absorbance of VAN in these tests.

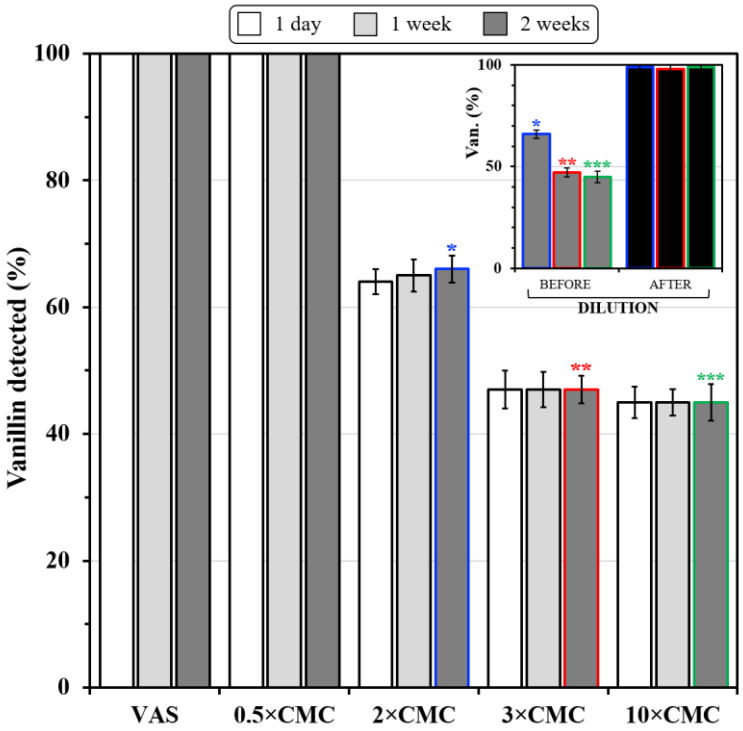

Figure 8. 2 - Results of EE in SDS micelles as a function of SDS concentration and t_s. In the top right corner the effect of SDS micelles disruption due the dilution of 10 times of the samples

As can be seen in Figure 8.2, all VAN present in the VAS "control" solution and in the 0.5X SDS-VAN solution was 100% detected. On the other hand, the concentration of VAN in 2X, 3X and 10X SDS-VAN solutions was lower than the VAN concentration used during samples

preparation. Almost 40% decrease of VAN concentration was observed in 2X SDS-VAN solution and approx. 60% of decrease was observed in 3X and 10X SDS-VAN solutions. These results can be explained considering a migration/encapsulation of VAN from the bulk water phase to the internal core of the formed SDS micelles. A fraction of VAN migrated into SDS micelles and it was surrounded by SDS molecules. This layer of SDS molecules altered the chemical surrounding of VAN and therefore their UV-Vis absorption. The decrease of VAN concentration was observed only in the SDS-VAN solutions in which a SDS concentration higher than the CMC was used and, therefore, SDS micelles were formed. No decrease of VAN concentration was detected in the sample where a SDS concentration lower than the CMC was used. In addition, detected VAN concentrations did not change as a function of t_s for all the solutions tested. These observation leaded to two conclusions: first, it can be stated that these solutions were stable overtime and VAN was not degraded. Second, the migration of VAN from the water phase into SDS micelles was extremely fast and much faster than that observed for AFG. The path of VAN to enter into the porous AFG matrix was much bigger in respect of that of a dynamic structure, such as a micelles. As migration in both systems was due to diffusion, it was expected for the rate of VAN transfer into AFG particles to be slower. In addition, this slower rate can be explained considering that ALG particle cores have a higher hydrophilic behaviour, in comparison to the core of SDS micelles. In fact, ALG particles are not only composed by carbohydrate polymer chains, which have a hydrophobic backbone, but also by water and hydrophilic groups present on the carbohydrate polymer chains themselves. On the contrary, the core of SDS micelles is formed by the rearrangement of hydrophobic tails of SDS leading to the formation of a very hydrophobic environment [23].

Additional experiments were conducted on SDS-VAN solutions after 2 weeks of storage. Since in the 2X, 3X and 10X SDS-VAN solutions the VAN concentration was lower than the expected one, considering the amount of active introduced in the samples, these were diluted 10 times with water in order to disrupt the SDS micelles. In fact, after dilution final SDS concentrations below the CMC were obtained. VAN concentrations were evaluated again via UV-Vis and results are reported in top-right corner of Figure 8.2. After micelles disruption all VAN that was introduced into 2X, 3X and 10X SDS-VAN solutions during their preparation was completely detected. The disruption of SDS micelles produced to the release of the entrapped VAN fraction into these moieties and the “free” VAN was then detected by UV-Vis analysis.

These experiments also confirmed that VAN was present into the SDS-VAN solutions, but its UV-Vis detection was hidden by its encapsulation into SDS micelles.

Overall, this work confirmed that by introducing a hydrophobic environment into the water phase, which impart an enthalpic advantage for VAN to be solubilised in water, the hydrophobic active will migrate into it. EE experiments of VAN in presence of ALG particles revealed that VAN migrated into particles as a function of time. It is possible to conclude that the inside of AFG particles behaves similarly to the hydrophobic core of SDS micelles. Therefore, the core of AFG, and of ALG particles in general, has a hydrophobic behaviour. Nevertheless, this hydrophobic property is less pronounced in comparison to SDS micelles, since the encapsulation of VAN happened instantaneously in SDS micelles, while it was extended overtime in ALG particles.

8.3.6 Release experiments in simulated GIT

Previous release experiments, reported in section 8.3.4 Rehydration of AFG with VAN solution, were conducted in water at 21.5 °C, showing that AFG, regardless of their particle dimensions, were not able to release the fraction of VAN encapsulated in their particles. Other release experiments were conducted using simulated gastric and intestinal fluids. These experiments were conducted on both VFG_2%_0.35% and VFG_2%_0.25% formulations as described in section 8.2.13 Simulated release in GIT, after 2 weeks of sample storage, in order to allow a significant encapsulation of VAN in AFG particles. An additional test was performed using water at 37 °C as release medium, to assess the temperature effect on VAN release. Release curves are reported in Figure 8.3, in addition with the EE of VAN in the samples after 2 weeks of storage.

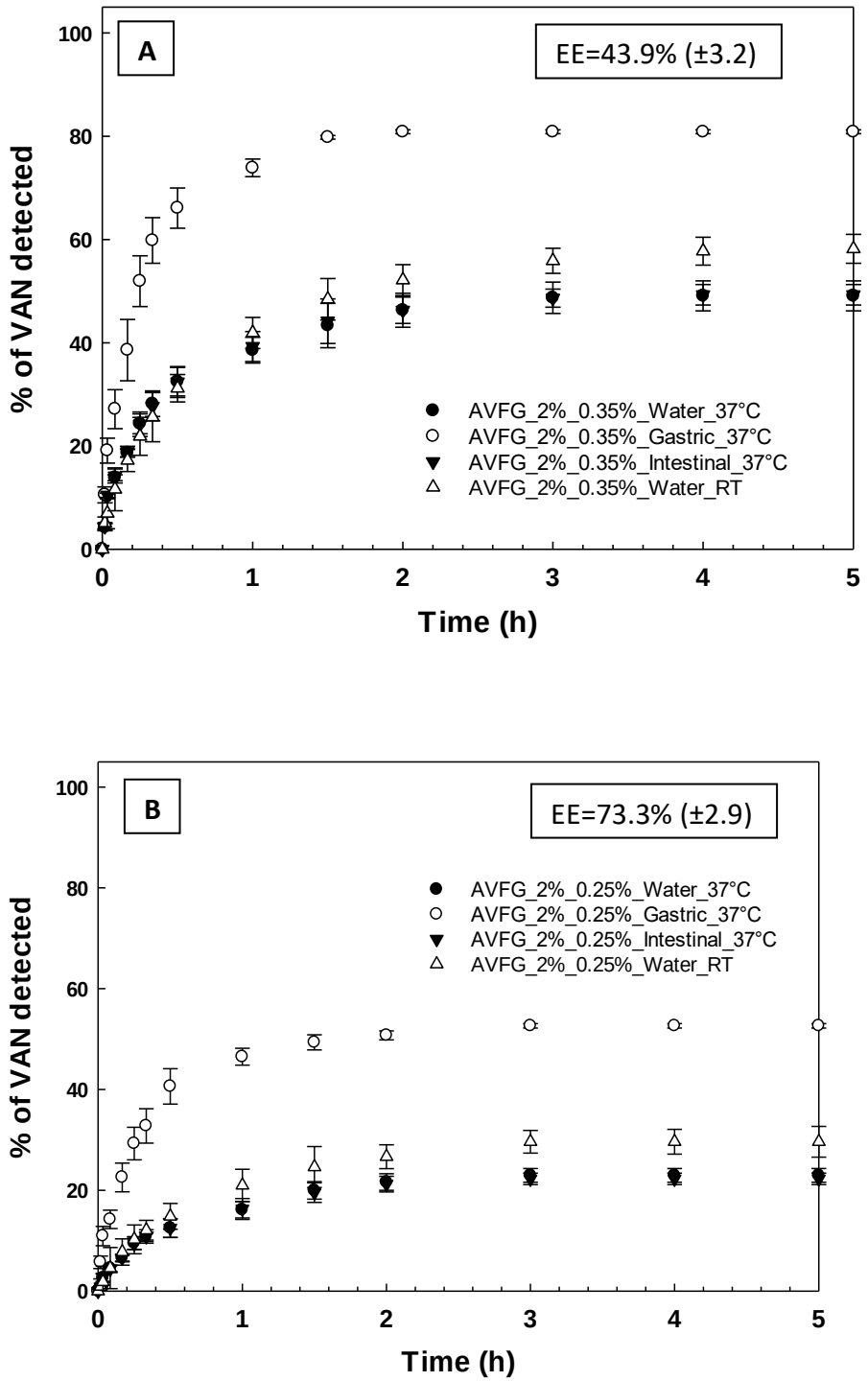

Figure 8. 3 - EE and release curves of VAN from VFG as a function of the release medium: A) VFG_2%_0.35% B) VFG_2%_0.25% (no significant differences [p > 0.05] were found between release experiments conducted under SIF, Water at RT and Water at 37°C, while significant differences [p < 0.05] were found between these experiments and release experiments conducted under SGF)

Comparing the release curves in which water was used as release medium it can be noticed that there were only marginal differences of VAN release by changing the temperature from

21.5 °C to 37 °C. A similar conclusion can be made when comparing experiments conducted in SIF and water. The SIF had a pH of 6.8, while the measured pH of "water-medium" was approx. 6.0, due to the water absorption of atmospheric CO_2 forming carbonic acid in solution (carbonation reaction). It can be concluded that this small difference in pH, as well as the presence of small concentrations of K^+,$H_2PO_4^-$, Na^+, Cl^- ions, did not affect the release of VAN from VFG materials. Ca^{2+}-alginate beads are known to dissolve in phosphate buffer overtime, due to Ca^{2+} exchange with Na^+ [25]. However, the observed undissolution of AFG in SIF can be explained considering that during AFG formation the eventual presence of non crosslinked Ca^{2+} was not removed from AFG by a washing step. Therefore, the presence of free Ca^{2+} ions can delay or block the dissolution of AFG in SIF. On the contrary, by using a SGF the VAN percentage released increased significantly. The EE of VAN into VFG_2%_0.35% was approx. 44% and in VFG_2%_0.25% was 73%. Therefore, the non-encapsulated VAN fractions were respectively 56% and 27%. During release studies in SGF medium approx. 80% of the VAN loaded in VFG_2%_0.35% was detected and approx. 50% in the case of VFG_2%_0.25%. SGF induced a release from AFG particles of approx. 24% of VAN initially introduced into both samples. VFG at the end of SGF-release experiments appeared clumpy and big aggregates could be identified. A study of Lim *et al*. (1997) about the diffusion of caffeine and theophylline from calcium alginate films revealed that their exposure to the acidic environment of SGF caused a significant increase of actives diffusion [26]. This effect was explained considering that the exposure of ALG gels to SGF produced a removal of Ca^{2+} ions, disrupting the cross-linked ALG network. This disruption increased the permeability of ALG films, leading to a higher release of actives. They also showed that a re-exposure of acid treated films to $CaCl_2$ regenerated the calcium content of these materials and their original active diffusion properties. A similar effect was reported by Aslani & Kennedy, when they studied the diffusion of acetaminophen from ALG gels [27]. In conclusion, the increased amounts of VAN detected into SGF can be attributed to the disruption of the ALG gel network, due to its exposure to a strong acidic environment (pH 1.2). In addition, these results confirmed that VAN was effectively encapsulated into VFG and the disruption of the gel network partially released the VAN fraction entrapped into particles.

Based on these results, AFG systems can potentially find applications as materials for the release of actives in the stomach. After ingestion these materials will start to release the VAN

fraction present in the water phase surrounding particles. When reaching the stomach, a higher release of active will be achieved, due to the low pH environment that will trigger the release of the fraction of active encapsulated into particles. In fact, the release plateaux during SGF experiments was reached after approx. 90 minutes, while, according to literature, the average time needed to obtain a 50% of stomach content to be emptied, after food consumption, is 2.5-3 hours [23]. Therefore, the release of the maximum amount of VAN will be obtained within the stomach, as a combination of release from particle cores and from the continuous water phase surrounding them. As the release of VAN during *in vitro* release tests in SIF, and also in water, was lower than the one observed in SGF it can be predicted that in the intestine AFG will not be able to release any additional amount of active. Therefore, it can be suggested to use AFG as matrices for stomach/low pH environment specific release formulations. On the contrary, these systems cannot be used for the sustained release in the intestine, since the majority of active will be released in the stomach.

8.4 Conclusions

Additional encapsulation experiments of VAN in ALG based materials were conducted in order to clarify the behavior of this active within AFG. Millimetre scale ALG particles were used to increase the size of ALG particles and, in this way, be able to separate the physically from the continuous water phase surrounding them. The effect of VAN encapsulation was studied into these bigger ALG particles by exposing them to a VAN solution and by monitoring the VAN migration in the particles overtime. The effect of changing the $CaCl_2$ and ALG concentrations during particle formation on the encapsulation behaviour of VAN was studied, revealing that the $CaCl_2$ concentration was responsible for the final rate of VAN loading into particles. A low $CaCl_2$ concentration produced a slow rate of VAN loading, but increasing this concentration above 1% w/w did not speed up the VAN loading rate. After that, FD was studied as an alternative method to load VAN in AFG. In fact, the properties of these materials were not affected by the FD process as reported in a previous study [6]. FD was able to stop the encapsulated fraction of VAN into AFG particles at the time when FD was performed. In fact, previous experiments clearly showed that hydrophobic actives were encapsulated into AFG as a function of t_s [7]. In addition, freeze dried blank AFG were rehydrated with a VAN solution and EE and release tests were then conducted. This revealed that dried AFG were able to

absorb VAN and their encapsulation rate was not different from the one observed for VFG, when VAN was introduced during pin-stirrer production. In addition, these tests revealed that dried materials retained their encapsulation behaviour for VAN. The encapsulation mechanism of VAN into ALG particles was due to the formation of hydrophobic interaction between VAN and the ALG matrix, as revealed the migration of VAN into SDS micelles, when these were introduced in a VAN-water solution. These tests revealed that AFG particles behaved similarly to SDS micelles, i.e. as hydrophobic moieties in water, and that VAN preferentially fitted hydrophobic environments instead of the continuous water phase of AFG. In general, hydrophobic actives are prone to be entrapped within the core of ALG particles, which leaded to an increase of encapsulation overtime. The entrapped fraction of hydrophobic actives in the particles was not released during release experiments conducted in water. However, release experiments conducted into different media revealed that VAN was partially unloaded from ALG particles when these were exposed to the acidic environment of SGF. Future studies should investigate if the exposure of AFG to SGF can change the later release behaviour in SIF. In fact, as reported by Mahdi *et al.* (2014) in the case of ibuprofen loaded in gellan gum fluid gels, the release of bioactives in SIF can be adjusted by changing the matrix-gel stiffness, by its exposure to low pH environments, such as SGF [28].

These studies are relevant from a scientific point of view, since they better clarified the behaviour of hydrophobic actives within AFG. This study revealed that AFG can be used as materials for the target release of hydrophobic drugs/nutraceuticals into the stomach or low pH environments. In addition, FD has been demonstrated to be a suitable method to extend AFG shelf life and to stop the encapsulation of hydrophobic actives in AFG overtime. In future, AFG should be used as ingredients of more complex food formulations to study the effect on using these materials for the production of food products and assess the impact of a real food matrix on the active encapsulation in AFG particles.

8.5 References

1. McClements, D.J., et al., *Enhancing Nutraceutical Performance Using Excipient Foods: Designing Food Structures and Compositions to Increase Bioavailability.* Comprehensive Reviews in Food Science and Food Safety, 2015. **14**(6): p. 824-847.

2. Wischke, C. and S.P. Schwendeman, *Principles of encapsulating hydrophobic drugs in PLA/PLGA microparticles.* International Journal of Pharmaceutics, 2008. **364**(2): p. 298-327.
3. Schrooyen, P.M.M., R.v.d. Meer, and C.G.D. Kruif, *Microencapsulation: its application in nutrition.* Proceedings of the Nutrition Society, 2001. **60**(4): p. 475-479.
4. Norton, Jarvis, and Foster, *A molecular model for the formation and properties of fluid gels.* International Journal of Biological Macromolecules, 1999. **26**(4): p. 255-261.
5. ter Horst, B., et al., *A gellan-based fluid gel carrier to enhance topical spray delivery.* Acta Biomaterialia, 2019. **89**: p. 166-179.
6. Smaniotto, F., et al., *Freeze drying and rehydration of alginate fluid gels.* Food Hydrocolloids, 2020. **99**: p. 105352.
7. Smaniotto, F., et al., *Use of Alginate Fluid Gel Microparticles to Modulate the Release of Hydrophobic Actives*. 2019.
8. Yong Lee, K. and D. J Mooney, *Alginate: Properties and biomedical applications*. Vol. 37. 2012. 106-126.
9. Ray, S., U. Raychaudhuri, and R. Chakraborty, *An overview of encapsulation of active compounds used in food products by drying technology.* Food Bioscience, 2016. **13**: p. 76-83.
10. Saha, D. and S. Bhattacharya, *Hydrocolloids as thickening and gelling agents in food: A critical review.* Journal of food science and technology, 2010. **47**: p. 587-97.
11. Tanaka, H., M. Matsumura, and I. Veliky, *Diffusion characteristics of substrates in Ca-alginate gel beads.* Biotechnology and bioengineering, 1984. **26**(1): p. 53-58.
12. Tu, J., et al., *Alginate microparticles prepared by spray–coagulation method: Preparation, drug loading and release characterization.* International Journal of Pharmaceutics, 2005. **303**(1): p. 171-181.
13. Hariyadi, D., et al., *Diffusion loading and drug delivery characteristics of alginate gel microparticles produced by a novel impinging aerosols method.* Journal of drug targeting, 2010. **18**: p. 831-41.
14. Fernández Farrés, I., M. Douaire, and I.T. Norton, *Rheology and tribological properties of Ca-alginate fluid gels produced by diffusion-controlled method.* Food Hydrocolloids, 2013. **32**(1): p. 115-122.
15. Fernández Farrés, Moakes, and Norton, *Designing biopolymer fluid gels: A microstructural approach.* Food Hydrocolloids, 2014. **42**: p. 362-372.
16. Piacentini, E., *Encapsulation Efficiency*, in *Encyclopedia of Membranes*, E. Drioli and L. Giorno, Editors. 2016, Springer Berlin Heidelberg: Berlin, Heidelberg. p. 706-707.
17. Pothakamury, U.R. and G.V. Barbosa-Cánovas, *Fundamental aspects of controlled release in foods.* Trends in Food Science & Technology, 1995. **6**(12): p. 397-406.
18. LeBlanc, J. G., *Vitamin C: an Update on Current Uses and Functions*. BoD–Books on Demand, 2019.
19. Ching, S., N. Bansal, and B. Bhandari, *Alginate gel particles–A review of production techniques and physical properties.* Critical reviews in food science and nutrition, 2015. **57**.
20. Probst, M., et al., *Molecular dynamics and x-ray investigation of an aqueous calcium chloride solution.* The Journal of Physical Chemistry, 1985. **89**(5): p. 753-759.
21. Soliman, E., et al., *Microencapsulation of Essential Oils within Alginate: Formulation and in Vitro Evaluation of Antifungal Activity.* Journal of Encapsulation and Adsorption Sciences, 2013. **3**: p. 48-55.

22. Chauhan, S., et al., *Study of Micellar Behavior of SDS and CTAB in Aqueous Media Containing Furosemide—A Cardiovascular Drug.* Journal of Solution Chemistry, 2010. **39**(5): p. 622-638.
23. Hammouda, B., *Temperature Effect on the Nanostructureof SDS Micelles in Water.* Journal of Research of the National Institute of Standards and Technology, 2013. **118**: p. 151.
24. Chobpattana, W., et al., *Mechanisms of Interaction Between Vanillin and Milk Proteins in Model Systems*. Vol. 67. 2002. 973-977.
25. Segale, L., Giovannelli, L., Mannina, P., Pattarino, F., *Calcium alginate and calcium alginate-chitosan beads containing celecoxib solubilized in a self-emulsifying phase*. Scientifica, 2016. doi: 10.1155/2016/5062706
26. Lim, E.B. and R.A. Kennedy, *Studies on diffusion in alginate gels. II. Effect of acid and subsequent re-exposure to calcium on the diffusion of caffeine and theophylline in alginate gel films.* Pharmaceutical development and technology, 1997. **2**(3): p. 285-292.
27. Aslani, P. and R.A. Kennedy, *Studies on diffusion in alginate gels. I. Effect of cross-linking with calcium or zinc ions on diffusion of acetaminophen.* Journal of controlled release, 1996. **42**(1): p. 75-82.
28. Mahdi, M.H., Conway, B.R., Smith, A.M., *Evaluation of gellan gum fluid gels as modified release oral liquids*. International Journal of Pharmaceutics, 2014. **475**(1–2): 335-343.

Chapter 9: CONCLUSIONS AND FUTURE RECOMMENDATIONS

9.1 Conclusions

The aim of this thesis was to advance the understanding of fluid gels by exploring potential applications in the field of bioactives encapsulation and release. Small molecular weight actives were introduced into AFG systems to investigate their encapsulation behaviour. Hydrophilic and hydrophobic actives were selected for this purpose and they were loaded in AFG matrices and their release was also investigated. In addition, the impact of FD on AFG properties was studied and this technique was investigated as a way to extend the shelf-life of these materials and of easy degradable bioactives loaded within them.

Before attempting the encapsulation of actives in AFG, their production using a pin-stirrer vessel was investigated. Their formation mechanism was studied and the effects of process parameters and constituents concentration, used during AFG production, on the final PSD and viscosity behaviour were deeply investigated.

- The $CaCl_2$/ALG ratio affects the final dimensions of ALG particles. Nanoparticles are obtained when a $CaCl_2$/ALG ratio below 0.155 is used and a higher ratio leads to the formation of microparticles. This is due to the fact that when a $CaCl_2$/ALG ratio lower than the CRMF (0.155) is used, ALG polymer chains are not completely cross-linked, which leads to the formation only of “nuclei of gelation” of nanometre dimensions [1]. On the contrary, only when a $CaCl_2$/ALG ratio higher than the CRMF is used a complete cross-linking of all G residues of ALG chains is achieved, producing the formation of particles of bigger, i.e. micrometre, dimensions [2].
- The flow behaviour of AFG is not dictated by the dimensions of particles, but by the concentration of ALG used during sample preparation and this is the only parameter affecting the final viscosity of AFG: the higher the concentration of ALG the higher the final viscosity of AFG.

The encapsulation of different actives, specifically VAN, TRP and NIC in AFG was then investigated. VAN and TRP were employed as model hydrophobic actives, while NIC as hydrophilic one, in order to correlate the active hydrophilicity/hydrophobicity to the encapsulation and subsequent release behaviours in AFG. In this studies, actives were introduced in AFG during their production in the pin-stirrer. Samples were characterised in terms of PSD, rheological properties, active EE and *in vitro* release behaviour, showing that:

- Actives presence does not affect the PSD and rheological behaviour of AFG, in the range of used concentrations (0.05%-0.10% w/w). This is probably due to the fact that actives do not alter the cross-linking between Ca^{2+} ions and ALG polymer chains.
- The EE, for all actives, following AFG production is very low and significantly increase upon storage only for hydrophobic actives. This is proposed to be due to the formation of hydrophobic interactions between low water soluble actives and AFG matrices. In general, actives diffuse into the gelled particles, thanks to their smaller sizes in comparison to gel pore dimensions. After their diffusion in AFG particles, in order to minimize their contact with the water medium surrounding particles, hydrophobic actives build some interactions with the ALG network. The formation of these interactions is time dependent, due to the time needed by the active to diffuse into the AFG particles from the bulk water phase, leading to an increase of EE overtime. What is more, during *in vitro* release tests, conducted under sink conditions, the fraction of hydrophobic active encapsulated cannot diffuse out of ALG particles, regardless of particle sizes. In addition, the amounts of hydrophobic actives released reduces by increasing t_s of samples, following an opposite trend of what observed for EE. Hydrophobic actives are, therefore, entrapped within AFG particles and they cannot be released from them. On the other hand, hydrophilic actives are not entrapped in AFG particles, since they do not form interactions with the gel network; they can diffuse in the particles, but they are not retained in them. When performing EE tests and/or release experiments these actives can back-diffuse from the particles core to the bulk phase and then to the release medium.
- In general, AFG showed the ability to slow down the release of actives loaded in their formulation, if compared to a water solution of the same active. This can be attributed to the presence of ALG gel network, which increases the viscosity of the system. In

fact, as suggested by Secouard *et al.* (2003), the viscosity of hydrocolloid formulations contributes significantly to active retention and delayed release [3].

The mechanism of hydrophobic actives encapsulation into ALG particles has been deeply investigated, specifically using VAN as model active. This investigation was conducted using not only AFG particles, but also other ALG-based particles/materials and other methods for the encapsulation of VAN. In particular, millimetre scale ALG particles were used to be able to physically separate them from their water surrounding phase. SDS micelles were used as proxy matrix to create hydrophobic moieties in water and study the loading of VAN into them, in order to mimic the internal core of AFG particles and confirm the hydrophobic character of these. It was concluded that:

- VAN can be loaded/entrapped into gelled ALG particles, regardless of their dimensions, i.e. nanometre, micrometre and millimetre; active-matrix interactions are prone to be developed into all these systems. A major difference between millimetre and nano/micrometre particles is about the effect of changing the $CaCl_2$ and ALG concentrations, during particle formation, on the rate of VAN encapsulation. In fact, the $CaCl_2$ concentration is responsible for the final rate of VAN loading in millimetre particles, while it does not seem to affect the rate of VAN loading in nano/micrometre particles. A study of Soliman *et al.* (2013) showed that the concentration of $CaCl_2$, used during the formation of ALG microparticles, changed the EE of essential oils [4]. This effect was observed within a range of $CaCl_2$ concentration between 0.125-2%. In the present study, nano/micrometre AFG particles were produced using $CaCl_2$ concentration of 0.25% and 0.35%, respectively. Probably no changes in VAN encapsulation were observed since the difference between the used $CaCl_2$ concentrations was too small. On the other hand, the $CaCl_2$ concentration used for the production of millimetre size ALG particles was changed over a broader range (between 0.5-2%), explaining why a difference of VAN encapsulation was observed for these systems. Overall, experiments conducted on millimetre size ALG particles confirmed that VAN, and hydrophobic actives in general, are prone to build interactions with this hydrocolloid.
- The behaviour of VAN of preferentially fit hydrophobic environments is confirmed by SDS experiments. The concentration of VAN in a water solution significantly decreases

when SDS micelles are introduced into the system. The core of SDS micelles is able to encapsulate a significant fraction of VAN, revealing the behaviour of this active to preferentially fit the hydrophobic internal compartment of micelles, instead of the water phase surrounding them. In addition, the disruption of SDS micelles, achieved by samples dilution, leads to the complete release of VAN fraction previously encapsulated. This confirms that the core of AFG particles has a hydrophobic character, similar to the one of SDS micelles. AFG particles are able to accommodate actives upon forming hydrophobic interactions.

Other release tests have been conducted on AFG loaded with VAN using different release conditions. These tests have been made in order to find release conditions/environments able to disrupt the hydrophobic interactions between VAN and the ALG matrix and, therefore, obtain the release of the VAN fraction encapsulated. This can be obtained by exposing VAN loaded AFG to acidic environments, like SGF. In fact, low pH environments disrupt the gel network, by breaking the ionic bridges between Ca^{2+} ions and ALG. This increases the permeability of the matrix, producing the release of the fraction of the active encapsulated.

The effects of FD and rehydration on AFG microstructure, on material properties, i.e. PSD and viscosity behaviour, and on the encapsulation behaviour of actives were investigated. NIC and VAN were chosen respectively as hydrophilic and hydrophobic model actives. This investigation showed that:

- Particle dimensions do not affect the kinetics of drying of AFG and after their rehydration the original particle sizes are completely restored.
- However, the bulk rheological performance (in terms of shear viscosity) can be completely recovered only for AFG formed by nanoparticles, i.e. in which a $CaCl_2$/ALG ratio lower than the CRMF was used during AFG formation. This is probably due to the fact that below that ratio, polymer chains are not fully cross-linked. Because of the presence of less cross-linking junctions, polymer chains have a higher mobility than fully cross-linked ones (when a $CaCl_2$/ALG ratio higher than the CRMF is used) and because of that, not-fully cross-linked polymer chains can rearrange to fit the water molecules between them during rehydration. In contrast, fully cross-linked polymer

chains present a lower mobility and they cannot completely fit back all water removed during the drying process.

- Actives presence within AFG do not affect the drying kinetics of these materials. This can be explained considering that actives used (VAN and NIC) do not interact significantly with the water present inside the gel network, for example by binding it. In addition, actives presence do not alter the water binding ability of ALG gels.
- Following the characterisation of AFG specific microstructure and material properties after FD and rehydration, this approach has been investigated as a way to encapsulate actives, specifically VAN, into freeze-dried AFG. As AFG properties are not affected by FD and rehydration, freeze-dried AFG can be loaded with actives upon their rehydration with an active containing water solution. It was disclosed that the rate of VAN loading, using this approach, is not dissimilar to the one observed by introducing VAN into AFG, during their pin-stirrer production.
- FD can be used to tailor the encapsulated fraction of hydrophobic actives into AFG particles. It was previously reported that the EE of hydrophobic actives increases as a function of time during their storage. FD can be used to block the amount of active encapsulated into AFG particles: by removing water, VAN is no longer able to diffuse into particles and, therefore, its encapsulated fraction does not increase any more as a function of time. The rehydration process restores the EE that samples had when FD was performed.
- The release behaviour of actives from AFG is not affected by the FD and rehydration processes for AFG formed by nanoparticles and it is marginally affected for microparticles AFG. This effect is probably linked with changes of rheological behaviour observed when rehydrating microparticle-based AFG materials.

Beside as a method to encapsulate and release of actives, FD can also be used as a method to extend the shelf-life of AFG and of easy degradable bioactives loaded within these materials. ASC was introduced into AFG systems to evaluate its degradation rate in the presence of the AFG matrix before and after the FD of the whole formulation. This study revealed that:

- The presence of AFG significantly accelerate the degradation of ASC, in comparison to an aqueous solution of this active, under the same storage conditions. The reason behind this enhanced degradation is probably due to an increased rate of anaerobic

degradation of ASC, which is catalysed by the presence of metal ions, like Ca^{2+} used for ALG cross-linking, as reported by Pinholt *et al.* [5]. What is more, the used $CaCl_2$/ALG ratio used during AFG production and, therefore, the final particle dimensions do not alter the rate of ASC degradation. This is probably due to the small difference of Ca^{2+} concentration used during samples production, specifically 0.25% $CaCl_2$ concentration for nanoparticles and 0.35% for microparticles based AFG, which does not produce an appreciable difference of ASC degradation rate.

- The FD process of AFG loaded with ASC significantly reduce the rate of ASC degradation, due to water removal. In addition, this procedure inhibit completely the formation of moulds, extending the shelf-life of AFG formulations, loaded or not with actives.

9.2 Recommendations for future work

This section aims to highlight areas of potential further research, based on the conclusions developed from this study.

1. **Investigate the effect of hydrophobic active size on their encapsulation in AFG.** In this work VAN and TRP were used as model hydrophobic actives to study actives encapsulation in AFG. However, these chemicals have similar molecular weights and hydrodynamic volumes. It will be beneficial to understand the effect of size/molecular weight of the active on its EE, rate of encapsulation and rate of release. In fact, when the drug's radius of gyration is similar to the pore size of the polymeric matrix, the diffusion of the active through the pores is hindered, producing a slower release overtime [6]. For example, a study of Pastor *et al.* (2015) showed that the pore size of silicon microparticles was essential to achieve a prolonged active release: when the mean pore size was similar to the radius of gyration of the loaded active a long retention time was observed, producing a prolonged release of the active over a time span of two weeks [7]. On the contrary, when microparticles were produced with larger pores a complete release was observed over a time span of two days. Similar effects were observed by Sandor *et al.* (2001), when investigating the effect of protein molecular weight on their release from PLGA microspheres [6]. The rate of proteins diffusion from microparticles decreased by increasing the molecular weight of the

loaded protein, suggesting that the release rate was function of the diffusion through the pores of the matrix. High molecular weight proteins experienced a prolonged time of release due their similar dimensions with matrix pores, which slowed down their diffusion.

2. **Investigate the active hydrophobicity limit that allows encapsulation in AFG.** It was observed that VAN and TRP were encapsulated into AFG particles, while NIC and ASC were not, due to their hydrophobic/hydrophilic behaviors. It will be beneficial to highlight the cut-off point of active hydrophilicity that will not permit the encapsulation of the active in AFG systems. In fact, VAN and TRP present a quite low water solubility, while NIC and ASC have a very high one. Conduct an encapsulation screening using actives of different water solubilities will clarify which is the water solubility limit that does not allow actives encapsulation in AFG.
3. **Investigate ways to accelerate the loading process of hydrophobic actives in AFG.** As shown in chapter 6 and 7 the encapsulation of hydrophobic actives increased as a function of time, but it was a slow process and 1-2 weeks were needed to load the maximum amount of actives possible. In order to obtain an industrially scalable process to encapsulate actives in these systems it is necessary to speed up the loading process. Potential ways to increase the encapsulation rate are:
    - Using of mild temperatures to increase the kinetic rate of encapsulation, but low enough to not increase the active degradation rate.
    - Using emulsifiers/surfactants and/or chemicals to be added into AFG formulations. In theory, by increasing the hydrophobic behavior of AFG particles, hydrophobic actives will migrate faster into the core of particles.
    - Dilute samples after their production. Assuming that AFG particles are homogeneously distributed through the sample, immediately after their production they are in the closest packed configuration. This is function of the dilution rate, used during sample preparation, between ALG particles and the water phase. By diluting AFG materials it will be achieved a disaggregation of particles and they will end to be more separated more one from another. Therefore, a larger surface area of particles will be exposed to the active containing phase, potentially increasing the rate and/or the amount of active diffusing from the water phase into particles. In addition, dilution can

maximize the loading rate/capacity by obtaining better diffusion conditions, such as reducing the diffusion pathway of the active from the water phase to the particle surface and/or by decreasing the bulk viscosity. In fact, the viscosity of the formulation can significantly change the diffusion of actives, as described by the Fick's law of diffusion. This law describes the mass transport phenomena of chemicals, through a phase, caused by their gradients of concentration [8]. Fick's first law of diffusion, reported in Equation 9.1, correlates the flux of mass transfer (*F*), on the *x* direction per unit of sectional area, with the concentration of the diffusing active (*c*) and with the diffusion coefficient (*D*) [9].

$$F = -D\frac{\partial c}{\partial x} \quad \text{(Equation 9.1)}$$

D coefficient, also called diffusivity, is proportional to the squared velocity of diffusing particles, which is function of the temperature, size of particles and the viscosity of the system [9]. Therefore, by reducing the viscosity of AFG systems, it can be increased the diffusivity of hydrophobic actives, present in the same phase, increasing the rate of active transfer into particles.

4. **Investigate the impact of modifications of the ALG gel network on its physical properties and on its capacity to effectively encapsulate actives.** It will be beneficial to understand how modifications of the ALG network will affect the PSD and rheological properties of AFG and if this will affect the behavior of actives loading/release. Interesting network modifications to investigate are:
    - Chemical modifications of the ALG polymer chain. It was observed that the encapsulation of hydrophobic actives in AFG increased as a function of t_s, due to the formation of hydrophobic interactions. In literature, different studies reported chemical modifications of ALG polymer chains to increase their hydrophobic behavior using different methods, like acylation or grafting with hydrophobic polymers, e.g. poly(methyl methacrylate), poly(butyl methacrylate) and poly(acrylonitrile) [10-12]. These modifications were specifically made to increase the hydrophobic nature of ALG matrix and tailor its drug encapsulation/release properties. By conducting similar modifications

it will be possible to increase the binding ability of AFG particles to hydrophobic actives and potentially accelerate their loading process.

- Cross-linking of ALG with different divalent/multivalent cations during AFG production. In this study AFG were produced using Ca^{2+} as cation to achieve gelation. However, it is not the only multivalent cation known to induce ALG gelation: Mg^{2+}, Sr^{2+}, Ba^{2+}, Al^{3+} and Fe^{3+} are cations able to cross-link ALG chains, but their ionic radii are different in size from that of Ca^{2+} [12]. Studying the effect of using smaller/bigger cations to achieve ALG gelation will be beneficial to understand their behavior on active encapsulation and/or release.

5. **Studying other hydrocolloid fluid gels for the encapsulation of actives.** In the past, ionically and thermally gelled hydrocolloids, e.g. gellan gum, agar and κ-carrageenan, were used for fluid gels production [13-15]. However, they were not or little investigated as matrices for actives encapsulation. The entrapment of skin cells in gellan gum fluid gel systems was studied by ter Horst *et al*. (2019), in order to enable their spray delivery onto burn wounds [13]. However, in this study, the fluid gel matrix was not used for loading cells into fluid gel particles, but to increase the retention time of skin cells on the wound after spraying. This was achieved thanks to the fluid gel contribution in increasing the formulation viscosity. It is possible to suggest future investigations about the use of other hydrocolloids for the encapsulation of actives. The present study can be used as guideline to conduct encapsulation experiments using the same actives used here and, therefore, highlight the hydrocolloid contribution on actives encapsulation/release. As a following step, fluid gels composed by a mixture of hydrocolloids can be studied to specific tailor the encapsulation, rheological and release properties as needed.
6. **Investigate the behaviour of AFG as ingredient of food formulations.** The impact on the final texture of more complex food formulations in which AFG are incorporated should be tested. In addition, it will be useful to understand the active encapsulation and release behaviours of AFG when they are applied into real foods. In fact, it will be possible to use these materials for two purposes:
    - **To encapsulate actives in AFG before their introduction in foods.** This will be beneficial especially when a hydrophobic active is loaded in AFG. In fact, the non-encapsulated active fraction will be released in the food itself and this

process will start during the mixing of AFG in the product. The encapsulated fraction will be released later in the stomach, where the low pH environment will disrupt the AFG network.

- **To add blank AFG to food systems as a sequestrant for chemicals already present in the formulation.** Food formulations are complex mixtures of ingredients and chemicals, which can be added on purpose or be already present within other ingredients. Since AFG can encapsulate low water soluble chemicals, in theory, they can act as absorbers of these chemicals during food storage and release them in the stomach. This can be useful to prevent chemicals degradation/reactions during storage. In addition, as this process will probably happen spontaneously during food storage, it will not be necessary to add an additional step, during food production, to load chemicals/actives.

7. **Studying approaches to control the release of actives from fluid gel particles.** Release experiments conducted on AFG loaded with VAN revealed that the non-encapsulated fraction of VAN can be released in water, while the encapsulated fraction can be released in acidic pH environments. In addition, EE tests showed that the ratio between encapsulated and non-encapsulated fractions is a function of t_s, i.e. the encapsulated fraction increases overtime. This property can be potentially used to develop a new class of stimuli responsive materials able to release the non-encapsulated active fraction in water, e.g. in neutral pH/water-based food products during storage, and the encapsulated one in low pH environments, e.g. in the stomach. Introducing active loaded AFG into the food product at different times will tune the amounts of active released under the two conditions/environments. However, future studies are necessary to disclose the feasibility of this potential way to control the release of actives, loaded into fluid gel particles.

9.3 References

1. Smaniotto, F., et al., *Freeze drying and rehydration of alginate fluid gels.* Food Hydrocolloids, 2020. **99**: p. 105352.
2. Braccini, I. and S. Pérez, *Molecular Basis of Ca2+-Induced Gelation in Alginates and Pectins: The Egg-Box Model Revisited.* Biomacromolecules, 2001. **2**(4): p. 1089-1096.

3. Secouard, S., et al., *Release of limonene from polysaccharide matrices: viscosity and synergy effect.* Food Chemistry, 2003. **82**(2): p. 227-234.
4. Soliman, E., et al., *Microencapsulation of Essential Oils within Alginate: Formulation and in Vitro Evaluation of Antifungal Activity.* Journal of Encapsulation and Adsorption Sciences, 2013. **3**: p. 48-55.
5. Pinholt, P., et al., *Rate Studies on the Anaerobic Degradation of Ascorbic Acid IV: Catalytic Effect of Metal Ions.* Journal of Pharmaceutical Sciences, 1966. **55**(12): p. 1435-1438.
6. Sandor, M., et al., *Effect of protein molecular weight on release from micron-sized PLGA microspheres.* Journal of Controlled Release, 2001. **76**(3): p. 297-311.
7. Pastor, E.L., et al., *Pore size is a critical parameter for obtaining sustained protein release from electrochemically synthesized mesoporous silicon microparticles.* PeerJ, 2015. **3**: p. e1277-e1277.
8. Poirier, D. and G. Geiger, *Fick's Law and Diffusivity of Materials*. 2016. p. 419-461.
9. Siepmann, J. and F. Siepmann, *Modeling of diffusion controlled drug delivery.* Journal of Controlled Release, 2012. **161**(2): p. 351-362.
10. Han, J., et al., *Alginate and chitosan functionalization for micronutrient encapsulation.* Journal of agricultural and Food chemistry, 2008. **56**(7): p. 2528-2535.
11. Yao, B., et al., *Hydrophobic modification of sodium alginate and its application in drug controlled release.* Bioprocess and biosystems engineering, 2010. **33**(4): p. 457-463.
12. Pawar, S.N. and K.J. Edgar, *Alginate derivatization: A review of chemistry, properties and applications.* Biomaterials, 2012. **33**(11): p. 3279-3305.
13. ter Horst, B., et al., *A gellan-based fluid gel carrier to enhance topical spray delivery.* Acta Biomaterialia, 2019. **89**: p. 166-179.
14. Fernández Farrés, I. and I.T. Norton, *The influence of co-solutes on tribology of agar fluid gels.* Food Hydrocolloids, 2015. **45**: p. 186-195.
15. Gabriele, A., F. Spyropoulos, and I.T. Norton, *Kinetic study of fluid gel formation and viscoelastic response with kappa-carrageenan.* Food Hydrocolloids, 2009. **23**(8): p. 2054-2061.